The role and regulation of VEGF-mediated ERK5 activity in endothelial cells

Thesis submitted in accordance with the requirements of the University of Liverpool for the degree of Doctor of Philosophy

by

GOPIKA NITHIA NITHIANANDARAJAH-JONES

November 2014

DECLARATION

This thesis is the result of my own work.
The material contained within this thesis has not been presented, nor is it currently being presented, either wholly or in part for any other degree or qualification.

Gopika Nithia Nithianandarajah-Jones

This research was carried out in the Department of Molecular and Clinical Pharmacology, Institute of Translational Medicine, University of Liverpool.

The role and regulation of VEGF-mediated ERK5 activity in endothelial cells

Extracellular signal-regulated kinase 5 (ERK5) is the newest member of the mitogen-activated protein kinase (MAPK) family following the discovery of ERK1/2, JNK and p38 MAPK. ERK5 consists of an N-terminal kinase domain, similar to the other MAPK members, and a large C-terminal domain, which is unique in structure and function from the other MAPK members. ERK5 is activated in response to a multitude of extracellular stimuli, including pro-angiogenic factors in endothelial cells. The physiological importance of ERK5 was highlighted following *Erk5* gene ablation in mice, where a severe disruption to cardiovascular development and loss of vascular integrity was observed, resulting in embryonic lethality.

This study investigated the differences in ERK5 activation between vascular endothelial growth factor (VEGF) stimulation of primary human dermal microvascular endothelial cells (HDMECs) compared to epidermal growth factor (EGF) stimulation of HeLa (immortalised epithelial cervical cancer cell line) cells. It was discovered that in contrast to other growth factors, VEGF appeared unique in its ability to induce ERK5 phosphorylation in HDMECs, stimulating ERK5 activity via a VEGFR-2/PLCγ-dependent pathway. Utilisation of the innovative Phos-tag™ reagent in SDS-PAGE facilitated the novel discovery that VEGF was only able to induce phosphorylation of the threonine (Thr)^{218}/tyrosine (Tyr)^{220} residues present within the activation loop of the kinase domain. In contrast, EGF stimulation of HeLa cells resulted in phosphorylation of ERK5 on Thr^{218}/Tyr^{220} as well as additional C-terminal residues such as Thr^{732}. It was further demonstrated that contrary to EGF, VEGF stimulation of HDMECs did not evoke a nuclear translocation of ERK5, instead, ERK5 appeared to localise to the cytoplasm and plasma membrane. The analysis of intracellular signalling pathways following treatment with small-molecule inhibitors against MAPK/ERK kinase 5 (MEK5) and ERK5 kinase activity, revealed that VEGF-mediated ERK5 activation regulated phosphorylation of AKT in HDMECs. Furthermore, with an apparent co-localisation of ERK5 and AKT in the cytoplasm and at the plasma membrane of HDMECs, it was hypothesised that the two proteins were interacting partners. Adenoviral-mediated expression of FLAG-tagged ERK5 revealed that VEGFR-2, ERK5 and AKT co-immunoprecipitated in HDMECs, suggesting the possibility of a complex between these proteins at the cell periphery following VEGF stimulation and VEGFR-2 internalisation. Taken together, this study shows that VEGF appears to induce a unique activation of ERK5 in endothelial cells, which facilitates its interaction with AKT and subsequent regulation of AKT phosphorylation, ultimately regulating endothelial cell survival.

Dedicated to Oliver Krishnan Jones

and Baby Girl Jones

"The greatest glory in living lies not in never falling, but in rising every time we fall"

- Nelson Mandela

Acknowledgements

I would first like to thank my supervisors Dr. Bettina Wilm, Dr. Chris Goldring and especially Dr. Mike Cross for their ideas and continuous guidance throughout my PhD. Thanks must also go to the BBSRC for funding the work in this thesis.

Thank you to the members of the Angio group: Ahmad, Awel, Maxine and Mohammad, with a special thanks to Emma for being my early morning lab buddy and her IF expertise!

I am very grateful to Dr. Parveen Sharma who has helped me understand the world of proteomics. You have endured some truly ridiculous questions, so thank you!

I would like to extend a massive thank you to Dr. Katie Holmes. I am extremely grateful to you for giving me the best possible start to my PhD. Science misses you!

Thank you to Agnès, Áine, Ali, Fiazia, Harriet, Holly and Jo for all the fun, gossip and laughs. Also, thank you for the blue block tea breaks in the early years, Matt, and Hayley for the motivational Skype chats from across the pond!

Danny, Jez, Kaine, Macca & Piers – thanks for remaining completely oblivious to what I do!

A huge thank you must also go to Alex, Katie and Laura. You have all kept me going with the catch-ups, pep-talks, visits and love you send my way. The three of you are truly amazing friends!

Nanna Buckley, thank you for feeding Oliver and me up every Monday!
I am incredibly grateful to my mum-in-law Sue, and stepdad-in-law Mick, for looking after Oliver every Tuesday and having us stay over every Monday night. I am so lucky to be able to call you my family.

To my big brother and sis-in-law, Hem and Kari, thank you for listening to my rants and then helping me forget about it all. I'm finished with all the studying now, so you can hurry up and get back over here!

Thank you to my wonderful parents. Mum and Dad, you gave me every opportunity in life and for that I will be eternally grateful. Hopefully, after all these years, you will finally clear the loft of all my primary and secondary school books…I really am done with studying now, I promise!

I have to thank my handsome little monkey, Oliver. You are an absolute blessing and your unconditional love has made this all worthwhile. I hope when you and your baby sister come across this in the future, you'll be proud of your Mummy.

Words cannot describe how thankful I am to my best friend and fantastic husband, Gav. Your constant encouragement, support and love over the years have kept me going through it all. You have an incredible amount patience to put up with me and I am truly grateful to have you by my side, every step of the way.

Table of Contents

Abbreviations

AKT	v-akt murine thymoma viral oncogene homolog (PKB)
Ala	Alanine (A)
AR	Amphiregulin
Arg	Arginine (R)
Asp	Aspartic acid (D)
ATP	Adenosine triphosphate
BAD	BCL2-antagonist of cell death
BAEC	Bovine aortic endothelial cell
BCL2	B-cell lymphoma-2
BDNF	Brain-derived neurotrophic factor
BLMEC	Bovine lung microvascular endothelial cell
BMK1	Big MAPK-1
BSA	Bovine serum albumin
BT474	Breast cancer cell line
C-	Carboxy-
CA	Constitutively-active
C2C12	Mouse myoblast cell line
CD	Common docking
CDK	Cyclin-dependent kinase
cDNA	Complementary DNA
CD31	Cluster of differentiation 31
COS7	Monkey kidney tissue-derived fibroblast-like, immortalised CV-1 cell line
CREB	cAMP-responsive element binding-protein
Cys	Cysteine (C)
DAG	Diacylglycerol
DMSO	Dimethylsulphoxide
DNA	Deoxyribonucleic acid
dsRNA	Double-stranded RNA
DUSP	Dual-specificity protein phosphatase
E	Embryonic day
EC	Endothelial cell
ECM	Extracellular matrix
EGF	Epidermal growth factor
EGFR	EGF receptor
eNOS	Endothelial nitric oxide synthase
EPR	Epiregulin
ER	Endoplasmic reticulum

ERK	Extracellular signal-regulated kinase
ETS	E26 transformation-specific factor
FAK	Focal adhesion kinase
FGM	Full growth medium
FasL	Fas ligand
FCS	Foetal calf serum
FDA	Food and drug administration
FGF	Fibroblast growth factor
Flk-1	Foetal liver kinase-1
Flt	Fms-related tyrosine kinase
FoxO3a	Forkhead box O3a
Gab1	Grb2-associated binder-1
Glu	Glutamic acid (E)
Grb2	Growth-factor-receptor-bound 2
GST	Gastrointestinal stromal tumour
HAEC	Human aortic endothelial cell
HB-EGF	Heparin-binding EGF-like growth factor
HDMEC	Human dermal microvascular endothelial cell
HEK293	Human embryonic kidney 293 cells
HeLa	Henrietta Lacks-derived immortalised epithelial cervical cancer cell line
HGF	Hepatocyte growth factor
HIF-1α	Hypoxia-inducible factor-1 alpha
HIF-1ß	Hypoxia-inducible factor-1 beta
HSPG	Heparan sulphate proteoglycan
HUVEC	Human umbilical vein endothelial cell
IF	Immunofluorescence
IFN-α	Interferon-alpha
IGF-1	Insulin-like growth factor 1
IL-6	Interleukin-6
IL-8	Interleukin-8
IP	Immunoprecipitation
IP_3	Inositol-1,4,5-trisphosphate
IP_3R	IP_3 receptor
JNK	c-Jun NH_2-terminal kinase
KDR	Kinase-insert domain-containing receptor
KLF2	Krüppel-like factor 2
KLF4	Krüppel-like factor 4
LB	Luria-Bertani

Lad	Lck-associated adaptor
Lck	Lymphocyte-specific protein tyrosine kinase
Lys	Lysine (K)
MAE	Murine aortic endothelial
MAPK	Mitogen-activated protein kinase
MAPKK	MAPK kinase
MAPKKK	MAPKK kinase
mCRC	Metastatic colorectal carcinoma
MCF-7	Michigan cancer foundation-7 breast cancer cell line
MEF	Myocyte enhancer factor
MEK	MAPK/ERK kinase
MEKK	MEK kinase
MKP	MAP kinase phosphatase
MMP	Matrix metalloproteinases
mRCC	Metastatic renal cell carcinoma
mRNA	Messenger RNA
mTOR	Mammalian target of rapamycin
mTORC	mTOR complex
N-	Amino-
NES	Nuclear export signal
NFAT	Nuclear factor of activated T-cells
NF-κB	Nuclear factor-kappaB
NGF	Nerve growth factor
NHDF	Normal human dermal fibroblast
NLS	Nuclear localisation signal
NO	Nitric oxide
Nrf2	NF-E2 related factor 2
NRP	Neuropilin
$p90^{RSK}$	90 kDa ribosomal S6 kinase
PAE	Porcine aortic endothelial
PAGE	Polyacrylamide gel electrophoresis
Phe	Phenylalanine (F)
PB1	Phox and Bem1p
PBS	Phosphate-buffered saline
PC12	Pheochromocytoma 12
PCR	Polymerase chain reaction
PDGF	Platelet-derived growth factor
PDGFR	PDGF receptor

PDK	Phosphoinositide-dependent kinase
PH	Pleckstrin-homology
PI3K	Phosphoinositide 3'-kinase
PIP_2	Phosphatidylinositol-4,5-bisphosphate
PIP_3	Phosphatidylinostitol-3,4,5-trisphosphate
PKB	Protein kinase B
PKC	Protein kinase C
PLCγ	Phospholipase C-gamma
PlGF	Placental growth factor
PMA	Phorbol 12-myristate 13-acetate
PML	Promyelocytic leukaemia protein
PML-NB	PML-nuclear body
PP2A	Protein phosphatase 2A
PR	Proline-rich
Pro	Proline (P)
PTB	Phosphotyrosine-binding
PTEN	Phosphatase and tensin homologue
qRT-PCR	Quantitative real-time PCR
RAF	Rapidly accelerated fibrosarcoma kinase
RAPTOR	Regulatory-associated protein of mTOR
RAS	Rat sarcoma protein
RCC	Renal cell carcinoma
RICTOR	Rapamycin-insensitive companion of mTOR
RIPA	Radio-immunoprecipitation assay
ROS	Reactive oxygen species
RNA	Ribonucleic acid
rpm	Revolutions per minute
rt	Room temperature
RTK	Receptor tyrosine kinase
SAPK	Stress-activated protein kinase
Sck	Shc-like protein
SDS	Sodium dodecyl sulphate
Ser	Serine (S)
SGK	Serum- and glucocorticoid-inducible kinase
SH2	Src homology 2
SH3	Src homology 3
Shb	Src homology 2 protein B
siRNA	Small-interfering RNA

SOS	Son of sevenless
SUMO	Small ubiquitin-related modifier
TBS	Tris-buffered saline
TBS-T	TBS Tween
TGF-α	Transforming growth factor-alpha
Thr	Threonine (T)
TNF-α	Tumour necrosis factor-alpha
TKD	Tyrosine kinase domain
TSAd	T-cell specific adapter
TSP-1	Thrombospondin-1
Tyr	Tyrosine (Y)
VCAM	Vascular cell adhesion molecule
VEGF	Vascular endothelial growth factor
VEGFR	VEGF receptor
VPF	Vascular-permeability factor
VRAP	VEGF receptor-associated protein
WB	Western blot
wt	Wild-type

Chapter One
General Introduction

1.1 Embryonic vascular development

1.1.1 Vasculogenesis

The *de novo* formation of the primitive vascular plexus during embryogenesis is referred to as vasculogenesis and is a multi-step process. The progression from the single-layered blastula into the tri-laminar gastrula gives rise to the three germ layers – the ectoderm, mesoderm and endoderm (Figure 1.1). Of these layers, cells derived from the mesoderm undergo differentiation to become angioblasts, which fuse together to form blood islands. Aggregation of these blood islands along with further differentiation into endothelial cells results in the primitive vascular network (Figure 1.1) (Risau and Flamme, 1995). In mice, aggregation of the angioblasts occur at embryonic day 6.5 (E6.5) and the primary vascular network is established at E8.0-E8.5 (Haar and Ackerman, 1971). It is essential that a functional plexus is constructed in order for murine embryos to survive beyond E9.5 (Srivastava and Olson, 2000).

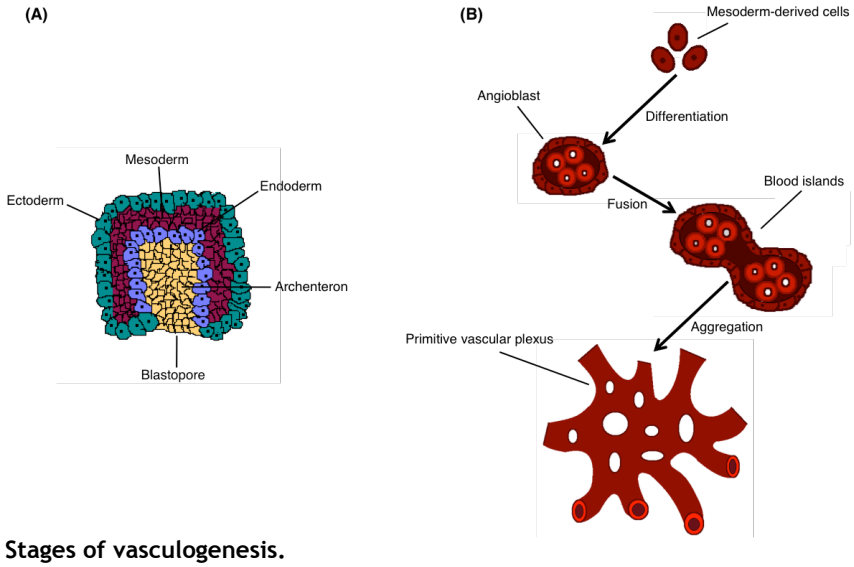

Figure 1.1 Stages of vasculogenesis.
(A) Structure of the gastrula. The tri-laminar gastrula is formed during gastrulation, in which the single-layered blastula undergoes cleavage at the primitive streak to result in the three germ layers – the ectoderm (teal), mesoderm (magenta) and endoderm (purple) – which envelop the archenteron (primitive gut; yellow). (B) Formation of the primitive vascular plexus. Mesoderm-derived cells differentiate into angioblasts. Fusion, aggregations and further differentiation of the blood islands give rise to the primitive vascular plexus in the yolk sac. Diagrams adapted from (A) (Brauckmann and Gilbert, 2004), and (B) (Heinke *et al.*, 2012).

1.1.2 Angiogenesis

Angiogenesis is defined as the formation of new blood vessels from pre-existing ones and occurs following the formation of the primary vascular network, therein remodelling the plexus to enable blood vessels to reach the extremities of the developing embryo (Risau, 1997; Carmeliet, 2000). Normal embryonic development is dependent upon angiogenesis, however this process remains in a state of quiescence postpartum, with only a few physiological exceptions including wound reparation (Li *et al.*, 2003) and endometriosis (Groothuis *et al.*, 2005).

Two distinct mechanisms of angiogenesis exist namely, intussusception and sprouting. During intussusceptive angiogenesis, interstitial cellular columns are inserted into the lumen of pre-existing vessels; the growth and stabilisation of these columns leads to a partitioning of the vessel and subsequent remodelling of the local vascular network (Risau, 1997). Sprouting angiogenesis however is somewhat more dynamic, whereby several diverse processes coordinate neovessel growth and stabilisation, shown schematically in Figure 1.2 (Klagsbrun and Moses, 1999; Vailhe *et al.*, 2001).

The initial neovessel growth in angiogenesis is stimulated by the presence of factors such as vascular endothelial growth factor (VEGF) and fibroblast growth factor (FGF) in the immediate microenvironment surrounding the endothelial cells (Folkman and Shing, 1992; Klagsbrun and Moses, 1999; Pearson, 2000). The binding of these angiogenic growth factors to their cognate receptors present on the endothelial cells of pre-existing vessels, induces a loss of pericyte coverage, an increase in vascular permeability and secretion of proteases to degrade the basement membrane and the surrounding interstitial matrix (Bergers and Song, 2005; van Hinsbergh *et al.*, 2006). The leading 'tip' endothelial cell migrates into the space created in the matrix along the concentration gradient of the angiogenic factor (Gerhardt and Betsholtz, 2003), succeeded by proliferating 'stalk' endothelial cells to collectively form an endothelial sprout with a lumen (Figure 1.2) (Vailhe *et al.*, 2001).

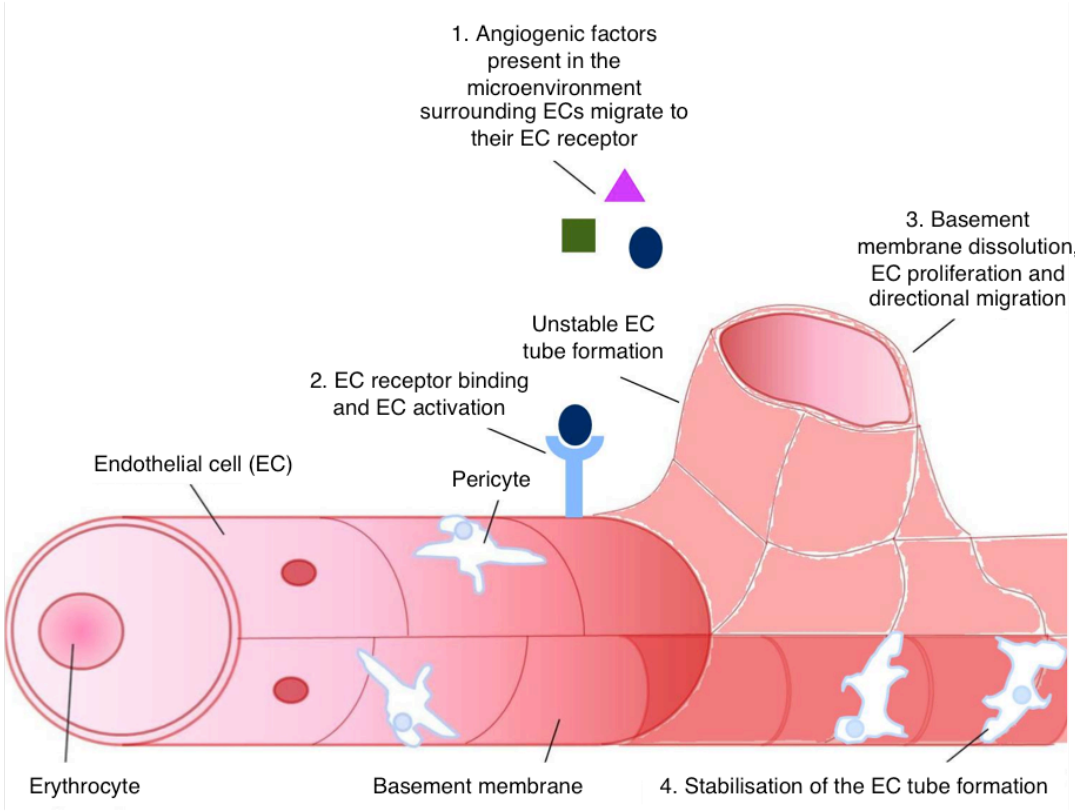

Figure 1.2 Sprouting angiogenesis.
Neovessel growth from a pre-existing blood vessel is stimulated by the presence of angiogenic factors in the microenvironment surrounding endothelial cells (ECs) (1). Upon binding of the growth factor to its cognate receptor on the EC, the cell becomes activated and secretes proteases (2). Degradation of the basement membrane and interstitial matrix creates a space into which the 'tip' EC migrates, followed by proliferating 'stalk' ECs to form an unstable vessel with a lumen (3). ECs secrete extracellular matrix proteins and growth factors in order to reconstruct the basement membrane and recruit pericytes for neovessel stabilisation (4). Diagram modified from (Klagsbrun and Moses, 1999).

The lumen is formed though the anastomoses of two sprouts and neovessel stabilisation, whereby the secretion of extracellular matrix proteins reconstructs the basement membrane, and mural cells such as pericytes are recruited to support the immature vessel (Figure 1.2) (Carmeliet, 2000; Jain, 2003; Fantin *et al.*, 2010). Vessel stabilisation is critical for survival of the vessel; its absence results in rapid apoptosis and as a consequence, vessel regression. This emphasises the equal importance of both the growth and stabilisation phases of sprouting angiogenesis (Benjamin *et al.*, 1998).

1.1.3 The vascular system

The vascular network that is generated as a consequence of vasculogenesis and angiogenesis is the first functional organ to develop during embryogenesis. It is a complex system that is of fundamental importance in all vertebrates as it facilitates the supply of oxygen and nutrients to their organs whilst simultaneously removing metabolic waste products. In addition to this, the vascular system permits the movement of immune cells to sites of infection or inflammation, as well as the rapid transport of endocrine signals to their effector organs (Rossant and Howard, 2002).

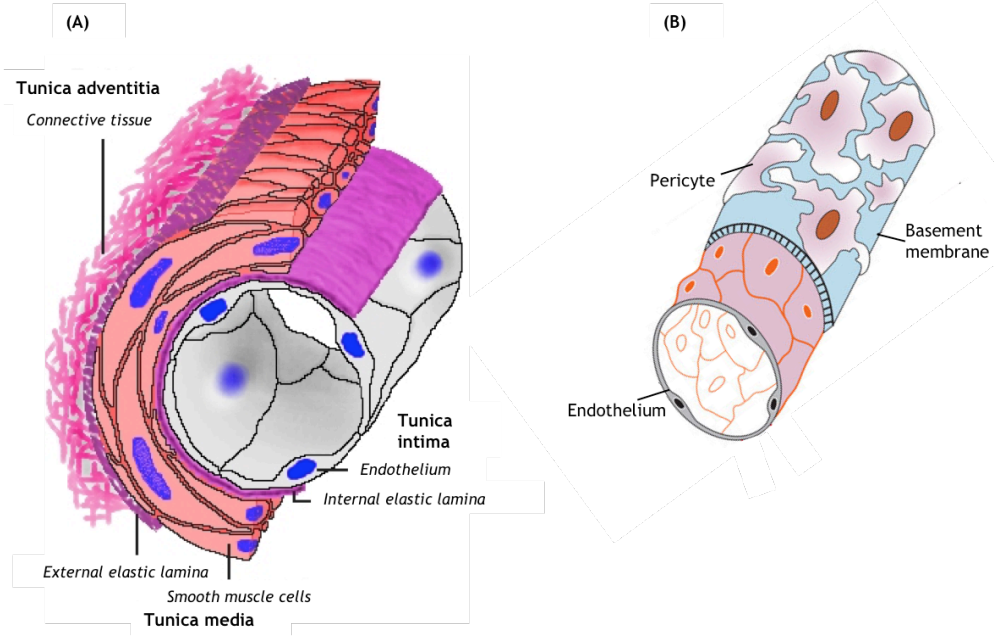

Figure 1.3 Cross-section of blood vessel structure.
Illustration of a large blood vessel such as an artery or vein (A) and a small vessel such as a capillary or arteriole (B). Diagrams adapted from (McGeachie, 2014) and (EducationalForum, 2014).

The cardiovascular system is a highly branched tubular network of blood vessels. The vessel lumens are lined with a monolayer of endothelial cells. Large blood vessels such as arteries and veins have three layers: the outermost layer (*adventitia*) comprises loose connective tissue, smaller blood vessels and nerves, the middle layer (*media*) consisting of multiple sheets of vascular smooth muscle cells, and the inner layer (*intima*) lining the luminal surface with a single layer of macrovascular endothelial cells, which is surrounded by the basement membrane (Figure 1.3). Small blood vessels such as capillaries and arterioles however, are lined by a monolayer of microvascular endothelial cells, encased

in the basement membrane and stabilised by specialised smooth muscle cells known as pericytes (Figure 1.3) (Lafleur *et al.*, 2003; Gallagher and van der Wal, 2006).

Endothelial cells display a significant amount of heterogeneity across the vascular tree; the most apparent difference being their morphology (Aird, 2007). Typically, endothelial cell are flat in structure, however in high endothelial venules they exhibit a cuboidal or plump shape (Kumar *et al.*, 1987; Girard and Springer, 1995; Miyasaka and Tanaka, 2004). In addition to this, endothelial cells from different organs also demonstrate diversity with regards to their function. For example, the basal and inducible permeability of endothelium are differentially regulated (Aird, 2007). The mechanisms of endothelial heterogeneity are mediated by spatial and time differences in the endothelium; blood vessels are located throughout the body, exposing the endothelial cells to a variety of tissue microenvironments (Aird, 2012). Furthermore, the molecular and biochemical properties of endothelial cells differ vastly across the vascular tree (Kumar *et al.*, 1987; Garlanda and Dejana, 1997; Jackson and Nguyen, 1997; Conway and Carmeliet, 2004; Hewett, 2009). Thus, since the majority of the human vasculature (over 95%) is comprised of microvessel endothelium, the use of these cells is more physiologically relevant for *in vitro* models of endothelial cell function and angiogenesis (Hewett, 2009).

1.1.4 Tumour angiogenesis and therapeutic targeting

The strictly coordinated process of physiological angiogenesis as previously described in Section 1.1.2, is critical to normal embryonic development. However, the pathogenesis of numerous diseases has been shown to be associated with dysregulated angiogenesis (Folkman, 1995) and of these pathologies, the role of angiogenesis in tumour development has been of significant interest. Since the 1970s, Folkman et al. have proposed and substantiated the theory that neoangiogenesis was the crux for tumour growth and metastasis (Folkman, 1971; Folkman, 1990; Folkman and Shing, 1992). Today, it is well established that the growth of solid tumours over 1-2 mm^3 requires an adequate blood supply to deliver nutrients and oxygen (Muthukkaruppan *et al.*, 1982), without which tumours can become necrotic or apoptotic (Holmgren *et al.*, 1995). Consequently, tumour angiogenesis has become one of the hallmarks of cancer (Hanahan and Weinberg, 2011).

A hypoxic environment is created by the limited capacity of oxygen to diffuse through the tumour mass (Dor *et al.*, 2001), and in response to this decreased concentration of oxygen, the transcription factor hypoxia-inducible factor-1 alpha (HIF-1α) is upregulated (Semenza, 2007). HIF-1α dimerises with HIF-1 beta (HIF-1ß) and regulates the expression of numerous hypoxia responsive genes, such as VEGFR-1 and VEGF-A (Carmeliet, 2005;

Ferrara, 2009). Additionally, angiostatic factors like endostatin and thrombospondin-1 (TSP-1) are decreased resulting in a phenotypic change referred to as the activation of the 'angiogenic switch' (Kazerounian *et al.*, 2008). This switch remains on, thus enabling and sustaining neoplasia (Hanahan and Folkman, 1996; Carmeliet, 2005).

Although tumour-induced vessels are functionally similar to normal vasculature in that they transport metabolites, they are structurally distinct. Unlike normal vessels, characteristics of tumour vessels include thin leaky walls due to the presence of fenestrae, irregularly-shaped vessels that are convoluted, the absence of a complete basement membrane and vessel immaturity due to a lack of pericyte stabilisation (Carmeliet, 2000; Hashizume *et al.*, 2000; Hellström *et al.*, 2001; Morikawa *et al.*, 2002). In addition to these attributes, endothelial cells derived from neoplasia display differential gene expression to those derived from normal vasculature (Seaman *et al.*, 2007). In particular, high levels of expression of VEGF and its receptors have been observed in a wide variety of human cancers (Plate *et al.*, 1993; Ferrara and Davis-Smyth, 1997; Nishida *et al.*, 2006), hence the rationale to focus on these targets for anti-angiogenic therapies (Holmes *et al.*, 2007; Soltau and Drevs, 2009).

The past decade has led to the introduction of numerous anti-VEGF(R) targeted therapies for a range of different carcinomas. The first U.S. Food and Drug Administration (FDA) approved anti-angiogenic agent was bevacizumab (Avastin®; a recombinant humanised monoclonal antibody against VEGF-A) in 2004, for the treatment of metastatic colorectal cancer (mCRC) in combination with chemotherapeutic agents (Hurwitz *et al.*, 2004). It has since been approved for use in metastatic renal cell carcinomas (mRCC) combined with interferon-alpha (IFN-α) (Escudier *et al.*, 2007b; Rini *et al.*, 2010) and it is suggested that its success is partly due to the normalisation of tumour vasculature, thereby enhancing delivery of chemotherapeutic agents into the tumour mass (Jain, 2005; Kerbel, 2006).

Subsequently, agents targeting receptor tyrosine kinases (RTKs) have been successfully developed; sorafanib (Nexavar®), sunitinib (Sutent®), pazopanib (Votrient®), axitinib (Inlyta®) were FDA approved in 2005, 2006, 2009 and 2012 respectively, for the treatment of various cancers including renal cell carcinoma (RCC), hepatocellular carcinoma and gastro-intestinal stroma tumours (GIST) (Escudier *et al.*, 2007a; Motzer *et al.*, 2007; Sonpavde and Hutson, 2007; Llovet *et al.*, 2008; Sternberg *et al.*, 2010; Rini *et al.*, 2011). The main mode of action for these small-molecule RTK inhibitors is to block the VEGF receptors (VEGFR-1, -2, -3) thereby preventing subsequent activation of the downstream signalling pathways, however they are multi-targeting, acting on receptors such as the

platelet-derived growth factor receptors (PDGFRs), as well as other kinases including Raf and c-kit (Sonpavde and Hutson, 2007; Wilhelm *et al.*, 2008).

Despite the success of these anti-VEGF(R) therapies there are numerous hurdles that are frequently encountered. A major adverse effect of these treatments is hypertension; VEGF causes vasodilation and hypotension (Ku *et al.*, 1993; Henry *et al.*, 2003), which is considered to be mediated by VEGFR-2 stimulation of nitric oxide (Ferrara, 2004). Additional side effects have been observed with the anti-VEGF(R) inhibitors, which are attributed to changes in normal vasculature, in particular endothelial dysfunction and pruning of healthy vessels (Inai *et al.*, 2004; Hayes, 2011). Furthermore, the benefits of these types of treatment are short-lived due to the rapid regrowth of tumour vasculature and consequently tumour growth, upon withdrawal of these therapies (Inai *et al.*, 2004; Mancuso *et al.*, 2006). Resistance to these treatments poses another challenge, as some patients are refractory to these therapies whereas others acquire resistance due to a substantial amount of redundant signalling and compensation mechanisms (Bergers and Hanahan, 2008; Eikesdal and Kalluri, 2009; Weis and Cheresh, 2011). These issues emphasise the importance for new anti-angiogenic targets to be identified and developed. Due to the significant cross-talk of intracellular signalling pathways upon the binding of angiogenic factors to their cognate receptors, rather than focussing efforts to inhibit multiple angiogenic signalling cascades, a more viable strategy of therapeutic inhibition may be to target the activity of intracellular signalling hubs where these pathways converge (Rossant and Howard, 2002; Weis and Cheresh, 2011).

1.2 VEGF/VEGFR-2 signalling in endothelial cells

1.2.1 VEGF

The term VEGF is a description of the family of homodimeric glycoproteins, as well as the prototypic growth factor which was first described as vascular-permeability factor (VPF) by Dvorak and colleagues (Senger *et al.*, 1983). In mammals, there are five structurally related members, VEGF (also designated VEGF-A and VEGF-A_{165}), VEGF-B, VEGF-C, VEGF-D and placenta growth factor (PlGF), with additional homologues such as the parapoxvirus *Orf* virus-encoded VEGF, denoted VEGF-E, and the snake venom VEGF, assigned VEGF-F (Lyttle *et al.*, 1994; Yamazaki *et al.*, 2003).

Furthermore, alternative splicing of the *VEGF-A* gene in humans results in six variants of differing amino acid lengths (denoted as $VEGF_{XXX}$) $VEGF_{121}$, $VEGF_{145}$, $VEGF_{165}$, $VEGF_{183}$, $VEGF_{189}$ and $VEGF_{206}$ (Houck *et al.*, 1991; Tischer *et al.*, 1991; Poltorak *et al.*, 1997; Jingjing *et al.*, 1999). With the exception of $VEGF_{121}$, the other VEGF splice variants contain a heparin-binding domain enabling their binding to cell surface heparan sulphate proteoglycans (HSPGs) and/or the extracellular matrix, as encoded for by exons 6 and 7 of *VEGF* (Tischer *et al.*, 1991; Park *et al.*, 1993). $VEGF_{121}$ lacks both exons 6 and 7 thus does not bind HSPGs, and as such is a freely diffusible acidic protein (Holmes *et al.*, 2007). Additionally, there exists a family of VEGF-A splice variants as a result of alternative splicing of exon 8. These variants are denoted $VEGF_{(XXX)}$b and are able to bind, but are unable to efficiently activate the cognate VEGF receptors, hence are described as anti-angiogenic (Harper and Bates, 2008).

Table 1.1 VEGF isoforms and their ability to bind to different receptors

VEGF Isoform	VEGFR-1	VEGFR-1 / VEGFR-2	VEGFR-2	VEGFR-2 / VEGFR-3	VEGFR-3	NRP1	NRP2
VEGF-A	✓	✓	✓	✓	✗	✓	✓
VEGF-B	✓	✗	✗	✗	✗	✓	✗
VEGF-C	✗	✗	✓	✓	✓	✗	✓
VEGF-D	✗	✗	✓	✓	✓	✗	✗
VEGF-E	✗	✗	✓	✓	✗	✓	✗
PlGf	✓	✓	✗	✗	✗	✓	✓

$VEGF_{165}$ is the most abundant and biologically active isoform in humans and is produced by a variety of cells such as macrophages, vascular smooth muscle cells and tumour cells (Berse *et al.*, 1992). It is secreted as a homodimeric protein, linked by covalent bonds and stabilised by intra- and inter-chain disulphide bonds (Pötgens *et al.*, 1994; Muller *et al.*, 1997). Under normal physiological conditions the expression of VEGF is low, however conditions such as growth factor stimulation (e.g. FGF-2), oxygen tension or an aberration in the pH level, result in increased VEGF levels (Shweiki *et al.*, 1992; Stavri *et al.*, 1995; Carmeliet and Jain, 2000). Furthermore, metabolic regulators and transcription factors such as reactive oxygen species (ROS) and the E26 transformation-specific (ETS) family are able to regulate VEGF expression (Ushio-Fukai and Nakamura, 2008; Randi *et al.*, 2009).

The VEGF family as a whole is essential for normal embryonic development via the processes of vasculogenesis, lymphangiogenesis and angiogenesis, however it is the original growth factor, VEGF-A, that plays a pivotal role (Coultas *et al.*, 2005). It was concurrently observed by two separate groups, that *Vegf*-$a^{-/-}$ and *Vegf*-$a^{+/-}$ heterozygous mice both exhibited fatal defects in vascular development (Carmeliet *et al.*, 1996; Ferrara *et al.*, 1996). The *Vegf*-$a^{-/-}$ mice died at embryonic day 9.5-10.5 (E9.5-10.5) whereas the *Vegf*-$a^{+/-}$ heterozygous mice died at E11.0-12.0 suggesting that embryonic vessel development may in fact be VEGF dose-dependent (Carmeliet *et al.*, 1996; Ferrara *et al.*, 1996; Holmes *et al.*, 2007). This dependence on VEGF was discovered to be essential in the early postnatal life of mice and diminished as the animal matured, eventually being lost after the fourth postnatal week, potentially due to having more stable vessels covered with pericytes (Kitamoto *et al.*, 1997; Gerber *et al.*, 1999). Interestingly, the consequence of a three-fold VEGF overexpression in mice was normal early vascular development, however these embryos later died between E12.5-E14.5, with observations of larger than normal hearts and abnormally thin ventricular walls (Miquerol *et al.*, 2000).

1.2.2 VEGF receptors

The VEGF ligands signal through three structurally related cell surface RTKs, denoted VEGF receptor (VEGFR) -1, -2 and -3, as well as two transmembrane non-tyrosine kinase co-receptors neuropilin (NRP) -1 and -2. The RTKs are expressed in a distinct manner – VEGFR-1 (Flt-1) is expressed on haematopoietic stem cells, macrophages and monocytes, VEGFR-2 (Flk-1/KDR) is expressed on vascular endothelial cells and VEGFR-3 (Flt-4) is expressed on lymphatic endothelial cells – however some overlap does occur with the expression of VEGFR-1 and -2 on other cell types (Holmes *et al.*, 2007; Koch and Claesson-Welsh, 2012). The various VEGF isoforms bind to different receptors, with VEGF-A binding to both VEGFR-1 and -2, whereas VEGF-B and PlGF exclusively bind to VEGFR-1. The pro-peptide forms of VEGF-C and VEGF-D bind to VEGFR-3, however the mature forms of these ligands can bind to VEGFR-2 as well. Finally, the viral VEGF-E ligand solely binds to VEGFR-2. Additionally, the binding of VEGFs to the NRP receptors has been shown to result in a complex with VEGFR-2 thus enhancing VEGFR-2 functionality (Whitaker *et al.*, 2001; Soker *et al.*, 2002; Holmes *et al.*, 2007).

1.2.2.1 VEGFR-1

VEGFR-1 (Flt-1) is expressed on endothelial cells, haematopoietic cells and monocytes, with the ability to bind VEGF-A, -B and PlGF. It has been reported that a splice variant of VEGFR-1 exists; devoid of the transmembrane and internal signalling domains, it is termed soluble VEGR-1 (sVEGFR-1). It is proposed that sVEGFR-1 acts as a decoy receptor to sequester VEGF and negatively regulate VEGFR-2 signalling (Shibuya *et al.*, 1990; Kendall and Thomas, 1993; Roberts *et al.*, 2004). The physiological role of VEGFR-1 was uncovered when it was observed that *Vegfr-1*$^{-/-}$ mice died at E8.5-9.0 due to an overproduction of haemangioblasts, leading to disorganised vasculature (Fong *et al.*, 1995; Fong *et al.*, 1999). Since then it has been demonstrated that in endothelial cells, ligand binding to VEGFR-1 as well as fixation of the extracellular domain of VEGFR-1 via the transmembrane domain, were essential for normal vascular development, whereas downstream signalling of VEGFR-1 was dispensable (Hiratsuka *et al.*, 1998; Hiratsuka *et al.*, 2005). Somewhat more recently it has been proposed that VEGFR-1 may act as a spatial control for VEGFR-2 signalling and branching of angiogenic sprouts by capturing VEGF (Kappas *et al.*, 2008).

1.2.2.2 VEGFR-2

VEGFR-2 is the main VEGF receptor on endothelial cells; 12,400 receptors/cell are reported to be present on human umbilical vein endothelial cells (HUVECs) (Chen *et al.*, 2001a) and 7,300 receptors/cell expressed on human dermal microvascular endothelial

cells (HDMECs) (Imoukhuede and Popel, 2011). Furthermore, a crucial role of VEGFR-2 in vascular development was emphasised when it was observed that VEGFR-2 null-mice died at E8.5-9.5 due to developmental defects of the haematopoietic cells, blood islands and endothelial cells (Shalaby *et al.*, 1995). Thus the high levels of VEGFR-2 expression on endothelial cells, as well as its physiological significance, form the basis of focussing on this receptor in HDMEC.

VEGFR-2, also known as kinase-insert domain receptor (KDR) in humans and foetal liver kinase (Flk)-1 in mice, is a class III transmembrane kinase receptor comprising of 1356 amino acids (Terman *et al.*, 1991). Flk-1 shares 85% sequence homology with KDR, however it is 2 amino acids shorter in length (Holmes *et al.*, 2007). It has been observed that VEGFR-2 exists in two forms, an immature form without significant glycosylation and of 150 kDa molecular weight, as well as a mature glycosylated form of 230 kDa that is expressed on the surface of the cell (Takahashi and Shibuya, 1997).

The extracellular domain of VEGFR-2 is made up of seven Ig-like domains, of which domains 2 and 3 bind VEGF (Figure 1.4) with a K_d of 75-125 pM (Fuh *et al.*, 1998; Shinkai *et al.*, 1998). The binding of VEGF to a VEGFR-2 monomer, induces a second VEGFR-2 monomer to bind to the tethered ligand, holding the two receptors in close proximity to stabilise the dimerisation with additional low-affinity interactions between the Ig-like domains (Ruch *et al.*, 2007; Yang *et al.*, 2010b). Consequently, the intracellular kinase domains of the receptors are correctly positioned for *trans*-autophosphorylation of several tyrosine (Tyr; Y) residues. Studies using mammalian cells that overexpress KDR, established five major phosphorylation sites namely, Y951 within the kinase-insert domain, Y1054 and Y1059 present in the kinase domain, and Y1175 and Y1214 in the carboxyl (C)-terminal tail of the receptor (Figure 1.4) (Takahashi *et al.*, 2001; Matsumoto *et al.*, 2005).

These phosphorylated tyrosine residues create binding sites for specific proteins that contain an Src homology 2 (SH2) domain. VEGF-receptor associated protein (VRAP) also known as T-cell specific adaptor molecule (TSAd) binds to phosphorylated (p-) Y951 (Wu *et al.*, 2000b; Matsumoto *et al.*, 2005), whereas p-Y1214 is the binding site for the adaptor protein Nck (non-catalytic region of tyrosine kinase adaptor protein 1) (Lamalice *et al.*, 2006). Phosphorylated Y1175 provides a docking site for numerous signalling molecules, including SH2-containing (Shc)-like protein (Sck), phospholipase C-gamma (PLC-γ) and SH2 protein B (Shb), (Cunningham *et al.*, 1997; Warner *et al.*, 2000; Takahashi *et al.*, 2001; Holmqvist *et al.*, 2004).

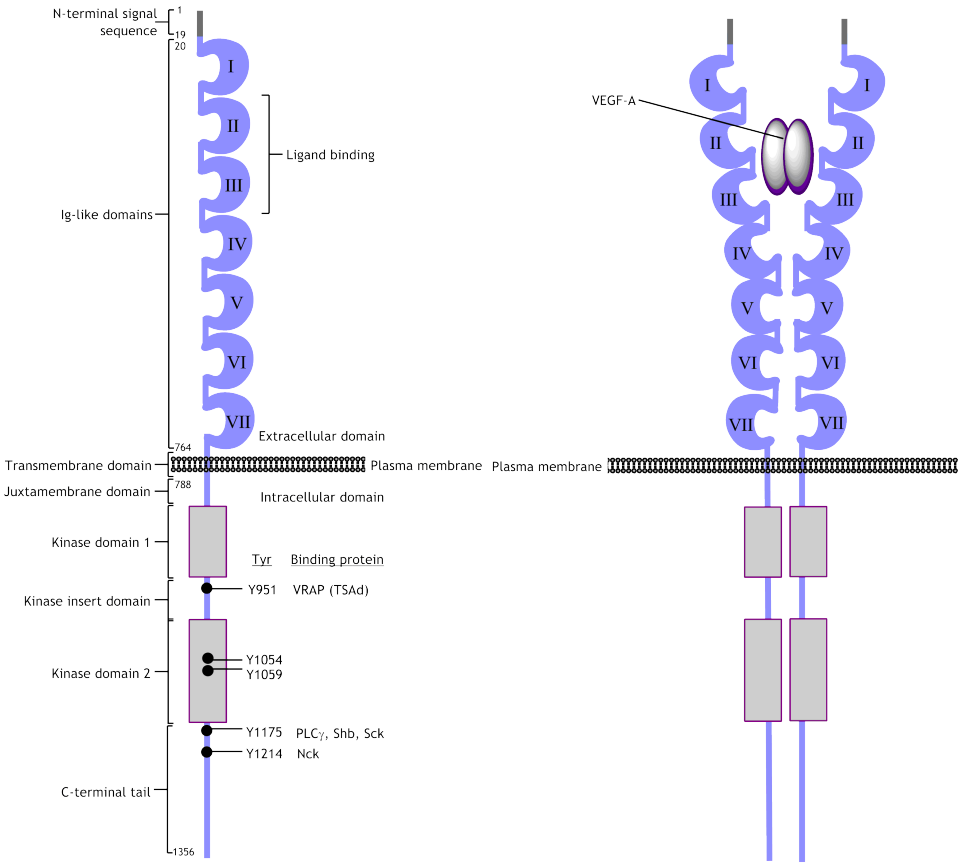

Figure 1.4 VEGFR-2 structure, tyrosine phosphorylation sites and dimerisation.
VEGFR-2 is a class III receptor tyrosine kinase composed of 1356 amino acids. There exist seven Ig-like domains (I-VII) on the extracellular domain, of which the domains II and III bind the ligand, VEGF-A. The intracellular domain comprises of two kinase domains, separated by a kinase insert domain. The five major phosphorylation sites identified, Y951, Y1054, Y1059, Y1175 and Y1214, along with their various binding proteins for downstream signalling, are highlighted. Figure adapted from (Holmes *et al.*, 2007).

1.2.2.3 VEGFR-3

VEGFR-3 (Flt-4) is expressed on all endothelial cells during development, however its expression is restricted to lymphatic endothelial cells in adults (Olsson *et al.*, 2006; Lohela *et al.*, 2009). VEGFR-3 is only able to bind VEGF-C and –D, and gene targeting studies have shown that it is *Vegfc* that is vital for sprouting lymphangiogenesis (Karkkainen *et al.*, 2002; Karkkainen *et al.*, 2004). The physiological role of VEGFR-3 was revealed upon *Flt-4* ablation in mice, which proved embryonically lethal at E9.5. *Flt-4*$^{-/-}$ embryos were observed to have an accumulation of fluid in the pericardium cause by leaky vasculature, prior to the onset of lymphangiogenesis (Dumont *et al.*, 1998).

1.2.2.4 VEGF co-receptors: NRP-1 and NRP-2

The transmembrane glycoproteins NRP-1 and NRP-2 are additional receptors for VEGF. NRPs are class III semaphorins with a conserved primary structure divided into four domains: CUB (a1/a2), FV/FVIII (b1/b2), MAM (c) and domain (d) comprising of a transmembranous and short cytoplasmic region (Figure 1.5a) (Parker *et al.*, 2012; Kumanogoh and Kikutani, 2013). The NRPs require an additional transmembrane molecule to exhibit kinase activity and in the case of VEGF binding, the co-receptor is a VEGF receptor (Figure 1.5b). Furthermore, NRPs are able to act as an isoform specific co-receptor for VEGF as they require the presence of exon 7 of the VEGF molecule, thus NRPs are able to bind $VEGF_{165}$, but not $VEGF_{121}$ (Neufeld *et al.*, 2002). The expression of NRP-1 is restricted to the heart vasculature wherein it functions as a co-receptor with VEGFR-2 (Soker *et al.*, 1998; Whitaker *et al.*, 2001). Rather interestingly, the VEGFR-2/NRP-1 heterodimer binds $VEGF_{165}$ with a four-fold greater affinity than the VEGFR-2 homodimer, and as a consequence, it has been shown to enhance VEGF-induced endothelial cell proliferation and migration (Soker *et al.*, 1998; Soker *et al.*, 2002). NRP-1 has been shown to be vital for normal vascular development, as global *Nrp-1*$^{-/-}$ mouse embryos die at E14.0 presenting with cardiovascular defects (Kawasaki *et al.*, 1999), and endothelial-specific *Nrp-1* deletion leads to vascular abnormalities (Gu *et al.*, 2003). NRP-2 plays an important role in lymphatic vessel development; *Nrp-2*$^{-/-}$ mice are viable but display decreased lymphatic growth (Yuan *et al.*, 2002). NRP-2 has also been observed to act as a co-receptor with VEGFR-2 and VEGFR-3 in endothelial cells, thereby enhancing VEGF-stimulated proliferation and migration (Favier *et al.*, 2006).

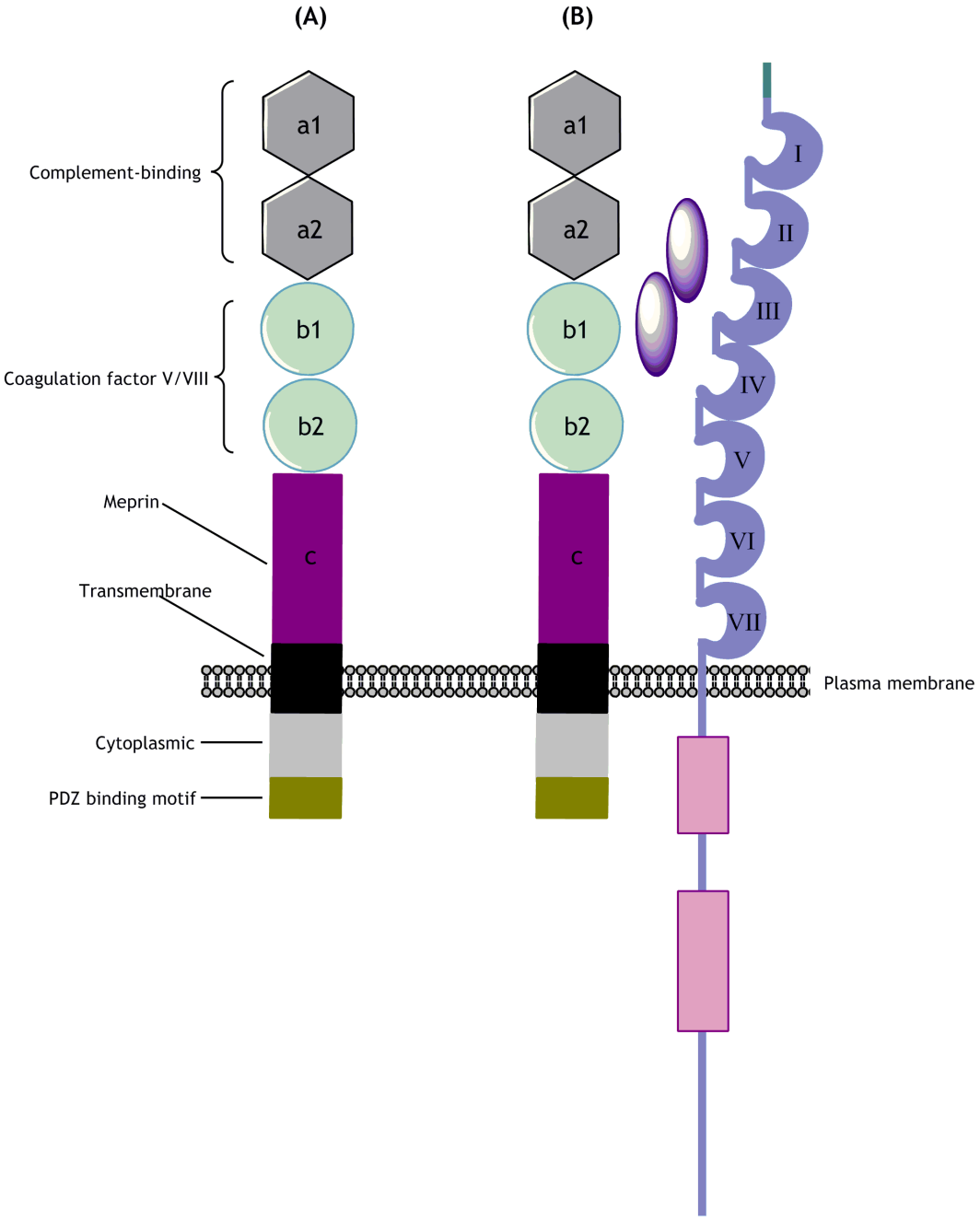

Figure 1.5 Primary structure of Neuropilins and their binding with VEGFRs.
(A) The NRPs consist of four domains, two repeats (a1/a2) of the CUB (complement C1r/C1s, Uegf, Bmp1) domain at the N-terminal, which are followed by two repeats (b1/b2) of the FV/FVIII (coagulation factor 5/8) domain, the MAM (Meprin, A-5 protein and receptor protein-tyrosine phosphatase μ) and a transmembrane/cytoplasmic region. NRP1 has an additional PDZ binding motif at the C-terminal. **(B)** A VEGF isoform containing exon 7 e.g. $VEGF_{165}$, binds to the FV/FVIII domain of NRP1 and domains II and III of VEGFR.

1.2.3 Intracellular VEGFR-2 signalling and the regulation of endothelial cell physiology

The propagation of the signal induced by VEGF-stimulated activation of VEGFR-2, confers a multitude of diverse functions in endothelial cells including proliferation, survival, migration, differentiation, transcriptional activation and permeability (Zachary, 2003; Holmes *et al.*, 2007). Various intracellular signalling pathways downstream of VEGFR-2 mediate these functions however only those implicated in cell proliferation and survival will be elaborated upon.

1.2.3.1 PLC-γ-mediated proliferation in endothelial cells

VEGFR-2 has a unique pathway through which it induces proliferation; it does not activate the extracellular signal-regulated kinases (ERKs, also known as mitogen-activated protein kinases or MAPKs) via the classical growth factor receptor-bound protein 2 (Grb2)-son of sevenless (Sos)-rat sarcoma (Ras) pathway, instead via PLC-γ activation and subsequently the protein kinase C (PKC) pathway (Takahashi *et al.*, 2001).

As previously mentioned in Section 1.2.2.2 p-Y1175 provides a docking site for PLC-γ, which in turn is phosphorylated prior to hydrolysing the membrane phospholipid, phosphatidylinositol (4,5)-bisphosphate (PIP_2), into inositol 1,4,5-trisphosphate (IP_3) and diacylglycerol (DAG) (Wu *et al.*, 2000a). The production of IP_3 increases the concentration of intracellular calcium whereas DAG activates PKC. Thus, various PKC isoforms have been associated with VEGF-mediated proliferation, including PKC-α, -ß, and –ζ (Xia *et al.*, 1996; Takahashi *et al.*, 1999; Wellner *et al.*, 1999).

Classically, the proliferation-inducing ERK1/2 pathway is activated by Ras, however the specific mechanism through which Ras is implicated in VEGFR-2 mediated signalling remains unclear. Initial studies suggested VEGF-stimulation of Ras occurred via a PKC and sphingosine kinase pathway in HUVECs (Meadows *et al.*, 2001; Shu *et al.*, 2002), however it remains possible that an unidentified adaptor molecule may be involved in coupling VEGFR-2 to the GrbB2-Sos-Ras pathway, as Ras hyperactivation has been shown to induce a pro-angiogenic phenotype (Meadows *et al.*, 2004; Bajaj *et al.*, 2010).

The significance of PLC-γ in angiogenesis was revealed with the use of *PLC-γ1* deficient mice embryos; a considerable decrease in vasculogenesis and erythropoiesis occurred resulting in death at E9.0 (Ji *et al.*, 1997; Liao *et al.*, 2002). In addition to this, it was observed that the VEGF/VEGFR-2/PLC-γ1 axis is required for arterial development, as *PLC-γ1* deficient zebrafish embryos did not respond to exogenous VEGF (Lawson *et al.*, 2003).

Furthermore, after initial observations revealing the importance of Y1173 in Flk-1 (Y1175 in KDR) (Takahashi *et al.*, 2001), later studies utilised mice with a Y1173F mutation (F represents phenylalanine) knock-in to emphasise these findings; defects in the endothelial and haematopoietic cells resulted in embryonic lethality at E8.5-9.5 similar to Flk-1 null mice (Shalaby *et al.*, 1995; Sakurai *et al.*, 2005). However, whether this is a consequence of a lack of PLC-γ activation and subsequently the ERK1/2 cascade, is unclear as Shb and Sck also bind to this residue (Warner *et al.*, 2000; Holmqvist *et al.*, 2004). It may be that PLC-γ activation regulates the function of proliferation in angiogenesis, whereas Shb and Sck binding to Y1173 may mediate other critical functions of angiogenesis. Studies have shown that *Shb* deficient mice exhibit dysfunctional microvasculature with a decrease in VEGF-induced vascular permeability and increased density of the arterioles as well as a reduced number of microvasculature branch points, possibly due to decreased levels of VE-cadherin (Funa *et al.*, 2009; Christoffersson *et al.*, 2012; Zang *et al.*, 2013). The phenotypic analysis of *Sck* deficient mice has yet to be determined.

1.2.3.2 PI3K/AKT-induced survival of endothelial cells

Phosphotidylinositide 3'-kinases (phosphoinositide 3' kinases or PI3Ks) are a family of related phosphate kinases capable of catalysing the phosphorylation of the 3-position hydroxyl group on the inositol ring of plasma membrane-associated phosphoinositides. Activation of PI3K occurs upon growth factor stimulation and generates membrane-bound phosphatidylinositol-3,4,5-trisphosphate (PIP_3) as a result of PIP_2 phosphorylation. As a consequence, the phosphoinositide-dependent kinases 1 and 2 (PDK1 and PDK2) are recruited to membrane-bound PIP_3 which subsequently phosphorylate the serine/threonine kinase protein kinase B (PKB/AKT) (Anderson *et al.*, 1998; Cantley, 2002). The binding of PDK1 and AKT to PIP_3 via their pleckstrin-homology (PH)-domains enables PDK1 to phosphorylate AKT on Thr^{308} in its catalytic domain (Alessi *et al.*, 1997; Stokoe *et al.*, 1997). Additionally, full AKT activity is obtained upon phosphorylation of Ser^{473} situated on the regulatory C-terminal, which is thought to occur via autophosphorylation as well as phosphorylation by other kinases (Coffer *et al.*, 1998; Lawlor and Alessi, 2001). Numerous potential kinases were reported to have PDK2 capabilities in phosphorylating AKT on Ser^{473}, however it is mammalian target of rapamycin (mTOR)-complex 2 (mTORC2) that has been best characterised in this role (Dong and Liu, 2005; Sarbassov *et al.*, 2005; Huang and Manning, 2009). In contrast, phosphatase and tensin homologue deleted on chromosome 10 (PTEN) antagonises the PI3K/AKT pathway; loss of *PTEN* results in hyperactive PI3K signalling, leading to various cancers, thus it is one of the most important tumour suppressor genes (Suzuki *et al.*, 2007; Salmena *et al.*, 2008; Omerovic *et al.*, 2010).

One of the most studied physiological consequences of the PI3K/AKT signalling pathway is cell survival, through phosphorylation and inhibition of pro-apoptotic proteins such as Bcl-2 associated death promoter (BAD), caspase 9 and the Forkhead family of transcription factors (Datta *et al.*, 1997; Cardone *et al.*, 1998; Brunet *et al.*, 1999). Additionally, it was shown that VEGF-mediated survival of HUVEC was dependent upon the VEGFR-2/PI3K/AKT axis (Gerber *et al.*, 1998). Many potential mechanisms have been proposed to elucidate this mechanism, the first of which was that Shb binding to p-Y1175 may play a role (Holmqvist *et al.*, 2004). Furthermore, the scaffold adaptor protein Grb2-associated binder-1 (Gab1) was initially observed to couple VEGFR-2 to PI3K/AKT via the p85 regulatory subunit of PI3K, thereby activating PI3K (Dance *et al.*, 2006), whereas Blanes et al. observed that autophosphorylation of Y801 on VEGFR-2 enabled direct binding of the p85 subunit of PI3K to induce its activation (Blanes *et al.*, 2007). However, evidence has since been provided to show that Y801F/Y1214F mutations on VEGFR-2 inhibited Gab1 phosphorylation, consequently impairing AKT activation in response to VEGF stimulation (Caron *et al.*, 2009). In support of this, a more recent computational study recapitulated the finding that Gab1 knockdown decreased AKT phosphorylation (Tan *et al.*, 2013). Thus the specific mechanism through which VEGF-mediated PI3K/AKT activation occurs still remains unclear.

1.3 Epidermal Growth Factor Receptor (EGFR) signalling

1.3.1 Epidermal Growth Factor (EGF)

In 1951 it was discovered that mouse tumours grafted onto chick embryos secreted a soluble, diffusible factor, which was able to stimulate the growth of nerve cells, thus termed nerve growth factor (NGF) (Levi-Montalcini and Hamburger, 1951). Purification of this crude NGF extract serendipitously revealed an additional growth factor that stimulated proliferation and keratinisation of epidermal cells, and was consequently termed epidermal growth factor (EGF) (Cohen and Levi-Montalcini, 1957; Cohen and Elliot, 1963). Subsequent studies revealed a homologous human EGF polypeptide isolated from human urine (Cohen and Carpenter, 1975; Starkey *et al.*, 1975). It was later discovered that urogastrone, a compound found in human urine that inhibits gastric acid secretion, was almost identical to EGF thus suggesting a potential new role for the growth factor (Gregory, 1975).

There are numerous other proteins that are structurally and functionally similar to EGF known as the EGF-like molecules including heparin-binding EGF-like growth factor (HB-EGF), transforming growth factor-α (TGF-α), amphiregulin (AR), epiregulin (EPR), and epigen, amongst others (Shoyab *et al.*, 1988; Massague, 1990; Higashiyama *et al.*, 1992; Toyoda *et al.*, 1995; Strachan *et al.*, 2001; Harris *et al.*, 2003). The mature forms of these growth factors are characterised by a conserved consensus sequence wherein 6 cysteine (cys; C) residues are spaced as follows: $CX_7CX_{4-5}CX_{10-13}CXCX_8GXRC$ (G represents glycine, R is arginine and X represents any amino acid) and form three intramolecular disulphide bonds (Harris *et al.*, 2003). The consensus sequence, known as the EGF motif, is essential for ligand binding to the family of EGF receptors.

1.3.2 EGF receptors

The EGF receptors (EGFRs), also known as the ErbB (derived from erythroblastic leukemia viral gene, to which these receptors are homologous) receptors, are similar to the VEGFRs in that they are transmembrane RTKs. In humans there are four structurally related members of the EGFR family: the original RTK ErbB1 (Her1, or EGFR-1 as it is referred to hereinafter), ErbB2 (Her2 in humans/Neu in rodents), ErbB3 (Her3) and ErbB4 (Her4) (Yarden and Sliwkowski, 2001).

EGF and the EGF-like molecules can bind to the various receptors to result in homo- or hetero-oligomers with differing downstream signalling properties, however it is the ubiquitously expressed and prototypic EGFR-1 that will be discussed further.

1.3.2.1 EGFR-1

EGFR-1 is a glycoprotein of 170 kDa, comprising an extracellular receptor domain, a single membrane-spanning region as well as an intracellular tyrosine kinase domain (TKD) (Figure 1.6) (Yarden and Sliwkowski, 2001). The extracellular region consists of four domains (I-IV), of which domains I and III are leucine-rich repeat (LRR)-like and II and IV are cysteine-rich. Prior to ligand binding, EGFR-1 exists in a tethered conformation, whereby intramolecular interactions between domains II and IV prevent dimerisation and activation (Ferguson *et al.*, 2003). High-affinity EGF binding to EGFR-1 disrupts these intramolecular interactions, causing a conformational change to the extracellular region and subsequently revealing a previously concealed dimerisation arm in domain II. This dimerisation arm enables an intermolecular interaction with a second ligand-bound/activated receptor (Figure 1.6) (Ferguson *et al.*, 2003; Dawson *et al.*, 2005).

Unlike VEGFR-2, dimerised EGFR does not undergo *trans*-phosphorylation of tyrosine residues present on the cytoplasmic kinase domains. Instead, the intracellular TKDs form an asymmetric dimer whereby the C-lobe of one TKD acts as an "activator" and interacts with the N-lobe of the second TKD, called the "receiver" (Zhang *et al.*, 2006) (Figure 1.6). This allosteric mechanism results in disruption of the monomeric *cis*-autoinhibitory interactions, enabling the "receiver" kinase to assume the active configuration with activation loop phosphorylation (Zhang *et al.*, 2006).

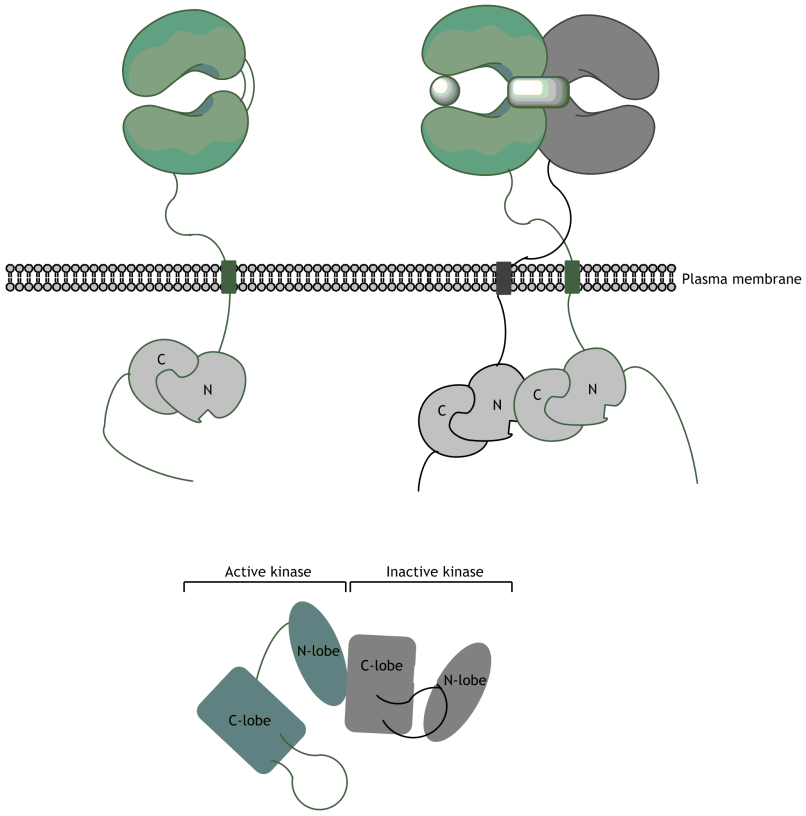

Figure 1.6 EGFR-1 structure, dimerisation and activation.
EGFR-1 undergoes a structural change upon ligand binding and results in the activation of the intracellular kinase domain. The binding of ligands, such as EGF, leads to the exposure of a binding arm unique to EGFR-1, which facilitates dimerisation. The intracellular domains form an asymmetric dimer, whereby one receptor acts as an "activator" and the other as a "receiver". Contact between the two receptors results in a conformational change in the N-lobe of the receiver receptor, consequently disrupting auto-inhibitory interactions present in the monomer. Figure adapted from (Lemmon and Schlessinger, 2010).

1.3.3 Downstream EGFR-1 signalling

EGFR-1 is able to form heterodimers with other members of the ErbB family, preferentially ErbB2, thus it is difficult to unambiguously ascertain substrates of EGFR-1. Phosphorylation of the cytoplasmic kinase domains of EGFR-1 presents specific docking sites for the SH2 or phosphotyrosine-binding (PTB) domains of various scaffold/adaptor proteins. Recruitment and subsequent activation of these adaptor proteins in turn activate a multitude of downstream substrates, thereby forming a complex, interlinked signalling network, however it is the two canonical signalling pathways, Ras>ERK1/2 and PI3K/AKT, that will be discussed in more depth.

1.3.3.1 Grb2, Shc and the Ras>ERK1/2 pathway

Two proteins that play major roles in relaying EGF-induced EGFR signalling to activate the Ras/MAPK pathway are Grb2 and Shc (Lowenstein *et al.*, 1992). Grb2 is found to have a cytosolic localisation and is constitutively bound to the Ras exchange factor, Sos. The SH2 domain of Grb2 is able to bind to EGFR upon activation and phosphorylation of the kinase and there are reports of direct Grb2-EGFR association at residues Y1068 and Y1086 of the receptor (Batzer *et al.*, 1994). Additionally, an indirect association of Grb2 and EGFR has been suggested through the binding of Shc to EGFR via its PTB domain, resulting in its tyrosine phosphorylation and consequent recruitment of the Grb2-Sos complex (Sasaoka *et al.*, 1994). This latter mode of recruitment is proposed to play a dominant role in EGF-stimulated Ras signalling (Sakaguchi *et al.*, 1998), however findings contrary to this were observed in a different cellular system, whereby Ras activation was not affected by the loss of Shc (Hashimoto *et al.*, 1999). The co-existence of these two pathways may be in order to perform different functional roles, or that cell-type specificity requires the dominance of one over the other. Nevertheless, the translocation of the Grb2-Sos complex to membrane-bound Ras assists the Ras-Sos interaction whereby Ras-bound GDP is exchanged for GTP, resulting in Ras activation, which subsequently activates the serine/threonine kinase, Raf-1 (Hallberg *et al.*, 1994). A cascade of intermediate kinases enables Raf-1 to activate ERK1 and ERK2 via phosphorylation, leading to their nuclear translocation wherein transcription factors are phosphorylated (Johnson and Vaillancourt, 1994). Furthermore, the Grb2-Sos complex undergoes dissociation due to ERK1/2 phosphorylation of Sos, thereby acting as an inherent negative feedback loop (Langlois *et al.*, 1995).

1.3.3.2 Gab1 and the PI3K/AKT activation

Initial studies suggested that phosphorylation of EGFR could result in a direct association between the p85 regulatory subunit of PI3K and EGFR as a consequence of Src-induced phosphorylation of residue Y920 on the receptor (Stover *et al.*, 1995). However it has since been reported that this interaction may in fact be due to EGFR/ErbB3 heterodimerisation, as the latter contains the required pYXXM motifs in order to bind the SH2 domains of the p85 subunit (Mattoon *et al.*, 2004). Thus it has been established that EGF induction of the PI3K/AKT pathway occurring via EGFR homodimerisation, must occur through an indirect association mediated by the docking protein Gab1.

It was observed that EGF stimulation of cells resulted in the tyrosine phosphorylation of Gab1, which facilitated the recruitment, binding (of the SH2 domains of the p85 regulatory subunit) and subsequent activation of PI3K (Holgado-Madruga *et al.*, 1996; Mattoon *et al.*, 2004). Furthermore, *Gab1* null mice presented significantly lower levels of PI3K activity, emphasising the importance of this adaptor protein in propagating the EGF/EGFR signal (Mattoon *et al.*, 2004).

1.3.4 EGFR-1 and carcinogenesis

EGFR-1 activation usually leads to cellular growth, however its aberrant signalling plays a pivotal role in the onset and progression of numerous types of cancer (Salomon *et al.*, 1995; Normanno *et al.*, 2001). Studies have shown that overexpression of EGFR-1, and the EGF-like peptides, can induce the neoplastic transformation of various cell types (Rosenthal *et al.*, 1986; Watanabe *et al.*, 1987; Di Marco *et al.*, 1989; Shankar *et al.*, 1989; Ciardiello *et al.*, 1990). More recently it has been demonstrated that EGFR-1 overexpression can be induced by the hypoxic microenvironment of tumours as a result of increased EGFR-1 mRNA translation (Franovic *et al.*, 2007), however it must also be noted that EGFR overexpression in the absence of gene amplification has also been observed (Salomon *et al.*, 1995; Normanno *et al.*, 2003).

The involvement of EGFR-1 in carcinogenesis increases in complexity however, the receptor is able to form heterodimers with other members of the EGF family of receptors, namely ErbB-2, -3 and -4 (Yarden and Sliwkowski, 2001). Furthermore, mutations in the TKD of EGFRs have been discovered in patients with various types of cancer, which has facilitated the selection of the correct cohort of patients likely to respond to anti-EGFR agents (Normanno *et al.*, 2006). Nevertheless, the integrated system through which an extracellular signal can be transmitted via other receptors, leads to the amplification and diversification of the signal (Normanno *et al.*, 2006). Consequently, a multitude of cellular

functions required for tumour development are regulated by these receptors, including angiogenesis, differentiation, growth and survival (Salomon *et al.*, 1995; Normanno *et al.*, 2006).

1.4 MAPK signalling

1.4.1 MAPK modules: organisation, activation and physiological role

The MAPKs are highly conserved enzymes expressed in all eukaryotic cells that are able to mediate a multitude of intracellular processes. A three-tiered hierarchical MAPK module exists, whereby the apical kinase, termed the MAPK kinase kinase (MAPKKK; MAPK/ERK kinase kinase; MEKK), first responds to extracellular stimuli such as growth factors, oxidative stresses and other stimuli (Boulton *et al.*, 1991; Widmann *et al.*, 1999) (Figure 1.7). The MAPKKK phosphorylates its downstream target, the dual-specificity MAPK kinase (MAPKK; MAPK/ERK kinase; MEK) on specific serine (Ser; S) and threonine (Thr; T) residues, which in turn phosphorylates the threonine and tyrosine (Tyr; Y) residues of the conserved T-X-Y motif present within the activation loop of the terminal MAPK (Widmann *et al.*, 1999; Zhang and Dong, 2007) (Figure 1.7). This sequential cascade enables phosphorylation and activation of the final MAPKs downstream effector proteins to generate a specific intracellular response (Lewis *et al.*, 1998; Yang *et al.*, 2003a; Yoon and Seger, 2006). These effector proteins include transcription factors, structural proteins, cytoplasmic enzymes and phospholipids (Chang and Karin, 2001), to regulate a variety of normal cellular function such as cell proliferation, differentiation, migration, survival and death (Yang *et al.*, 2003a; Qi and Elion, 2005).

As with most intracellular signalling pathways, MAPK signalling is also relatively complex and diverse; each MAPKK can be phosphorylated by more than one MAPKKK (Chang and Karin, 2001). Furthermore, there exists a cross-talk between the MAPKs to regulate critical functions, however the specificity of signal transfer to MAPKs is maintained by scaffold proteins and distinct docking interactions between individual components of each MAPK cascade (Whitmarsh and Davis, 1998; van Drogen and Peter, 2002; Morrison and Davis, 2003). Consequently, an efficient signal transfer produces the required cellular response (Tanoue and Nishida, 2003; Raman *et al.*, 2007).

Mammalian cells contain four distinct, classical MAPK cascades: extracellular signal-regulated kinases (ERK) 1/2, c-Jun NH_2-terminal kinases (JNK) 1/2/3, p38 proteins α/β/γ/δ and ERK5 (Nishida and Gotoh, 1993; Abe *et al.*, 1996; Robinson and Cobb, 1997; Chang and Karin, 2001). Dual-phosphorylation of the Thr and Tyr residues within a T-X-Y motif in the activation loop of the kinase domain of the terminal MAPK results in its activation (X represents glutamic acid, proline, or glycine in the ERK, JNK and p38 subfamilies respectively (Widmann *et al.*, 1999)). ERK5 is the most recently identified MAPK and has been associated with a multitude of cellular processes including cellular proliferation, migration, survival and angiogenesis.

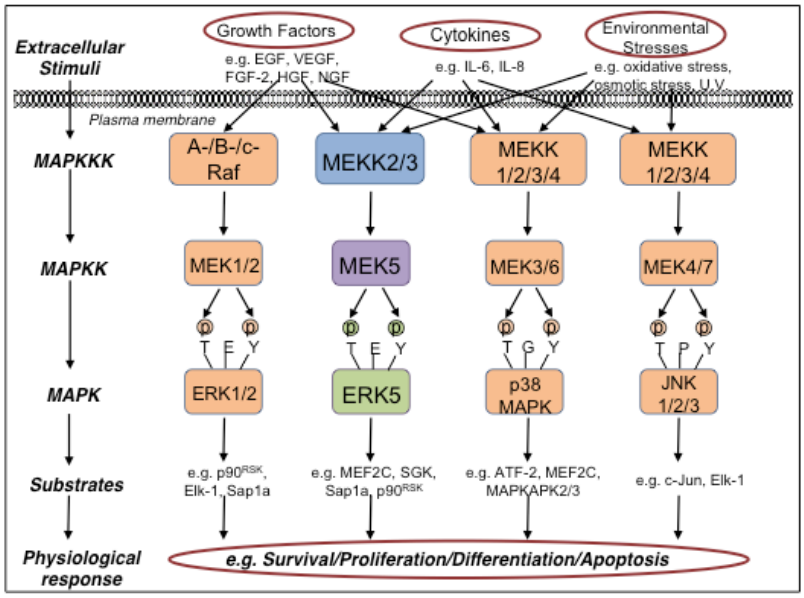

Figure 1.7 Mitogen-activated protein kinase (MAPK) signalling cascades in mammalian cells.
The four distinct MAPK cascades namely ERK1/2, ERK5, p38 MAPKs (α,β,γ,δ) and JNK 1/2/3, are arranged into a hierarchal three-tier system known as a MAPK module. Mitogens such as cytokines or growth factors, environmental stresses including oxidative or osmotic stress, as well as other extracellular stimuli, act via specific receptors to stimulate the MAPK cascade activation. The response begins with phosphorylation of an apical MAPKKK (or MEKK), activation of which sequentially phosphorylates and concomitantly activates the downstream MAPKK (or MEK). The MAPKK in turn dual-phosphorylates (denoted by a circled **P**) specific threonine (T) and tyrosine (Y) residues of the conserved T-X-Y motif present within the kinase domain, where X is glutamic acid (E) in ERK1/2 and ERK5; glycine (G) in p38 MAPKs and proline (P) in JNKs, to activate the terminal MAPK. A variety of downstream cytosolic or nuclear substrates, including other protein kinases such as p90RSK/SGK and transcription factors (MEF2C, Elk-1, Sap1a) are phosphorylated by the MAPKs to elicit a range of transcriptional or non-transcriptional changes that result in specific cellular responses e.g. cellular proliferation/differentiation, sustained cellular survival of the initiation of cell death by apoptosis.

1.4.2 Extracellular signal-regulated kinase 5 – ERK5

1.4.2.1 Discovery of ERK5

Nearly two decades ago, two independent research groups simultaneously cloned ERK5. Zhou et al. utilised a yeast two-hybrid screen, initially identifying the upstream MEK5 and consequently discovering a novel binding partner, ERK5 (Zhou *et al.*, 1995). The second group, Lee and colleagues, screened a human placenta cDNA library using degenerate PCR to identify a novel MAPK gene; they termed this big MAPK (BMK)-1 due to its large size relative to ERK1/2 (Lee *et al.*, 1995). ERK5 and BMK1 were later found to be identical. Both research groups demonstrated that ERK5 was ubiquitously expressed, but particularly abundant in the heart, skeletal muscle, placenta, lungs and kidneys (Lee *et al.*, 1995; Zhou *et al.*, 1995). Furthermore, it has since been documented that ERK5 is universally expressed in various different cell lines and is localised in both nuclear and cytoplasmic compartments (Buschbeck and Ullrich, 2005).

1.4.2.2 Structure of ERK5

The human *ERK5* gene (also called *MAPK7*) is 5,824 bases in length, with an open reading frame of 2451 bp and encodes for a protein of 816 amino acids (Figure 1.8). There are four alternatively spliced transcript variants, which encode for two isoforms of ERK5. Variants 1, 3 and 4 (also known as BMK1-α, -γ and -ß respectively) all encode for the longer isoform (isoform 1). BMK1-α is the prototypic transcript from which BMK-γ and -ß have a differing 5' untranslated region (UTR). Transcript variant 2 is deficient of a 5' segment that includes the translation start codon, thus resulting in an N-terminal truncated isoform (isoform 2) at which transcription occurs at an in-frame start codon further downstream (NCBI, 2014).

The N-terminus of isoform 1 (amino acids 1-406) begins with a region required for cytoplasmic targeting (a.a. 1-77), followed by the kinase domain (a.a. 78-406) which shares 66% sequence identity to the kinase domain of ERK2 (Zhou *et al.*, 1995) (Figure 1.8). The kinase domain can be further separated into a region essential for MEK5 interaction (a.a. 78-139) and for oligomerisation (a.a. 140-406) (Yan *et al.*, 2001) (Figure 1.8). The dual-phosphorylation T-E-Y motif at which MEK5 is able to dual-phosphorylate ERK5, is positioned at a.a. 218-220. It is important to note that this numbering is historical, as an updated sequence situates these residues at a.a. 219-221. However, in line with the majority of published studies and commercially produced antibodies, this project will refer to these activation loop residues as Thr^{218}/Tyr^{220}.

ERK5 contains a common docking (CD) domain, similar to other MAPKs, consisting of a short sequence of negatively-charged amino acid residues (a.a. 350-358) (Figure 1.8), thereby allowing ERK5 to form associations with certain docking (D)-domain-containing substrates (Tanoue and Nishida, 2002).

ERK5 is unique to the MAPK family as it contains an extended C-terminal tail of 410 amino acids (Figure 1.8), giving it a molecular weight of approximately 102kDa, consequently making it more than twice the molecular weight of many other MAPKs (Zhou *et al.*, 1995).

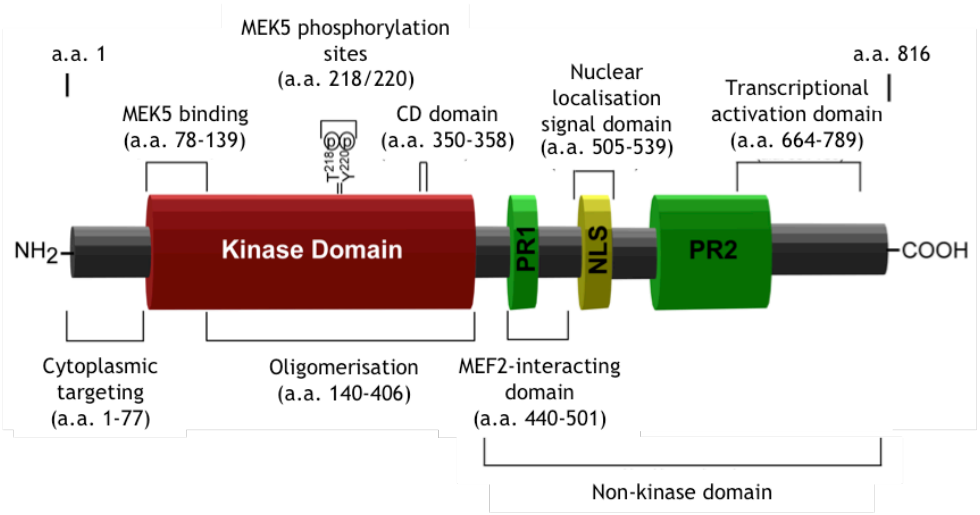

Figure 1.8 Structure of ERK5 and functional domains.
ERK5 consists of 816 amino acid (a.a.) residues, with an N-terminal kinase domain and a large C-terminal tail of approximately 400 a.a. The N-terminus contains a region for cytoplasmic targeting (a.a. 1-77), before the kinase domain (a.a. 78-406), which is comprised of a MEK5 binding region (a.a. 78-139), a common docking (CD) domain (a.a. 350-358) and the oligomerisation region, which spans over a.a. 140-406. It is within the kinase domain of ERK5 that the residues (Thr^{218}/Tyr^{220}), which are phosphorylated by MEK5, exist. The extended C-terminal tail contains two Proline-rich (PR) domains – PR1 (a.a. 434-465) and PR2 (a.a. 578-701) – a MEF2-interacting region (a.a. 440-501), the nuclear localisation signal (NLS) domain (a.a. 505-539) and a transcriptional activation domain (a.a. 664-789).

Within this C-terminal domain exists a nuclear localisation signal (NLS) domain (a.a. 505-539) important for ERK5 nuclear targeting (Yan *et al.*, 2001; Buschbeck and Ullrich, 2005) (Figure 1.8), two proline-rich (PR) domains termed PR1 (a.a. 434-465) and PR2 (a.a. 578-701) which are considered to be potential binding sites for Src-homology 3 (SH3)-domain-containing proteins (Zhou *et al.*, 1995; Yan *et al.*, 2001) (Figure 1.8) and a myocyte enhancer factor 2 (MEF2)-interacting region (a.a. 440-501) (Yan *et al.*, 2001). Recently, a potent transcriptional activation domain (a.a. 664-789) (Figure 1.8) was identified (Kasler

et al., 2000) This region undergoes autophosphorylation thus enabling it to directly regulate gene transcription; an additional unique trait of ERK5 compared to the other MAPKs (Morimoto *et al.*, 2007). Furthermore, it has been shown that truncation of this C-terminal tail gives rise to an increased kinase activity of ERK5, which previous studies have suggested might infer an auto-inhibitory function of the C-terminal tail (English *et al.*, 1998), however it is more likely that MEK5 activity is increased thereby increasing the number of activated ERK5 molecules (Buschbeck and Ullrich, 2005).

Although it has been established that ERK5 has constant nuclear localising activity due to its bipartite NLS (Yan *et al.*, 2001; Kondoh *et al.*, 2006), it has recently been proposed that ERK5 also possesses nuclear export activity (Raviv *et al.*, 2004; Buschbeck and Ullrich, 2005). It is considered that ERK5 exists in a folded conformation in its quiescent unphosphorylated state whereby an intramolecular interaction between the N- and C-terminals is facilitated. This interaction is suggested to either dampen the signal of the NLS due to the folded conformation of ERK5, or generate a nuclear export signal (NES) thereby sequestering ERK5 in the cytoplasm (Figure 1.9).

However upon dual-phosphorylation of Thr^{218} and Tyr^{220} by MEK5, the presumed intramolecular NES interaction is disrupted resulting in ERK5 undergoing a conformational change and translocating to the nucleus (Kondoh *et al.*, 2006) (Figure 1.9). Dephosphorylation reverts ERK5 to a folded conformation, increasing NES strength relative to NLS, and relocating ERK5 to the cytoplasm (Kondoh *et al.*, 2006; Plotnikov *et al.*, 2011).

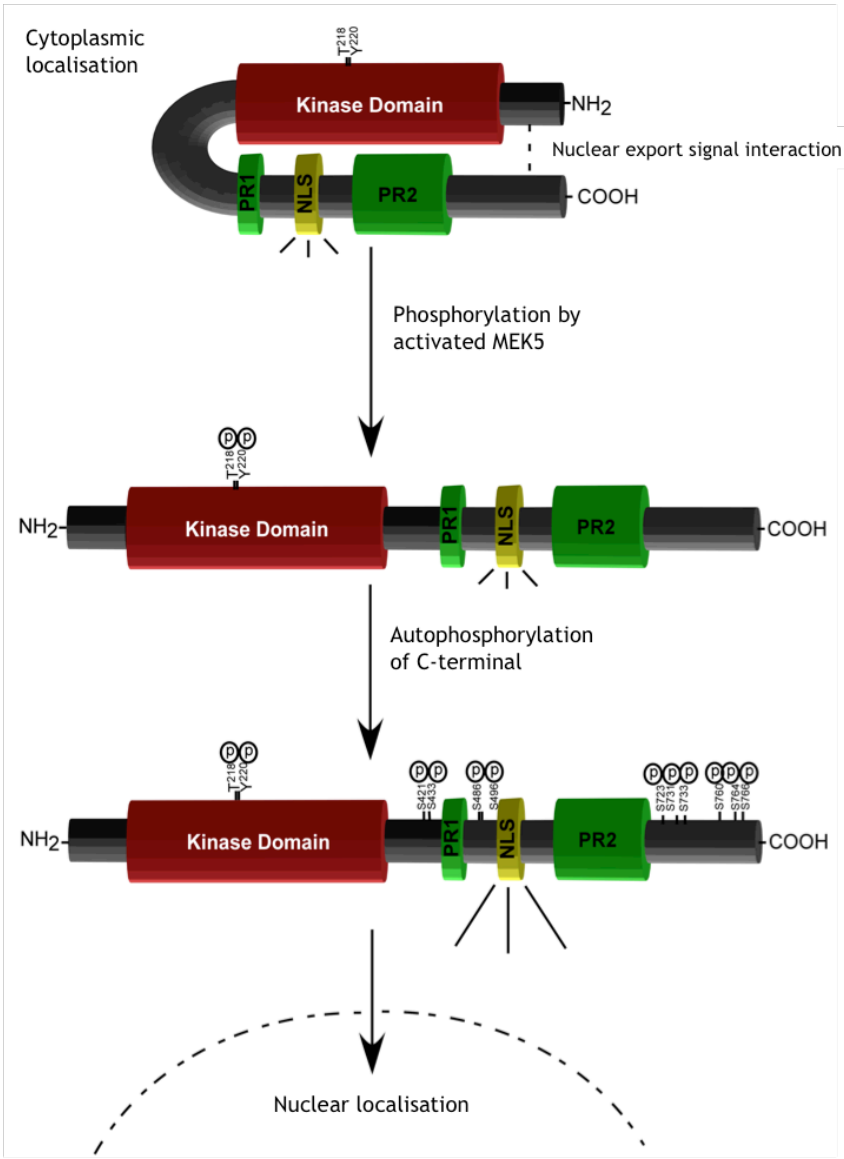

Figure 1.9 ERK5 intracellular localisation.
It has been proposed that ERK5 possesses nuclear export activity (Raviv *et al.*, 2004; Buschbeck and Ullrich, 2005) and that in its unphosphorylated state, ERK5 exists in a folded conformation, thereby enabling a molecular interaction between the N- and C-terminals. It is considered that this conformation may either reduce the nuclear localisation signal (NLS) or generate a nuclear export signal (NES), causing ERK5 to be sequestered in the cytoplasm. Phosphorylation of ERK5 by MEK5 results in a conformational change that disrupts the NES interaction and facilitates translocation of ERK5 into the nucleus (Kondoh *et al.*, 2006).

The intricacies and idiosyncrasies of ERK5 are continually being revealed, however progress in the field has been hampered by a lack of reagents, most notably a reliable phospho-Thr^{218}/Tyr^{220} ERK5 antibody for western blotting and immunofluorescence.

1.5 The ERK5 signalling pathway

1.5.1 ERK5 activation

Since its initial identification as a stress-activated MAPK activated by both oxidative and osmotic stresses (Abe *et al.*, 1996), evidence has shown ERK5 to be stimulated by a plethora of extracellular stimuli; such as VEGF, EGF, FGF-2 and platelet-derived growth factor (PDGF) (Kato *et al.*, 1998; Hayashi and Lee, 2004; Kesavan *et al.*, 2004). Additionally, ERK5 is activated by trophic factors in neurons, namely brain-derived neurotrophic factor (BDNF) (Cavanaugh *et al.*, 2001) and nerve growth factor (NGF) (Watson *et al.*, 2001; Finegan *et al.*, 2009) as well as certain inflammatory cytokines, for example interleukin 6 (IL-6) (Carvajal-Vergara *et al.*, 2005). Furthermore, physiological and pathological conditions including laminar shear-stress, ischaemia and hypoxia are also able to activate ERK5 (Takeishi *et al.*, 1999; Yan *et al.*, 1999; Sohn *et al.*, 2002).

The MAPKKKs activated by these extracellular stimuli and upstream of ERK5 are MEKK2 and MEKK3, which are able to specifically phosphorylate the Ser^{311}/Thr^{315} residues of MEK5 (Chao *et al.*, 1999; Sun *et al.*, 2001). MEKK2 and MEKK3 share 94% sequence identity (Blank *et al.*, 1996), including the presence of Phox (PX) and Bem1p (PB1) domains in their N-terminal regions. MEK5 also contains a PB1 domain; heterodimerisation of the PB1 domains of MEK5 and MEKK2/MEKK3 enables the transmission and maintenance of the specific signal transduction between MEKK2/MEKK3 and MEK5 (Nakamura and Johnson, 2003). MEKK2 and MEKK3 are sufficiently divergent in their N-terminals to permit differential regulation of the ERK5 signalling cascade (Lamark *et al.*, 2003). MEKK2 has been shown to bind to the SH2-domain containing scaffold protein, Lck-associated adaptor (Lad), which then complexes with MEK5 to enhance ERK5 activation (Sun *et al.*, 2001). Furthermore, the MEKK2-Lad complex is required for EGF-stimulated, Src-dependent activation of ERK5 (Sun *et al.*, 2003). MEK5 is the sole upstream MAPKK able to directly activate ERK5. This activation occurs by the preferential phosphorylation of the Thr^{218} residue of the T-E-Y motif present within the activation loop of the ERK5 kinase domain, by MEK5 (Mody *et al.*, 2003). MEK5 can only confer full catalytic activity to ERK5 by dual-phosphorylation of both the Thr^{218}/Tyr^{220} residues of ERK5. Once activated, ERK5 is able to phosphorylate MEK5 (Mody *et al.*, 2003) and undergo autophosphorylation, in addition to potential phosphorylation by an alternative kinase, of numerous residues on its C-terminal thereby enhancing the transcriptional activity of ERK5 (Morimoto *et al.*, 2007).

The MEK5 phosphorylation motif $S^{311}XXXT^{315}$ bears great similarity to the phosphorylation motif of MEK1 ($S^{218}XXXS^{222}$), thus it was suggested that analogous to the canonical Ras>Raf-1>MEK1/2>ERK1/2 signalling pathway, Ras/Raf-1 may also be able to activate MEK5

(English *et al.*, 1998). Initial findings proposed a Ras-dependent, yet Raf-independent pathway of ERK5 activation upon co-transfection of HEK 293 cells with constitutively active Ras with ERK5 (English *et al.*, 1998), however subsequent studies revealed the cell-type specific nature of Ras-mediated activation of ERK5; ERK5 was strongly activated by constitutively active Ras in PC12 cells and C2C12 myoblasts, but not in HeLa or COS7 cells (English *et al.*, 1998; Kato *et al.*, 1998; Kamakura *et al.*, 1999). An interesting observation was unearthed in 2005 however, whereby insulin-stimulated activation of ERK5 in adipocytes appeared to be inhibited by a dominant-negative farnesyltransferase, indicating a requirement for prenylation of Ras in order to activate ERK5 (Sharma and Goalstone, 2005). Thus until further clarification, Ras/Raf-1 activation of ERK5 remains dependent upon cell type.

It has recently been shown that during mitosis, ERK5 is able to undergo MEK5-independent phosphorylation of alternative residues by cyclin-dependent kinases (CDK), thereby revealing potential novel modes of ERK5 activation (Diaz-Rodriguez and Pandiella, 2010; Inesta-Vaquera *et al.*, 2010).

1.5.2 Regulation of ERK5 activity

MAPKs are typically inactivated by dephosphorylation of the T-X-Y motif by a MAP kinase phosphatase (MKP) subfamily of dual-specificity phosphatases (DUSPs) (Dickinson and Keyse, 2006). However, a DUSP that dephosphorylates Thr^{218}/Tyr^{220} of ERK5 has yet to be identified. Instead, the phosphotyrosine-specific phosphatase PTP-SL (protein tyrosine phosphatase STEP-like) is proposed to dephosphorylate ERK5 at the Tyr^{220} residue, consequently hindering its translocation to the nucleus (Buschbeck and Ullrich, 2005). ERK5 was observed to phosphorylate PTP-SL, however this interaction appeared to be minor in comparison to the significantly increased phosphatase activity of PTP-SL upon its binding to ERK5 (Buschbeck and Ullrich, 2005).

Furthermore, post-translational modifications have been shown to regulate ERK5 activity; in HUVECs, a small ubiquitin-like modifier 3 (SUMO3) protein covalently binds to ERK5 on Lys^6 and Lys^{22} following exposure to advanced glycation end-products (AGE) or H_2O_2, thereby inhibiting its transcriptional promoter activity induced by sheer stress without affecting ERK5 phosphorylation (Woo *et al.*, 2008).

1.5.3 ERK5 substrates

The most significant role of ERK5 reportedly is to regulate a number of downstream transcription factors of which the myocyte enhancer factor (MEF) family, MEF2A, C, and D, are the best characterised (Kato *et al.*, 1997; Yang *et al.*, 1998; Kato *et al.*, 2000). ERK5 phosphorylates MEF2C on Ser^{387} (Kato *et al.*, 1997), which increases MEF2C transcriptional activity and subsequently increases c-Jun gene expression (Kato *et al.*, 1997). It has been shown that MEF2D is a substrate specific to ERK5 (Yang *et al.*, 1998; Kato *et al.*, 2000), whereas both ERK5 and the p38 MAPK control the activities of MEF2A and C (Han *et al.*, 1997; Ornatsky *et al.*, 1999). As previously mentioned in Section 1.4.2.2 ERK5 contains a MEF2-interacting region and a transcriptional activation domain in its C-terminal tail, both of which are necessary for regulating MEF2 activity (Kasler *et al.*, 2000); a truncated C-terminal ERK5 mutant lacks the ability to stimulate MEF2 activity (Yan *et al.*, 2001).

In addition to the MEF2 family of substrates, ERK5 is also able to directly enhance the transcription of c-Myc, CREB and Sap1a (English *et al.*, 1998; Kamakura *et al.*, 1999), the latter of which occurs via a serum response element that may also be involved in activating the c-Fos promoter. Both ERK5 and ERK1/2 are capable of phosphorylating c-Fos on Ser^{387}, however it has been observed that ERK5 activation leads to phosphorylation of alternative sites on c-Fos, leading to maximal c-Fos transactivation. Furthermore, phosphorylation of these sites in c-Fos requires the C-terminal tail of ERK5 (Terasawa *et al.*, 2003).

ERK5, like other MAPKs, phosphorylates substrates on Ser/Thr residues immediately preceding a Pro residue. Interestingly, residue Thr^{28} in the ERK5 N-terminal domain and residues Ser^{421}, Ser^{433}, Ser^{496}, Ser^{731} and Thr^{733} in the C-terminal tail are not followed by a Pro residue, but undergo phosphorylation (Mody *et al.*, 2003) thus further suggesting the possible involvement of an additional kinase. In addition to this, MEK5 can be phosphorylated by ERK5 at specific non-proline directed residues Ser^{129}, Ser^{137}, Ser^{142} and Ser^{149} (Mody *et al.*, 2003). Together these findings suggest that the substrate specificity of ERK5 may differ from that of other MAPK family members.

1.5.4 ERK5 and endothelial cells

1.5.4.1 Knockout of ERK5 signalling axis components

The physiological role of the ERK5 signalling cascade was determined *in vivo*, utilising gene ablation of specific components of the pathway in mice (Regan *et al.*, 2002; Sohn *et al.*, 2002; Hayashi *et al.*, 2004; Hayashi and Lee, 2004; Kesavan *et al.*, 2004) (Table 1.2).

Erk5-deficient mice died around E10.5 due to defects in normal cardiac development, maturation of vasculature and angiogenesis. In addition to this, an increased expression of VEGF was observed in these mice compared to the wild-type, however this was not considered to be the primary factor leading to death (Sohn *et al.*, 2002); over-expression of VEGF resulted in normal development up to E12.5, with cardiovascular abnormalities leading to lethality only being evident at E12.5-14.5 (Miquerol *et al.*, 2000).

Furthermore, it is suggested that the increased VEGF expression may be due to deregulation of hypoxia-inducible factor-1 alpha (HIF-1α), preventing its ubiquitination and proteolysis and resulting in aberrant angiogenesis (Pi *et al.*, 2005). Phenotypic abnormalities of *Erk5* ablation include immature vasculature and rounded, disorganised endothelial cells (ECs) leading to loss of vascular integrity, with increased vessel leakiness, leading to death by haemorrhage (Regan *et al.*, 2002; Sohn *et al.*, 2002; Yan *et al.*, 2003). Additionally, ablation of upstream genes of the ERK5 signalling axis resulted in similar phenotypic disruptions in *Mek5*-deficient (Wang *et al.*, 2005) and *Mekk3*-deficient (Yang *et al.*, 2000) mice, thus highlighting the critical function that the ERK5 signalling cascade plays in both vasculogenesis and angiogenesis (Table 1.2).

1.5.4.2 Conditional knockouts and endothelial cell apoptosis

Generation of endothelial-specific *Erk5*-knockout mice revealed that the initial defect upon *Erk5* ablation occurs within the endothelium (Hayashi *et al.*, 2004); these mice displayed cardiovascular defects and died around E10.0, analogous to the global *Erk5*-knockout mice. However, cardiomyocyte-, hepatocyte- and neuronal-specific *Erk5*-knockout mice did not exhibit developmental effects (Hayashi *et al.*, 2004; Li *et al.*, 2013) (Table 1.2). Ablation of *Erk5* in adult mice resulted in decreased vascular integrity followed by death within 2-3 weeks owing to leaky blood vessels caused by EC apoptosis (Hayashi *et al.*, 2004).

Table 1.2 Phenotypic consequences after gene ablation of components of the ERK5 signalling cascade in mice.

Genotype	Phenotype	Reference
Mekk3$^{-/-}$	Severe defects in early angiogenesis resulting in **embryonic lethality at E11.0**; vasculogenesis not affected	(Yang *et al.*, 2000)
Mekk2$^{-/-}$	Mice develop normally, are viable and fertile	(Kesavan *et al.*, 2004)
	Mice develop normally and are viable, but display altered cytokine expression in thymocytes	(Guo *et al.*, 2002)
	Mice develop normally and are viable, but demonstrate reduced cytokine expression in embryonic stem-cell derived mast cells	(Garrington *et al.*, 2000)
Mek5$^{-/-}$	Impaired cardiac development, decreased proliferation and increased apoptosis in the head, head and dorsal regions leading to **embryonic death at E10.5**	(Wang *et al.*, 2005)
Erk5$^{-/-}$	**Embryonically fatal at E9.5-10.5** with stunted growth and underdeveloped vasculature within the yolk sac	(Hayashi *et al.*, 2004)
	Defective cardiac development, heart looping, angiogenesis and vascular maturation; **embryonic lethality at E9.5-10.5**	(Regan *et al.*, 2002)
	Embryonic death at E10.5-11.0 owing to angiogenic defects in the embryo and placenta; evidence of embryonic endothelial cell apoptosis	(Yan *et al.*, 2003)
	Embryonic growth retardation, particularly of the head and lower trunk with dilated pericardial sacs; impaired angiogenesis in the embryo and placenta; **embryonically fatal at E10.5-11.5**	(Sohn *et al.*, 2002)
Erk5$^{-/-}$ *cardiomyocyte*	Mice develop normally and are viable	(Hayashi *et al.*, 2004)
	Pathophysiological challenges in adult mice result in reduced hypertrophic remodelling, are more vulnerable to hypertrophic stress and can undergo cardiac dysfunction under a prolonged, increased workload	(Kimura *et al.*, 2010)
Erk5$^{-/-}$ *endothelial*	Identical phenotype to that of global *Erk5*$^{-/-}$ mice; **embryonically fatal at E9.5-10.5 due to cardiovascular defects**	(Hayashi *et al.*, 2004)
Erk5$^{-/-}$ *hepatocyte*	Mice develop normally and are viable	(Hayashi and Lee, 2004)
Erk5$^{-/-}$ *inducible knockout*	Degeneration of the cardiovascular system with apoptosis of endothelial cells resulting in **lethality of adult mice within 2 weeks** of induced *Erk5*-gene ablation	(Hayashi *et al.*, 2004)
Erk5$^{-/-}$ *neuronal*	Significant reduction in the density of adult-born neurons in the granule cell layer of the olfactory bulb, delayed cell cycle exit of mitotic neuroblasts in the subventricular zone resulting in inhibited neuronal differentiation, disrupted neuronal maturation, migration and cell survival	(Li *et al.*, 2013)
Mef2c$^{-/-}$	**Embryonic death at E9.5** owing to right ventricle malformation as a consequence of failed right loop morphogenesis of the heart tube; disorganisation of endothelial cells results in failure to form a vascular plexus	(Lin *et al.*, 1997)
		(Lin *et al.*, 1998)
	Cardiac and vascular malformations leads to **embryonic fatality at E9.5**	(Bi *et al.*, 1999)

The ability of ERK5 to protect ECs from apoptosis relies on ERK5 phosphorylation of MEF2C (Hayashi *et al.*, 2004); the phenotype of *Mef2c*$^{-/-}$ mice is similar to that of *Erk5*$^{-/-}$ mice, with embryonic lethality as a consequence of cardiac and vascular malformations (Hayashi and Lee, 2004; Roberts *et al.*, 2009). Interestingly, it was observed that *Erk5*$^{-/-}$ embryos infected with an adenovirus encoding a constitutively active Mef2c were only partially protected from EC apoptosis (Hayashi *et al.*, 2004) suggesting the existence of additional downstream effectors of ERK5 that regulate apoptosis (Olson, 2004).

Recent *in vitro* studies using HDMECs demonstrated that ERK5 is required for VEGF-induced phosphorylation of AKT to suppress apoptosis and facilitate cellular survival during tubular morphogenesis of the endothelial cells via VEGFR-2 (Roberts *et al.*, 2010). Furthermore, ERK5 has also been implicated in PDGF-induced activation of AKT in porcine aortic endothelial cells (PAEs) (Lennartsson *et al.*, 2010) and FLT3-mediated activation of AKT in the Ba/F3 pro-B-cell line (Razumovskaya *et al.*, 2011). Taken together, these data suggest that ERK5 may play a critical role in coupling growth factor receptors to activation of AKT and regulating cell survival (Datta *et al.*, 1997). It is unlikely that ERK5 directly phosphorylates AKT as it is well established that AKT is activated via phosphorylation of Thr^{308} in the activation loop via mammalian target of rapamycin complex 2 (mTORC2) (Jacinto *et al.*, 2006; Sarbassov *et al.*, 2006), as well as Ser^{473} in the C-terminus by phosphoinositide-dependent kinase-1 (PDK1) (Alessi *et al.*, 1996). The precise mechanism through which ERK5 regulates AKT phosphorylation and activation remains obscure, however it may be that ERK5 regulates the activity of a phosphatase, such as protein phosphatase 2 (PP2A) (Pankov *et al.*, 2003), or MAP-kinase phosphatase 3 (MKP3) (Razmara *et al.*, 2012), which have been shown to regulate AKT dephosphorylation (Nithianandarajah-Jones *et al.*, 2012).

1.5.4.3 Shear-stress and atheroprotection

Endothelial cell injury caused by various factors including tobacco smoke, diabetes and hypertension (Hayashi and Lee, 2004), can lead to endothelial dysfunction, reduced laminar shear stress, endothelial apoptosis and eventually atherosclerosis (Traub and Berk, 1998). It was demonstrated that steady laminar shear stress resulted in an ERK5-mediated anti-apoptotic effect in bovine lung microvascular endothelial cells (BLMECs) (Pi *et al.*, 2005). This study revealed that activation of ERK5 by constitutively-active MEK5 (CA-MEK5) improved EC viability and reduced apoptosis, whereas dominant-negative ERK5 resulted in EC apoptosis, increased endothelial permeability and plaque destabilisation (Pi *et al.*, 2005). In HUVECs however, an atheroprotective effect was observed whereby ERK5 activation negatively regulated TNF-α-mediated expression of adhesion molecules such as

vascular adhesion molecule-1 (VCAM-1) and E-selectin (Akaike *et al.*, 2004). Additionally, a more recent study utilised a novel MEK5 inhibitor, BIX 02188, to reveal that the MEK5>ERK5 pathway mediates flow-dependent inhibition of TNF-α signalling in BLMECs (Li *et al.*, 2008).

ERK5 was been observed to be required for flow-induced expression of Krüppel-like factor 2 (KLF2) in HUVECs (Parmar *et al.*, 2006) and human glomerular endothelial cells (Slater *et al.*, 2012). KLF2 has been implicated in negatively regulating inflammation and promoting vascular stabilisation (Dekker *et al.*, 2002; SenBanerjee *et al.*, 2004; Boon and Horrevoets, 2009). Further to KLF2, the expression of KLF4-dependent genes have been shown to be induced by ERK5 activation, which are also important in flow-dependent protective responses in endothelial cells (Ohnesorge *et al.*, 2010; Clark *et al.*, 2011). Furthermore, statins have been implicated in ERK5-mediated KLF4-dependent gene expression in endothelial cells, thereby suggesting that some of the pleiotropic vasoprotective effects of these drugs may act via ERK5 activation (Ohnesorge *et al.*, 2010).

In addition to this, it has been observed that the flow–induced activation of ERK5 conveys a cytoprotective response via activation of NF-E2 related factor 2 (Nrf2)-upregulated genes (Kim *et al.*, 2012). Consequently, depletion of ERK5 expression using siRNA or a MEK5 inhibitor (BIX02189, discussed in more detail in Section 1.5.5.4) resulted in a loss of Nrf2 transcriptional activity (Kim *et al.*, 2012). Even more recently, it has been shown that in HUVECs, MAPK-activated protein kinase-1 (MAPKAP-K1, also known as p90RSK) directly inhibits the transcriptional activity of ERK5 thereby inducing an inflammatory response in the ECs and promoting vascular dysfunction (Le *et al.*, 2013).

1.5.5 ERK5 and carcinogenesis

1.5.5.1 Aberrant cell proliferation, migration and adhesion

Cancer represents a progression from normal cellular homeostasis to a neoplastic condition with the cellular acquisition of a number of defined hallmarks: sustained proliferative signalling, evading suppressors, resisting cell death, enabling replicative immortality, inducing angiogenesis, activating invasion and metastasis, reprogramming energy metabolism and evading immune destruction (Hanahan and Weinberg, 2011). The role of MAPKs, in particular ERK1/2, in cancer progression has been a focus of intense research over the last two decades (Dhillon *et al.*, 2007) and attention is now also shifting to the potential role of ERK5 in the development of cancer and disease progression (Lochhead *et al.*, 2012).

It was demonstrated by Kato and colleagues that EGF-induced proliferation of the non-tumourigenic breast epithelial cell line MCF10A, and cervical cancer cell line HeLa, were dependent upon ERK5 activity (Kato *et al.*, 1998). It was later found that EGF stimulation of ERK5 was essential for the phosphorylation of the serine-threonine kinase serum- and glucocorticoid-induced protein kinase (SGK) at Ser^{78} to allow entry into S-phase, and subsequent proliferation (Hayashi *et al.*, 2001). Furthermore, it was observed that in a range of cells, ERK5 regulated cyclin D1 expression to allow cell-cycle progression from G_1- to S-phase (Mulloy *et al.*, 2003), yet it has since been shown that ERK5 activity peaks at G_2-M phase and is necessary to regulate NF-κB activity prior to expression of mitosis-promoting genes, to allow cell proliferation (Cude *et al.*, 2007).

Additional studies have shown a role for ERK5 in the proliferation of the breast cancer cell lines, MCF-7 and BT474 (Esparís-Ogando *et al.*, 2002). More recently, it has been shown that ERK5 suppresses the promyelocytic leukaemia protein (PML) in the PML nuclear body by direct phosphorylation on Ser^{403} and Thr^{409}; consequent upregulation of p21 expression is prevented – an important proliferation modulator (Yang *et al.*, 2010a). This suppression has since been shown to enable the cells to overcome the G1-S transition checkpoint in cell-cycle progression, thereby reducing inhibition of tumour cell proliferation (Yang and Lee, 2011) (Figure 1.10).

The RAS oncogene is mutated in approximately 20-30% of cancers (Prior *et al.*, 2012). ERK5 has been shown to be activated by Ras in PC12 and C2C12 cells (English *et al.*, 1998; Kato *et al.*, 1998; Kamakura *et al.*, 1999) and it has been demonstrated that oncogenic forms of SRC activate the ERK5 pathway in fibroblasts, leading to a loss of actin stress fibres (Barros and Marshall, 2005) and formation of invasive adhesions also known as podosomes (Schramp *et al.*, 2008).

Cellular invasion and metastasis are critical for tumour spread. Sawhney et al. have shown that in breast cancer cells, ERK5 forms a complex with the $a_vß_3$ integrin and FAK to regulate adhesion and migration, and that overexpression of constitutively active MEK5 leads to hyperphosphorylation of FAK (Sawhney *et al.*, 2009). Furthermore, it has been demonstrated that overexpression of MEK5 in prostate cancer induces expression of matrix metalloproteinase-2 (MMP-2) (Ramsay *et al.*, 2011) and MMP-9 (Mehta *et al.*, 2003). Collectively, these data suggest that ERK5 may have an important role in cell attachment to the extracellular matrix (ECM) and in cell migration (Nithianandarajah-Jones *et al.*, 2012).

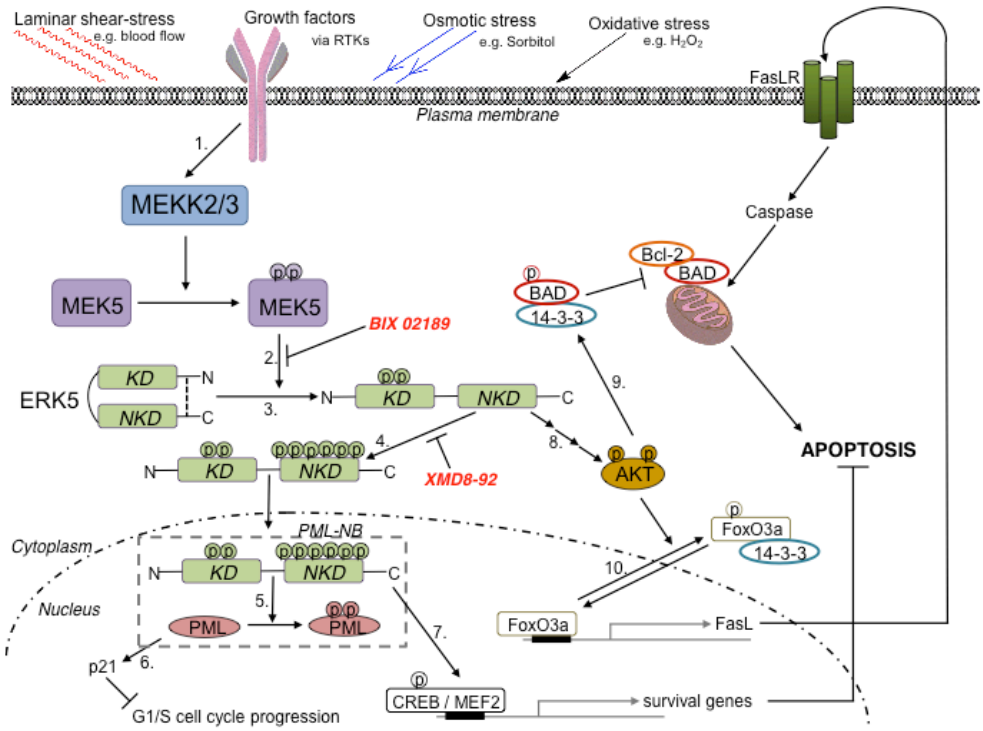

Figure 1.10 Mechanisms of ERK5-mediated cell survival.
1. Various extracellular stimuli such as growth factors, oxidative and osmotic stresses as well as laminar shear-stress, can activate the ERK5 MAPK module; 2. ERK5 is directly phosphorylated on Thr^{218}/Tyr^{220} in the kinase domain by MEK5. Inhibition of this phosphorylation can occur using the MEK5-selective inhibitor, BIX 02189; 3. Phosphorylation of ERK5 leads to a conformational change and results in disruption of the proposed N- and C-terminal nuclear export signal (NES) interaction; 4. Active ERK5 undergoes autophosphorylation of the C-terminal non-kinase domain (NKD) and consequently translocates into the nucleus. Inhibition of ERK5 by XMD8-92 prevents this autophosphorylation and thus disrupts activation of the nuclear localisation signal; 5. Once in the nucleus, ERK5 is able to phosphorylate promyelocytic leukemia protein (PML) in the PML nuclear body (PML-NB); 6. Non-phosphorylated PML upregulates p21, which is necessary for G1/S cell cycle progress; 7. Nuclear ERK5 is also able to phosphorylate transcription factors such as CREB and MEF2 resulting in a survival response; 8. ERK5 regulates phosphorylation of AKT on Thr^{308} and Ser^{473} by an unknown mechanism; 9. AKT phosphorylation of BAD, sequesters it to the 14-3-3 protein and inhibits its interaction with BCL2 and translocation to the mitochondria; 10. Phosphorylated FoxO3a by AKT, is also sequestered by the 14-3-3 protein in the cytoplasm, thus preventing it from upregulating the Fas ligand (FasL), which subsequently results in an apoptotic feedback loop and FasL-mediated caspase activation.

1.5.5.2 Breast and prostate cancer

The genesis and progression of breast carcinomas is linked to certain oncogenic stimuli, in particular the ErbB family of RTKs in response to binding with members of the EGF family of ligands (Wang and Tournier, 2006); HER2 overexpression is detected in 20-30% of breast carcinomas. ERK5 expression has been detected in the majority of patients during the early stages of breast cancer, with overexpression occurring in approximately 20% (Montero *et al.*, 2009), supporting previous studies that demonstrate the upregulation of the ERK5 pathway in HER2 overexpressing cells (Hayashi and Lee, 2004). Montero et al.

also proposed ERK5 as an independent prognosis factor, as levels of ERK5 appeared to be inversely proportional to disease free survival time, thereby illustrating the potential of ERK5 as a biomarker to better predict the outcome of breast cancer in its early stages (Montero *et al.*, 2009; Nithianandarajah-Jones *et al.*, 2012).

ERK5 expression in prostate cancer is similar to that of breast cancer, whereby it correlates to poor prognosis. There is an additional significant link between ERK5 expression and bone metastases, leading to death (McCracken *et al.*, 2008). Studies have shown that MEK5/ERK5 induces the transcription of activator protein (AP)-1, which in turn upregulates matrix metallopeptidase (MMP)-9 to degrade the extracellular matrix surrounding the cells, and enhance the metastatic potential of the cancer (Mehta *et al.*, 2003). Furthermore, PC3 cells overexpressing ERK5 had significantly increased levels of proliferation, motility and invasion, as well as being considerably more efficient in forming tumours, thus emphasising the relationship between the presence of ERK5 and the aggression of prostate cancer (McCracken *et al.*, 2008).

1.5.5.3 Tumour-associated angiogenesis

As previously described in Section 1.1.4, tumour-associated angiogenesis is distinctly different from its physiological counterpart; the microvessels are leaky and twisted, blood flow can be intermittent, static and even reversed, and there is often a lack of supporting pericyte cells (De Bock *et al.*, 2011). The critical role that ERK5 plays in physiological angiogenesis was demonstrated when *Erk5*-deficient mice exhibited defective vasculature (Hayashi *et al.*, 2004; Hayashi and Lee, 2004). It was subsequently reported that the ERK5 signalling pathway was essential for tumour-associated angiogenesis; vascular development was inhibited and exogenous tumour growth was reduced in mice with deleted ERK5 in human tumour xenograft models (Hayashi *et al.*, 2005). Additionally, studies have demonstrated the ability of pro-angiogenic factors such as VEGF and FGF to stimulate ERK5 activation in HUVECs (Hayashi *et al.*, 2004) and have shown the specific requirement for ERK5 to mediate VEGF-stimulated tubular morphogenesis, but not cellular proliferation in HDMEC (Roberts *et al.*, 2010). Thus taken together, these data indicate the potential of ERK5 as an anti-angiogenic drug target.

1.5.5.4 Small-molecule inhibitors of ERK5

Studies into small-molecule kinase inhibitors of the MEK5/ERK5 pathway have recently uncovered two indolinone-6-carboxamides (developed by Boehringer Ingelheim) that selectively inhibit MEK5 over MEK1/2 (Tatake *et al.*, 2008). *In vitro,* BIX02188 and BIX02189 are able to block MEK5 activity and have IC_{50}s of 4.3 nmol/L and 1.5 nmol/L

respectively. In HeLa and HEK293 cells, both osmotic stress-induced ERK5 and MEF2C activation are inhibited (Tatake *et al.*, 2008). The use of these compounds in PC12 cells implicate MEK5/ERK5 in NGF-induced neurite outgrowth and stabilisation of tyrosine hydroxylase (Obara *et al.*, 2009). Currently no data is available with respect to growth factor-induced activation of ERK5, or of the pharmacodynamics or pharmacokinetics of these two carboxamides. Although MEK5 is the only upstream kinase to directly phosphorylate ERK5, recent findings that ERK5 phosphorylation occurs via a MEK5-independent, CDK-dependent pathway (Inesta-Vaquera *et al.*, 2010), implies that these MEK5-targeting BIX inhibitors may prove to be insufficient in inhibiting the ERK5 signalling cascade within mitotic tumour cells.

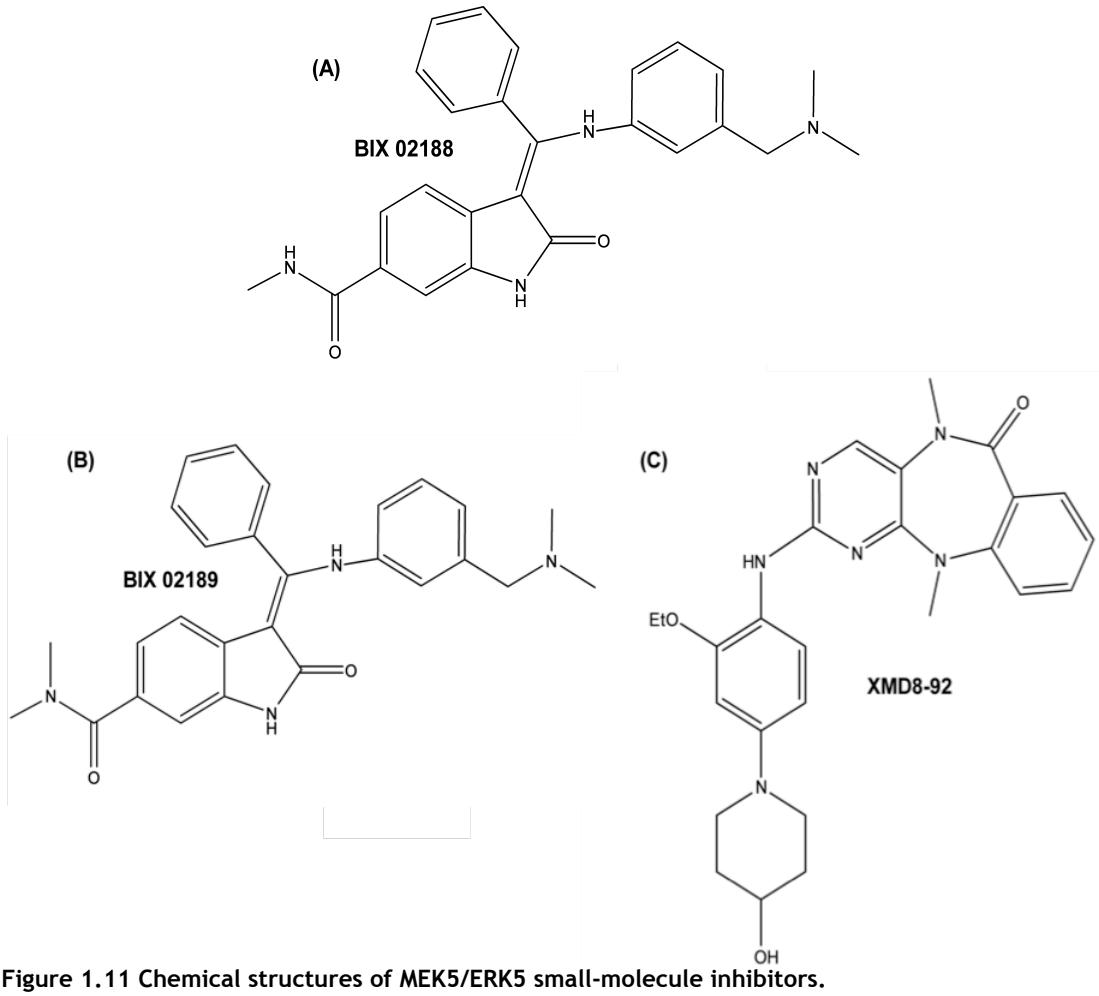

Figure 1.11 Chemical structures of MEK5/ERK5 small-molecule inhibitors.
(A) BIX 02188, *Chemical name (3Z)-3-[[[3-[(Dimethylamino)methyl]phenyl]amino]phenylmethylene]-2,3-dihydro-2-oxo-1H-indole-5-carboxamide*, and (B) BIX 02189, *Chemical name 3-[[[3-[(Dimethylamino)methyl]phenyl]amino]phenylmethylene]-2,3-dihydro-N,N-dimethyl-2-oxo-1H-indole-6-carboxamide*, both developed by Boehringer Ingelheim are selective MEK5 inhibitors, with an IC_{50} of 4.3 nmol/L and 1.5 nmol/L, respectively; (C) XMD8-92, *Chemical name 2-[[2-Ethoxy-4-(4-hydroxy-1-piperidinyl)phenyl]amino]-5,11-dihydro-5,11-dimethyl-6H-pyrimidol[4,5-b][1,4]benzodiazepine-6-one*, is a highly selective ERK5 inhibitor, with an IC_{50} of 240 nmol/L.

XMD8-92 is a highly-selective inhibitor of ERK5 activity, which arose after modifications were made to the ATP-competitive polo kinase inhibitor BI-2536 (Yang *et al.*, 2010a). XMD8-92 inhibits EGF-stimulated ERK5 activation with an IC_{50} of 240 nmol/L *in vitro* and selectively inhibits EGF-induced phosphorylation of ERK5 over ERK1/2 up to a concentration of 5μM. Yang et al. utilised XMD8-92 in mice with lung and cervical xenograft tumours to show inhibition of tumour growth by 95%, through phosphorylation and suppression of PML as described in Section 1.5.5.1, thereby blocking tumour cell proliferation (Yang *et al.*, 2010a). Furthermore, unlike the loss of vascular integrity caused by endothelial-specific ERK5 deletion (Hayashi *et al.*, 2004), it has been observed that XMD8-92 treatment does not appear to affect vasculature stability in mice owing to the reversible nature of inhibition of ERK5 activity (Yang *et al.*, 2010a).

1.6 Project aims

The objective of this study was to further elucidate the activation of ERK5 in VEGF-stimulated primary human dermal microvascular endothelial cells (HDMECs) in contrast to EGF-stimulated HeLa cells.

In order to achieve this objective, this project aimed to:

1. Characterise the activation and phosphorylation status of ERK5 in response to various growth factors in the two cell types, as well as determining the potential tyrosine residues on VEGFR-2 and downstream signalling pathways through which ERK5 is activated.
2. Utilise small-molecule inhibitors of MEK5 and ERK5 to determine the phosphorylation status of ERK5 and the role of agonist stimulated ERK5 in regulating AKT activation in HDMECs and HeLa.
3. Identify the intracellular localisation of ERK5 in HDMEC, compared to HeLa, following agonist stimulation.
4. Identify potential novel binding partners of ERK5 in HDMECs using immunoprecipitation of ERK5, followed by mass spectrometry analysis.

Chapter Two
Materials and Methods

2.1 Materials

2.1.1 General reagents

Full-range (12-225 kDa) rainbow molecular weight marker and Hybond ECL nitrocellulose membrane were purchased from GE Healthcare (Amersham, UK). Ultrapure ProtoGel® solution was bought from Geneflow Ltd. (National Diagnostics, Staffordshire, UK).

ProLong® Gold antifade reagent, Lipofectamine™ RNAiMAX and Lipofectamine™ 2000 transfection agents, as well as RNase*Zap*® were bought from Invitrogen™; NuPAGE® 4-12% Bis-Tris gels, LDS sample buffer [4X] and SilverQuest™ Silver Staining kit were purchased from Novex®. Invitrogen™ and Novex® products were sourced from Life Technologies™ (Paisley, UK).

Aprotinin, leupeptin, pepstatin, phenylmethylsulphonyl fluoride (PMSF), agar, agarose (electrophoresis grade), glycerol, 3-(N-morpholino)-propanesulphonic acid (MOPS), polyoxyethylenesorbitan monolaurate (Tween-20) and sodium dodecyl sulphate (SDS) 20% (w/v) solution, were purchased from Melford (Ipswich, UK). Prestained protein marker (broad range 10-230 kDa) was bought from New England Biolabs (UK) Ltd. (Hitchin, UK).

Ammonium chloride, ammonium peroxodisulphate (APS), ampicillin solution, bicinchoninic acid solution, copper (II) sulphate solution, dimethyl sulphoxide (DMSO), sterile DNase- and RNase-free dH_2O, ethidium bromide (EtBr), ethylenediaminetetraacetic acid (EDTA), gelatin from porcine skin, kanamycin solution, Luria Bertani (LB) broth powder, manganese (II) chloride tetrahydrate, sodium orthovanadate (Na_3VO_4), N,N,N',N'-tetramethylethylenediamine (TEMED), Tris-EDTA (TE) buffer solution (pH 8.0) and Triton X-100 were bought from Sigma-Aldrich (Poole, UK).

Enhanced chemiluminescence (ECL) western blotting detection reagents, glycine, sodium chloride (NaCl), Tris-Base were bought from Thermo Fisher Scientific™ (Loughborough, UK). Phos-tag™ AAL-107 was bought from Wako Chemicals GMBH (Neuss, Germany).

2.1.2 Agonists and inhibitors

Recombinant human vascular endothelial growth factor (VEGF)-A_{165} and basic fibroblast growth factor (FGF-2) were purchased from R&D Systems Inc. (Minneapolis, MN, USA). Recombinant human hepatocyte growth factor (HGF), epidermal growth factor (EGF), dimeric platelet-derived growth factor (PDGF)-BB and transforming growth factor (TGF)-α were bought from Peprotech EC (Rocky Hill, NJ, USA). BIX 02189 was purchased from

Selleck Chemicals (Stratech Scientific Ltd., Suffolk, UK). XMD 8-92 was bought from Tocris Bioscience (Bristol, UK).

2.1.3 Antibodies

Table 2.1 Primary antibodies against total proteins used in this study

Antibody	Source	Cat. No.	Dilution	Host Species	Appl.
Actin (I-19)	Santa Cruz Biotechnology (CA, USA)	sc-1616-R	1:2000	Rabbit	WB
AKT	New England Biolabs (Hitchin, UK)	#9271	1:1000 1:50	Rabbit	WB IP
EGFR-#1	New England BioLabs (Hitchin, UK)	#2232	1:1000	Rabbit	WB
ERK5	New England Biolabs (Hitchin, UK)	#3372	1:1000 1:100 1:50	Rabbit	WB IF IP
ERK5	R&D Systems	AF2848	1:40	Goat	IP
FLAG® M2	Sigma-Aldrich (Poole, UK)	F1804	1:2000	Mouse	WB
FLAG® M2 Affinity Gel	Sigma-Aldrich (Poole, UK)	A2220	1:25	Mouse	IP
GAPDH XP	New England Biolabs (Hitchin, UK)	#5174	1:2000	Rabbit	WB
Lamin B1 (H-90)	Santa Cruz Biotechnology (CA, USA)	sc-20682	1:2000	Rabbit	WB
MEK5	Abcam (Cambridge, UK)	ab45146	1:10000	Rabbit	WB
PECAM1 (CD31)	Santa Cruz Biotechnology (CA, USA)	sc-1506	1:1000	Goat	WB
PLC-γ1	New England Biolabs (Hitchin, UK)	#2822	1:1000	Rabbit	WB
p44/42 MAPK (ERK1/2)	New England Biolabs (Hitchin, UK)	#9102	1:1000 1:100	Rabbit	WB IF
c-Raf	New England BioLabs (Hitchin, UK)	#9422	1:1000	Rabbit	WB
H-Ras (C-20)	Santa Cruz Biotechnology (CA, USA)	sc-520	1:200	Rabbit	WB
K-Ras (C-19)	Santa Cruz Biotechnology (CA, USA)	sc-521	1:200	Rabbit	WB
N-Ras (F-155)	Santa Cruz Biotechnology (CA, USA)	sc-31	1:200	Mouse	WB
VEGF Receptor 2 (55B11)	New England Biolabs (Hitchin, UK)	#2479	1:1000 1:200	Rabbit	WB IF

Applications: WB – Western blotting; IF – Immunofluorescence; IP – Immunoprecipitation

Table 2.2 Primary antibodies against phosphorylated proteins used in this study

Antibody	Source	Cat. No.	Dilution	Host Species	Appl.
Phospho-AKT (S^{473}) XP	New England Biolabs (Hitchin, UK)	#4060	1:2000	Rabbit	WB
Phospho-EGFR1	New England Biolabs (Hitchin, UK)	#2234	1:1000	Rabbit	WB
Phospho-ERK5 (T^{218}/Y^{220})	New England Biolabs (Hitchin, UK)	#3371	1:1000	Mouse	WB
Phospho-ERK5 (T^{218}/Y^{220})	Dr. Atanasio Pandiella Instituto de Biolgia Molecular y Celular del Cancer, CSIC-Universidad de Salamanca	N/A	1:3000	Rabbit	WB
Phospho-ERK5 (T^{732})	Dr. Atanasio Pandiella (as above)	N/A	1:1000	Rabbit	WB
Phospho-PKC (pan)	New England BIoLabs (Hitchin, UK)	#9371	1:1000	Rabbit	WB
Phospho-PLCγ1 (Y^{783})	New England Biolabs (Hitchin, UK)	#2821	1:1000	Rabbit	WB
Phospho-p44/42 MAPK (T^{202}/Y^{204}) XP	New England Biolabs (Hitchin, UK)	#4370	1:2000	Rabbit	WB
Phospho-VEGFR2 (Y^{1175})	New England Biolabs (Hitchin, UK)	#3770	1:1000	Rabbit	WB

Applications: WB – Western blotting

Table 2.3 Secondary antibodies used in this study

Antibody	Source	Cat. No.	Dilution	Appl.
Alexa Fluor® 488 Donkey Anti-Rabbit IgG (H+L)	Molecular Probes® (Life Technologies™; Paisley, UK)	A21206	1:1000	IF
Alexa Fluor® 568 Donkey Anti-Rabbit IgG (H+L)	Molecular Probes® (Life Technologies™; Paisley, UK)	A10042	1:1000	IF
Hoechst 33342	Molecular Probes® (Life Technologies™; Paisley, UK)	H1399	1:5000	IF
HRP-conjugated AffiniPure Donkey Anti-Goat IgG (H+L)	Jackson ImmunoResearch Laboratories, Inc. (PA, USA)	705-035-147	1:10000	WB
HRP-conjugated AffiniPure Goat Anti-Mouse IgG (H+L)	Jackson ImmunoResearch Laboratories, Inc. (PA, USA)	115-035-166	1:5000	WB
HRP-conjugated AffiniPure Goat Anti-Rabbit IgG (H+L)	Jackson ImmunoResearch Laboratories, Inc. (PA, USA)	111-035-144	1:5000	WB
Protein G Plus Agarose Suspension	Calbiochem® (EMD Millipore; Feltham, UK)	IP04	1:10	IP

Applications: WB – Western blotting; IF – Immunofluorescence; IP - Immunoprecipitation

2.1.4 Bacterial strains and media

Table 2.4 Bacterial strains and media used in this study

Bacterial strain	Source	Media	Application
One Shot® *ccd*B Survival™ 2 T1^R Competent Cells (*E.coli* strain)	Invitrogen™ (Life Technologies™; Paisley, UK)	LB broth / agar plates + 50 µg/mL kanamycin or + 50 µg/mL ampicillin	pENTR™1A Entry Vector or pAd/CMV/V5-DEST™ Destination Vector
One Shot® TOP10 Chemically Competent *E.coli*	Invitrogen™ (Life Technologies™; Paisley, UK)	LB broth / agar plates + 50 µg/mL kanamycin or + 50 µg/mL ampicillin	pENTR™1A-plasmids pAd/CMV/DEST™-plasmids

2.1.5 Cell culture

2.1.5.1 General materials

Glass coverslips (16 mm diameter) were bought from Agar Scientific (Stansted, UK). All other cell culture materials were purchased from Greiner Bio-One (Stonehouse, UK), Starlab UK (Milton Keynes, UK) or Thermo Fisher Scientific™ (Loughborough, UK), unless otherwise stated.

2.1.5.2 Cell types, culture media and solutions

Table 2.5 Cell types used in this study

Abbr. Name	Cell type and details	Source
HDMEC	Human dermal microvascular endothelial cells (Lot No. 6060707.1) Isolated from juvenile, Caucasian male	PromoCell (Heidelberg, Germany)
HeLa	Human epithelial cervical cancer cell line Isolated from adult, African-American female	European Collection of Cell Cultures supplied by Sigma-Aldrich (Poole, UK)
MAE	Murine aortic endothelial cells Isolated from mouse aorta (vector cells)	Prof. Lena Claesson-Welsh, Rudbeck Laboratory, Dept. Immunology, Genetics & Pathology, Uppsala University, 75185, Sweden
MAE Flk-1 wt	Murine aortic endothelial cells Isolated from mouse aorta, stably expressing transfected murine VEGFR-2 (Flk-1)	Prof. Lena Claesson-Welsh (as above)
MAE Flk-1 Y949F	Murine aortic endothelial cells Isolated from mouse aorta, stably expressing transfected murine VEGFR-2 (Flk-1) with a point mutation at Tyr^{949} to Phe^{949} in the cytoplasmic domain	Prof. Lena Claesson-Welsh (as above)

MAE Flk-1 Y1173F	**Murine aortic endothelial cells Isolated from mouse aorta, stably expressing transfected murine VEGFR-2 (Flk-1) with a point mutation at Tyr^{1173} to Phe^{1173} in the cytoplasmic domain**	**Prof. Lena Claesson-Welsh (as above)**
MAE Flk-1 Y1212F	**Murine aortic endothelial cells Isolated from mouse aorta, stably expressing transfected murine VEGFR-2 (Flk-1) with a point mutation at Tyr^{1212} to Phe^{1212} in the cytoplasmic domain**	**Prof. Lena Claesson-Welsh (as above)**
HEK 293A	**Human embryonal kidney cell line Subclone of 293 cell line, suitable for generating recombinant adenovirus**	**Invitrogen™ (Life Technologies™; Paisley, UK)**

Table 2.6 Cell culture media and solutions used in this study

Name	Culture media composition	Source
Endothelial full growth medium	**EBM MV2 basal medium (Cat. No. C-22221) with SupplementPack (Cat. No. C-39221): 0.05 mL/mL FCS, 5 ng/mL EGF, 10 ng/mL FGF-2, 20 ng/mL Long R3 IGF-1, 0.5 ng/mL $VEGF_{165}$, 1 µg/mL Ascorbic Acid, 0.2 µg/mL Hydrocortisone**	**PromoCell (Heidelberg, Germany)**
Endothelial 1% low serum medium	**EBM MV2 basal medium supplemented with 0.01 mL/mL FCS (Cat. No. 37350)**	**PromoCell (Heidelberg, Germany)**
Complete medium	**Dulbecco's Modified Eagle Medium (DMEM) (Cat. No. D6429) containing 4500 mg/L glucose, L-glutamine, sodium pyruvate and sodium bicarbonate supplemented with 0.1 mL/mL FBS (Cat. No. 10270106)**	**Sigma-Aldrich® (Poole, UK) Gibco® (Life Technologies™; Paisley, UK)**
0.1% low serum medium	**Dulbecco's Modified Eagle Medium (DMEM) (Cat. No. D6429) containing 4500 mg/L glucose, L-glutamine, sodium pyruvate and sodium bicarbonate supplemented with 0.001 mL/mL FBS (Cat. No. 10270106)**	**Sigma-Aldrich® (Poole, UK) Gibco® (Life Technologies™; Paisley, UK)**
Opti-MEM® reduced serum medium, GlutaMAX™	**Opti-Minimal Essential Medium (Cat. No. 51985-0XX) containing GlutaMAX™-I, (HEPES, sodium pyruvate, sodium bicarbonate)**	**Gibco® (Life Technologies™; Paisley, UK,**
Trypsin	**0.05% Trypsin-EDTA (1X), Phenol Red (Cat. No. 25300-054)**	**Gibco® (Life Technologies™; Paisley, UK,**
Gelatin	**0.5% (w/v) gelatin from porcine skin in ddH_2O, autoclaved**	**Sigma-Aldrich® (Poole, UK)**
Versene	**Dulbecco's phosphate buffered saline without Ca^{2+}/Mg^{2+} supplemented with 0.001 mL/mL EDTA**	**Lonza (Basel, Switzerland)**
PBS Cell Wash	**Dulbecco's phosphate buffered saline with Ca^{2+}/Mg^{2+}**	**Lonza (Basel, Switzerland)**
Ice-cold PBS Lysis Wash	**Dulbecco's phosphate buffered saline without Ca^{2+}/Mg^{2+} stored at 4°C**	**Lonza (Basel, Switzerland)**

2.1.6 Deoxyribonucleic acid (DNA) and ribonucleic acid (RNA)

2.1.6.1 General materials

siRNA duplexes were purchased from Dharmacon Inc. (Lafayette, USA). Gateway® entry vector, Gateway®-adapted ViraPower adenoviral expression vector, oligonucleotide primers and 2x Power SYBR® Green mastermix were bought from Life Technologies™ (Paisley, UK). RNeasy mini RNA extraction kit, QIAshredder kit, RNase-Free DNase set and QIAprep Spin Miniprep/Maxiprep kits were purchased from Qiagen (Crawley, UK). Vivapure® AdenoPACK™ 20 was bought from Sartorius UK (Surrey, UK). Optically clear heat-sealing film was purchased from Starlab UK (Milton Keynes, UK) and Adeno-X Rapid Titer Kit was bought from Takara Bio Europe SAS (Clontech; Saint-Germain-en-Laye, France).

2.1.6.2 Plasmid constructs

Table 2.7 Plasmid constructs used in this study

Plasmid	Description	Source
pcDNA3.1-ERK5(wt)	pcDNA3.1 mammalian expression vector containing human wild-type ERK5 cDNA and a FLAG epitope tag at the N-terminus (Kato *et al.*, 1997)	Dr. J.D. Lee, The Scripps Research Institute, La Jolla, CA, USA
pcDNA3.1-ERK5(AEF)	pcDNA3.1 mammalian expression vector containing dominant-negative mutant human ERK5 cDNA, whereby the T^{218} and Y^{220} activation domain phosphorylation sites were mutated to A^{218} and F^{220}, and a FLAG epitope tag at the N-terminus (Kato *et al.*, 1997)	Dr. J.D. Lee (as above)
pCMV5-MEK5(D)	pCMV5 mammalian expression vector containing a constitutively active rat MEK5α-1 cDNA, whereby the S^{313} and T^{317} phosphorylation sites were replaced with D^{313} and D^{317}, and 3 copies of the HA epitope tag added to the C-terminus (Kato *et al.*, 1997)	Dr. J.D. Lee (as above)
pENTR™1A-ERK5(wt)	Gateway® pENTR™1A entry clone containing human wild-type ERK5 cDNA, and a FLAG epitope tag at the N-terminus	This study.
pENTR™1A-ERK5(AEF)	Gateway® pENTR™1A entry clone containing dominant-negative mutant human ERK5 cDNA, whereby the T^{218} and Y^{220} activation domain phosphorylation sites were mutated to A^{218} and $F^{220,}$ and a FLAG epitope tag at the N-terminus	This study.
pENTR™1A-MEK5(D)	Gateway® pENTR™1A entry clone containing a constitutively active rat MEK5α-1 cDNA, whereby the S^{313} and T^{317} phosphorylation sites were replaced with D^{313} and D^{317}, and a HA_3 epitope tag at the C-terminus	This study.
pAd/CMV/FLAG-ERK5(wt)	Gateway®-adapted ViraPower™ adenoviral expression clone containing human wild-type ERK5 cDNA and a FLAG epitope tag at the N-terminus	This study.

pAd/CMV/FLAG-ERK5(AEF)	**Gateway®-adapted ViraPower™ adenoviral expression clone containing dominant-negative mutant human ERK5 cDNA, whereby the T^{218} and Y^{220} activation domain phosphorylation sites were mutated to A^{218} and F^{220}, and a FLAG epitope tag at the N-terminus**	**This study.**
pAd/CMV/HA_3-MEK5(D)	**Gateway®-adapted ViraPower™ adenoviral expression clone containing a constitutively active rat MEK5α-1 cDNA, whereby the S^{313} and T^{317} phosphorylation sites were replaced with D^{313} and D^{317}, and a HA_3 epitope tag at the C-terminus**	**This study.**

2.2 Methods

2.2.1 Adenoviral expression clone construction

2.2.1.1 Restriction digests, gel extraction and ligation reactions

Restriction digests were performed in a volume of 100 µL on 5 µg of DNA, in the presence of bovine serum albumin (BSA) and a restriction enzyme buffer, with a 2- to 10- fold excess of the appropriate restriction enzymes, and made up to 100 µL with nuclease-free dH_2O. The N-terminal FLAG-tagged ERK5(wt) and ERK5(AEF) cDNA sequences were cut out of the pcDNA3.1 expression vectors using the restriction enzymes *XhoI* and *XbaI*, and the C-terminal HA_3-tagged MEK5(D) cDNA sequence was cut out of the pCMV5 expression vector using *KpnI* and *XmaI*. The pENTR™1a entry vector was cut open with the *DraI* and *EcoRV* restriction enzymes. Restriction digest mixtures were mixed by gentle pipetting and incubated at the enzyme's optimum temperature for 4 h, prior to inactivating the enzymes by heating to 75ºC for 15 min. The 5' and 3' ends of the cDNA were blunted by incubating the 100 µL restriction digest mixtures with 20 µL of 10 mM dNTP mix and 5 µL of T4 polymerase. The entry vector was treated with 5µL Calf Alkaline Phosphatase (CAP) for 1 h at 37ºC, to remove 5' phosphates and prevent the religation of single digests thereby reducing false positives, and then heated to 75ºC for 15 min to inactivate the enzyme.

The insert and vector restriction digests were run on a 1% (w/v) agarose gel and the appropriate bands were extracted using the Wizard® SV Gel Extraction Kit (Cat #9281; Promega, Southampton, UK).

The digested insert was incubated with the digested vector in the presence of T4 ligase, ligase buffer and nuclease-free dH_2O in a volume of 10 µL for 18 h at 21ºC in order to ligate the two products. The background level of self-ligated vector was checked by including a vector-only (no cDNA) ligation reaction.

2.2.1.2 Chemical transformation of competent cells

One Shot® TOP10 Chemically Competent *E.coli* cells were transformed with the ligation reaction products. Competent cells were thawed on ice and 100 µL was added to each ligation reaction and placed on ice for 30 min. Each reaction was incubated at 42ºC for 90 s and then placed on ice for 3 min. 900 µL of warm Luria Bertani (LB) media was then added to each reaction, which was then incubated for 1 h at 37ºC, under continuous rotation at 250 rpm. 200 µL of each transformed construct was streaked out onto kanamycin LB plates and incubated overnight at 37ºC. Three colonies for each construct were selected and incubated in separate 5 mL cultures for 8 h at 37ºC. DNA was then extracted from each culture using the QIAprep Spin Miniprep kit (described below), the concentration determined by spectrophotometric measurement of the absorbance at 260 nm (A_{260}) using a NanoDrop ND-1000 spectrophotometer and the associated software (Labtech International, Lewes, UK) and the sample sent to Source BioScience LifeSciences for sequencing.

Once the correct sequence and alignment were confirmed, one DNA extraction product from each entry clone was selected and used to transform chemically competent cells as described above. Following this, the starter culture of each transformed construct was amplified in 100 mL of kanamycin LB media, the cells were harvested using the QIAprep Spin Maxiprep kit (described below) and the DNA concentration determined by spectrophotometry.

<u>QIAprep Spin Miniprep and Maxiprep kit</u>

The principles behind both the Miniprep and Maxiprep plasmid purification kits were the same, with the only difference being the volume of culture being purified. Initially, bacterial lysates were neutralised, cleared through centrifugation and the cleared lysate (supernatant) was then loaded directly onto an equilibrated, anion-exchange tip and allowed to enter the resin by gravity flow. Due to the low-salt and pH conditions, the plasmid DNA was able to selectively bind to the resin. Other impurities such as RNA and proteins were removed from the resin with a medium-salt wash, after which addition of a high-salt buffer to the resin eluted the ultrapure plasmid DNA. Isopropanol precipitation was then used to concentrate and desalt the DNA, which was then collected by centrifugation, air-dried and resuspended in sterile nuclease-free dH_2O.

The following protocol states volumes for the Miniprep in normal font and those for the Maxiprep, in underlined font. All buffers indicated are those provided in the commercially available Qiagen kits.

Bacterial cultures were centrifuged at 6000 x g for 15 min at 4ºC, the supernatant discarded and the bacterial pellet was resuspended in 0.3 mL or 10 mL of Buffer P1, by vortexing. To the suspension, 0.3 mL or 10 mL of Buffer P2 was added, mixed by vigorous inversion (not vortexing) of the capped tube and incubated at room temperature for 5 min. The addition of 0.3 mL or 10 mL of chilled Buffer P3 prior to immediate mixing by vigorous inversion and incubation on ice for 5 min, enhanced the precipitation of contaminants such as genomic DNA and cell debris, which was separated by room temperature centrifugation at 13,300 rpm for 10 min or two 4ºC centrifugation steps, the first for 30 min, followed by transference of the supernatant to fresh capped tubes, and a second spin for 15 min. To equilibrate a QIAGEN-tip, 1 mL or 10 mL of Buffer QBT was added to the column and allowed to empty by gravity flow, after which the cleared sample supernatant was added to the column and allowed to enter the resin by gravity flow. Impurities were removed from the column with two washes of 2 mL or 30 mL Buffer QC, and the DNA was eluted with 0.8 mL or 15 mL Buffer QF into fresh tubes. The addition of 0.7 volumes of room temperature isopropanol to the eluted DNA, followed by centrifugation at 13,300 rpm for 30 min at room temperature or 4ºC, enabled precipitation of the DNA. The pelleted DNA was then washed with 1 mL or 5 mL of room temperature 70% (v/v) ethanol, centrifuged at 13,300 rpm for 10 min and the resulting supernatant carefully removed and discarded. The pellet was air-dried for 5 min prior to redissolving the DNA in nuclease-free dH_2O.

2.2.1.3 LR recombination reaction and expression clone selection

The entry clones (pENTR™1A + ERK5(wt)/ERK5(AEF)/MEK5(D)) underwent a LR recombination reaction with the pAd/CMV destination vector (Gateway®-adapted ViraPower™ adenoviral expression vector) prior to chemical transformation of competent cells and selection of an expression vector. In a final volume of 8 µL, 150 ng of the entry clone was mixed with 300 ng of the destination vector, in the presence of TE buffer (pH 8.0). 2 µL of LR Clonase™ II enzyme mix (provided with the kit) was then added to each sample, mixed well by pipetting and incubated at 25ºC for 18 h. To each reaction, 1 µL Proteinase K solution (provided with the kit) was added and incubated at 37ºC for 10 min, after which competent *E.coli* were transformed as previously described in Section 2.2.1.2 and streaked onto ampicillin LB plates. Colonies were then selected, grown and the extracted DNA (Miniprep kit) was sent off for sequencing, as before. One DNA extraction

product from each destination clone, with the correct sequence and alignment, was selected and used to transform chemically competent cells as described above, prior to amplification in 100 mL of ampicillin LB media and harvesting the cells using the Maxiprep kit.

2.2.2 Preparing adenoviral stocks

2.2.2.1 *PacI* digestion, phenol:chloroform extraction and ethanol precipitation

Each destination clone (pAd/CMV + ERK5wt/ERK5(AEF)/MEK5(D)) and the empty destination vector (pAd/CMV) were digested with the *PacI* restriction enzyme to expose the viral inverted terminal repeats to enable proper viral replication and packaging, and remove the bacterial sequences (i.e. ampicillin resistance gene and pUC origin). 5 µg of plasmid was digested with *PacI* restriction enzyme in the presence of restriction enzyme buffer, BSA, made up to 100 µL with nuclease-free dH_2O and mixed well with gentle pipetting. The mix was incubated at 37ºC for 4 hours after which the enzyme was inactivated by heating to 65ºC for 20 min.

Each fragment was then purified using phenol:chloroform extraction. An equal volume (100 µL) of phenol:chloroform:isoamyl alcohol (or PCI; 25:24:1) was added to each restriction fragment, vortexed to mix and then centrifuged at 13,300 rpm for 1 min. The aqueous layer containing the DNA, was transferred into a fresh microcentrifuge tube and 1 volume of PCI was added, vortexed and centrifuged as before. The transferred aqueous layer was further purified, first by incubating it with 2.5 volumes of 100% ice-cold ethanol and 1/10 volume of 3 M sodium acetate (pH 5.2) at -80ºC for 1 h. The products were then centrifuged at 13,300 rpm for 20 min at 4ºC and the supernatant was carefully removed. The pellet was rinsed with 70% ethanol, centrifuged at 13,300 rpm for 15 min at 4ºC and the supernatant was aspirated off. The pellet was then resuspended in 10 µL sterile, nuclease-free dH_2O.

2.2.2.2 Generating crude and secondary adenoviral stocks

Table 2.8 Cell density of HEK 293A cell line

12-well plate (cells/well)	6-well plate (cells/well)	10 cm dish (cells/dish)
5.0×10^5 (for viral titering)	**5.0×10^5**	**3.0×10^6**

Each well of a 6-well tissue culture plate was seeded with HEK 293A cells, at a density as mentioned in Table 2.8, in 2 mL complete medium and incubated in a humidified 37ºC, 5% (v/v) CO_2 Sanyo MCO-17AC cell culture incubator for 24 h, after which the culture medium was replaced with fresh complete medium (1.5 mL). For each *PacI*-digested product, 1 µg of linearised plasmid was diluted with 250 µL of Opti-MEM® and gently mixed by pipetting. Separately, 3 µL of Lipofectamine™ 2000 was diluted in 250 µL of Opti-MEM® for each plasmid, mixed gently and incubated at room temperature for 5 min. After this, the diluted Lipofectamine™ 2000 solution was combined with each diluted plasmid to result in a 500 µL transfection mix and gently mixed, prior to incubation at room temperature for 20 min, to enable the formation of liposome-nucleic acid complexes. The transfection mix was then added drop-wise to each well, the culture plate was gently swirled to ensure even distribution and the cells were incubated in the cell culture incubator for 24 h. After this incubation period, the transfection medium was removed from the cells and replaced with 2 mL complete medium. Every 48-72 h, cells were replenished with 2 mL fresh complete medium until approximately 80% cytopathic effect was observed at which point adenovirus-containing cells were harvested by squirting cells and media off the plate with a tissue culture pipette and transferred to a sterile, 15 mL capped tube.

The harvested adenovirus-containing cells were then subjected to three freeze/thaw cycles (freeze at -80ºC for 30 min followed by thawing in a 37ºC water bath for 15 min) causing the cells to lyse and release the intracellular viral particles to result in a crude viral lysate. The viral lysate was then centrifuged at 3000 rpm for 15 min at room temperature to pellet the cell debris and the supernatant containing the crude viral particles was transferred into cryovials in 1 mL aliquots at stored at -80ºC.

The crude viral lysate was used to generate an amplified secondary stock for purification and titering. For each adenovirus, HEK 293A cells were seeded at a density as mentioned in Table 2.8 on a 10 cm cell culture dish, in 10 mL of complete medium for 24 h at 37ºC. Each dish was then infected with the drop-wise addition of 100 µL of crude adenoviral stock, swirled gently to mix and then incubated at 37ºC for 72 h. The adenovirus-containing cells were harvested with a tissue culture pipette and transferred with the media to a sterile, 15 mL capped tube, prior to three freeze/thaw cycles, centrifugation and transferring and storing the supernatant containing viral particles, as described above.

2.2.2.3 Purifying and concentrating adenoviral stocks

To purify each adenovirus construct, HEK 293A cells were seeded on 6 x 10 cm cell culture dishes at a density as previously mentioned in Table 2.8, in 7 mL of complete medium per dish, for 24 h at 37ºC. Cells were then infected with the secondary adenoviral stock as described in Section 2.2.2.2 and incubated at 37ºC until 80-90% cytopathic effect was observed. Infected cells were harvested with a tissue culture pipette and centrifuged at 3,500 x g for 15 min to pellet the cells. The supernatant was decanted into a sterile container and set aside, however 2 mL of the supernatant was used to resuspend the cell pellet prior to subjecting the cells to three freeze/thaw cycles. The cells were then centrifuged as before to pellet the cell debris and the viral supernatant was recombined with the original supernatant and gently mixed.

The adenoviruses were purified using reagents and materials provided with the Vivapure® AdenoPACK™ 20 (Sartorius UK). Benzonase® was added to each culture to result in a final concentration of 12.5 U/mL, mixed well and incubated at 37ºC for 30 min to enable the digestion of cellular nucleic acids. The digested supernatant was then loaded onto a Vivaclear Maxi and centrifuged at 500 x g for 30 min at room temperature. The flow-through was collected and measured, to which 1/9 volume of loading buffer (10x) was slowly added under agitation, to prevent osmotic shock to the viral particles. Each adenoviral sample was then added to separate, equilibrated AdenoPACK 20 Maxi columns, centrifuged at 500 x g for 30 min and the flow-through discarded. The columns were washed twice with Washing Buffer (1x; diluted from 10x) and centrifuged at 500 x g for 5 min, removing the flow-through each time.

The adenoviruses were eluted off the membrane, by addition of 1 mL Elution Buffer, centrifugation at 500 x g for 30 s, 10 min incubation, followed by centrifugation at 500 x g for 5 min. The adenoviruses were dialysed with 9 mL PBS containing 2.5% glycerol (v/v) on Vivaspin 20 centrifugal concentrators and centrifuged at 800 x g for 30 min, concentrating the adenoviruses to a volume of approximately 200 µL.

2.2.2.4 Titering adenoviral stocks

A viral titer of optical particle units (opu) was obtained by diluting 2 µL of each adenovirus with 8 µL PBS containing 0.1% (v/v) SDS, determining the absorbance at 260 nm (OD_{260}) by spectrophotometry and using the following calculation:

$$OD_{260} \times 5 \text{ (dilution factor)} \times (1.1 \times 10^9) = \text{viral titer (opu/µL)}$$

A viral titer of infectious units (ifu) was obtained by following the Adeno-X Rapid Titer Kit protocol. In brief, HEK 293A cells were seeded on a 12-well plate at a density as mentioned in Table 2.8, in 1 mL complete medium and infected with 100 µL of 10-fold serial dilutions of the viral samples for 48 h. Infected cells were then fixed with ice-cold 100% methanol and probed with an anti-hexon antibody and its corresponding secondary (HRP-conjugated) antibody. Each well was then treated with DAB (3,3'-diaminobenzidine) substrate to develop the brown/black colour for positive-infected cells and washed with PBS Cell Wash (Table 2.6) before quantification using a 20X objective and applying the following calculation to result in a viral titer of ifu/µL:

$$\frac{\textit{(\# infected cells/field) x 594 (fields/well)}}{\textit{100 µL (volume of virus) x } 10^{-6}\textit{ (dilution factor)}}$$

Complete adenoviral FLAG-ERK5 sequence and final viral titer is provided in Appendix I.

2.2.3 Cell culture

2.2.3.1 Sterile cell culture technique

Cells were cultured in sterile conditions at all times. A Howie coat and nitrile gloves were worn and sterile cell culture equipment were used within a TriMAT^2 Class II microbiological safety cabinet. All work surfaces were disinfected using 70% (v/v) ethanol before and after cell culture work. Prior to use, culture media were warmed to 37ºC in a water bath. Cells were maintained at a humidified 37ºC, 5% (v/v) CO_2 Sanyo MCO-17AC cell culture incubator.

2.2.3.2 Gelatin-coating of cell culture materials

HDMEC were cultured or seeded on gelatin-coated dishes, plates or coverslips. Sterile dishes, plates and 16 mm coverslips were coated with 0.5% (w/v) gelatin and incubated in the cell culture incubator for at least 5 min prior to use. Gelatin was aspirated prior to plating out HDMEC.

2.2.3.3 Thawing of cryopreserved cell stocks

Cryopreserved cells were stored in vapour phase Nitrogen (approximately -135ºC). Cryovials were thawed for 2-3 min in a 37ºC water bath, disinfected with 70% (v/v) ethanol and the cells were transferred into a 15ml capped tube containing 9 mL of pre-warmed, appropriate culture medium (full growth/complete medium). Cells were pelleted by centrifugation at 1000 rpm for 5 min, the supernatant was aspirated off and the cells were resuspended in 10 mL culture medium. Cells were transferred to a 10 cm gelatin-coated dish (HDMEC) or non-gelatinised T-75 cm^2 flask (all other cell types) then incubated for 24 h, after which the cell culture medium was replaced with 10 mL fresh culture medium.

2.2.3.4 Routine culture of cells

As previously mentioned, cells were maintained in their appropriate full growth/complete medium in a cell culture incubator. HDMEC were cultured on gelatin-coated 10 cm^2 dishes, whereas all other cells were cultured in T75 cm^2 flasks.

Cells that reached 80-90% confluency, approximately 2-3 days after seeding, were split to the next *passage*. Each 10 cm^2 dish or T75 cm^2 flask of cells was washed with 6-10 mL Versene (Table 2.6) and treated with 1-3 mL of Trypsin (Table 2.6), respectively and returned to the incubator for 3-5 min. After this time, 95-100% of the cells will have detached (which can be observed under a light microscope) and cells were resuspended in their appropriate cell culture medium, homogenised with vigorous pipetting and reseeded in the splitting ratio as described in Table 2.9.

Table 2.9 Cell splitting ratio

Cell type	Culture medium	Splitting ratio
HDMEC	Full growth medium	1:6
HeLa	Complete medium	1:5
MAE (all variants)	Complete medium	1:10
HEK 293A	Complete medium	1:5

2.2.3.5 Cell counting and seeding

Cells were counted to ensure an accurate number of cells were seeded for experiments. Trypsin was used to detach cells from the culture dish or flask, as described in Section 2.2.3.4 and cells were resuspended in 7 mL of their appropriate culture medium. 100 µL of cells was pipetted onto a Neubauer haemocytometer (Sondheim, Germany) for counting.

The original cell density was calculated as follows:

Number (#) of cells counted = cells per 0.1 mm^3

∴ # of cells counted x 10,000 = cells per 1 cm^3 i.e. cells / mL

Multiply by 8 mL = total # of cells

The cell number for experiments may then be calculated. Cells were then transferred into a fresh capped tube, centrifuged at 1000 rpm for 5 min, the medium aspirated and cells resuspended in the required volume of appropriate culture medium.

To ensure reproducibility, cells were seeded for protein analysis experiments as denoted in Table 2.10 and immunofluorescence analysis experiments in Table 2.11.

Table 2.10 Cell density for protein analysis experiments

Cell type	12-well plate (cells/well) in 1 mL of media	6-well plate (cells/well) in 2 mL of media	10 cm dish (cells/dish) in 8 mL of media
HDMEC	5.0×10^4	1.0×10^5	4.0×10^5
HeLa	6.5×10^4	1.3×10^5	5.2×10^5
MAE (all)	5.0×10^4	1.0×10^5	N/A

Table 2.11 Cell density for immunofluorescence experiments

Cell type	12-well plate (cells/well) in 1 mL of media
HDMEC	3.0×10^4
HeLa	4.0×10^4

2.2.4 Cell treatments

2.2.4.1 Cell infection with adenoviral expression vectors

HDMEC and HeLa were routinely infected in 6-well plates for Western immunoblotting (Section 2.2.9), or 10 cm dishes for mass spectrometry (Section 2.2.8). Cells were seeded at the appropriate density as described in Table 2.10 in full growth medium or complete medium respectively, and incubated for 24 h at 37ºC. Adenoviral expression vectors were diluted from their stock solution in full growth medium or complete medium to the desired

multiplicity of infection (MOI; ratio of infectious units to the number of cells) using the following calculation:

 # cells x desired MOI = # infectious units (ifu)

 # ifu / viral titer (ifu/µL) = # µL stock virus needed for desired MOI

Cells were then infected with drop-wise addition of the diluted virus, the cell culture plates were gently swirled to ensure even distribution, and incubated at 37ºC for 30 h. Following this incubation, cells were washed with PBS Cell Wash and serum starved overnight in 1% low serum medium or 0.1% low serum medium respectively, prior to agonist stimulation (Section 2.2.4.4) and cell lysis (Section 2.2.4.5).

2.2.4.2 Cell transfection with small interfering RNA (siRNA)

A list of siRNA duplexes used in this study can be found in Appendix II.

HDMEC and HeLa were routinely transfected in 6-well plates for protein analysis by Western immunoblotting and thus were seeded at a density as described in Table 2.10 in their appropriate culture medium respectively, and incubated at 37ºC for 24 h. Lipofectamine™ RNAiMAX transfection reagent was diluted to give a final concentration of 0.2% (v/v) in 250 µL of Opti-MEM® and in a separate microcentrifuge tube, siRNA stock solution (20 µM) was diluted to a final concentration of 10 nM in 250 µL of Opti-MEM®. These two components were incubated separately for 5 min at room temperature, then combined and mixed by gentle pipetting to result in a 500 µL transfection mix which was then incubated at room temperature for 30 min to enable the formation of the liposome-nucleic acid complexes. Media on the cells was replaced accordingly with 2 mL of fresh full growth medium or complete medium, prior to drop-wise addition of the siRNA transfection mix and gentle swirling of the cell culture plate to ensure even distribution. Cells were incubated at 37ºC for 6 h with the transfection mix, after which they were washed twice with 2 mL PBS Cell Wash, and incubated with 2 mL full growth medium or complete medium for a further 24 h at 37ºC. Following this 24 h incubation, cells were washed with PBS Cell Wash and serum starved overnight in 1% low serum medium or 0.1% low serum medium respectively, prior to treatment with inhibitors (Section 2.2.4.3) and/or agonist stimulation (Section 2.2.4.4) and cell lysis (Section 2.2.4.5).

For experiments conducted on 12-well plates, all volumes were halved i.e. 125 µL of Opti-MEM® per incubation, resulting in a 250 µL transfection mix in 1 mL of media.

2.2.4.3 Intracellular kinase inhibition using small-molecule inhibitors

The small-molecule kinase inhibitors used in this study, BIX 02189 and XMD8-92, were diluted in sterile dimethylsulphoxide (DMSO) into stock solutions of 50 mM and 30 mM respectively, and stored in aliquots at -80ºC. For experimental use, the inhibitors were thawed and either diluted in DMSO or appropriate low serum medium to result in 0.1% (v/v) final concentration of DMSO in each case. Furthermore, 0.1% (v/v) DMSO in appropriate low serum medium was utilised as a vehicle control, as DMSO had no observed effects on the cells at this concentration. Cells were pre-incubated with vehicle control or inhibitor medium for 1 h, prior to agonist stimulation (Section 2.2.4.4) and cell lysis (Section 2.2.4.5). Cells were treated with varying concentrations of inhibitors, the specifics of which are provided in the text for individual experiments.

2.2.4.4 Agonist stimulation of cells

As previously mentioned, prior to agonist stimulation, cells were serum starved overnight at 37ºC, in their appropriate low serum medium. A list of the growth factors used in experiments can be found in Section 2.1.2. The two most commonly used growth factors in these experiments were vascular endothelial growth factor (VEGF) to stimulate HDMEC and epidermal growth factor (EGF) to stimulate HeLa cells. All growth factors were initially diluted in sterile-filtered PBS containing 0.1% (w/v) BSA to 100 mg/mL stock concentrations and stored in aliquots at -80ºC. For experimental use, growth factors were thawed and diluted in appropriate low serum medium to 50 ng/mL final concentration, unless otherwise stated in the text. Cells were incubated with various agonists for different lengths of time, thus the specifics of these are provided in the text for each experiment.

2.2.4.5 Cell lysis – Protein extraction

Protein lysates were prepared by placing cell culture plates on ice, prior to washing cells twice with ice-cold PBS Lysis Wash (Table 2.6). Unless otherwise stated in the text, lysates for Western immunoblotting were generated with the addition of modified radio-immunoprecipitation assay (RIPA) lysis buffer and lysed cells were scraped and transferred into microcentrifuge tubes. Protein lysates were centrifuged at 14,000 rpm for 20 min at 4ºC, prior to being transferred into fresh, pre-chilled microcentrifuge tubes and mixing samples with 1/3 volumes of 4x LDS. Protein samples were then boiled at 90ºC for 5 min, vortexed and frozen at -80ºC for at least 1 h before their use in Western immunoblotting (Section 2.2.9).

Constituents of RIPA lysis buffer:

20 mM Tris-HCl; pH 7.5, 150 mM NaCl, 2.5 mM EDTA, 10% (v/v) glycerol, 1% Triton-X-100, 1 mM Na_3VO_4, 10 µg/mL aprotinin, 10 µg/mL leupeptin, 10 µg/mL pepstatin, 1 mM PMSF, 0.1% (w/v) SDS and 0.5% (w/v) sodium deoxycholate.

Protein lysates for immunoprecipitation and mass spectrometry were produced with the addition of sucrose lysis buffer and lysed cells were scraped and transferred into microcentrifuge tubes. Lysates were then centrifuged at 14,000 rpm for 20 min at 4ºC, prior to being transferred into fresh, pre-chilled microcentrifuge tubes and proceeding with the immunoprecipitation protocol (Section 2.2.7).

Constituents of sucrose lysis buffer:

250 mM Tris-HCl; pH 7.6, 1 mM $MgCl_2$, 1 mM ß-mercaptoethanol, 0.1% (v/v) Triton-X-100, 1 mM Na_3VO_4, 10 µg/mL aprotinin, 10 µg/mL leupeptin, 10 µg/mL pepstatin, 1 mM PMSF.

2.2.5 Subcellular protein fractionation

HDMEC and HeLa were seeded on sterile 10 cm dishes at a density as denoted in Table 2.10 for 48 h in full growth medium or complete medium, respectively. Cells were then serum starved overnight in their appropriate low serum medium, prior to agonist stimulation, washing with ice-cold PBS Lysis Wash and harvesting cells with Trypsin. Cells were then pelleted by centrifugation at 500 x g for 5 min at 4ºC, washed with ice-cold PBS Lysis Wash, repelleted in fresh, pre-chilled microcentrifuge tubes and the supernatant discarded. The cell pellet was kept on ice prior to commencing with the protocol as provided in the Subcellular Protein Fractionation Kit for Cultured cells (purchased from Thermo Fisher Scientific™; Loughborough, UK).

Unless otherwise stated, all extraction buffers contained protease inhibitors, all incubations and centrifugations were at 4ºC, incubations involved gentle, rotary mixing and all extraction samples were kept on ice in fresh, pre-chilled microcentrifuge tubes. In brief, the procedure involved ice-cold cytoplasmic extraction buffer (CEB) being added to and incubated with the cell pellet for 10 min, after which the sample was centrifuged at 500 x g for 5 min and the supernatant (cytoplasmic extract) was transferred to a fresh tube. Ice-cold membrane extraction buffer (MEB) was then added to the pellet, vortexed for 5 s and incubated for 10 min prior to centrifugation at 3000 x g for 5 min. The supernatant (membrane extract) was transferred to a fresh tube, and nuclear extraction buffer (NEB) was added to the pellet, vortexed for 15 s and incubated for 30 min.

Centrifugation of the sample at 5000 x g for 5 min, separated the soluble nuclear extract into the supernatant and was transferred to a fresh tube, after which chromatin-bound extraction buffer (room temperature NEB containing 100 mM $CaCl_2$ and 300 units Micrococcal Nuclease – both provided in the kit) was added to the pellet, vortexed for 15 s and incubated in a 37ºC water bath for 5 min. Further vortexing for 15 s, followed by centrifugation at 16,000 x g for 5 min, enabled the supernatant (chromatin-bound nuclear extract) to be transferred to a fresh tube prior to adding room temperature pellet extraction buffer to the cell pellet, vortexing for 15 s and incubation at room temperature for 10 min. A final centrifugation at 16,000 x g for 5 min separated the cytoskeletal extract into the supernatant which was transferred to a fresh tube. Subcellular protein fractions were mixed with 1/3 volumes of 4x LDS, boiled at 90ºC for 5 min, vortexed and frozen at -80ºC for at least 1 h before their use in Western immunoblotting.

2.2.6 Immunofluorescence

2.2.6.1 Cell staining

HDMEC and HeLa cells were seeded on sterile 16 mm glass coverslips, placed within wells of a 12-well plate, at a density as mentioned in

Table 2.11, for 48 h in full growth medium or complete medium respectively. Cells were then serum starved overnight in their appropriate low serum medium, prior to agonist stimulation, washing cells with ice-cold PBS Lysis Wash and cell fixation and permeabilisation with ice-cold methanol for 10 min at -20ºC. Unless otherwise stated in the text, all subsequent washes were with Tris-buffered saline (TBS; 20mM Tris, 0.137M NaCl) containing 0.1% (v/v) Tween-20 (TBS-T) and all washes and incubations were at room temperature with gentle rotation. Each well was initially washed three times with PBS Cell Wash, 5 min each, after which cells were incubated with blocking buffer (TBS-T containing 1% (w/v) BSA and 5% (v/v) donkey serum) for 1 h. Cells were washed once prior to their incubation with primary antibodies, which were made up in TBS-T containing 1% (w/v) BSA, at a dilution as denoted in Table 2.1 and Table 2.2, for 1 h. Each well was then washed three times and incubated with the appropriate fluorescent-labelled secondary antibodies, which were made up in TBS-T containing 1% (w/v) BSA at a dilution as mentioned in Table 2.3 for 1 h in the dark. Cells were then washed twice, and Hoechst diluted in TBS-T containing 1% (w/v) BSA (Table 2.3) was added to the cells and incubated for 10 min in the dark, after which cells were washed three times.

2.2.6.2 Image acquisition and analysis

The glass coverslips were then carefully removed from the wells using forceps and mounted onto glass slides, using ProLong® Gold antifade reagent and sealed with clear nail varnish. Samples were stored in the dark at 4ºC until observation using an inverted Zeiss Axio Observer microscope, with Filter Sets 49 (DAPI/Hoechst; #488049-9901=000), 38 (GFP/FITC/Alexa 488; #000000-1031-346) and 31 (Alexa 568; #000000-1031-350) and the associated Zen software for image acquisition.

2.2.7 Immunoprecipitation

Unless otherwise stated, all incubations and washes were conducted at 4ºC, under rotation and all centrifugations were at 4ºC. Primary antibodies that were not pre-conjugated to agarose beads, were incubated for 8 h with Protein G Plus in Wash/Binding buffer (25 mM Tris, 150 mM NaCl; pH 7.2) containing 0.1% (w/v) BSA, at the dilutions mentioned in Table 2.1 and Table 2.2. Primary antibody-coupled-agarose beads were then centrifuged at 13,300 rpm for 1 min and the blocking buffer supernatant discarded. Protein lysates generated as described in Section 2.2.4.5, were then added to the primary antibody-coupled-agarose beads and incubated overnight, with end-over-end mixing at 4ºC. The samples were centrifuged at 13,300 rpm for 5 min, the supernatant removed and kept aside on ice, and the beads were then washed three times with Wash buffer for 5 min each. Samples for mass spectrometry were further washed twice with 25 mM ammonium bicarbonate, a fraction taken out for Western blotting and silver staining, and stored in 100 µL of ammonium bicarbonate at -80ºC prior to running samples on a mass spectrometer (Ultimate 3000 RSLC™ nano system coupled to a QExactive™ mass spectrometer; both Thermo Scientific). Samples for Western blotting were mixed with 1 volume of 2x LDS sample buffer, boiled at 90ºC for 5 min, vortexed, centrifuged for 30 s and stored at -80ºC for at least 1 h, prior to use.

2.2.8 Mass spectrometry (LC-MS/MS)

In order to identify proteins prior to analysis by mass spectrometry, samples were initially evaluated using SDS-PAGE (2.2.9.1), followed by Western blotting (0) and silver staining (2.2.8.1).

2.2.8.1 Silver staining

The SilverQuest™ Silver Staining kit (Life Technologies) was utilised, only ultrapure water was used and all incubations were performed on a rotary shaker at a speed of 1 revolution/sec at room temperature.

After electrophoresis, the gel was removed from the cassette and placed in a clean staining tray. The gel was briefly rinsed with water prior to incubating it with 100 mL of fixative (40% (v/v) ethanol, 10% (v/v) acetic acid) for 20 min. The fixative was discarded and the gel was washed with 30% (v/v) ethanol for 10 min, after which the gel was incubated with 100 mL of Sensitizing solution for 10 min. The Sensitizing solution was then removed and the gel was washed with 100 mL of 30% (v/v) ethanol for 10 min, followed by 100 mL of water for 10 min. The gel was then incubated with 100 mL of Staining solution for 15 min, after which the gel was washed with 100 mL of water for 30 sec. To develop the gel, 100 mL of Developing solution was added to the gel and incubated for up to 8 min until the desired band intensity had been reached, at which point 10 mL of Stopper solution was added to the gel (still submerged in Developing solution) and the colour change from pink to colourless indicated the development had stopped. The gel was washed with 100 mL of water for 10 min and scanned using an Epson® 4490 photo scanner.

2.2.8.2 Proteomic analysis

The label-free analysis was performed by Professor Rob Beynon's Proteomics Group (Institute of Integrative Biology, University of Liverpool, Crown Street, Liverpool L69 7ZB) using an UltiMate 3000 RSLC™ nano system (Thermo Scientific) coupled to a QExactive™ mass spectrometer (Thermo Scientific). The sample was loaded onto the trapping column (Thermo Scientific, PepMap100, C18, 75 µm x 20 mm) using partial loop injection for seven minutes at a flow rate of 4 µL/min with 0.1% (v/v) formic acid (FA). The sample was resolved on the analytical column (Easy-Spray, C18, 75 µm x 500 mm, 2 µm column) using a gradient of 97% solution A (0.1% FA) : 3% solution B (99.9% acetonitrile (ACN), 0.1% FA) to 60% solution A : 40% solution B over 240 min at a flow rate of 300 nL/min. The program used for data acquisition consisted of 70,000 resolution full-scan MS scan and the 10 most abundant peaks were selected for MS/MS. Database searching was performed using MASCOT (Matrix Science). A p-value of 0.05, the built in MASCOT decoy search, reported a peptide false discovery rate (FDR) of 0.5%. The data was processed with Progenesis (version 4, Nonlinear Dynamics, Newcastle-upon-Tyne, UK).

2.2.9 Western immunoblotting

2.2.9.1 SDS-PAGE

Sodium dodecyl sulphate polyacrylamide gel electrophoresis (SDS-PAGE) was carried out using pre-cast, 15-well NuPAGE® Novex® 4-12% Bis-Tris polyacrylamide gels in the XCell *SureLock*™ Mini-Cell electrophoresis system, with 800 mL 1x MOPS running buffer (0.05 M MOPS, 0.05 M Tris, 1 mM EDTA, 0.1% (v/v) SDS). The Mini-Cell running unit was loaded with 1 or 2 pre-cast gels, placed into the tank and secured into position by locking the tension wedge. The loading chamber was then filled with MOPS buffer to ensure there were no leaks, after which the combs were removed and each well rinsed out with MOPS buffer to remove any unpolymerised acrylamide. Protein lysates in LDS were prepared as previously described in Section 2.2.4.5, of which up to 25 µL was loaded into each well, with the first well of every gel being loaded with 3 µL of full-range rainbow marker mixed with 22 µL 1x LDS sample buffer. After all the samples were loaded, the remaining MOPS buffer was poured into the tank, the lid was placed on to the running unit and the tank connected to a power supply prior to running the gels at constant amperage of 50 mA, 250 V, 15 W for up to 2 h.

Following electrophoresis, the Mini-Cell was disassembled, the plastic cassettes containing electrophoresed NuPAGE® gels were opened and the stacking gel and 'foot' of the gel discarded. The resolving gel was then allowed to equilibrate in 25 mL 1x Tris-Glycine transfer buffer (12 mM Tris, 96 mM glycine, 20% (v/v) methanol) prior to transferring the proteins onto nitrocellulose membrane.

2.2.9.2 Phos-tag™ SDS-PAGE

The Phos-tag™ Acrylamide reagent was utilised in order to enable specific monitoring of phosphorylated proteins. This resulted in a retarded mobility and a distinct upward band shift of the phosphorylated form, from the non-phosphorylated protein, thus permitting the use of a total antibody to detect both the phosphorylated and non-phosphorylated forms.

Phos-tag™ gels were set up and run using the Bio-Rad Mini-PROTEAN® Tetra Cell electrophoresis system, whereby a 1.5 mm glass spacer plate was assembled with a glass short plate in the gel casting unit. Each Phos-tag™ resolving gel was made up in the order as mentioned in Table 2.12, leaving the addition of the APS and TEMED solutions, until just prior to the resolving gel solution being poured between the glass plates.

Table 2.12 Composition of 7% Phos-tag™ SDS-PAGE gels

	Resolving gel	Stacking gel
Resolving gel buffer (1.5 M Tris-HCl, pH 8.8, 0.4% (v/v) SDS	2.5 mL	N/A
Stacking gel buffer (0.5 M Tris-HCl, pH 6.8, 0.4% (v/v) SDS	N/A	2.5 mL
Ultrapure Protogel® solution (30% (w/v) Acrylamide, 0.8% (w/v) Bis-Acrylamide (37.5:1))	2.3 mL	1.3 mL
$MnCl_2$ (10mM)	210 µL	N/A
Phos-tag™ Acrylamide reagent (5mM; 3% (v/v) MeOH)	140 µL	N/A
dH_2O	4.85 mL	6.2 mL
APS (10% (w/v) in dH_2O)	100 µL	100 µL
TEMED	10 µL	10 µL

On top of each gel, 300 µL dH_2O was gently pipetted to eliminate air bubbles and ensure an even edge to the top of the gel, and the gel was left to polymerise for 1 h. Following polymerisation, the dH_2O was poured off and the excess blotted, before adding the stacking gel (Table 2.12) and immediately inserting a 15-well, 1.5 mm comb. The stacking gel was then allowed to polymerise for 1 h. The Tetra Cell running units were loaded with 2 gels or 4 gels, positioned within the tank and each loading chamber filled with 1x SDS running buffer (0.025 M Tris-HCl, 0.192 M glycine, 0.1% (v/v) SDS; pH 8.3) to ensure there were no leaks. Following this, the combs were removed and each well flushed out with SDS buffer to remove any unpolymerised acrylamide, prior to loading the samples in each well, with the first well of every gel being loaded with 12.5 µL prestained protein marker. After loading all the samples, the remaining SDS buffer was poured into the tank, the lid placed on to the running unit and connected to a power supply, prior to running the gels at constant amperage of 8 mA or 16 mA, 250V, 15 W for 22 h.

The manganese ions present in the Phos-tag™ gels act as a cofactor and enable the formation of a stable complex with the phosphate group of the proteins during electrophoresis. However, after electrophoresis these ions must be eliminated from the gel in order to increase the efficiency at which the proteins can be transferred onto nitrocellulose membrane.

The Tetra Cell was disassembled, the glass plates containing electrophoresed Phos-tag™ gels were opened and the stacking gel and 'foot' of the gel discarded. The resolving gel was carefully placed into 25 mL 1x transfer buffer containing 100 mM EDTA and gently agitated for 10 min. Following this, the EDTA transfer buffer was poured off and the gel was gently agitated for a further 10 min in 25 mL fresh 1x transfer buffer.

2.2.9.3 Western blot analysis

Proteins resolved by SDS-PAGE or Phos-tag™ SDS-PAGE, were transferred onto nitrocellulose membrane using the XCell II™ Blot Module. Sponges provided with the blotting unit were pre-soaked in 1x transfer buffer, along with nitrocellulose membrane cut to 7.5 cm x 8.5 cm. The two electrophoresed gels were sandwiched between pre-soaked filter papers cut to 7.5 cm x 8.5 cm, and these two stacks were placed on top of one another but separated by a pre-soaked sponge. This stack in turn was placed upon another pre-soaked sponge within the blotting unit. A further three pre-soaked sponges were placed on top of the stack, followed by the unit lid, after which the blotting unit was placed into the Mini-Cell tank and secured into position with the tension wedge. The blotting chamber was then filled with 1x transfer buffer, the rest of the tank with cold dH_2O and the lid was placed on top prior to transferring the proteins at a constant amperage of 140 mA or 125 mA, 300 V, 15 W for 2 h.

Nitrocellulose membranes with transferred proteins were briefly washed with 1x TBS-T to remove any traces of methanol, which would impede antibody binding. Membranes were then incubated, with gentle rocking, in 25 mL of blocking buffer (5% (w/v) BSA in TBST) at room temperature for 1 h to block non-specific antibody binding sites. Membranes were then incubated with the appropriate primary antibody diluted in 2% (w/v) BSA in TBS-T (as described in Table 2.1 and Table 2.2) at 4ºC for 16 h with gentle agitation. Following incubation with the primary antibody, membranes were washed six times with 1x TBS-T for 10 min with gentle rocking, prior to incubation with the appropriate horseradish peroxidase (HRP)-linked secondary antibody diluted in 2% (w/v) BSA in TBS-T (Table 2.3) at 4ºC for 1.5 h, with gentle agitation. Membranes were then washed for 10 min each time – five washes with 1x TBS-T, followed by a wash with 1x TBS, prior to incubating the membrane with a 1:1 mixture of enhanced chemiluminescence (ECL) reagent 1 and reagent 2 at room temperature for 2 min. The membranes were then encased in a plastic sleeve within an X-ray film cassette and taken into a darkroom before exposing them to X-ray films for various lengths of time, developing and fixing the films.

2.2.9.4 Quantification of protein expression by densitometry

Developed X-ray films were scanned using an Epson® 4490 photo scanner and the image imported into ImageJ (http://imagej.nih.gov/ij/). The image was grey-scaled and the colour inverted to remove any background interference, after which a box set to the size of the largest band was positioned over each band to measure the relative intensity (a setting within the program). To correct for protein loading, the quantified protein of interest band was then related back to its corresponding, quantified Actin band. The untreated control sample in each experiment was assigned an arbitrary value of 1.0, to which bands from all other conditions were relatively expressed.

2.2.9.5 Statistical analysis

Densitometric values from Western blot experiments that had been repeated three or more times were subjected to statistical analysis. A repeated measures ANOVA was performed in SPSS 20 on densitometric values to determine the overall significant difference in the means of the experimental conditions. In the case of sphericity violation ($p<0.05$ in Mauchly's Test of Sphericity), a Greenhouse-Geisser correction was utilised. A post hoc test using the Bonferroni correction allowed for pair-wise comparison of each experimental condition to the basal control condition, in order to determine which specific means significantly differed. The means are presented as bar charts with standard deviation bars. The significance levels $p<0.05$, $p<0.01$ or $p<0.001$ were applied accordingly to each experiment and any significant differences were indicated with asterisks.

Chapter Three
Characterisation of ERK5 activation

3.1 Introduction

The ERK5 protein is ubiquitously expressed in various tissues and cell lines (Regan *et al.*, 2002; Yan *et al.*, 2003; Buschbeck and Ullrich, 2005) but studies suggest that ERK5 may play different, yet specific roles in particular cell types (Sohn *et al.*, 2002; Hayashi and Lee, 2004; Wang *et al.*, 2005; Wang and Tournier, 2006; Spiering *et al.*, 2009). As such, ERK5 has been implicated in the regulation of cell adhesion, differentiation, migration, proliferation and survival in various cellular contexts (Kato *et al.*, 1998; Dinev *et al.*, 2001; Wang and Tournier, 2006; Carter *et al.*, 2009; Sawhney *et al.*, 2009). Additionally, the progression of certain pathologies including cancer, cardiac hypertrophy and ischemia implicate a pivotal role for ERK5 (Takeishi *et al.*, 1999; Wang and Tournier, 2006; Montero *et al.*, 2009).

The physiological role of ERK5 was highlighted with experiments utilising gene ablation of components of the ERK5 signalling pathway in mice (Hayashi and Lee, 2004), and as previously discussed, it was apparent that *Erk5*$^{-/-}$ (Regan *et al.*, 2002; Sohn *et al.*, 2002; Yan *et al.*, 2003), *Mek5*$^{-/-}$ (Wang *et al.*, 2005) and *Mekk3*$^{-/-}$ (Yang *et al.*, 2000) deficient mice died around E9.5-11.5 due to severe defects in the vasculature. Subsequent studies utilised conditional tissue-specific *Erk5* knockout mice; developmental defects similar to those observed in the global *Erk5*$^{-/-}$ mice were also detected with endothelial-specific *Erk5* knockout mice (Hayashi *et al.*, 2004). However, the cardiomyocyte and hepatocyte *Erk5* knockouts did not affect development (Hayashi *et al.*, 2004; Hayashi and Lee, 2004), thus revealing the significant role of ERK5 in endothelial cell development and survival.

The activation of ERK5 in endothelial cells was initially investigated using H_2O_2 to stimulate HUVECs whereby it was demonstrated that oxidative stress was able to activate ERK5 (Abe *et al.*, 1996). Following this, Yan and colleagues showed that ERK5 could be stimulated by fluid shear stress in bovine aortic endothelial cells (BAECs) (Yan *et al.*, 1999). In the same study, the pro-angiogenic molecules VEGF and FGF-2 were unable to induce ERK5 activity in the BAECs; however, it has since been shown in HUVECs that these same growth factors are able to stimulate ERK5 activation (Hayashi *et al.*, 2004). It has more recently been observed that ERK5 plays a unique role in HDMEC, regulating VEGF-mediated AKT activation and suppressing apoptosis to facilitate tubular morphogenesis of cells in a collagen gel (Roberts *et al.*, 2010).

Due to the vast structural and functional heterogeneity of endothelial cells across the vascular bed, studies into the role of ERK5 in endothelial cell function often present with conflicting data. Furthermore, EGF-stimulated HeLa cells have been utilised to date as a

benchmark for ERK5 activation in the context of tumour cell proliferation, suggesting a profound difference in ERK5 function between endothelial cells and HeLa cells. Thus, this chapter describes experiments performed in order to analyse the regulation of ERK5 activity between these two cell types.

This project utilises conventional and innovative methods of SDS-PAGE to identify the key differences in the intracellular ERK5 signalling of these cell types. Additionally, murine aortic endothelial (MAE) cell lines stably transfected with various Flk-1 receptor mutants, as well as small-molecule kinase inhibitors, were employed to define potential regulators and effectors of ERK5 and elucidate differences in agonist-dependent ERK5 phosphorylation.

3.2 Characterisation of ERK5 activation

3.2.1 Detection of ERK5 activity

After the initial discovery of ERK5 in 1995, the detection of ERK5 activation predominantly involved protein separation by SDS-PAGE with an 8% (w/v) acrylamide gel, followed by Western blotting using a polyclonal anti-ERK5 antibody (Duff *et al.*, 1995; Abe *et al.*, 1996; Abe *et al.*, 1997). This resulted in a 'bandshift' whereby phosphorylated ERK5 exhibited reduced electrophoretic mobility, thus migrating slower than the non-phosphorylated form of ERK5. However since then, many commercial antibodies against ERK5 have become readily available, as have pre-cast, gradient percentage acrylamide gels for SDS-PAGE.

A range of pro-angiogenic growth factors - VEGF, FGF-2, HGF, EGF, PDGF-BB and TGF-α – were utilised in order to assess the profile of ERK5 activation in HeLa and HDMEC, by means of a mobility bandshift. Following cell stimulation with the pro-angiogenic factors, cells were lysed with RIPA, and analysed by SDS-PAGE and Western blotting using an 8% (w/v) acrylamide gel and the commercially available ERK5 antibody (#3372; New England BioLabs, Hitchin, UK) respectively (Figure 3.1).

It was found that in HeLa cells, VEGF, FGF-2 and PDGF-BB did not stimulate ERK5 activation as only a single ERK5 band was detected, similar to that of the control basal condition (Figure 3.1a). However, stimulation with HGF, EGF and TGF-α resulted in an ERK5 mobility bandshift.

Individual quantification of the stimulated lower ERK5 and upper p-ERK5 mobility bands were compared to an arbitrary value of 1.0, set for both the ERK5 and p-ERK5 bands in the basal condition.

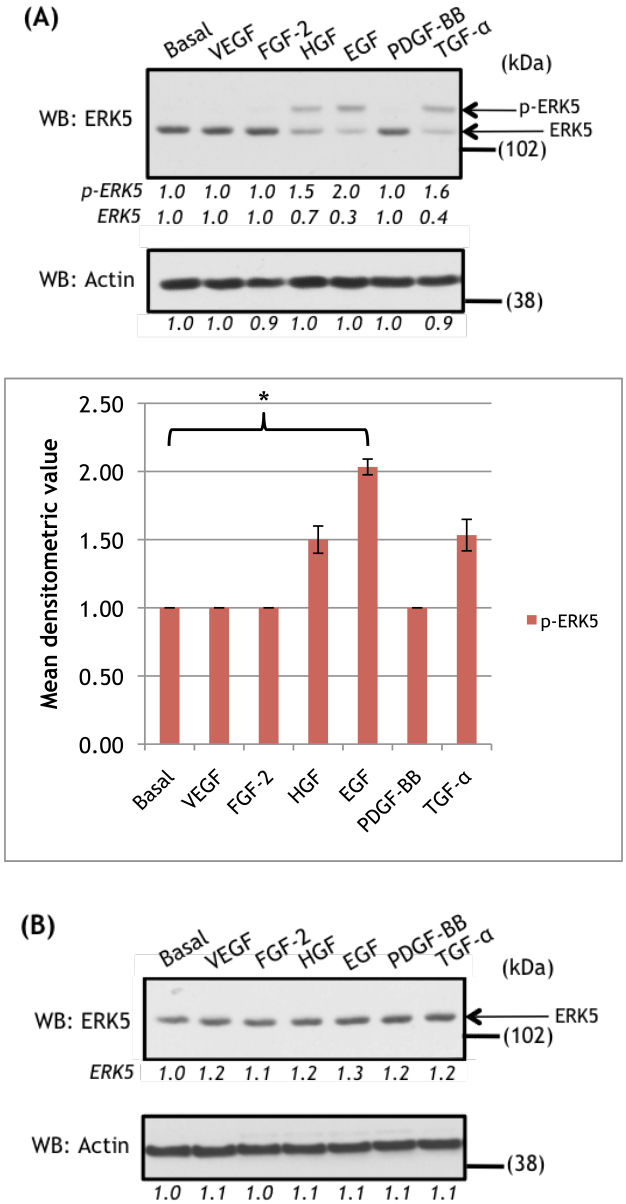

Figure 3.1 Characterisation of ERK5 activation by electrophoretic mobility bandshift.
(A) HeLa cells were seeded on 6-well plates for 24 h, prior to overnight serum starvation. Cells were stimulated with 50 ng/mL of VEGF, FGF-2, HGF, EGF, PDGF-BB or TGF-α for 10 min, followed by RIPA lysis. (B) HDMEC were seeded gelatin-coated 6-well plates for 24 h, followed by overnight serum starvation. Cells were stimulated with 50 ng/mL of VEGF, FGF-2, HGF, EGF, PDGF-BB or TGF-α for 10 min, and lysed with RIPA. Protein lysates from (A) and (B) were resolved on an 8% (w/v) acrylamide gel, followed by Western blotting (WB) with antibodies against ERK5 (#3372, NEB) and Actin (I-19, SCB) as a loading control. *Densitometric analysis of protein phosphorylation or protein expression relative to Actin is displayed beneath each blot. The basal control condition was set arbitrarily as 1.0. This result is representative of three independent experiments (*p<0.05).*

EGF stimulated ERK5 activation in HeLa to a greater degree than any other agonist (Figure 3.1a) and was statistically significant ($p<0.05$). HGF and TGF-α addition also led to increased ERK5 phosphorylation, but these two agonists did not activate ERK5 as effectively as EGF (Figure 3.1a).

In stark contrast to the HeLa cells, agonist stimulation of HDMEC followed by separation by SDS-PAGE and Western blotting, did not result in a mobility bandshift of ERK5 activation with any of the pro-angiogenic factors (Figure 3.1b). Therefore, in order to detect ERK5 activation in this cell type, phosphorylation of the Thr^{218}/Tyr^{220} residues of the T-E-Y motif present in the ERK5 activation loop (Zhou *et al.*, 1995) were probed with a commercially produced phospho-specific ERK5 (p-ERK5) antibody (#3371 New England Biolabs, Hitchin, UK).

3.2.2 Dual-phosphorylation of ERK5

The same agonist-stimulated HeLa and HDMEC lysates used in Figure 3.1 underwent SDS-PAGE on a 4-12% NuPAGE gel prior to Western blotting with the aforementioned Thr^{218}/Tyr^{220}-specific p-ERK5 antibody (Figure 3.2).

The use of this p-ERK5 antibody on the HeLa lysates confirmed the previous ERK5 activation results produced with the mobility bandshift, i.e. EGF was a potent activator of ERK5, as demonstrated by a two-fold increase compared to the control basal condition (Figure 3.2a).

Furthermore, HGF and TGF-α also stimulated ERK5 phosphorylation, but to a lesser degree. Once again, stimulation of HeLa with VEGF, FGF-2 and PDGF-BB had a negligible effect on the phosphorylation of ERK5.

The activation of ERK5 in HDMEC as detected by the p-ERK5 antibody, was only noticeably induced upon stimulation with VEGF (Figure 3.2b). VEGF stimulation evoked ERK5 phosphorylation 1.6 times that of the basal condition, whereas FGF-2, HGF, EGF, PDGF-BB and TGF-α only marginally phosphorylated ERK5.

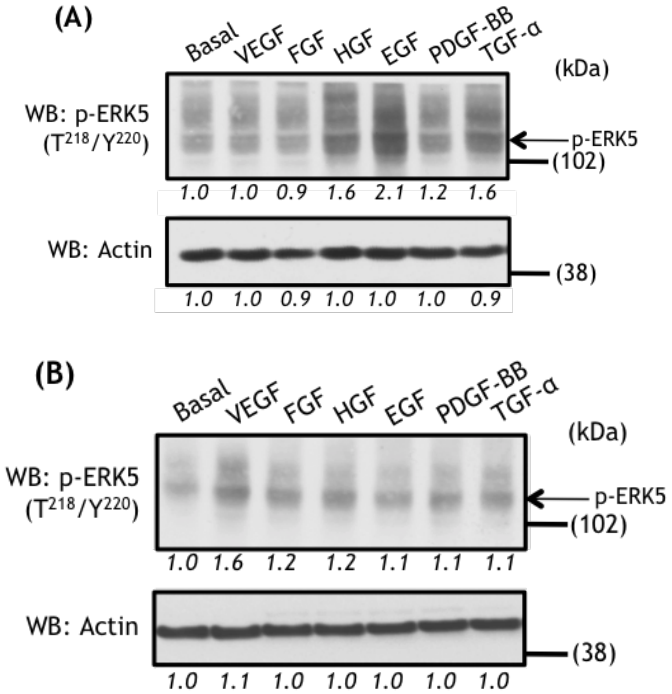

Figure 3.2 Characterisation of ERK5 activation using phospho-specific antibodies.
(A) HeLa protein lysates used in Figure 3.1a and (B) HDMEC protein lysates used in Figure 3.1b were resolved on a 4-12% NuPAGE® gel, followed by Western blotting (WB) with an antibody against phospho-ERK5 (p-ERK5) (T^{218}/Y^{220}) (#3371, NEB). *Densitometric analysis of protein phosphorylation or protein expression relative to actin is displayed beneath each blot. The basal control condition was set arbitrarily as 1.0. This result is representative of three independent experiments.*

As this ERK5 activation was not detected by mobility bandshift, it was considered that ERK5 might be differentially phosphorylated in HeLa cells and HDMEC, however it was necessary to initially exclude the possibility that different isoforms of ERK5 might be present in the two cell types. As previously discussed in Section 1.4.2.2, four alternatively spliced transcript variants of ERK5 exist, which encode for two different isoforms of ERK5. Thus, total RNA was extracted from HeLa cells and HDMEC grown in their normal growth medium and sent to Dr Jürgen Müller (Warwick Medical School, University of Warwick, Coventry, CV4 7AL, UK) for sequence analysis. Sequencing data from the mRNA revealed that the ERK5 transcripts in both cell types were in fact identical. The full sequence data can be found in Appendix III.

Subsequently, due to the clear evidence that Thr^{218}/Tyr^{220} are phosphorylated in response to VEGF in the HDMEC and EGF in the HeLa (Figure 3.2), it was hypothesised that the enhanced mobility bandshift observed in HeLa but not in HDMEC, was instead due to the phosphorylation of the numerous serine and threonine residues in the C-terminal tail of ERK5. Thus, Thr^{218}/Tyr^{220} phosphorylation alone is not sufficient in decreasing the

electrophoretic mobility of p-ERK5 compared to non-phosphorylated ERK5; a result previously reported in HEK293 cells (Mody *et al.*, 2003). Therefore, in order to ascertain the potential differences in phosphorylation between the two cell types, the innovative Phos-tag™ reagent was utilised in an acrylamide gel.

3.2.3 Phosphorylation events of ERK5

Kinoshita and colleagues reported that phosphorylated proteins could be visualised with the use of an alkoxide-bridged dinuclear metal (Mn^{2+}) complex as a novel phosphate-binding tag molecule (Phos-tag™) (Kinoshita *et al.*, 2006). This Phos-tag™ reagent has a vacancy on the two metal ions, which provides suitable access for capturing phosphomonoester dianions bound to Ser, Thr and Tyr residues. Thus, phosphorylated proteins bound to Phos-tag™ migrate slower through a polyacrylamide gel than their corresponding non-phosphorylated proteins, resulting in the visualisation of multiple bands during Western blotting (Figure 3.3) (Kinoshita *et al.*, 2006).

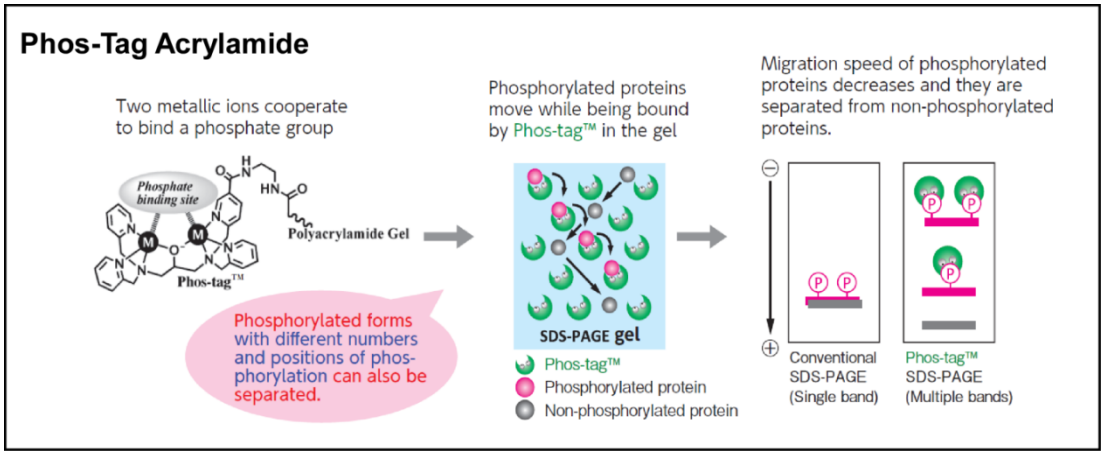

Figure 3.3 Mode of action of Phos-tag acrylamide
Image from: http://www.wako-chem.co.jp/english/labchem/product/life/Phos-tag/Acrylamide.htm

The recommended concentrations for the Phos-tag™ reagent were 10% (w/v) acrylamide, 100 µM Phos-tag and 140 µM $MnCl_2$. However, with the equipment available – XCell *SureLock*™ and XCell II™ Blot system – the substantial heat produced during electrophoresis rendered the gel unusable. Hence it was necessary to optimise the conditions for protein electrophoresis and transfer. During optimisation of these conditions, it became apparent that a lower total concentration of acrylamide present (%T; see Table 3.1) in the gel would enhance the electrophoretic mobility of both the non-phosphorylated and phosphorylated protein bands, whilst enabling the reduction in the amount of Phos-tag™

reagent used. Furthermore, it proved valuable to increase the ratio of Mn^{2+} ion to Phos-tag™ to an excess of 3:1, thus ensuring all reagent molecules were primed to capture phosphorylated proteins.

The Phos-tag™ optimisation conditions that were unsuccessful in distinctly separating the phosphorylation events of ERK5, are indicated in normal type font in Table 3.1 (data not shown).

Table 3.1 Optimisation Phos-tag™ SDS-PAGE conditions

%T (w/v) Acrylamide gel	Final Phos-tag™ conc^{n} (μM)	Final $MnCl_2$ conc^{n} (μM)	Electrophoresis system, amperage & time	Western blot system, amperage & time
10%	**100**	**200**	**XCell *SureLock*™; 30mA, 2h**	**XCell II™ Blot; 125mA, 2h**
8%	100	200	XCell *SureLock*™; 10mA, 6h	XCell II™ Blot; 125mA, 2h
8%	70	210	XCell *SureLock*™; 10mA, 6h	XCell II™ Blot; 125mA, 2h
8%	70	210	XCell *SureLock*™; 8mA, 22h	XCell II™ Blot; 125mA, 2h
7%	70	210	XCell *SureLock*™; 8mA, 22h	XCell II™ Blot; 125mA, 2h
7%	70	210	Mini-PROTEAN®; 8mA, 22h	Mini Trans-Blot®; 125mA, 2h
7%	70	210	Mini-PROTEAN®; 8mA, 22h	XCell II™ Blot; 125mA, 2h

After these initial experiments, it was evident that the XCell II™ Blot Module enabled clearer transfer of proteins onto the nitrocellulose membrane than the Mini Trans-Blot®. Thus, the XCell II™ Blot was utilised in an experiment that compared the quality of ERK5 phosphorylation band separation using the XCell *SureLock*™ and Mini-PROTEAN® electrophoresis systems, and the optimised conditions indicated in bold type font in Table 3.1 (Figure 3.4).

EGF-stimulated HeLa and VEGF-stimulated HDMEC protein lysates were separated for 22 h at 8 mA on a 7% (w/v) acrylamide, 70 μM Phos-tag™, 210 μM $MnCl_2$ gel either using the XCell *SureLock* electrophoresis system or the Mini-PROTEAN system. However, both gels were transferred using the XCell II Blot Module at 125 mA for 2h prior to Western blotting with an antibody against ERK5 (Figure 3.4).

Using the XCell *SureLock* system, it was apparent that the protein lysates did not migrate through their lanes in a stable manner, as the bands were not horizontally aligned (Figure 3.4a). This was attributed to inefficient heat conduction from the plastic cassettes to the surrounding buffer, produced during electrophoresis. Nevertheless, in both cell types and all conditions, a higher migrating band (*) that did not fully resolve from the ERK5 band was observed and was termed "p-ERK5" in Figure 3.4a.

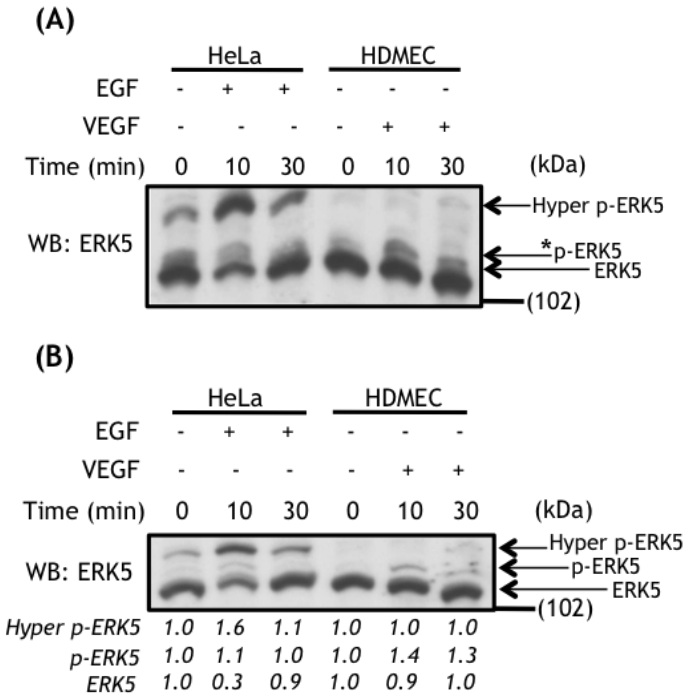

Figure 3.4 Optimisation of Phos-tag™ gel SDS-PAGE to detect ERK5 activation.
HeLa cells and HDMEC were seeded on 6-well plates for 24 h, prior to overnight serum starvation. HeLa were stimulated with EGF (50 ng/mL) and HDMEC with VEGF (50 ng/mL), for 10 or 30 min, followed by RIPA lysis. Lysates were separated for 22 h at 8 mA on a 7% (w/v) acrylamide, 70 μM Phos-tag™, 210 μM $MnCl_2$ gel using either (A) an Invitrogen XCell *SureLock*™ Mini-Cell electrophoresis system or, (B) a Bio-Rad Mini-PROTEAN® Tetra Cell electrophoresis system. Both gels were transferred for 2 h at 125 mA, using an Invitrogen XCell II™ Blot Module prior to Western blotting (WB) with an antibody against ERK5. *Densitometric analysis of protein phosphorylation or protein expression relative to the basal control condition of each cell type, is displayed beneath each blot. The basal control condition for each cell type and each migrated form of ERK5 was set arbitrarily as 1.0.*

The HeLa cells exhibited an additional band migrating much slower than the p-ERK5 band suggesting this represented a hyper-phosphorylated ERK5 and was designated the "hyper p-ERK5" band (Figure 3.4a). This band was present in unstimulated HeLa, but significantly increased in intensity at 10 min EGF stimulation and then somewhat decreased again at 30 min stimulation, yet still remained more intense than the unstimulated condition. Importantly, this hyper p-ERK5 band was not detected in unstimulated or VEGF-stimulated HDMEC (Figure 3.4a).

Protein separation using the Mini-PROTEAN® system appeared to result in greater stability of migration, as all detected bands were horizontally aligned. Furthermore, all observed bands were distinct from one another, making it possible to quantify their intensity relative to the respective basal condition migration band for each cell type (Figure 3.4b).

EGF stimulation of HeLa for 10 min resulted in a faint band that migrated slower than that of ERK5, suggestive of a phosphorylation event and was termed "p-ERK5" (Figure 3.4b), however at 30 min post-stimulation, this band disappeared. This p-ERK5 band was also present in VEGF-stimulated HDMEC at 10 min, remaining sustained for 30 min.

A clear hyper p-ERK5 band was observed in all conditions of HeLa cells whilst using the Mini-PROTEAN® system (Figure 3.4b), the intensity of which, followed that observed in Figure 3.4a. Once again however, this band was not detected in either the unstimulated or VEGF-stimulated HDMEC conditions (Figure 3.4b). Overall these data suggested a potential difference in the agonist-stimulated phosphorylation of ERK5 in HeLa and HDMEC.

3.2.4 ERK5 activation in HeLa cells

The same agonist stimulated HeLa lysates used in Figure 3.1a and Figure 3.2a were separated on a 7% (w/v) acrylamide, 70 μM Phos-tag™, 210 μM $MnCl_2$ gel for 22 h at 8 mA, after which an antibody against ERK5 was used for Western blotting. In addition to this, the same lysates were resolved on a 4-12% NuPAGE® gel prior to Western blotting with antibodies against phospho-AKT (#4060) and phospho-ERK1/2 (#4370) (Figure 3.5).

Similar to results observed in Figure 3.1a and Figure 3.2a, stimulation of HeLa cells with VEGF, FGF-2 or PDGF-BB did not induce any phosphorylation of ERK5 as detected by Phos-tag™ SDS-PAGE, compared to the basal condition (Figure 3.5). Furthermore, VEGF and FGF-2 did not elicit phosphorylation of AKT or ERK1/2 compared to the unstimulated basal condition, whereas PDGF-BB evoked AKT phosphorylation 2.3 times that of the basal condition and slightly lower phosphorylation of ERK1/2.

HeLa stimulated with HGF, EGF and TGF-α all resulted in hyper p-ERK5, with a significant decrease in p-ERK5 ($p<0.05$) (Figure 3.5). EGF stimulation of ERK5 was much greater than with HGF and TGF-α, however hyper p-ERK5 stimulation with both EGF and TGF-α appeared to be statistically significant ($p<0.01$). In addition to this, HGF stimulation resulted in an increase in AKT phosphorylation to a higher degree than EGF and TGF-α, and these three agonists phosphorylated ERK1/2 to a lesser degree.

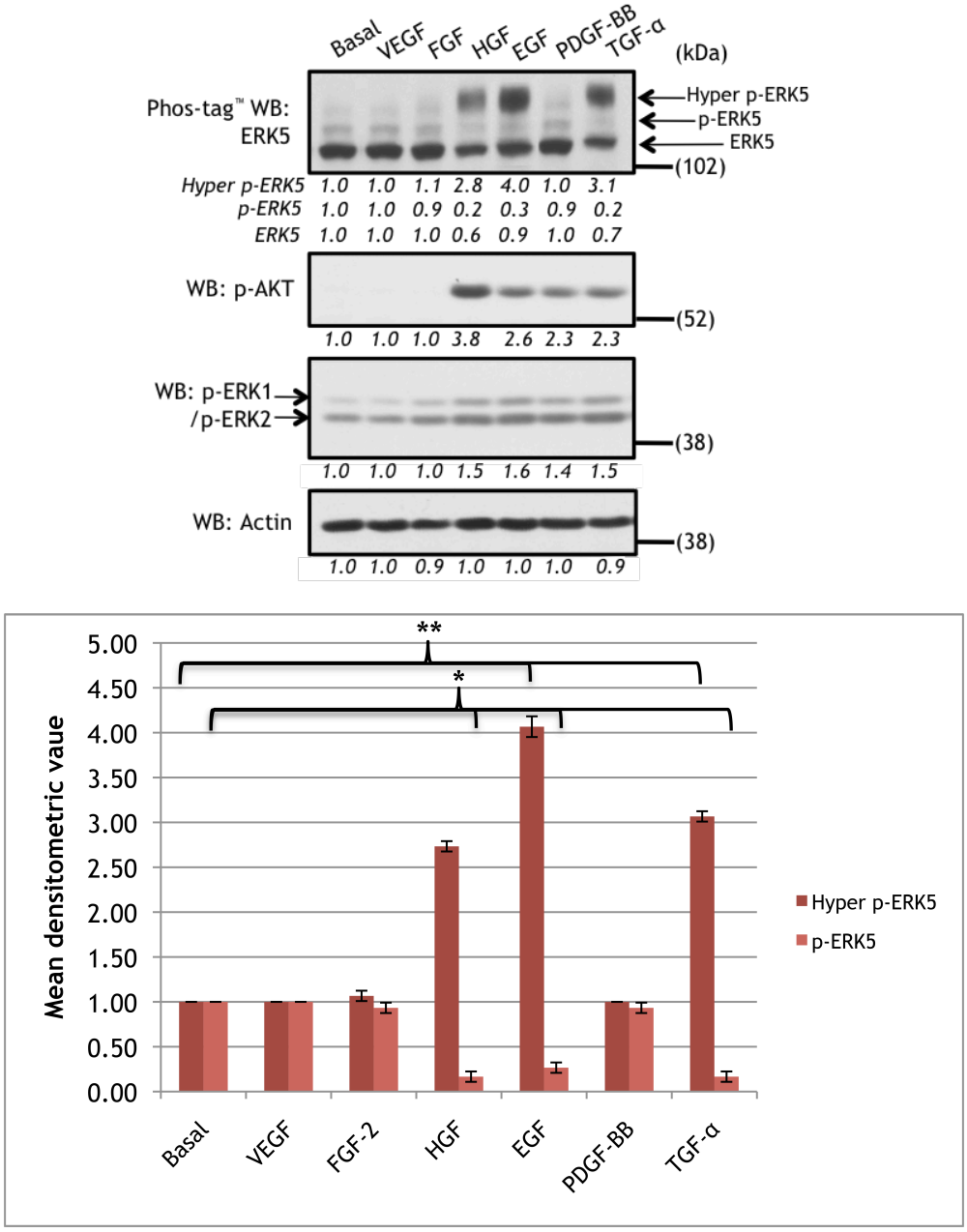

Figure 3.5 Characterisation of ERK5 activation in HeLa cells using Phos-tag™ SDS-PAGE.
HeLa protein lysates used in Figure 3.1a and Figure 3.2a were separated on a 7% (w/v) acrylamide Phos-tag™ gel, followed by Western blotting (WB) with an antibody against ERK5. Lysates were also resolved on a 4-12% NuPAGE® gel prior to Western blotting (WB) with antibodies against phospho-AKT (#4060, NEB) and phospho-ERK1/2 (#4370, NEB). *Densitometric analysis of protein phosphorylation or protein expression relative to the basal control condition, is displayed beneath each blot. The basal control condition was set arbitrarily as 1.0 for each protein. This result is representative of three independent experiments (*p<0.05, **p<0.01).*

3.2.5 VEGF stimulates ERK5 activation in HDMEC

Agonist stimulated HDMEC lysates used in Figure 3.1b and Figure 3.2b were also resolved on a 7% (w/v) acrylamide, 70 μM Phos-tag™, 210 μM $MnCl_2$ gel for 22 h at 8 mA, followed by Western blotting using an antibody against ERK5. The same lysates were also separated on a 4-12% NuPAGE® gel prior to Western blotting with antibodies against phospho-PLCγ (#2821), phospho-PKC (pan) (#9371), phospho-AKT and phospho-ERK1/2 (Figure 3.6).

The Phos-tag™ gel revealed ERK5 activation results in a similar pattern of bands to that seen in Figure 3.2b, namely that VEGF was the most potent stimulator of ERK5 phosphorylation in HDMEC, resulting in a significant increase in p-ERK5 ($p<0.01$) (Figure 3.6). The only other agonist that marginally activated ERK5 was HGF. Interestingly, both VEGF and HGF also stimulated AKT phosphorylation in HDMEC to a strong degree, as well as phosphorylation of four identifiable PKC isoforms – α, δ, ε and η.

Additionally, ERK1/2 appeared to be phosphorylated upon stimulation with VEGF, FGF-2 and HGF, with increased band intensities of 1.9, 1.7 and 1.6 respectively (Figure 3.6).

Interestingly, VEGF was unique in its ability to phosphorylate PLCγ (Figure 3.6) compared to the negligible values for the other agonists, suggesting VEGF-mediated ERK5 activity may exist downstream of, and thus be linked to, PLCγ activation.

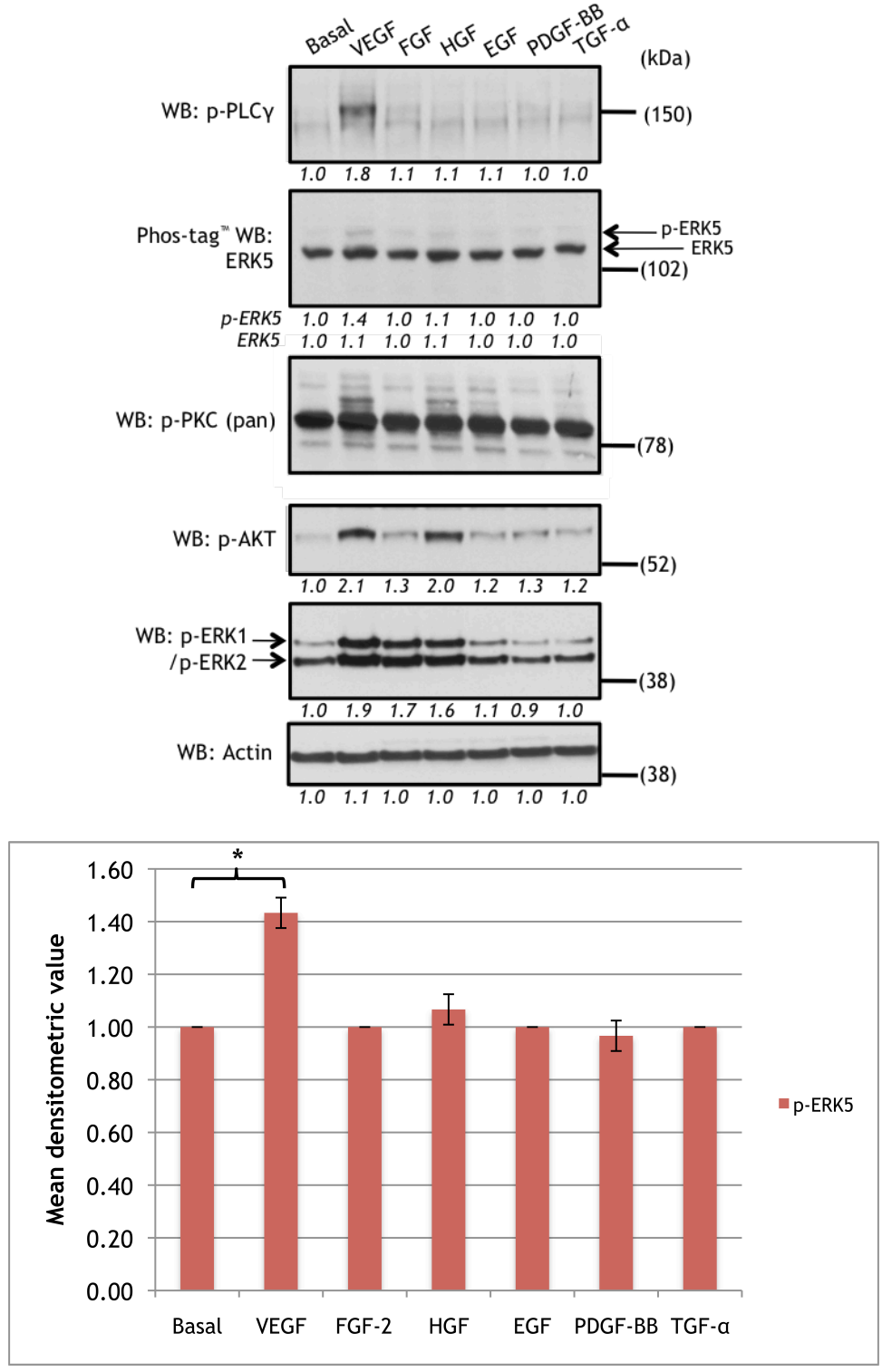

Figure 3.6 Characterisation of ERK5 activation in HDMEC using Phos-tag™ SDS-PAGE.
HDMEC protein lysates used in Figure 3.1b and Figure 3.2b were separated on a 7% (w/v) acrylamide Phos-tag™ gel, followed by Western blotting (WB) with an antibody against ERK5. Lysates were also resolved on a 4-12% NuPAGE® gel prior to Western blotting (WB) with antibodies against phospho-PLCγ (#2821), phospho-PKC (pan) (#9371, NEB) phospho-AKT and phospho-ERK1/2. *Densitometric analysis of protein phosphorylation or protein expression relative to the basal control condition, is displayed beneath each blot. The basal control condition was set arbitrarily as 1.0 for each protein. This result is representative of three independent experiments (*p<0.01).*

3.3 VEGF-induced activation of ERK5 occurs via Tyr1175 residue on VEGFR-2

VEGF-A is known to activate VEGFR-1 and VEGFR-2 in endothelial cells, however it is the binding to VEGFR-2 that stimulates a plethora of downstream signalling pathways resulting in a multitude of cellular functions (Holmes *et al.*, 2010). The Tyr^{1175} residue located on the intracellular C-terminal domain of VEGFR-2 undergoes trans-autophosphorylation upon VEGF binding to the extracellular region of the receptor. Furthermore, phosphorylated Tyr^{1175} acts as a docking site for PLCγ which itself is phosphorylated and activated (Cunningham *et al.*, 1997; Takahashi *et al.*, 2001). To determine the role of VEGFR-2 in the activation of ERK5, murine aortic endothelial (MAE) cells stably expressing a range of murine VEGFR-2 (Flk-1) mutants were obtained from Prof. Claesson-Welsh, Rudbeck Laboratory, Uppsala University, Sweden. The original MAE cells (designated MAE vector) had been stably transfected with wild-type Flk-1 (assigned MAE WT) or Flk-1 point mutants known to affect downstream signalling pathways. Flk-1 is two amino acids shorter in length than human VEGFR-2, thus the Flk-1 receptor mutants contained point mutations at Tyr^{949}, Tyr^{1173}, Tyr^{1212} residues (corresponding to the human Tyr^{951}, Tyr^{1175}, Tyr^{1214} residues) to give Phe^{949}, Phe^{1173}, Phe^{1212}.

An initial experiment screened the MAE vector cells with the same pro-angiogenic growth factors that were used to stimulate HeLa and HDMEC in Section 3.2, alongside a positive control of VEGF-stimulated HDMEC (Figure 3.7). It was confirmed that the MAE vector cells did not express endogenous Flk-1, as stimulation with VEGF and subsequent Western blotting with a p-VEGFR2 antibody did not result in a phosphorylation band comparable to that of the VEGF-stimulated HDMEC positive control. Interestingly however, the MAE vector cells appeared to be strongly stimulated by EGF, with the presence of an intense p-EGFR1 band migrating at an apparent molecular weight of 175 kDa suggesting the presence of EGFR-1 on these cells.

In addition to this, it was observed that HGF, EGF, PDGF-BB and TGF-α stimulation resulted in the phosphorylation of AKT and ERK1/2 in the MAE vector cells, whereas VEGF and FGF-2 had negligible effects on the phosphorylation of these two proteins, thereby reflecting the absence of the cognate receptors of these latter agonists on the MAE vector cells.

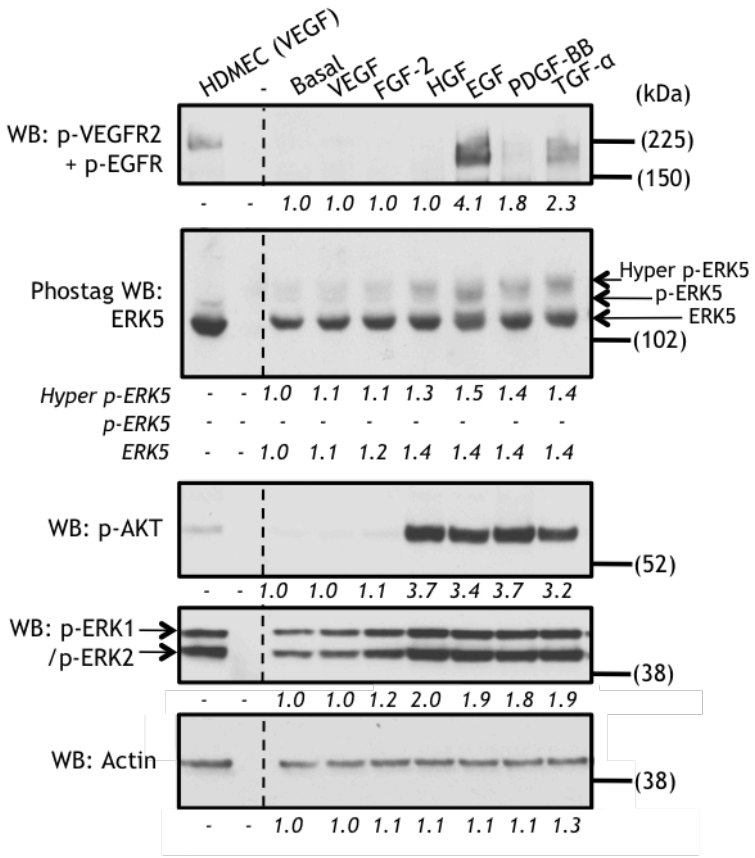

Figure 3.7 Agonist screen on MAE vector cells.
MAE vector cells were seeded on 6-well plates for 24 h, prior to overnight serum starvation. Cells were stimulated with 50 ng/mL of VEGF, FGF-2, HGF, EGF, PDGF-BB or TGF-α for 10 min, followed by RIPA lysis. Proteins were separated on a 4-12% SDS-PAGE gel as well as on a 7% (w/v) acrylamide Phos-tag™ gel, alongside a positive control of HDMEC stimulated with 50 ng/mL of VEGF. Membranes were incubated with antibodies against phospho-VEGFR2 (#3770, NEB)+phospho-EGFR (#2234, NEB), ERK5, phospho-AKT, phospho-ERK1/2 and Actin as a loading control. *Densitometric analysis of protein phosphorylation or protein expression relative to the basal control condition, is displayed beneath each blot. The basal control condition was set arbitrarily as 1.0 for each protein. This result is representative of two independent experiments.*

The MAE vector cells were screened alongside the MAE WT and receptor mutant cells following VEGF stimulation for 10 and 30 min, to confirm the presence of Flk-1 on the stably transfected cells as well as observe the phosphorylation kinetics of ERK5 and various other proteins (Figure 3.8). It is important to note that each cell type was densitometrically compared to its own basal condition, which was set at an arbitrary value of 1.0.

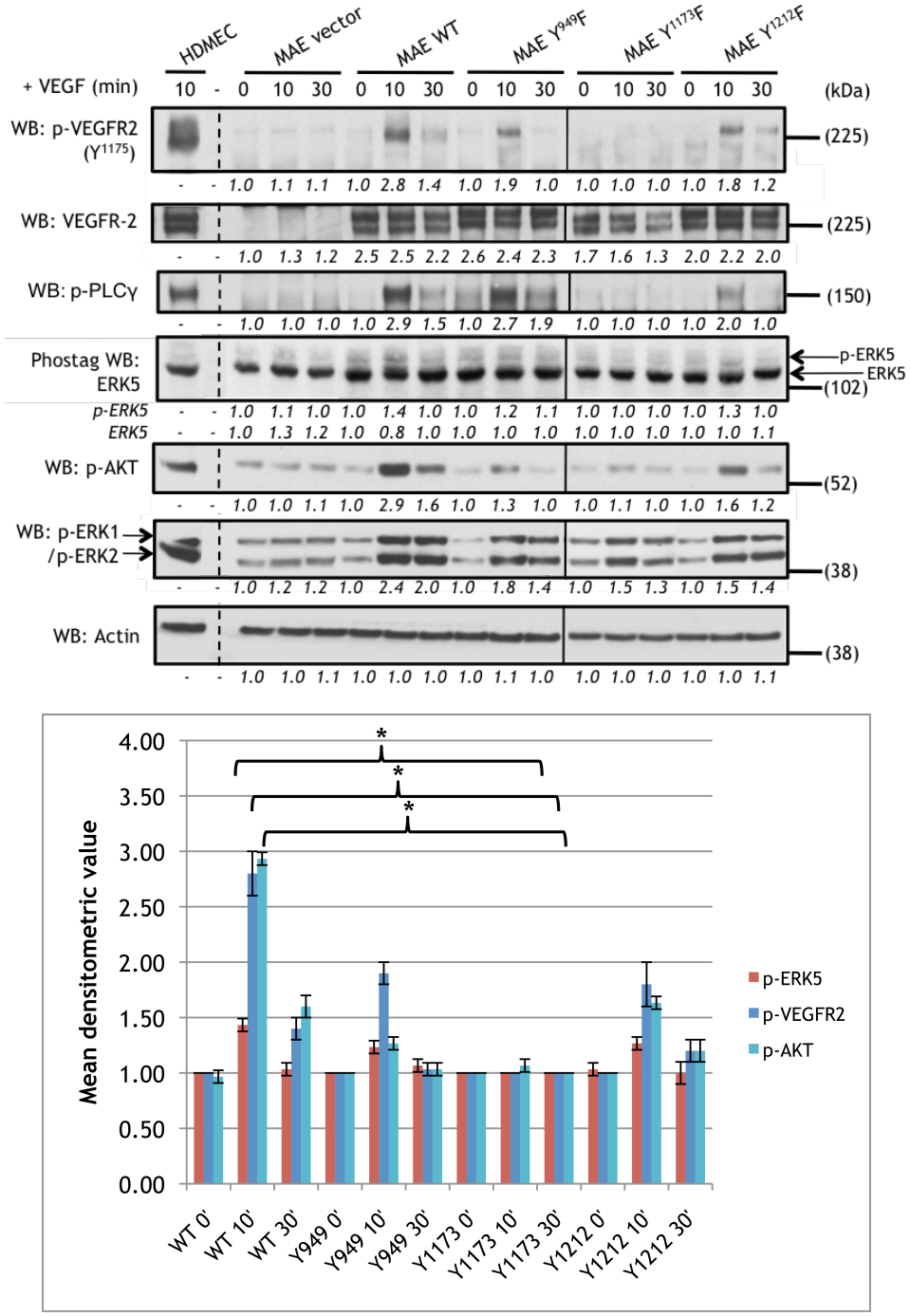

Figure 3.8 Screen of MAE mutant cell lines.
MAE vector cells and MAE cells expressing the Flk-1 WT, $Y^{949}F$, $Y^{1173}F$ or $Y^{1212}F$ receptors were seeded on 6-well plates alongside HDMEC as a positive control. Cells were incubated for 24 h, prior to overnight serum starvation, VEGF stimulation (50 ng/mL) for 10 or 30 min and RIPA lysis. Proteins were separated on a 4-12% SDS-PAGE gel, as well as on a 7% (w/v) acrylamide Phos-tag™ gel, alongside the 10 min VEGF (50 ng/mL) stimulated HDMEC positive control. Membranes were then incubated with antibodies against phospho-VEGFR2, VEGFR-2 (#2479 NEB), phospho-PLCγ, ERK5, phospho-AKT, phospho-ERK1/2 and Actin, for Western blotting (WB). *Densitometric analysis of protein phosphorylation or protein expression relative to the basal control condition of each cell type, is displayed beneath each blot. The basal control condition was set arbitrarily as 1.0 for each protein and each cell type. This result is representative of three independent experiments (*p<0.05).*

It was evident that the MAE WT and mutant receptor cells expressed VEGFR-2, as both the mature and immature forms of the receptor were observed in these cells in comparison to the absence of the receptor in the MAE vector cells (Figure 3.8). In addition to this, with the use of the p-VEGFR2 (Tyr^{1175}) antibody, it was possible to confirm the inability of the MAE cells expressing Flk-1 $Y^{1173}F$, to be phosphorylated on this site.

The phosphorylation of PLCγ was significantly increased with 10 min VEGF stimulation in both the MAE WT and MAE cells expressing Flk-1 $Y^{949}F$, and a two-fold increase in phosphorylation was observed in the MAE cells expressing Flk-1 $Y^{1212}F$. As expected, the lack of phosphorylation of the MAE cells expressing Flk-1 $Y^{1173}F$ prevented the docking and subsequent phosphorylation of PLCγ (Figure 3.8).

Rather interestingly, this deficiency in PLCγ phosphorylation in the MAE cells expressing Flk-1 $Y^{1173}F$ resulted in a statistically significant lack of ERK5 phosphorylation as detected by Phos-tag™ SDS-PAGE ($p<0.05$) (Figure 3.8), whereas the MAE cells expressing Flk-1 $Y^{949}F$ and Flk-1 $Y^{1212}F$ were shown to phosphorylate ERK5 at 10 min VEGF stimulation, compared to the MAE WT.

AKT phosphorylation at 10 min in the MAE WT cells upon VEGF stimulation was nearly three times that of its basal condition and sustained p-AKT was observed at 30 min. Although at 10 min VEGF stimulation the MAE cells expressing Flk-1 $Y^{949}F$ and $Y^{1212}F$ also had increased p-AKT compared to their respective basal conditions, the increase was not as marked as the MAE WT cells. Additionally, some sustained p-AKT was observed in the MAE cells expressing Flk-1 $Y^{1212}F$. The MAE cells expressing Flk-1 $Y^{1173}F$ appeared to have little, if any, AKT phosphorylation at both the 10 min or 30 min stimulation time points (Figure 3.8), with a significant difference at 10 min ($p<0.05$).

Furthermore, VEGF appeared to stimulate ERK1/2 phosphorylation in the MAE WT and the three mutant receptors at 10 min relative to their respective basal conditions, with sustained phosphorylation at 30 min within each cell type.

These results are suggestive of both ERK5 and AKT lying downstream of VEGFR-2 and that phosphorylation of the Tyr^{1175} residue was required in order for these two kinases to be activated in endothelial cells.

3.4 ERK5 undergoes differential phosphorylation following VEGF and EGF stimulation in murine endothelial cells

Due to the apparent difference in ERK5 activation in HeLa and HDMEC, it was considered that this may be attributable to the activation of ERK5 via the separate EGF- and VEGF-stimulated intracellular signalling pathways, rather than differences in cell type. Thus, the presence of both EGFR-1 and murine VEGFR-2 on the MAE WT cells was exploited in order to ascertain whether the differential activation of ERK5 was characteristic of cell type, as well as extracellular stimuli.

MAE vector and MAE WT cells were stimulated with VEGF, EGF, or VEGF+EGF for 10 min alongside positive controls of basal and VEGF-stimulated HDMEC and basal and EGF-stimulated HeLa (Figure 3.9) and protein lysates were separated on both conventional and Phos-tag™ SDS-PAGE.

In corroboration with previous results in Section 3.3, it was observed that EGF stimulated ERK5 phosphorylation in the MAE vector cells, as only a hyper p-ERK5 band was detected (Figure 3.9) similar to the EGF-stimulated HeLa cells. VEGF was unable to induce ERK5 activity in the MAE vector cells due to their lack of VEGFR-2 expression. Stimulation of the MAE WT cells with VEGF resulted in a p-ERK5 band 1.5 times that of its basal condition, whereas EGF stimulation of these cells led to a hyper p-ERK5 band 2.5 times greater than its respective basal condition. Interestingly however, the co-stimulation of the MAE WT cells with VEGF and EGF appeared to slightly increase the intensity of the p-ERK5 band yet decrease the hyper p-ERK5 band (Figure 3.9).

The use of conventional SDS-PAGE to ascertain ERK5 activation by mobility bandshift illustrated that only the EGF stimulation of the MAE vector, MAE WT and HeLa cells resulted in a bandshift denoting ERK5 activation (Figure 3.9). Thus, the stimulation of the MAE WT and HDMEC with VEGF did not lead to a mobility bandshift and in addition to this, the co-stimulation of the MAE WT cells appeared to restrict the ability of ERK5 to undergo a mobility bandshift as observed with EGF alone (Figure 3.9).

The phosphorylation of AKT in the MAE WT cells upon individual agonist stimulation was observed to be much greater with EGF rather than VEGF (Figure 3.9). Furthermore, the co-stimulation condition appeared to present phosphorylated AKT as a cumulative of the separate agonist conditions.

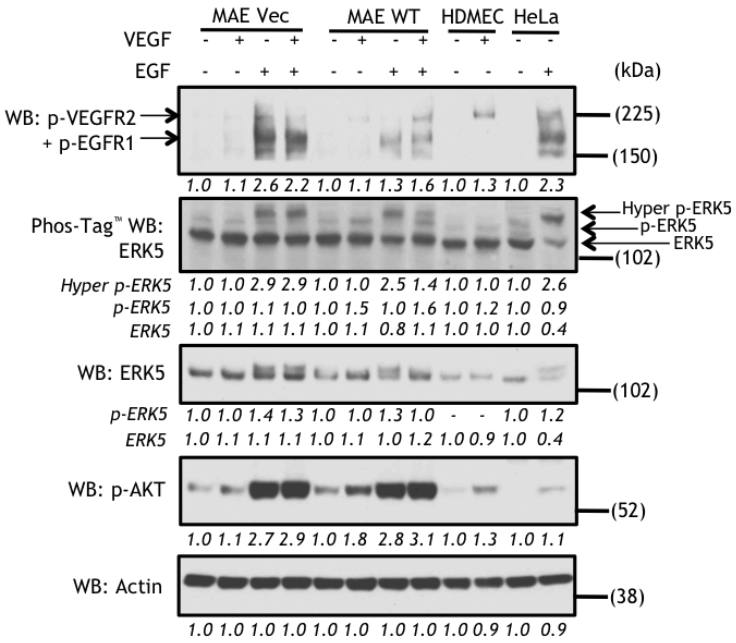

Figure 3.9 ERK5 is differentially activated by VEGF and EGF.
MAE vector and MAE WT cells were seeded on 6-well plates with HDMEC and HeLa plated alongside. Cells were incubated for 24 h, serum starved overnight, stimulated with VEGF, EGF or VEGF+EGF (50ng/mL for each agonist) for 10 min and RIPA lysed. Proteins were separated on an 8% (w/v) acrylamide gel, as well as on a 7% (w/v) acrylamide Phos-tag™ gel, alongside HDMEC and HeLa basal and stimulated conditions (50 ng/mL of VEGF and EGF respectively). Membranes were incubated with antibodies against p-VEGFR2+p-EGFR1, ERK5, p-AKT and Actin. *Densitometric analysis of protein phosphorylation or protein expression relative to the basal control condition of each cell type (set arbitrarily as 1.0), is displayed beneath each blot. This result is typical of three independent experiments.*

Altogether, these findings indicate that VEGF and EGF stimulate differential ERK5 phosphorylation within the same cell type. Additionally, co-stimulation with these agonists appears to affect ERK5 phosphorylation, not in a cumulative manner as would be expected, but instead in a mode where VEGF stimulation of ERK5 seems to decrease the effect of EGF-stimulated hyper p-ERK5 compared to that of EGF stimulation alone.

3.5 Small-molecule kinase inhibitors

The two small-molecule kinase inhibitors commonly used in blocking MEK5 and ERK5 activity are BIX 02189 and XMD8-92 respectively. The indolinone-6-carboxamide, BIX 02189 selectively inhibits MEK5 over MEK1/2 and has an IC_{50} of 1.5 nmol/L (Tatake *et al.*, 2008), whilst the highly-selective ATP-competitive kinase inhibitor XMD8-92 inhibits EGF-stimulated ERK5 activation with an IC_{50} of 240 nmol/L (Yang *et al.*, 2010a). Interestingly,

XMD8-92 has been shown to phosphorylate and consequently suppress PML, thereby blocking tumour cell proliferation; the growth of lung and cervical xenograft tumours were inhibited by 95% (Yang *et al.*, 2010a). These two inhibitors were validated by dose response experiments conducted in HDMEC and HeLa cells to ensure receptor activation, as well as other intracellular signalling pathways, were not affected in a non-specific manner with these agents (Figure 3.10, Figure 3.11, Figure 3.12, and Figure 3.13).

3.5.1 BIX 02189 inhibits ERK5, but not ERK1/2, activity

In HDMEC, the addition of 0.1 μM BIX 02189 appeared to marginally increase the p-ERK5 band as detected in the Phos-tag™ gel, compared to the basal or 0.1% (v/v) DMSO vehicle control. The subsequent doses of 0.3 μM, 1 μM and 3 μM reduced this phosphorylation to below those of the controls (Figure 3.10). Furthermore, the higher concentrations of 10 μM and 30 μM were able to decrease p-ERK5 to that of the unstimulated control conditions, with the 10 μM condition yielding a significant decrease ($p<0.05$) (Figure 3.10).

The phosphorylation of ERK1/2 was not affected by the addition of BIX 02189 up to a concentration of 10 μM, thereby suggesting that VEGF-mediated ERK1/2 activity occurs independently of the ERK5 signalling pathway (Figure 3.10). In spite of this, the 30 μM dose of BIX 02189 decreased p-ERK1/2 and p-AKT indicating a more global, toxic effect of the drug at this concentration (Figure 3.10).

BIX 02189 did not appear to have an effect on p-AKT up to 0.3 μM, with 1 μM and 3 μM only marginally decreasing its phosphorylation (Figure 3.10). However the 10 μM concentration decreased p-AKT to half that of the stimulated controls, suggesting that VEGF-mediated ERK5 phosphorylation may be required for AKT activity (Figure 3.10).

A rather interesting result was the increase in p-VEGFR2 with the addition of 10 μM BIX 02189, suggesting that MEK5 may either play a role in the internalisation of VEGFR-2, or it activates phosphatases that dephosphorylate the receptor.

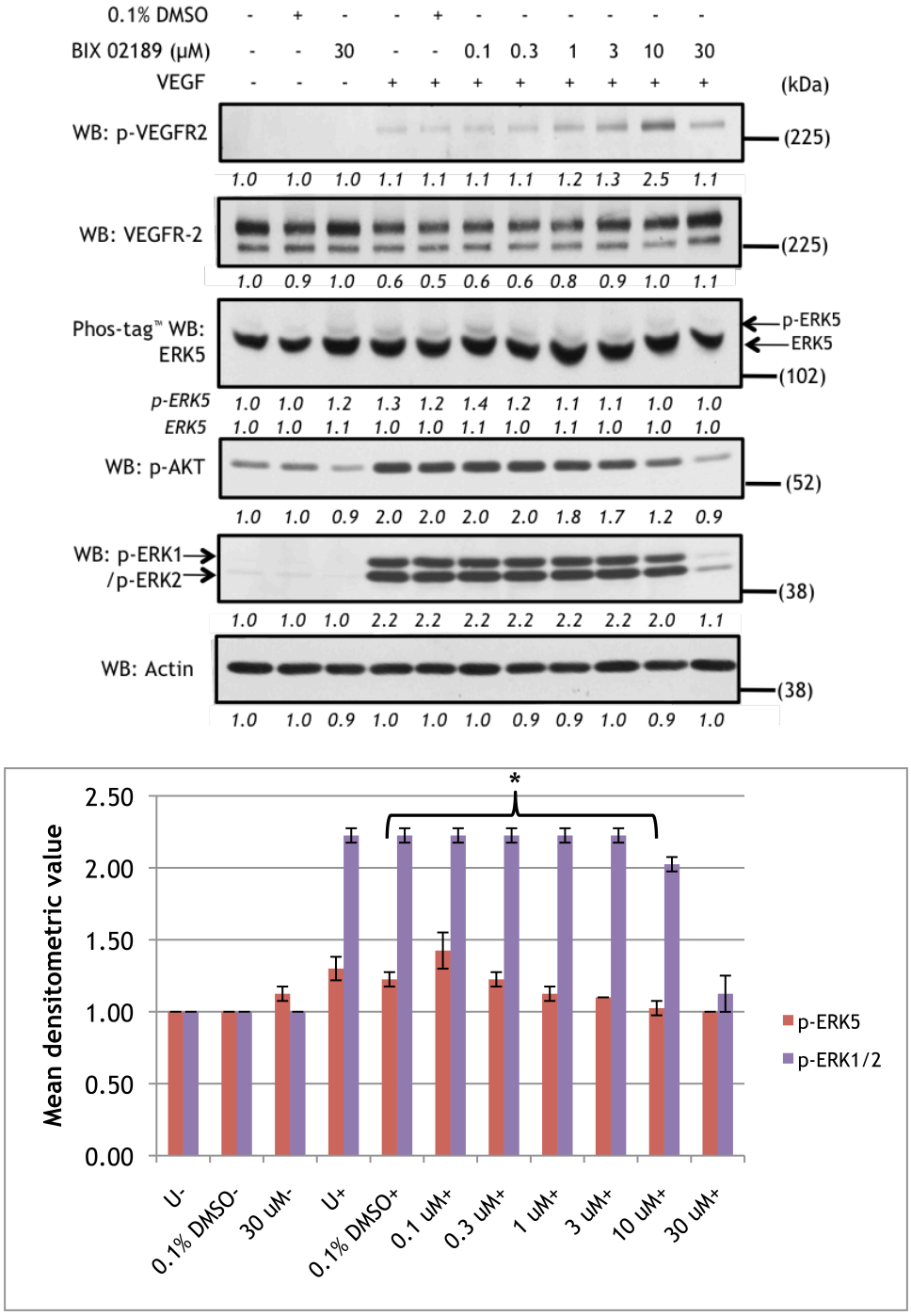

Figure 3.10 BIX 02189 dose response in HDMEC.
HDMEC were plated on 6-well plates for 48 h prior to overnight serum starvation. Cells were then pre-incubated with 0.1 μM, 0.3 μM, 1 μM, 3 μM, 10 μM and 30 μM BIX 02189 or 0.1% DMSO for 1 h, prior to VEGF stimulation (50 ng/mL) for 10 min and RIPA lysis. Proteins were separated on 4-12% NuPAGE® gel as well as on a 7% (w/v) acrylamide Phos-tag™ gel followed by incubating with antibodies against p-VEGFR2, VEGFR-2, ERK5, p-AKT, p-ERK1/2 and Actin for Western blotting (WB). *Densitometric analysis of protein phosphorylation or protein expression relative to the basal control condition (set arbitrarily as 1.0), is displayed beneath each blot. This result is representative of four independent experiments ($p<0.05$).*

In the HeLa cells, the stimulation of the basal and 0.1% (v/v) DMSO vehicle controls with EGF resulted in a slight decrease in p-ERK5, but a three-fold increase in hyper p-ERK5 as detected by Phos-tag™ gel. This result was interpreted as a single, slower electrophoretic band (p-ERK5) on a conventional SDS-PAGE (Figure 3.11).

The addition of 0.1 μM or 0.3 μM BIX 02189 appeared to reduce hyper p-ERK5 ($p<0.01$) yet slightly increase p-ERK5, possibly in an attempt to abrogate the inhibition of MEK5 by the drug. This result was reflected on conventional SDS-PAGE, as the p-ERK5 band was also affected (Figure 3.11). The subsequent doses of 1 μM, 3 μM, 10 μM and 30 μM, all decreased p-ERK5 and significantly decreased hyper p-ERK5 ($p<0.001$) in the Phos-tag™ gel, as well as the p-ERK5 band in SDS-PAGE (Figure 3.11).

BIX 02189 did not have an effect on ERK1/2 phosphorylation at any of the concentrations, however there was a noticeable increase of p-AKT at 30 μM (Figure 3.11).

These data demonstrate that the phosphorylation of additional residues of ERK5 is dependent upon EGF-mediated MEK5 dual-phosphorylation of ERK5. Furthermore, these data have revealed that a BIX 02189 dose of 10 μM was sufficient in inhibiting MEK5/ERK5 activity without affecting the parallel ERK1/2 pathway in both HDMEC and HeLa cells.

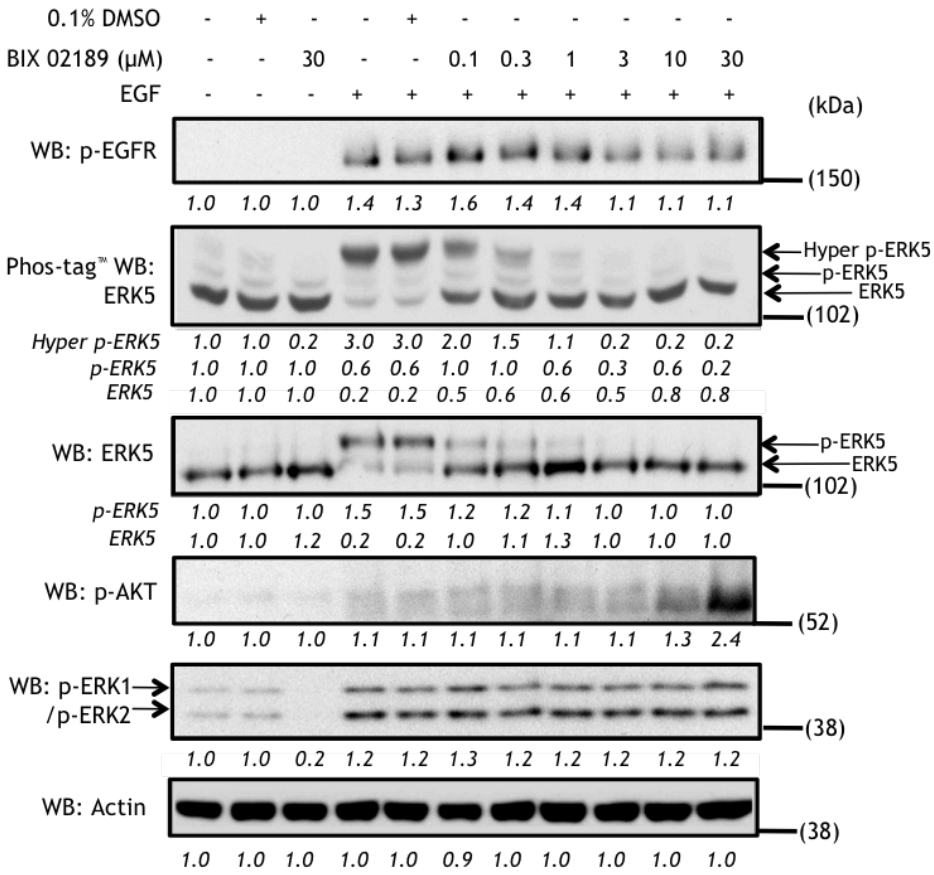

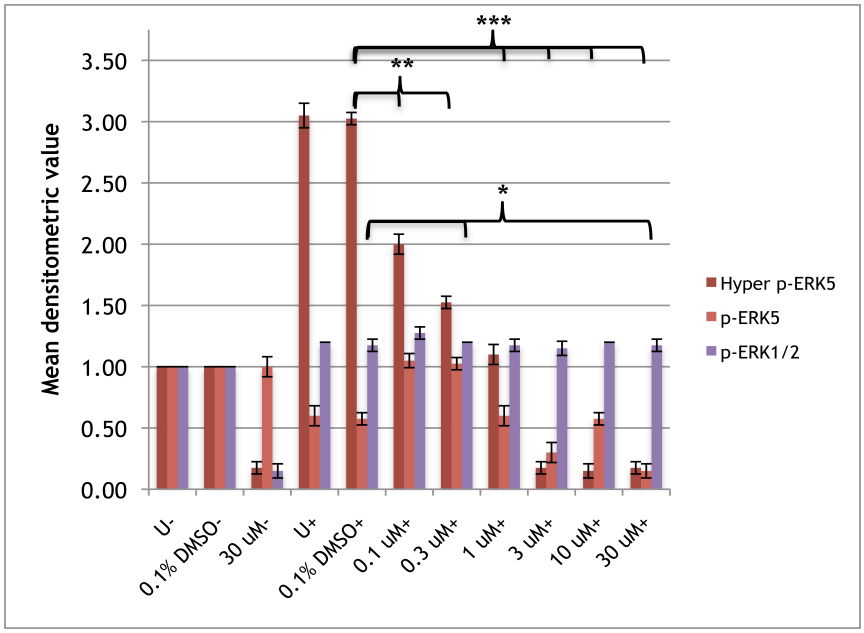

Figure 3.11 BIX 02189 dose response in HeLa.
HeLa were plated on 6-well plates for 48 h prior to overnight serum starvation. Cells were then pre-incubated with 0.1 μM, 0.3 μM, 1 μM, 3 μM, 10 μM and 30 μM BIX 02189 or 0.1% DMSO for 1 h, prior to EGF stimulation (50 ng/mL) for 10 min and RIPA lysis. Proteins were separated on 4-12% NuPAGE® gel as well as on a 7% (w/v) acrylamide Phos-tag™ gel followed by incubating with antibodies against p-EGFR1, ERK5, p-AKT, p-ERK1/2 and Actin for Western blotting (WB). *Densitometric analysis of protein phosphorylation or protein expression relative to the basal control condition (set arbitrarily as 1.0), is displayed beneath each blot. This result is typical of four independent experiments (*p<0.05, **p<0.01, ***p<0.001).*

3.5.2 XMD8-92 inhibits hyper phosphorylation of ERK5

It was observed that upon adding XMD8-92 to HDMEC and utilising Phos-tag™ SDS-PAGE, VEGF-mediated phosphorylation of ERK5 was not inhibited even at 30 μM (Figure 3.12). Alongside this, ERK1/2 activity remained unaffected by the addition of this drug, whereas the phosphorylation of AKT was slightly increased at concentrations up to 3 μM, above which AKT activity decreased back to levels akin to the control conditions (Figure 3.12).

In HeLa cells, the addition of 0.1 and 0.3 μM resulted in a slight decrease in hyper p-ERK5, which became somewhat more apparent at the 1 μM and 3 μM concentrations and significantly decreased at the 10 μM and 30 μM concentrations ($p<0.01$), as observed by Phos-tag™ gel (Figure 3.13). Conventional SDS-PAGE was able to detect a decrease in p-ERK5 from 0.3 μM and was reduced to a level similar to that of the unstimulated controls at 3 μM. Once again, alongside the Phos-tag™ decreases in hyper p-ERK5, the p-ERK5 band appeared to increase, perhaps in an attempt to reinstate phosphorylation of the additional residues (Figure 3.13).

The phosphorylation of both ERK1/2 and AKT were unaffected by any concentrations of XMD8-92. Altogether, these data illustrate that XMD8-92 inhibits the hyper phosphorylation of ERK5 at a concentration between 10 μM and 30 μM and in addition to this, AKT activity is not dependent upon ERK5 hyper phosphorylation.

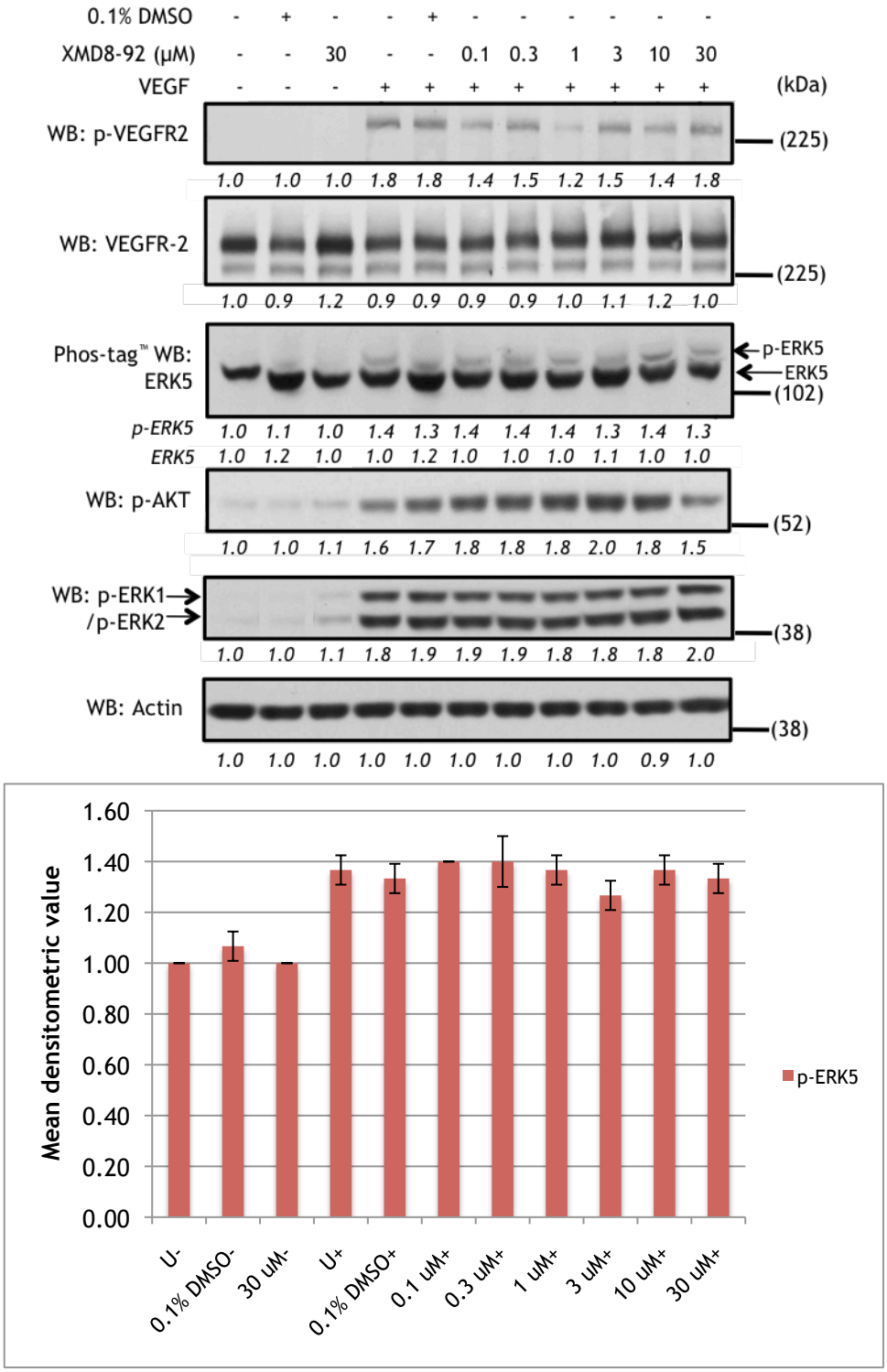

Figure 3.12 XMD8-92 dose response in HDMEC.
HDMEC were plated on 6-well plates for 48 h prior to overnight serum starvation. Cells were then pre-incubated with 0.1 μM, 0.3 μM, 1 μM, 3 μM, 10 μM and 30 μM XMD8-92 or 0.1% DMSO for 1 h, prior to VEGF stimulation (50 ng/mL) for 10 min and RIPA lysis. Proteins were separated on 4-12% NuPAGE® gel as well as on a 7% (w/v) acrylamide Phos-tag™ gel followed by incubating with antibodies against p-VEGFR2, VEGFR-2, ERK5, p-AKT, p-ERK1/2 and Actin for Western blotting (WB). *Densitometric analysis of protein phosphorylation or protein expression relative to the basal control condition (set arbitrarily as 1.0), is displayed beneath each blot. This result is representative of three independent experiments.*

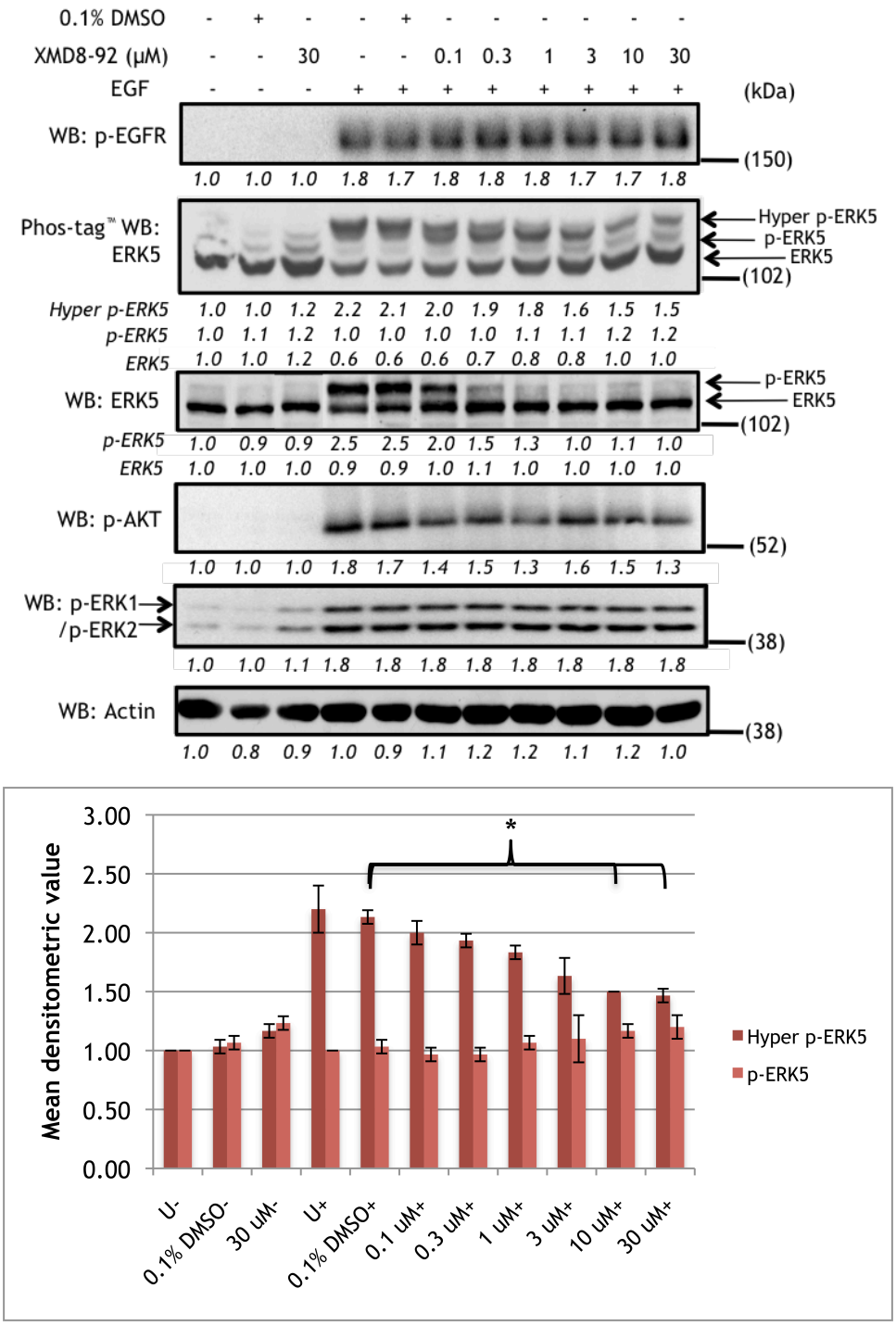

Figure 3.13 XMD8-92 dose response in HeLa.
HeLa were plated on 6-well plates for 48 h prior to overnight serum starvation. Cells were then pre-incubated with 0.1 μM, 0.3 μM, 1 μM, 3 μM, 10 μM and 30 μM XMD8-92 or 0.1% DMSO for 1 h, prior to EGF stimulation (50 ng/mL) for 10 min and RIPA lysis. Proteins were separated on 4-12% NuPAGE® gel as well as on a 7% (w/v) acrylamide Phos-tag™ gel followed by incubating with antibodies against p-EGFR1, ERK5, p-AKT, p-ERK1/2 and Actin for Western blotting (WB). *Densitometric analysis of protein phosphorylation or protein expression relative to the basal control condition (set arbitrarily as 1.0), is displayed beneath each blot. This result is typical of three independent experiments ($p<0.01$).*

3.6 Discussion

The strong activation of ERK5 in HeLa seen upon EGF stimulation (Figure 3.1a, Figure 3.2a and Figure 3.5) corroborates findings from previous studies although these include a variety of cell types (Kato *et al.*, 1998; Kamakura *et al.*, 1999; Hayashi *et al.*, 2004; Kondoh *et al.*, 2006). With the use of conventional SDS-PAGE, a phospho-specific ERK5 antibody against the Thr^{218}/Tyr^{220} residues and Phos-tag™ SDS-PAGE, it was possible to ascertain that in HeLa cells, ERK5 not only undergoes phosphorylation in the activation loop of the kinase domain (Figure 3.2a), but also at additional residues. As a consequence of this extensive phosphorylation, ERK5 was able to produce a mobility bandshift with conventional SDS-PAGE (Figure 3.1a), as well as a dual bandshift (p-ERK5 and hyper p-ERK5) with Phos-tag™ SDS-PAGE (Figure 3.5) in the HeLa cells.

TGF-α possesses some structural similarity to EGF and is able to bind to the EGF receptor (Tam *et al.*, 1984; Schreiber *et al.*, 1986) with an affinity indistinguishable from EGF in an equilibrium competition assay (Ebner and Derynck, 1991), consequently potentiating the activation of ERK5 in HeLa cells through EGFR-1. In addition to this, it has recently been shown that although the HGF receptor (cMET) is usually expressed in cells of an epithelial origin, they are also expressed in HeLa cells and dimerise upon ligand binding (Dietz *et al.*, 2013). The number of cMET receptors on the surface of HeLa cells is significantly lower than that of the EGF receptor (4600-8700 cMET receptors/HeLa (Dietz *et al.*, 2013) compared to 22,000 high affinity EGFR/HeLa and 25,000 low affinity EGFR/HeLa (Berkers *et al.*, 1991)). Thus, the activation of ERK5 upon HGF stimulation is less than that of EGF, which can be seen by the presence of a less intense phosphorylation band for HGF compared to that of EGF (Figure 3.1a, Figure 3.2a and Figure 3.5). Furthermore, the Phos-tag™ SDS-PAGE revealed that although TGF-α may bind to EGFR-1 with a similar affinity as EGF, the former agonist did not appear to phosphorylate ERK5 to the same extent as EGF, highlighting the potency of EGF-mediated ERK5 activation.

In stark contrast to ERK5 activation in HeLa cells, it was impossible to detect ERK5 activation in HDMEC using the mobility bandshift method with conventional SDS-PAGE (Figure 3.1b). However, the use of the p-Thr^{218}/Tyr^{220} antibody and Phos-tag™ SDS-PAGE enabled the detection of ERK5 phosphorylation in HDMEC upon stimulation with VEGF (Figure 3.2b and Figure 3.6).

Interestingly, this study revealed that both VEGF and HGF were able to stimulate AKT phosphorylation with much more potency than other agonists in HDMEC (Figure 3.6). It has previously been reported that in human malignant mesothelioma cells both AKT and ERK5 are activated by HGF stimulation (Altomare *et al.*, 2005; Ramos-Nino *et al.*, 2008), whereas in human aortic endothelial cells (HAEC), AKT and ERK1/2 are phosphorylated (Nakagami *et al.*, 2001).

Studies have associated the cMET signalling pathway in tumour growth, survival, and metastasis; additionally promoting angiogenesis by acting synergistically with VEGF (van Belle *et al.*, 1998; Xin *et al.*, 2001). Furthermore, stimulation with VEGF has been reported to lead to increased tyrosine phosphorylation of PI3K and AKT (Guo *et al.*, 1995).

Although there is evidence that FGF-2, HGF and EGF are able to phosphorylate PLCγ in other cell lines (Nishibe *et al.*, 1990; Mohammadi *et al.*, 1991; Okano *et al.*, 1993), it was observed in this study that VEGF was unique in its ability to stimulate PLCγ amongst growth factors (Figure 3.6); a finding which has previously been observed in HDMEC (Holmes *et al.*, 2010).

Utilisation of MAE cells stably expressing Flk-1 receptor mutants confirmed that the Tyr^{1173} residue (Tyr^{1175} in humans) was essential for PLCγ phosphorylation (Figure 3.8), which corroborates previous studies (Takahashi *et al.*, 2001). Additionally, this residue was also responsible for the activation of ERK5, implying the presence of ERK5 downstream of VEGFR-2 (Tyr^{1175}) and PLCγ (Figure 3.8). With the knowledge that p-PLCγ hydrolyses PIP_2 into IP_3 which increases intracellular Ca^{2+}, and DAG an activator of PKC (Wu *et al.*, 2000a), it is possible that ERK5 activity may be regulated by various PKC isoforms, which has previously been shown in a multitude of cell types (Diaz-Meco and Moscat, 2001; Li *et al.*, 2005; Zhao *et al.*, 2010). Contrary to these studies however, other groups have shown that ERK5 activation does not occur via PKC (Abe *et al.*, 1996; Kato *et al.*, 1998; Yan *et al.*, 1999) suggesting that activation of this pathway is highly dependent on cell type.

Further to this, the MAE Tyr^{1173}Phe mutant displayed reduced p-AKT, which may be attributed to decreased activation of PI3K in response to the hindered binding of Shb to the Tyr^{1173} residue (Holmqvist *et al.*, 2004), whereas ERK1/2 activity remained unaffected demonstrating that ERK5 and ERK1/2 activity are independent of one another and regulated separately.

With the suggestions that VEGFR-2 and PLCγ are required for the VEGF-mediated phosphorylation of ERK5 in endothelial cells, attention turned to the apparent difference

in ERK5 phosphorylation in HeLa cells namely, the hyper p-ERK5 band. The MAE WT cells enabled exploitation of the presence of both the VEGF and EGF cognate receptors on an endothelial cell type. Furthermore, utilising both Phos-tag™ and conventional SDS-PAGE allowed for discrimination of the different phosphorylation events of ERK5 amongst agonists and cell types (Figure 3.9).

This study revealed for the first time that observed differences in ERK5 phosphorylation were not dependent upon cell type, instead upon agonist. The data presented in this chapter show that VEGF is able to phosphorylate ERK5 at the very least on the Thr^{218}/Tyr^{220} residues within the activation loop, resulting in a p-ERK5 band on Phos-tag™ SDS-PAGE (Figure 3.9). However, this phosphorylation event alone is not substantial enough to generate a mobility bandshift on conventional SDS-PAGE (Figure 3.9); a similar discovery was made in HEK293 cells (Mody *et al.*, 2003). In contrast to this, EGF is able to phosphorylate ERK5 at Thr^{218}/Tyr^{220} as well as additional residues, most probably in the C-terminal tail, and as a consequence gives rise to a hyper p-ERK5 band on Phos-tag™ SDS-PAGE and a mobility bandshift on conventional SDS-PAGE (Figure 3.9). An additional interesting discovery amongst these results is that of ERK5 phosphorylation upon VEGF and EGF co-stimulation; there is an apparent decrease in hyper p-ERK5 compared to that of EGF stimulation alone. One theory may be that VEGFR-2 and EGFR-1 activate different intracellular pools of ERK5, whereby VEGFR-2 sequesters ERK5 in an intracellular localisation that precludes it from being further phosphorylated by EGFR-1.

The data generated with the use of the small-molecule kinase inhibitors targeting MEK5 and ERK5, further demonstrated these VEGF- and EGF-mediated differences in ERK5 phosphorylation (Figure 3.10, Figure 3.11, Figure 3.12, and Figure 3.13). It was evident that inhibition of MEK5 kinase activity with BIX 02189 prevented dual-phosphorylation of ERK5 in both VEGF-stimulated HDMEC and EGF-stimulated HeLa (Figure 3.10 and Figure 3.11), as well as the subsequent phosphorylation of additional C-terminal residues in HeLa (Figure 3.11). XMD8-92 appears to be a type I, ATP-competitive inhibitor that affects the kinase activity of ERK5 i.e. hyper p-ERK5 in EGF-stimulated HeLa (Figure 3.12 and Figure 3.13) and not activation of the T-E-Y motif, a finding that has previously been reported by way of mobility band shift (Deng *et al.*, 2011). Thus, data from this project provides evidence to support findings from previous studies that have demonstrated no effect on vasculature stability upon XMD8-92 treatment (Yang *et al.*, 2010a). Further elucidation of VEGF and EGF-mediated differences in ERK5 phosphorylation and the effect this may have on its intracellular localisation, as well as on cell survival, is discussed in the next chapter.

Chapter Four
Differential regulation of ERK5 in HDMEC and HeLa

4.1 Introduction

VEGF has been shown to activate ERK5 in HUVECs (Hayashi *et al.*, 2004) and HDMECs (Roberts *et al.*, 2010), yet numerous studies have utilised the stimulation of ERK5 by EGF to determine ERK5 activation, intracellular localisation and subsequently, develop small-molecule inhibitors of ERK5 (Kato *et al.*, 1998; Kamakura *et al.*, 1999; Hayashi *et al.*, 2001; Raviv *et al.*, 2004; Kondoh *et al.*, 2006; Tatake *et al.*, 2008; Yang *et al.*, 2010a). As a consequence, EGF-mediated ERK5 activation and its function in tumour cell proliferation is perceived to be the dogma. However, the discovery that the initial defect of *Erk5* ablation occurs within the endothelium (Hayashi *et al.*, 2004), along with the finding that ERK5 is required for VEGF-induced AKT phosphorylation during tubular morphogenesis in HDMEC (Roberts *et al.*, 2010), emphasised the physiological relevance of characterising ERK5 activation in endothelial cells. Hence, it was hypothesised that EGF- and VEGF-mediated ERK5 activation and function differed.

Data from the previous chapter revealed an important discovery with respect to VEGF- and EGF-mediated activation of ERK5 in HDMEC and HeLa, whereby the two growth factors were able to induce differential phosphorylation events of ERK5 (*Chapter 3*). VEGF-stimulated HDMEC resulted in phosphorylation of the Thr^{218}/Tyr^{220} residues of ERK5, whereas EGF was able to induce this dual-phosphorylation, as well as phosphorylation of additional residues thought to be in the C-terminal.

It was possible to discriminate these phosphorylation events with the use of Phos-tag™ SDS-PAGE, a technique that will be further utilised in this chapter, along with small interfering RNA (siRNA) to identify the differences in the role and regulation of VEGF- and EGF-induced phosphorylation of ERK5 in HDMEC and HeLa.

The use of RNA interference (RNAi) technology has been demonstrated to be an effective method of post-transcriptional gene silencing (Sharp, 2001). This method introduces foreign small double-stranded RNA (dsRNA), complementary to the sequence of the gene of interest, which is recognised by an RNA III nuclease (termed Dicer) and cleaved into short RNA duplexes measuring 21-28 nucleotides (hence the term small interfering RNA) (Bernstein *et al.*, 2001; Zhang *et al.*, 2002). The siRNAs are incorporated into a silencing complex termed RISC (RNA-induced silencing complex), enabling the complex to be guided to the target mRNA sequence, resulting in the degradation of the mRNA sequence and subsequently preventing the translation of the mRNA (Hammond *et al.*, 2000).

Additionally, with the use of immunofluorescence and subcellular protein fractionation, the effect this differential ERK5 activation has on the intracellular localisation of ERK5 will be explored.

Furthermore, the use of the specific small-molecule inhibitors of MEK5 and ERK5, BIX 02189 and XMD8-92 will be utilised in order to determine the role of VEGF- and EGF-mediated AKT activity as a result of ERK5 phosphorylation.

4.2 VEGF fails to induce C-terminal phosphorylation of ERK5

The differential phosphorylation of ERK5 by VEGF and EGF was further investigated with the use of phospho-specific antibodies against the Thr^{218}/Tyr^{220} residues in the activation loop of the kinase domain as well as against Thr^{732}, a residue present on the C-terminal tail of ERK5. These antibodies were generated and kindly gifted by Dr. Atanasio Pandiella and his lab group (Instituto de Biolgia Molecular y Celular del Cancer, CSIC-Universidad de Salamanca, Spain). HDMEC and HeLa were stimulated with VEGF and EGF respectively for different times and the protein lysates were run on Phos-tag™ gels in order to assign specific phosphorylation events to the individual bands.

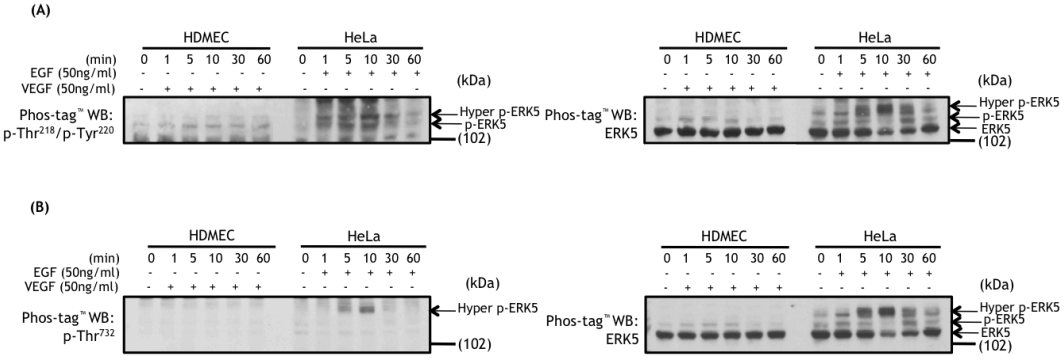

Figure 4.1 VEGF fails to induce C-terminal phosphorylation of ERK5.
HDMEC and HeLa were plated on 12-well plates for 24 h prior to overnight serum starvation. Cells were then stimulated with VEGF or EGF accordingly, for 1, 5, 10, 30 and 60 min after which they were lysed with RIPA. HDMEC and HeLa lysates were run alongside each other and separated on a 7% (w/v) acrylamide, 70 μM Phos-tag™, 210 μM $MnCl_2$ gel at 8 mA for 22 h, followed by Western blotting (WB) with antibodies against **(A)** phospho-Thr^{218}/Tyr^{220} or **(B)** phospho-Thr^{732}, prior to being stripped and re-incubated with an antibody against ERK5. *This result is representative of two independent experiments.*

It was observed that with the p-Thr^{218}/Tyr^{220} antibody, these residues were phosphorylated by VEGF from 1 min, with the highest phosphorylation seen at 5 min and 10 min. However, phosphorylation of these residues was somewhat sustained through to 60 min (Figure 4.1a - left). EGF stimulation of these kinase domain residues in HeLa also resulted in phosphorylation at 1 min and once again, the 5 min and 10 min time points possessed the strongest phosphorylation (Figure 4.1a - left). These residues did appear to be phosphorylated at 30 and 60 min but less so than at the earlier time points. There are two distinct bands evident in HeLa cells with the p-Thr^{218}/Tyr^{220} antibody, the lower band (*) denotes the phosphorylation of the T-E-Y residues, whereas (**) represents phosphorylation of C-terminal residues in addition to the T-E-Y residues (Figure 4.1a - left).

Stripping this phospho-specific antibody off the membrane and re-probing with the ERK5 antibody enabled determination of the migration distance of these specific residues (Figure 4.1 - right). Thus, the ERK5 antibody revealed that the band designated "p-ERK5" in Phos-tag™ gels from the previous chapter, i.e. the only species of phosphorylated band in HDMEC and the "faster" of the two phosphorylated bands in HeLa could be attributed to phosphorylation of the Thr^{218}/Tyr^{220} residues (marked * in Figure 4.1a - right).

Comparing the p-ERK5 band in HDMEC to that of the phospho-specific antibody, similar results were observed – strong phosphorylation at the 1, 5, and 10 min time points, with less intensity at 30 and 60 min (Figure 4.1 - right). However, the kinetics of the p-ERK5 band in HeLa differ to that seen using the phospho-specific antibody, due to the ability of ERK5 to undergo hyper-phosphorylation due to EGF stimulation.

The use of the p-Thr^{732} antibody on the same lysates uncovered an interesting and novel discovery. Stimulation of HDMEC with VEGF did not appear to phosphorylate the Thr^{732} residue at any of the time points, however EGF-stimulated HeLa revealed phosphorylation of this C-terminal residue at 5 min which increased at 10 min (Figure 4.1 - left). Once again, stripping and re-probing the membrane with the ERK5 antibody, and measuring the migration distance of this phosphorylation band showed the "hyper p-ERK5" band (as assigned in the previous chapter) could be attributable to phosphorylation of C-terminal residues of ERK5 in addition to phosphorylation of the Thr^{218}/Tyr^{220} residues (Figure 4.1 - right).

Taken together, these data show that VEGF only evokes phosphorylation of Thr^{218}/Tyr^{220} in the kinase domain, whereas EGF can stimulate phosphorylation of these residues in the kinase domain as well as residues present in the C-terminal tail.

4.3 EGF-mediated C-terminal phosphorylation of ERK5 requires HRAS

The previous data suggest that VEGFR-2 couples to ERK5 activation in a manner distinct to EGFR-1 and that phosphorylation of the Thr^{218}/Tyr^{220} motif in the activation loop of the kinase domain does not necessarily facilitate autophosphorylation of subsequent C-terminal residues. In an attempt to explain this, specific signalling proteins differentially activated downstream of EGFR-1 and VEGFR-2, in particular the RAF-1/RAS molecules (Hallberg *et al.*, 1994; Sasaoka *et al.*, 1994; Sakaguchi *et al.*, 1998; Doanes *et al.*, 1999; Takahashi *et al.*, 2001; Zachary, 2003), were knocked down using siRNA to determine which protein would affect ERK5 phosphorylation.

RAF-1 activation has been implicated downstream of EGFR-1 and RAS activation, leading to phosphorylation of ERK1/2 (Hallberg *et al.*, 1994; Johnson and Vaillancourt, 1994), thus its potential role in VEGF-/EGF-mediated ERK5 phosphorylation was examined. In HDMEC, p-ERK5 was not affected by siRNA knockdown of RAF-1 (Figure 4.2a). However in HeLa cells, a slight decrease in hyper p-ERK5 was detected compared to that of the untransfected/non-targeting siRNA EGF-stimulated control (Figure 4.2b).

The abundance of the RAS isoforms differs greatly amongst cell types. In a variety of endothelial cells (HAEC and murine microvascular lung and cardiac cells) H-RAS is the major isoform (60-70% of the total), followed by N-RAS (approximately 20%) and the K-RAS comprising of the remainder (Haeussler *et al.*, 2013). In HeLa cells, K- and N-RAS occur in relatively equal quantities, each comprising about 40-45% of the total amount of RAS, with H-RAS only accounting for <10% of the total (Omerovic *et al.*, 2008). Despite this stark disparity in RAS isoform abundance, siRNA knockdown of any of the RAS isoforms did not affect p-ERK5 in HDMEC (Figure 4.2a). Interestingly, only siRNA knockdown of H-RAS in HeLa cells (the lowest abundant isoform) resulted in a notable decrease in hyper p-ERK5 compared to the EGF-stimulated control conditions (Figure 4.2b).

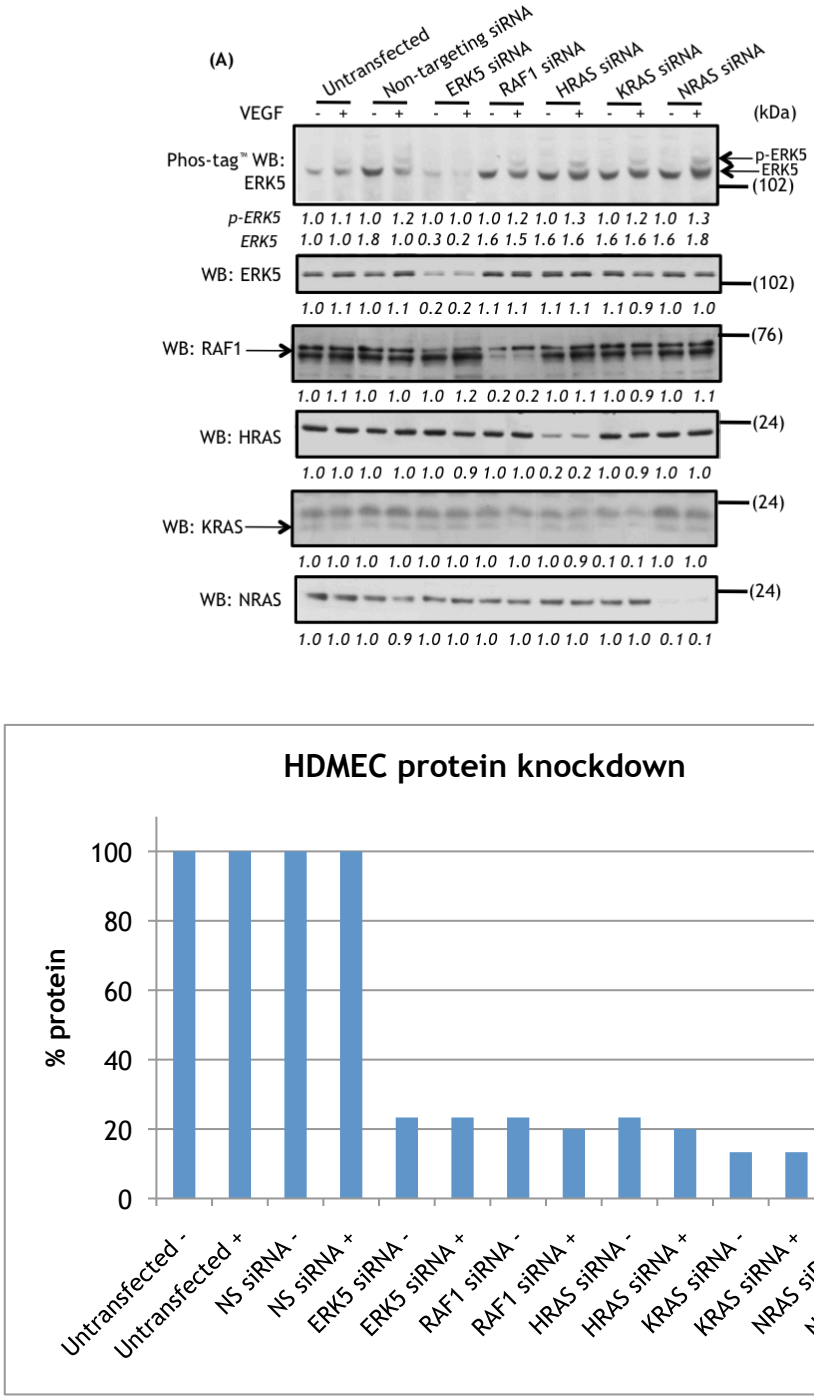

Figure 4.2a C-terminal phosphorylation of ERK5 requires HRAS activation.
(A) HDMEC were plated on 6-well plates for 24 h, prior to a 6 hr siRNA transfection with the appropriate control and target duplexes. Cells were then serum starved overnight, stimulated with 50 ng/mL VEGF for 10 min and RIPA lysed. Lysates were separated on a 4-12% NuPAGE® gel, 15% SDS-PAGE as well as a 7% (w/v) acrylamide, 70 µM Phos-tag™ gel, followed by Western blotting (WB) with antibodies against ERK5, RAF-1 (#9422, NEB), HRAS (sc-520), KRAS (sc-521) and NRAS (sc-31). Bar chart represents percentage of protein knockdown achieved. *This result is representative of three independent experiments.*

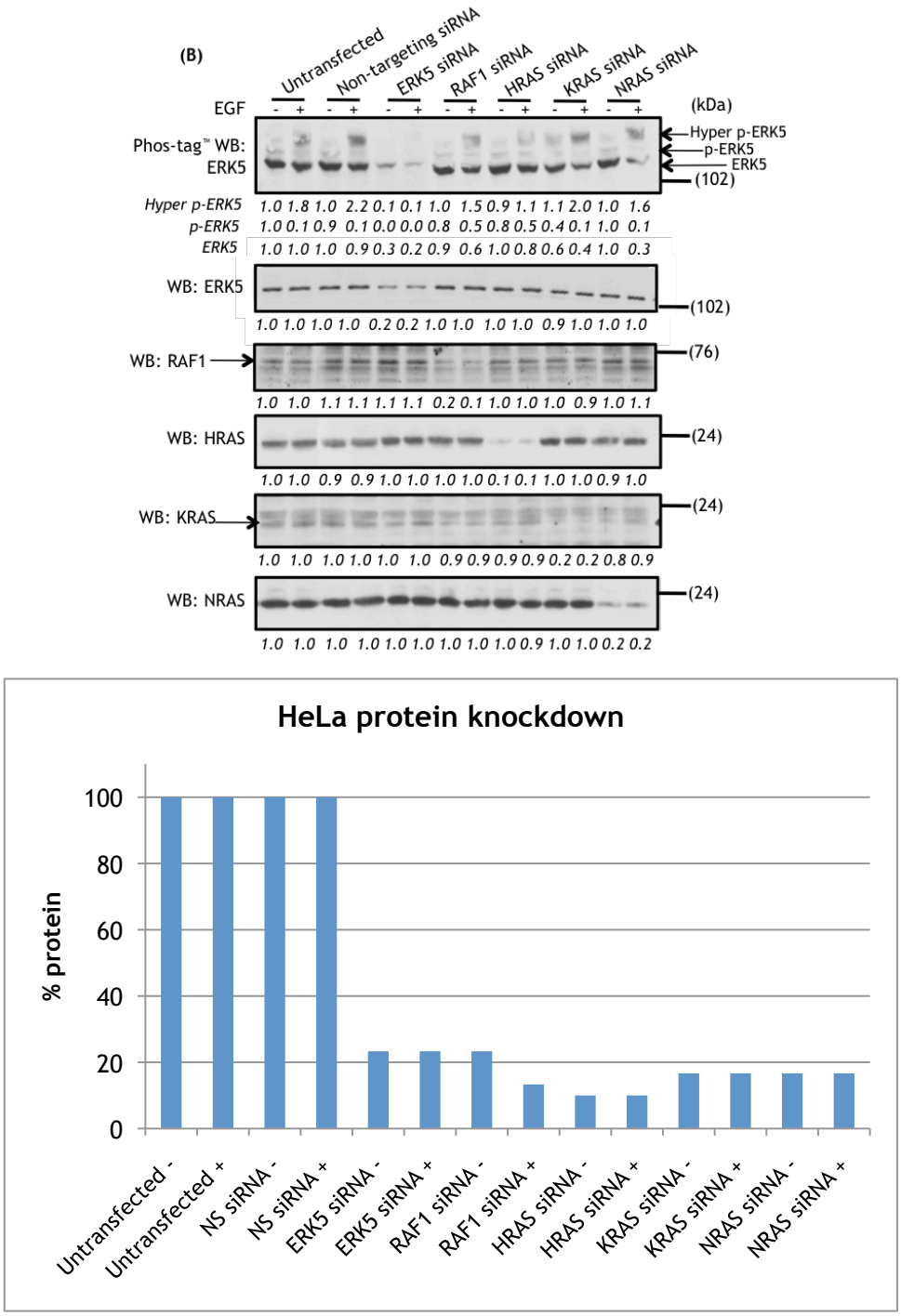

Figure 4.2b C-terminal phosphorylation of ERK5 requires HRAS activation.
(B) HeLa were plated on 6-well plates for 24 h, prior to a 6 hr siRNA transfection with the appropriate control and target duplexes. Cells were then serum starved overnight, stimulated with 50 ng/mL EGF for 10 min and RIPA lysed. Lysates were separated on a 4-12% NuPAGE® gel, 15% SDS-PAGE as well as a 7% (w/v) acrylamide, 70 µM Phos-tag™ gel, followed by Western blotting (WB) with antibodies against ERK5, RAF-1 (#9422, NEB), HRAS (sc-520), KRAS (sc-521) and NRAS (sc-31). Bar chart represents percentage of protein knockdown achieved. *This result is representative of three independent experiments.*

4.4 Thr^{218}/Tyr^{220} phosphorylation alone is not sufficient to facilitate nuclear localisation

The intracellular localisation of ERK5 has been suggested to alter according to the phosphorylation status, and hence the conformation, of ERK5. Kondoh and colleagues proposed that in its quiescent unphosphorylated state, ERK5 is tethered in a folded configuration due to an intramolecular interaction between the N- and C-terminals (Kondoh *et al.*, 2006). It is considered that this conformation either generates a nuclear export signal (NES), or dampens the signal of the nuclear localisation signal (NLS) domain, thus sequestering ERK5 in the cytoplasm. Dual-phosphorylation of the Thr^{218}/Tyr^{220} residues by MEK5 is thought to disrupt the intramolecular NES interaction enabling the translocation of ERK5 to the nucleus (Kondoh *et al.*, 2006).

The aforementioned data in this project portrays a key difference in VEGF- and EGF-mediated ERK5 phosphorylation, thus the possible effect on the intracellular localisation of ERK5 was investigated with the use of immunofluorescence.

HeLa cells were stimulated with EGF (Figure 4.3) and HDMEC stimulated with VEGF, for 10 or 30 min (Figure 4.4). In HeLa cells, ERK5 translocated from the cytoplasm to the nucleus upon stimulation with EGF at 10 min (Figure 4.3). Furthermore, 30 min stimulation with EGF resulted in almost complete translocation of ERK5 into the nucleus (Figure 4.3).

Interestingly in HDMEC, 10 min VEGF stimulation did not appear to have any effect on ERK5 localisation, remaining sequestered in the cytoplasm (Figure 4.4). In spite of ERK5 still having a cytoplasmic localisation upon 30 min VEGF stimulation, a somewhat more plasma membranous localisation was observed, with the presence of clusters of ERK5 on the cell periphery (Figure 4.4).

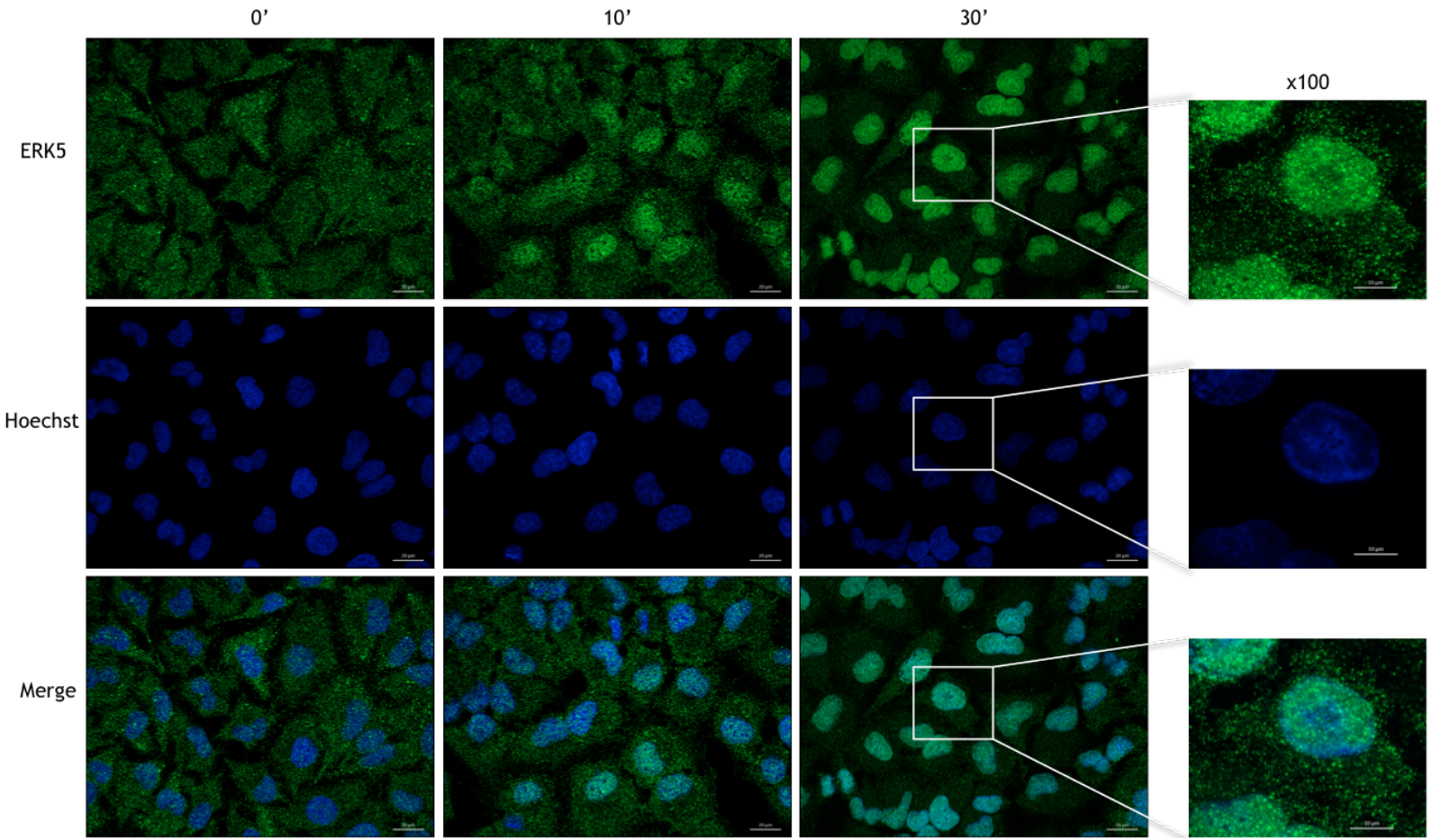

Figure 4.3 Intracellular localisation of ERK5 in HeLa cells.
HeLa were plated on 16 mm coverslips for 24 h, prior to overnight serum starvation and stimulation with 50 ng/mL EGF for 10 or 30 min. Cells were then fixed with ice-cold MeOH, blocked in 5% BSA/PBS with donkey serum and stained with an antibody against ERK5, prior to staining with a fluorescent secondary antibody and image acquisition with an inverted Zeiss Axio Observer microscope and the associated Zen software.

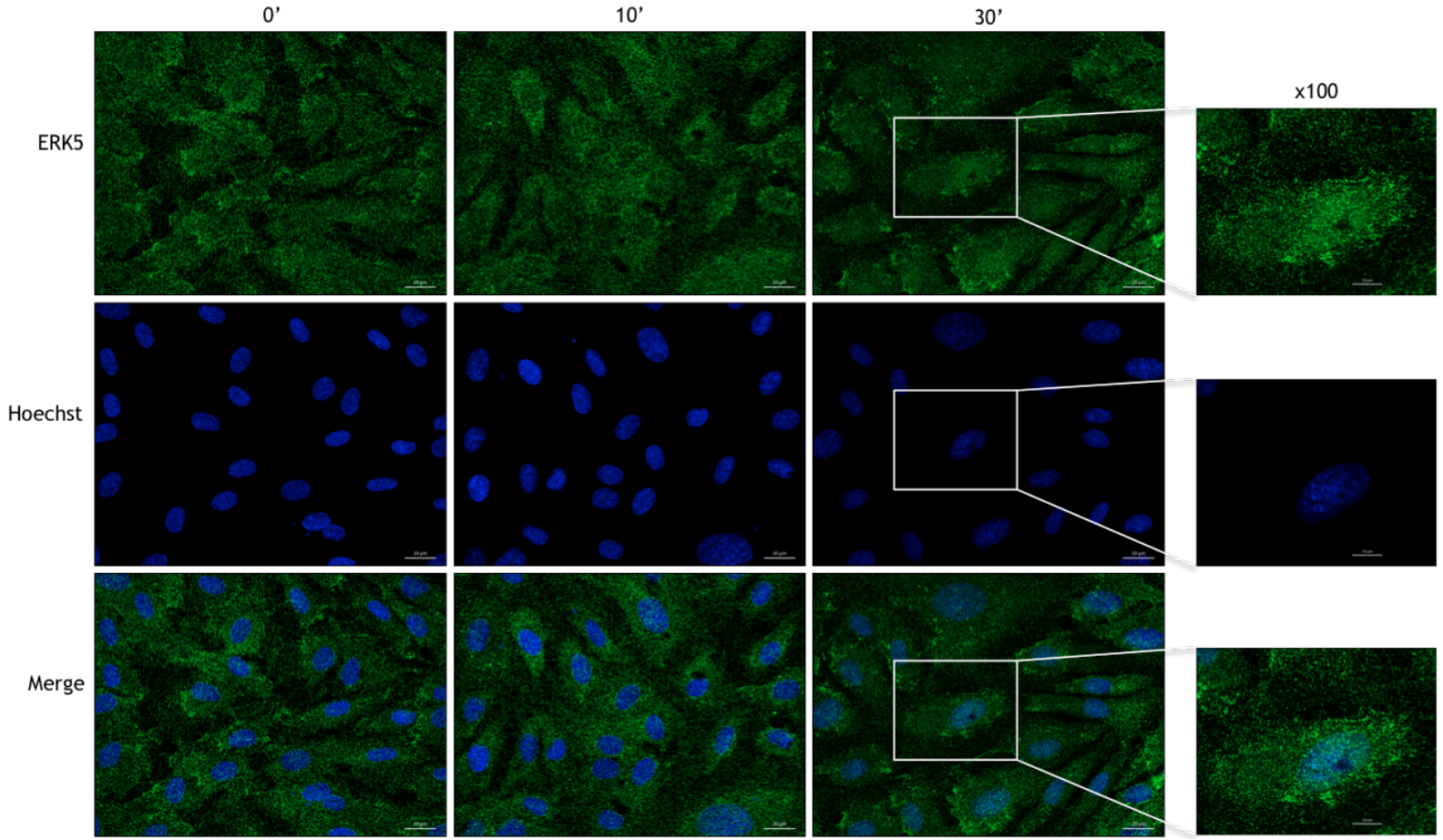

Figure 4.4 Intracellular localisation of ERK5 in HDMEC.
HDMEC were plated on 16 mm coverslips for 24 h, prior to overnight serum starvation and stimulation with 50 ng/mL VEGF for 10 or 30 min. Cells were then fixed with ice-cold MeOH, blocked in 5% BSA/PBS with donkey serum and stained with an antibody against ERK5, prior to staining with a fluorescent secondary antibody and image acquisition with an inverted Zeiss Axio Observer microscope and the associated Zen software.

To further explore the potential localisation of ERK5 in VEGF-stimulated HDMEC, a subcellular protein fractionation kit was utilised to separate the cellular compartments over various stimulation time points (Figure 4.5).

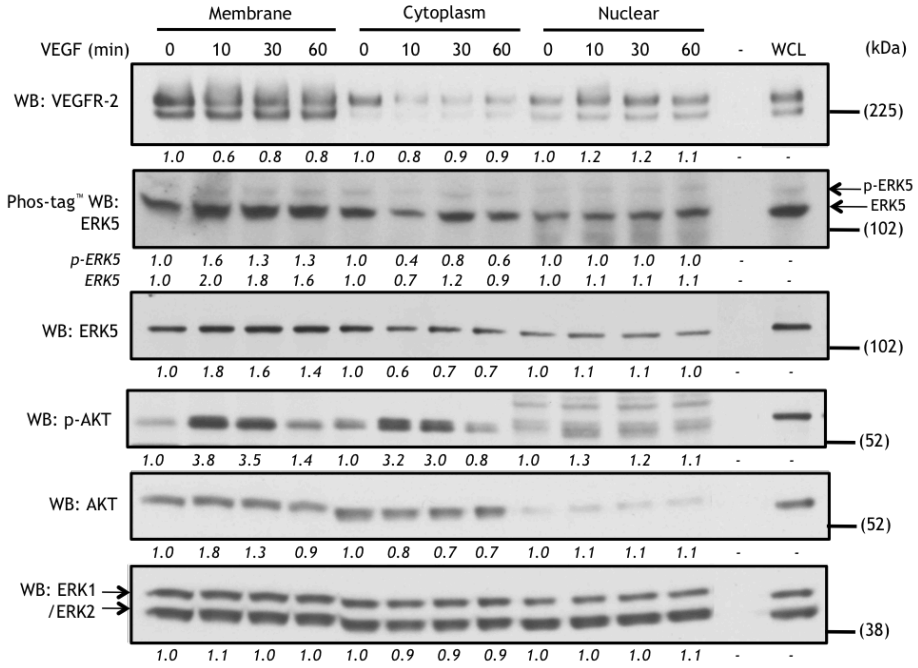

Figure 4.5 Subcellular protein fractionation of HDMEC.
HDMEC were seeded on 10 cm plates for 24 h prior to overnight serum starvation and stimulation with 50 ng/mL VEGF for 10, 30 and 60 min. Cells were then lysed with the appropriate buffers from the Thermo Fisher Subcellular Fractionation Kit. Lysates were separated on a 4-12% NuPAGE gel as well as a 7% (w/v) acrylamide, 70 µM Phos-tag™ gel, followed by Western blotting (WB) with antibodies against VEGFR-2, ERK5, AKT and ERK1/2. *Densitometric analysis of protein phosphorylation or protein expression relative to the basal control condition of each subcellular region, is displayed beneath each blot. The basal control condition was set arbitrarily as 1.0 for each protein and each subcellular region. This result is representative of two independent experiments.*

The use of subcellular controls (CD31 - membrane, GAPDH - cytoplasm and Lamin - nuclear) established that each fraction contained some presence of contaminants from other compartments, however the enrichment of each subcellular protein in comparison to the whole cell lysate was evident (Appendix IV). Following this, the localisation of VEGFR-2, ERK5, AKT and ERK1/2 was studied.

As expected, VEGFR-2 localised predominantly to the membrane during the 10, 30 and 60 min stimulation time points (Figure 4.5). Small amounts were detected in the nucleus upon VEGF stimulation, which may be attributable to internalisation and translocation of the receptor to the nucleus; a phenomenon observed to occur in endothelial cells (Santos *et al.*, 2007) and has since been shown to be a dynamic process (Domingues *et al.*, 2011).

From the 0 min basal to the 10 min stimulation time point, the amount of ERK5 in the cytoplasm decreased, yet in the same time frame the ERK5 quantity increased in the membranous fraction nearly two-fold (Figure 4.5). The presence of ERK5 at the membrane decreased slightly, yet remained somewhat sustained at the expense of its existence in the cytoplasm.

The use of Phos-tag™ SDS-PAGE with these fraction lysates similarly highlighted the increase of both the unphosphorylated and phosphorylated forms of ERK5 at the membrane after 10 min VEGF stimulation, with a noticeable decrease of both forms in the cytoplasm at the same time point (Figure 4.5). Once again, the amounts of both ERK5 and p-ERK5 at the membrane slightly decreased at the 30 and 60 min time points, however they still remained higher than the basal condition. Dissimilar to previous observations, the 30 min time point in the cytoplasm revealed a replenishment in the amount of ERK5 which decreased again at 60 min, however at both time points p-ERK5 was lower than that of the basal condition (Figure 4.5).

Interestingly, the levels of AKT follow a pattern similar to that of ERK5. Over the time points, the amount of AKT in the cytoplasm decreases however at the membrane, there is a peak of AKT at 10 min, followed by a slight decrease at the 30 min time point. The difference to this trend is at 60 min, where the level of AKT drops to just below that of the basal condition (Figure 4.5).

The intracellular localisation of p-AKT differed to that of AKT; a three-fold increase in p-AKT was observed at the 10 min and 30 min time points in the cytoplasm, followed by a decrease to below basal levels at 60 min (Figure 4.5). Additionally the increased levels of AKT previously observed at the membrane resulted in increased p-AKT at 10 min and 30 min and a decreased, yet somewhat sustained, phosphorylation at 60 min (Figure 4.5).

The constant levels of ERK1/2 throughout all time points and in each cellular fraction suggest that VEGF does not affect its intracellular localisation (Figure 4.5).

Taken together, these data suggest that the inability of VEGF to induce C-terminal phosphorylation of ERK5 affects the intracellular localisation of ERK5, subsequently resulting in a more cytoplasmic/plasma membranous rather than nuclear localisation as observed with EGF stimulation of HeLa.

4.5 ERK5 co-localises with AKT in HDMEC but not HeLa

The earlier subcellular fractionation data suggested that the localisation of AKT appeared to mimic that of ERK5, thus utilising co-staining and immunofluorescence, the intracellular localisation of ERK5 and phosphorylated AKT were investigated in HDMEC (Figure 4.6) and HeLa cells (Figure 4.7).

VEGF-stimulated HDMEC revealed an increase in p-AKT fluorescence in the cytoplasm at 10 min and this further increased at 30 min, compared to the basal (Figure 4.6). The high fluorescence of p-AKT detected in the nucleus of HDMEC was surprising considering the low levels detected in the subcellular fractionation.

The merged images highlight that although increased p-AKT is detected in the cytoplasm at the 10 min time point, it does not co-localise with ERK5 until 30 min, visualised as white fluorescence in the cytoplasm and at the cell periphery (Figure 4.6).

In HeLa cells, the levels of p-AKT increased in the cytoplasm at 10 min EGF stimulation, but this decreased back to basal levels at 30 min stimulation (Figure 4.7). Consequently, the co-staining reveals that at the 10 min time point there is no co-localisation evident, as the punctate green and magenta fluorescence remain distinct from one another in the merged image (Figure 4.7). Once again due to the pre-existing nuclear p-AKT staining in the basal condition as well as in the stimulated conditions, the apparent co-localisation of ERK5 and AKT at the 30 min time point may be a circumstantial observation (Figure 4.7). Furthermore, it must be considered that the presence of numerous proteins within the confined area of the nucleus may be incorrectly interpreted as co-localisation.

These data draw attention to the key difference that sustained stimulation of HDMEC with VEGF results in an intracellular co-localisation of ERK5 and phosphorylated AKT within the cytoplasm and at the fringes of the cell, whereas neither acute, nor sustained EGF stimulation of HeLa cells produces co-localisation of these two proteins.

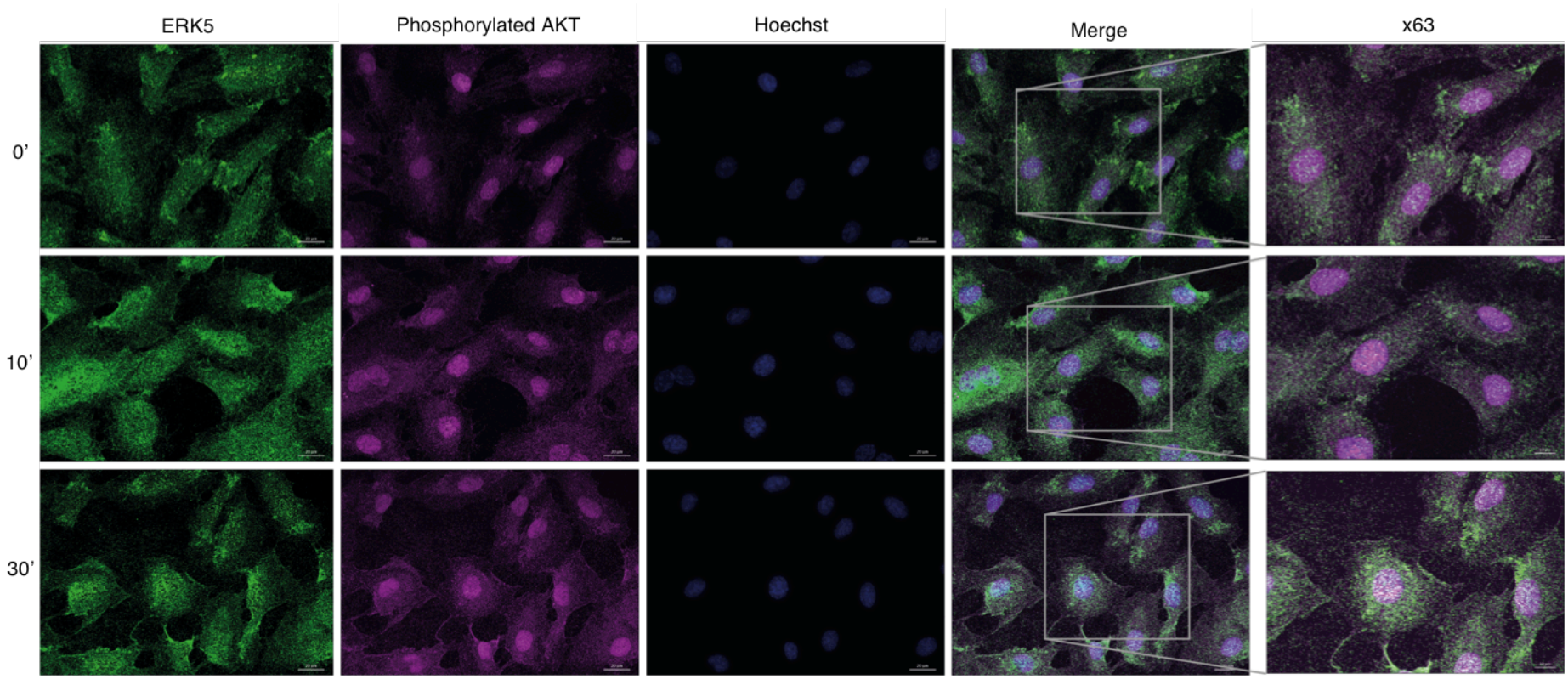

Figure 4.6 ERK5 and AKT co-staining in HDMEC reveals co-localisation within the cytoplasm and the cell periphery.
HDMEC were seeded at 3.0 x 10^4 cells per 16 mm coverslips for 24 h. Cells were serum started overnight, then stimulated for 10 or 30 min with 50 ng/mL VEGF. Cells were then stained with an antibody against ERK5 (green), p-AKT (magenta) and the nucleus with Hoechst (blue) for detection of intracellular co-localisation.

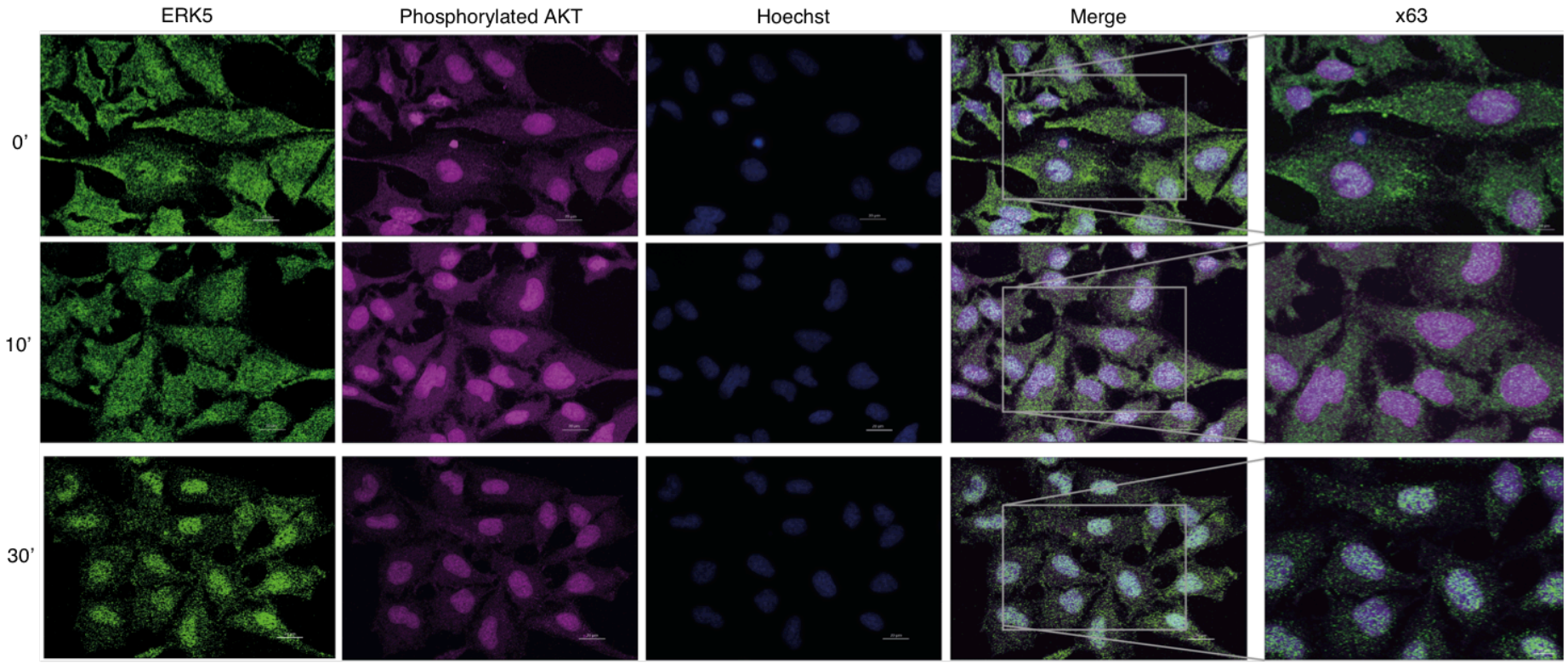

Figure 4.7 ERK5 and AKT co-staining in HeLa reveals a lack of co-localisation.
HeLa were seeded at 4.0 x 10^4 cells per 16 mm coverslips for 24 h. Cells were serum starved overnight, then stimulated for 10 or 30 min with 50 ng/mL EGF. Cells were then stained with an antibody against ERK5 (green), p-AKT (magenta) and the nucleus with Hoechst (blue) for detection of intracellular localisation.

4.6 MEK5 kinase activity is required for VEGF-stimulated AKT activity in HDMEC

It has recently been observed that ERK5 is required for VEGF-induced phosphorylation of AKT in HDMEC during tubular morphogenesis (Roberts *et al.*, 2010) and additional studies implicate ERK5 in growth-factor induced activation of AKT in other cells (Lennartsson *et al.*, 2010; Razumovskaya *et al.*, 2011). Taken together with the subcellular fractionation and co-localisation data shown earlier in this study, this suggests that ERK5 may play a role in coupling growth factor receptors to AKT, leading to its activation and subsequently regulating cellular survival. To further investigate the potential involvement of VEGF, EGF as well as activated ERK5, in the regulation of AKT activity, the commercially available MEK5 and ERK5 inhibitors were pre-incubated with HDMEC or HeLa prior to acute agonist stimulation.

The dose-response data for these inhibitors from the previous chapter (Figure 3.10 - Figure 3.13), determined the optimum concentration of the MEK5 inhibitor BIX 02189 was 10 μM and the ERK5 in HDMEC and HeLa without affecting other pathways such as ERK1/2 phosphorylation in a non-specific manner.

VEGF stimulation of the untreated HDMEC and 0.1% (v/v) DMSO vehicle control gave rise to the phosphorylation of VEGFR-2, ERK5, AKT and ERK1/2 to similar levels, thus confirming that the signalling pathways were not affected by the presence of DMSO at this concentration (Figure 4.8).

The MEK5 inhibitor, BIX 02189, significantly reduced VEGF-induced phosphorylation of ERK5 as detected by Phos-tag™ SDS-PAGE ($p<0.05$), with no observed effects on ERK1/2 phosphorylation (Figure 4.8). Two important observations were highlighted with this BIX-treated, VEGF-stimulated condition – there was a marked increase in VEGFR-2 phosphorylation and a significant decrease in AKT phosphorylation ($p<0.01$). Thus, it is proposed that the inhibition of MEK5 kinase activity with BIX 02189 prevents MEK5 from dual-phosphorylating the Thr^{218}/Tyr^{220} residues of ERK5 and as a consequence, ERK5 activation and p-AKT is decreased (Figure 4.8). The increase in p-VEGFR2 is thought to occur in response to a decrease in receptor internalisation and degradation, due to MEK5 inhibition by BIX 02189. In the presence of BIX 02189, the levels of VEGFR-2 after VEGF stimulation are maintained, suggesting that MEK5 may play a role in the internalisation of the receptor (Figure 4.8).

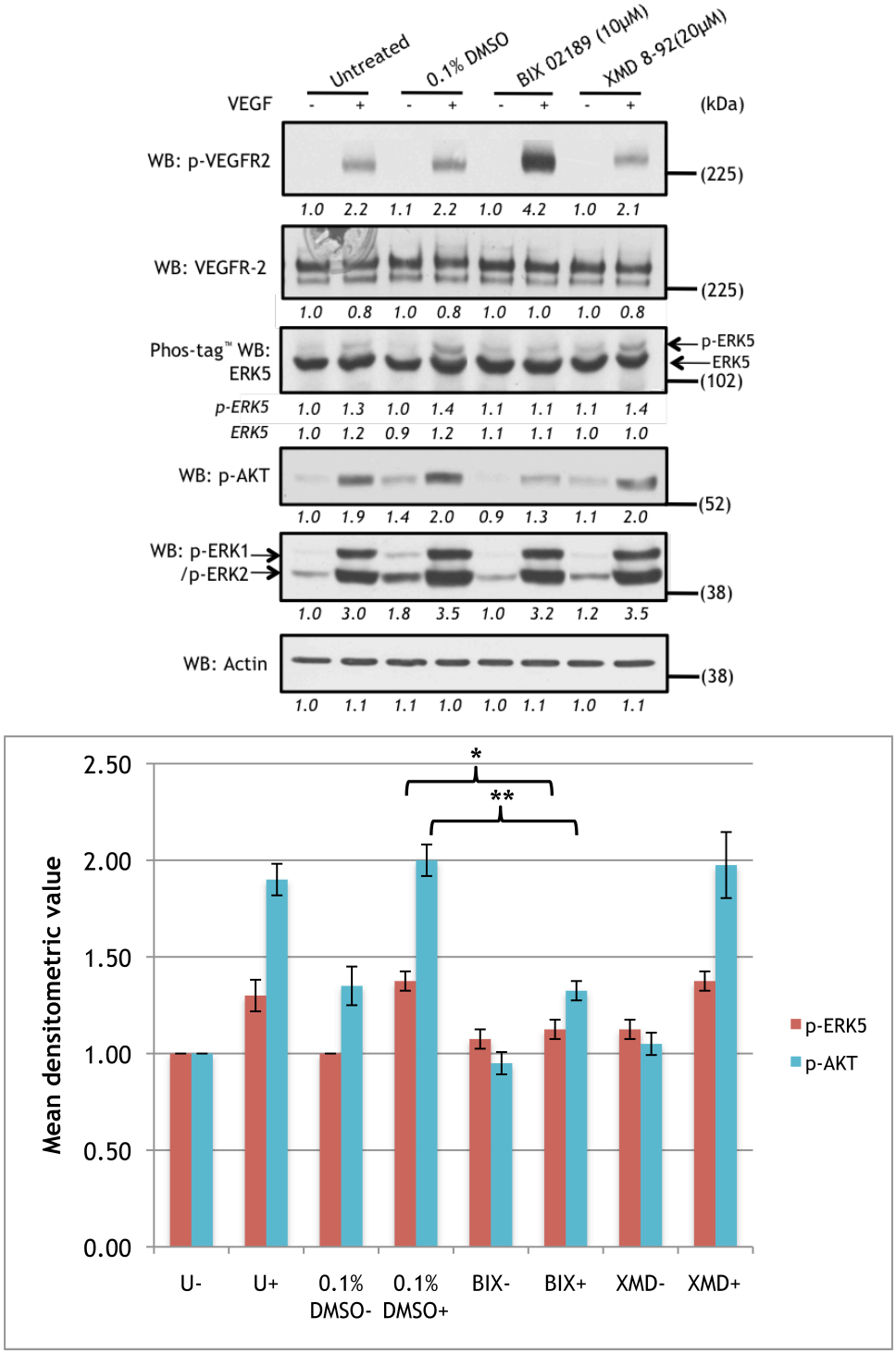

Figure 4.8 VEGF-stimulated AKT activity in HDMEC is dependent upon MEK5 kinase activity. HDMEC were plated on 12-well plates for 24 hours, followed by overnight serum starvation. Cells were pre-incubated with 0.1% (v/v) DMSO as a vehicle control, BIX 02189 (10 μM) or XMD8-92 (20 μM) for 1 hour, prior to addition of VEGF (50 ng/mL final concentration) for 10 min and RIPA lysis. Protein lysates were separated on 4-12% NuPAGE® gels as well as a 7% (w/v) acrylamide, 70 μM Phos-tag™ gel. Membranes were incubated with antibodies against p-VEGFR2, VEGFR-2 ERK5, p-AKT, p-ERK1/2 and Actin. *This experiment is representative of four individual experiments (*p<0.05, **p<0.01).*

Treatment with the ERK5 inhibitor, XMD8-92 did not appear to have any effect on the phosphorylation of VEGFR-2, ERK5, AKT or ERK1/2, further confirming the hypothesis that C-terminal phosphorylation of ERK5 does not occur in VEGF-stimulated HDMEC, but also that C-terminal phosphorylation is not required in the regulation of AKT activity (Figure 4.8).

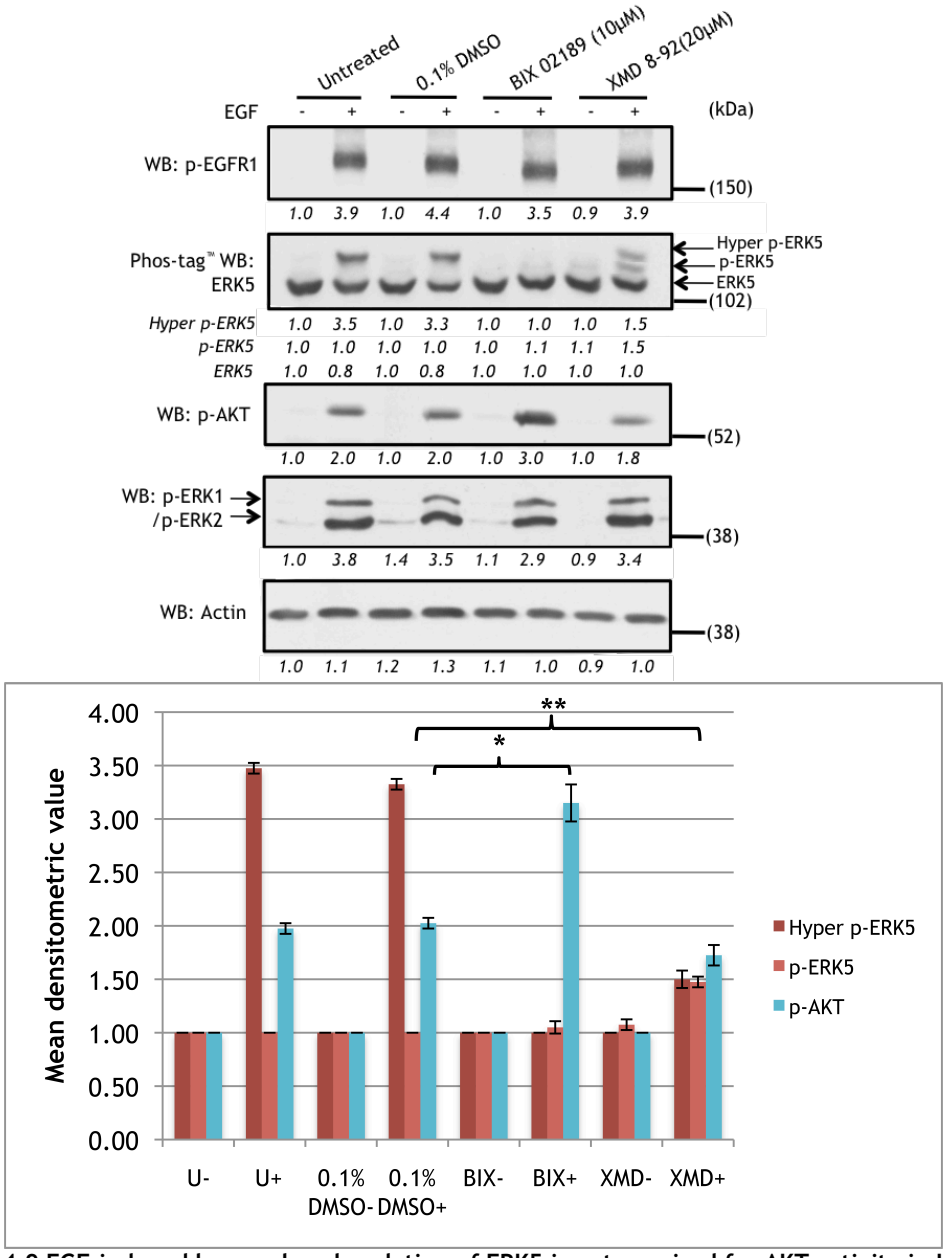

Figure 4.9 EGF-induced hyper phosphorylation of ERK5 is not required for AKT activity in HeLa. HeLa were plated on 12-well plates for 24 hours, followed by overnight serum starvation. Cells were pre-incubated with 0.1% (v/v) DMSO as a vehicle control, BIX 02189 (10 μM) or XMD8-92 (20 μM) for 1 hour, prior to addition of EGF (50 ng/mL final concentration) for 10 min and RIPA lysis. Protein lysates were separated on 4-12% NuPAGE® gels as well as a 7% (w/v) acrylamide, 70 μM Phos-tag™ gel. Membranes were incubated with antibodies against p-EGFR1, ERK5, p-AKT, p-ERK1/2 and Actin. *This experiment is representative of four individual experiments (*p<0.05, **p<0.01).*

The use of BIX 02189 in HeLa cells significantly reduced EGF-induced p-ERK5 and hyper p-ERK5 ($p<0.01$). However, in contrast to results observed in the HDMEC, AKT phosphorylation increased 1.5-fold ($p<0.05$) with no notable effect on EGFR-1 phosphorylation observed (Figure 4.9), suggesting a potential negative feedback loop with EGF, which is inhibited by BIX 02189.

As expected, inhibition with XMD8-92 prevented EGF-induced hyper-phosphorylation of ERK5, yet p-ERK5 was still evident (Figure 4.9). No other significant differences were observed, implying C-terminal phosphorylation is not required for AKT activity.

These results suggest that VEGF- and EGF-induced AKT activity have opposing dependencies regarding MEK5 kinase activity. In HDMEC, phosphorylation of AKT requires VEGF-mediated MEK5 kinase activity and consequently ERK5 activation. In HeLa however, AKT activation may exist within a negative feedback loop with EGF, which is inhibited by the presence of BIX 02189. Nevertheless, it is apparent that C-terminal phosphorylation of ERK5 does not play a role in AKT activity.

4.7 Discussion

Current literature reports that phosphorylation of the Thr^{218}/Tyr^{220} residues of ERK5 leads to kinase activity and concomitant autophosphorylation of C-terminal Ser/Thr residues (Mody *et al.*, 2003; Buschbeck and Ullrich, 2005; Morimoto *et al.*, 2007). This study has uncovered a novel discovery in that VEGFR-2 activation of ERK5 shows that kinase activity and phosphorylation of C-terminal residues are not necessarily mutually inclusive events. VEGF induces phosphorylation of the Thr^{218}/Tyr^{220} residues, however it fails to induce phosphorylation of C-terminal residues of ERK5 (Figure 4.1). Dual-phosphorylation of T-E-Y alone is insufficient to decrease the electrophoretic mobility on conventional SDS-PAGE, hence the lack of mobility bandshift observed in VEGF-stimulated HDMEC in the previous chapter (Section 3.2.1) – a finding which has previously been observed in HEK293 cells (Mody *et al.*, 2003).

In contrast, this study has shown that EGF stimulation of ERK5 activity results in phosphorylation of Thr^{218}/Tyr^{220}, as well as C-terminal residues including Thr^{732} (Figure 4.1). Interestingly, although this Thr^{732} residue directly precedes a proline residue, VEGF was unable to induce its phosphorylation, suggesting that an alternative pathway may feed into the phosphorylation of C-terminal residues upon EGF stimulation.

Subsequent experiments aimed to further identify potential downstream signalling proteins that may contribute to this difference in growth factor-induced ERK5 phosphorylation, thus siRNA was utilised against RAF-1, HRAS, KRAS and NRAS – molecules known to be differentially activated by VEGFR-2 and EGFR-1 (Hallberg *et al.*, 1994; Sasaoka *et al.*, 1994; Sakaguchi *et al.*, 1998; Doanes *et al.*, 1999; Takahashi *et al.*, 2001; Zachary, 2003). Results from these experiments uncovered the possible involvement of HRAS in EGF-mediated C-terminal phosphorylation of ERK5, as a significant decrease in hyper p-ERK5 was observed upon HRAS knockdown (Figure 4.2). It is important to note that although the protein level of KRAS appeared to be knocked-down by approximately 85% in both HDMEC and HeLa, the non-specific nature of the antibody used to detect the protein in Western blotting, makes this result somewhat unreliable. Thus additional evidence would be required to ensure the lack of KRAS involvement in EGF-mediated C-terminal phosphorylation of ERK5. A previous study reported no effect on EGF-induced ERK5 activation in HeLa cells in the presence of a dominant-active (G12V) RAS (Kato *et al.*, 1998), the mutation favoured by HRAS (Prior *et al.*, 2012), however with the hypothesis that dominant-active HRAS would only induce C-terminal phosphorylation of ERK5, it would not affect the EGF-mediated phosphorylation of T-E-Y. Nevertheless, as EGF activation of the various RAS isoforms has already been demonstrated in HeLa (Omerovic *et al.*, 2008), the use of a RAS activation assay would confirm the involvement, or lack thereof, of VEGF-activated RAS in HDMEC.

Despite the aforementioned differences in VEGF- and EGF-mediated phosphorylation of ERK5, it was observed that phosphorylation of both Thr^{218}/Tyr^{220} in the activation loop, as well as residues present on the C-terminal, was required for nuclear localisation of ERK5. Thus, as EGF was able to phosphorylate all these residues in HeLa, ERK5 translocated from the cytoplasm into the nucleus after 10 min stimulation, with translocation more evident at 30 min (Figure 4.3). However, VEGF-mediated phosphorylation of ERK5 on Thr^{218}/Tyr^{220} in the absence of C-terminal phosphorylation renders the protein unable to undergo translocation to the nucleus, instead localising in the cytoplasm and at the plasma membrane (Figure 4.4, Figure 4.5) in HDMEC. The data produced from the subcellular fractionation experiment revealed an interesting finding in that along with ERK5 having a more cytoplasmic/plasma membranous localisation, AKT also appeared to follow suit (Figure 4.5). It is important to consider the purity of these subcellular fractions in this interpretation however, as the subcellular controls in Appendix IV demonstrated some presence of contaminants from other compartments. Nevertheless, the co-localisation of the two proteins was investigated using immunofluorescence co-staining (Figure 4.6 and Figure 4.7).

The data from these co-staining experiments revealed that upon sustained VEGF stimulation (30 min), ERK5 and p-AKT appeared to co-localise as visualised by white fluorescence in the cytoplasm and at the periphery of the cell (Figure 4.6), a result also observed in the subcellular fractionation (Figure 4.5). Interestingly however, this co-localisation was not evident in acute or sustained EGF-stimulated HeLa cells, as separate punctate fluorescence for each protein was observed (Figure 4.7). This disparity in VEGF- and EGF- induced co-localisation with p-AKT suggests that ERK5 may play different roles in various cell types dependent upon growth factor stimulus.

With the use of specific MEK5 and ERK5 small-molecule inhibitors, the association between ERK5 and AKT was further exposed; it was apparent that VEGF-mediated AKT activity in HDMEC required MEK5 kinase activity, but not ERK5 kinase activity (Figure 4.8), whereas EGF-mediated AKT activity appeared to increase upon addition of BIX 02189 (Figure 4.9). The positive correlation between ERK5 and AKT upon VEGF stimulation is one that has been previously observed in HDMEC with respect to cell survival and tubular morphogenesis (Roberts *et al.*, 2010). Additional studies have implicated ERK5 in PDGFR-ß-mediated activation of AKT in PAE cells (Lennartsson *et al.*, 2010) and FLT3-mediated activation of AKT in the Ba/F3 pro-B-cell line (Razumovskaya *et al.*, 2011), however a very recent study has proposed a novel, positive feedback loop between ERK5 and AKT in PDGF-stimulated mesangial cells (Bera *et al.*, 2014). This feedback loop is suggested to lie downstream of PI3K, yet in parallel to the ERK1/2 signalling pathway, however no data are shown with respect to the phosphorylation levels of the receptor upon inhibition of PI3K, AKT or ERK5 (Bera *et al.*, 2014).

Small-molecule inhibitor data from this chapter and Chapter 3 have revealed an interesting association between VEGFR-2 and MEK5 (Figure 4.8 and Figure 3.10). The addition of BIX 02189 in VEGF-stimulated HDMEC resulted in increased receptor phosphorylation compared to that of the untreated stimulated condition (Figure 4.8). It has been established that VEGFR-2 is internalised upon VEGF stimulation (Santos *et al.*, 2007), hence the observed decrease in receptor levels between the untreated basal and untreated stimulated condition (Figure 4.8). However in the presence of BIX 02189, VEGFR-2 levels are maintained upon VEGF stimulation, suggesting the possible involvement of MEK5 kinase activity in VEGFR-2 internalisation.

Intriguingly, EGF-mediated AKT activity in HeLa was observed to increase upon MEK5 kinase inhibition (Figure 4.9), whereas the inhibition of ERK5 C-terminal phosphorylation with XMD 8-92 did not appear to have any effect on p-AKT levels (Figure 4.9). These data

suggest that ERK5 and AKT may exist within a negative feedback loop with EGF which is inhibited by the presence of BIX 02189 but not XMD8-92.

The specific mechanism through which ERK5 regulates VEGF-induced AKT phosphorylation still remains unclear. It has been considered that ERK5 may phosphorylate and consequently inactivate a phosphatase that regulates AKT phosphorylation, e.g. PP2A or MKP3 (Pankov *et al.*, 2003; Razmara *et al.*, 2012), rather than ERK5 directly phosphorylating AKT, as it is well established that mTORC2 and PDK1 are responsible for AKT activation via phosphorylation at Thr^{308} and Ser^{473} (Alessi *et al.*, 1996; Jacinto *et al.*, 2006; Sarbassov *et al.*, 2006). A recent study demonstrated the requirement of ERK5 in VEGF-mediated AKT phosphorylation in HDMEC, whereby siRNA against ERK5 resulted in a decrease in p-AKT (Roberts *et al.*, 2010). This finding is supported by novel data from this study; inhibition of VEGF-induced ERK5 phosphorylation of Thr^{218}/Tyr^{220} with BIX 02189 leads to a 50% decrease in AKT phosphorylation (Figure 4.8). However the inability of the ERK5 kinase inhibitor XMD8-92 to affect VEGF-stimulated AKT activation (Figure 4.8) suggests that only the Thr^{218}/Tyr^{220} phosphorylation of ERK5 is critical for VEGF-mediated AKT regulation, rather than the ability of ERK5 to subsequently phosphorylate downstream targets. Additionally, the intracellular localisation of ERK5 and AKT is significant, as this reveals a potential interaction between the two proteins, which may result in either a direct or indirect mode of AKT phosphorylation by ERK5. Thus in an attempt to further investigate the association between ERK5 and AKT in VEGF- and EGF- stimulated cells, experiments in the next chapter utilise adenoviral gene transduction to overexpress FLAG-epitope tagged ERK5 in the primary HDMECs followed by immunoprecipitation and mass spectrometry analysis.

Chapter Five
Proteomic analysis of ERK5-interacting proteins in HDMEC

5.1 Introduction

The data from Chapter 4 revealed a potential link between ERK5 and AKT in VEGF-stimulated HDMEC; immunofluorescence highlighted an intracellular co-localisation of the two proteins and small-molecule inhibitors uncovered the dependency of AKT phosphorylation on MEK5 kinase activity. In contrast, with EGF-stimulated HeLa cells, AKT did not appear to co-localise with ERK5 and inhibition of MEK5 kinase activity did not inhibit EGF-stimulated AKT activity.

Previous studies have identified MEF2D as an ERK5-interacting protein using yeast 'two-hybrid' screen, *in vitro* GST-pull down assays, as well as antiserum to detect immunoprecipitation of MEF2 associated proteins *in vivo* (Yang *et al.*, 1998; Kasler *et al.*, 2000). However, as it is unclear if ERK5 is able to directly phosphorylate AKT on Thr^{308} and Ser^{473}, there remains a distinct possibility that unidentified ancillary proteins interact with ERK5 to facilitate AKT phosphorylation. A complex containing multiple proteins could prove difficult to detect at endogenous levels, thus overexpression of ERK5 using adenoviral-mediated gene delivery was utilised to express a FLAG-epitope tagged ERK5 in HDMEC and HeLa. The FLAG-tag could then be exploited during immunoprecipitation prior to Western blotting. In addition to this, mass spectrometry was utilised to further confirm potential binding partners of ERK5. Achieving high transfection efficiency in primary human cells such as endothelial cells is known to be notoriously difficult. The discontinued transfection reagent TransPass™ HUVEC transfection reagent (NEB®, 2013) reports to have been able to achieve a 40% transfection efficiency in HDMEC, whereas the current Lipofectamine™ 2000 transfection (LifeTechnologies™) reports to achieve <2% transfection efficiency in HUVECs. The study from which this project has progressed previously utilised Amaxa® Nucleofector® technology (Lonza, 2014) to transfect HDMECs, but this led to low cell viability.

Recombinant adenoviruses are the most commonly used vectors utilised as gene transfer vectors *in vivo* and *in vitro*. They are advantageous due to their high transduction efficiency and ability to infect both dividing as well as resting cells without actively integrating into the host genome, therein resulting in transient gene expression (Anton *et al.*, 2012). Adenoviruses enter the target cells by binding to the Coxsackie/Adenovirus receptor (CAR) (Bergelson *et al.*, 1997) prior to being internalised via integrin-mediated endocytosis (Russell, 2000) and transported into the nucleus. Here, transcription and translation of E1 proteins occurs, two early phase events that are essential for the subsequent expression of adenoviral late genes and viral replication.

The ViraPower™ adenoviral expression system utilised in this project generates a replication-incompetent adenovirus due to the deletion of E1 and E3 in the destination vector (pAd/CMV-DEST) capable of delivering a gene of interest, i.e. FLAG-ERK5. The HEK293A producer cells contain a stably integrated copy of E1, thus they are infected with the pAd/CMV-DEST thereby supplying it with the E1 proteins required to facilitate early phase transcription and translation of the adenovirus. The pAd/CMV-DEST contains the human cytomegalovirus (CMV) promoter, which controls the expression of FLAG-ERK5, hence it is termed pAd/CMV/FLAG-ERK5. The adenoviral FLAG-ERK5 was used as a gene delivery vehicle, whereby HDMEC and HeLa cells were transduced with the adenovirus, with no occurrence of viral replication.

Mass spectrometry (MS) of small molecules has been used for over 50 years in combination with a wide variety of ionisation techniques such as chemical ionisation, electron ionisation and fast atom bombardment. However, these methods of ionisation were not readily applicable to larger molecules such as peptides and proteins, hence the introduction of mild ionisation technologies.

The original concept of matrix-assisted laser desorption/ionization (MALDI) was developed in 1988, whereby a laser bombards sample molecules in an absorbing matrix, resulting in an ionised sample (Karas and Hillenkamp, 1988). Since then, MS-based technologies have become much more sophisticated enabling the identification and quantification of low-abundance proteins. Methods such as electrospray ionisation (ESI) (Fenn *et al.*, 1989), isotope-coded affinity tags (ICATs) (Gygi *et al.*, 1999), stable-isotope labelling by amino acids in cell culture (SILAC) (Ong *et al.*, 2002), isotope-coded protein label (ICPL) (Schmidt *et al.*, 2005), isobaric tags for relative and absolute quantification (iTRAQ) (Ross *et al.*, 2004) have all aided in the detection of previously undetectable, low-abundance proteins. This project utilised label-free analysis using an UltiMate 3000 RSLC™ nano system (Thermo Scientific) coupled to a QExactive™ mass spectrometer (Thermo Scientific).

This chapter details experiments conducted to characterise the potential interaction of ERK5 and AKT in both HDMEC and HeLa cells and the further analysis of potential VEGF-stimulated ERK5-interacting proteins in HDMEC.

5.2 RIPA vs sucrose lysis buffer for immunoprecipitation

Radio-immunoprecipitation assay (RIPA) buffer is a commonly used cell lysis reagent, due to its robustness in lysis and extracting proteins (abcam®). Nowadays, the original isotopic assay method is rarely performed, however the acronym for this buffer endured. The presence of three non-ionic and ionic detergents results in a vigorous lysis buffer. As RIPA buffer was utilised in the preparation of protein lysates for Western blotting, it was also initially used in the preparation of immunoprecipitation lysates (Figure 5.1).

Immunoprecipitation was conducted in order to initially precipitate, isolate and concentrate ERK5 out of the HDMEC or HeLa protein lysates with the use of an antibody previously bound to agarose beads. Subsequently, SDS-PAGE and Western blotting was utilised in an attempt to ascertain potential interacting partners of ERK5. MEK5 has previously been shown to bind ERK5, via the PB1 domain and 34 amino acid C-terminal extension of MEK5 (Nakamura *et al.*, 2006), hence blotting for MEK5 acts as a positive control for the ERK5 IP experiments.

Furthermore, data from the previous chapter highlighted a potential role for MEK5 in VEGFR-2 internalisation and degradation in HDMEC and as a consequence, the receptor may also be in close proximity to ERK5. In contrast, no association was observed between MEK5 kinase activity and EGFR-1 in the previous chapter, thus blotting for EGFR-1 after IP could provide evidence to confirm this theory. Additionally, an antibody against AKT was also utilised in order to further elucidate the potential interaction between ERK5 and AKT in HDMEC.

It was evident that in both the HeLa and HDMEC, relatively low levels of ERK5 expression were detected in both the IP and total lysates after RIPA lysis (Figure 5.1). The high detergent content of RIPA results in a highly denaturing lysis buffer, deeming it somewhat incompatible for its use in IP. Consequently, a sucrose lysis buffer was considered for the preparation of IP lysates as it stabilises lysosymal membranes and reduces the release of proteases (Figure 5.2).

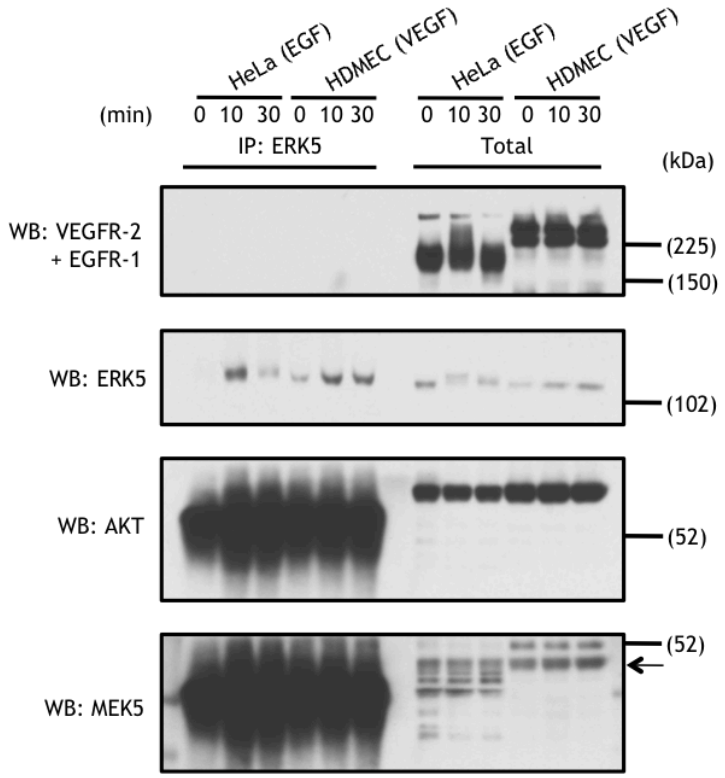

Figure 5.1 Immunoprecipitation of endogenous ERK5 after lysis with RIPA buffer.
HeLa and HDMEC were seeded on 10 cm dishes for 24 h, prior to overnight serum starvation. Cells were then stimulated with EGF or VEGF (50 ng/mL) for 10 or 30 min, followed by RIPA lysis. Lysates were immunoprecipitated (IP) overnight, at 4°C with an antibody against ERK5 (AF2848) that had been previously bound to Protein G Plus agarose beads. The beads were then spun down and washed, prior to the addition of 1 volume of LDS and boiling at 90°C. Samples were separated on 4-12% NuPAGE® gels and membranes were incubated with antibodies against VEGFR-2+EGFR-1, ERK5, AKT and MEK5 for Western blotting (WB). Arrows indicate the protein band of interest amongst other non-specific bands. This result is representative of three individual experiments.

Cells lysed with the sucrose lysis buffer displayed higher levels of ERK5 in both the IP and total lysates, compared to that detected after RIPA lysis (Figure 5.2). The presence of proteins additional to AKT and MEK5 detected in the total lysates, were not considered problematic due to the enhanced detection of our proteins of interest. However, in both lysis methods, the presence of the heavy IgG-γ chains from the un-coupled ERK5 antibody (50-55 kDa) obscured the detection of AKT and MEK5 in the IP lysates (Figure 5.1 and Figure 5.2).

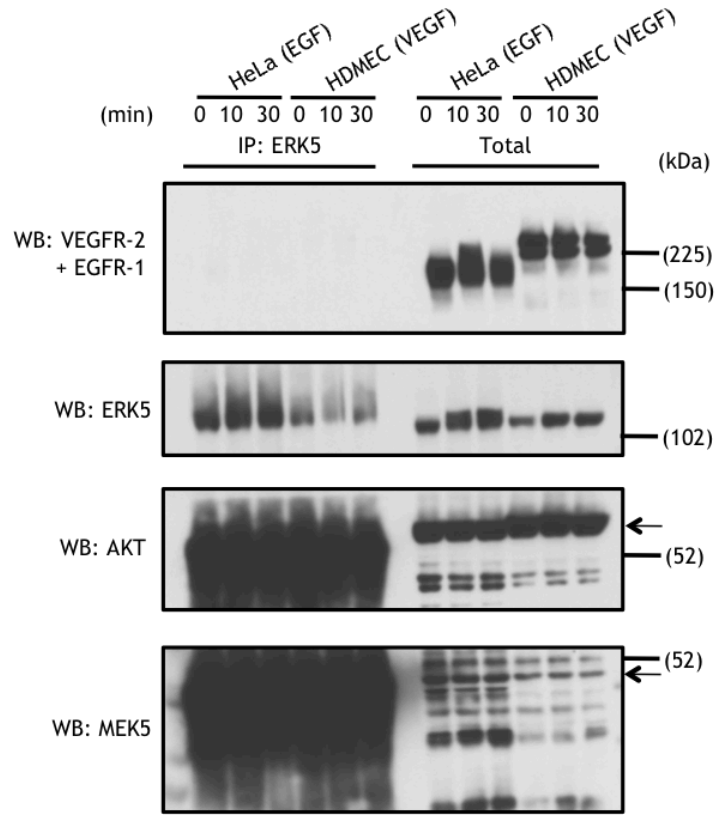

Figure 5.2 Immunoprecipitation of endogenous ERK5 after lysis with sucrose buffer.
HeLa and HDMEC were seeded on 10 cm dishes for 24 h, prior to overnight serum starvation. Cells were then stimulated with EGF or VEGF (50 ng/mL) for 10 or 30 min, followed by sucrose lysis. Lysates were immunoprecipitated (IP) overnight, at 4°C with an antibody against ERK5 (AF2848) that had been previously bound to Protein G Plus agarose beads. The beads were then spun down and washed, prior to the addition of 1 volume of LDS and boiling at 90°C. Samples were separated on 4-12% NuPAGE® gels and membranes were incubated with antibodies against VEGFR-2+EGFR-1, ERK5, AKT and MEK5 for Western blotting (WB). Arrows indicate the protein band of interest amongst other non-specific bands. This result is representative of three individual experiments.

This could be overcome with the use of an agarose conjugated ERK5 antibody (sc-1284 AC) to prevent free antibody, and subsequently free IgG-γ chains, from concealing the 50kDa region. However, this pre-conjugated antibody proved somewhat less effective in immunoprecipitating ERK5 than the one originally used (AF2848) (Figure 5.3). Additionally, very low expressions of co-precipitating proteins were detected in endogenous levels (data not shown). Figure 5.3 illustrates the various antibodies tested for efficient IP of ERK5, as well as the Protein G Plus agarose beads control.

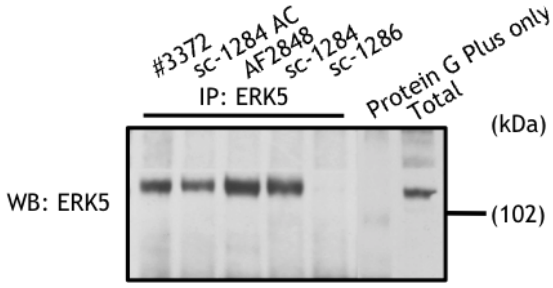

Figure 5.3 Antibodies against ERK5 utilised to ascertain immunoprecipitation efficiency.
HDMEC were seeded on 10 cm dishes for 24 h, prior to overnight serum starvation. Cells were then stimulated with VEGF (50 ng/mL) for 10 min, followed by sucrose lysis. Lysates were immunoprecipitated (IP) overnight, at 4°C with antibodies against ERK5 (#3372 NEB, sc-1284 AC SC, AF2848 R&D, sc-1284 SC and sc-1286 SC) that had been previously bound to Protein G Plus agarose beads, alongside a Protein G plus agarose beads only control. The beads were then spun down and washed, prior to the addition of 1 volume of LDS and boiling at 90°C. Samples were separated on 4-12% NuPAGE® gels and membranes were incubated with an antibody against ERK5 (#3372 NEB).

5.3 Overexpression of ERK5, reveals AKT as a potential interacting partner in HDMEC but not HeLa

The use of adenoviral-mediated gene delivery to overexpress FLAG-tagged ERK5 in HDMEC and HeLa cells offered a two-fold advantage: ERK5 could be overexpressed in an attempt to increase the binding of potential ERK5-interacting proteins, and the FLAG-epitope tag could be utilised for efficient immunoprecipitation with an anti-FLAG antibody covalently coupled to agarose beads, reducing the potential presence of the heavy IgG-γ chains.

In order to determine the level of ERK5 expression required for subsequent experiments, HeLa and HDMEC were transduced with a range of adenoviral multiplicity of infection (MOI) and analysed using Western blotting (Figure 5.4 and Figure 5.5). It was evident that the adenovirus efficiently transduced overexpression of ERK5 in both cell types, with overexpression noticeable from a MOI of 5 in HeLa (Figure 5.4) and as little as MOI of 1 in HDMEC (Figure 5.5). The use of an anti-FLAG® M2 antibody enabled confirmation of the expression of the FLAG-epitope tag, and in both cell types the tag was first detected at a MOI of 5 (Figure 5.4 and Figure 5.5).

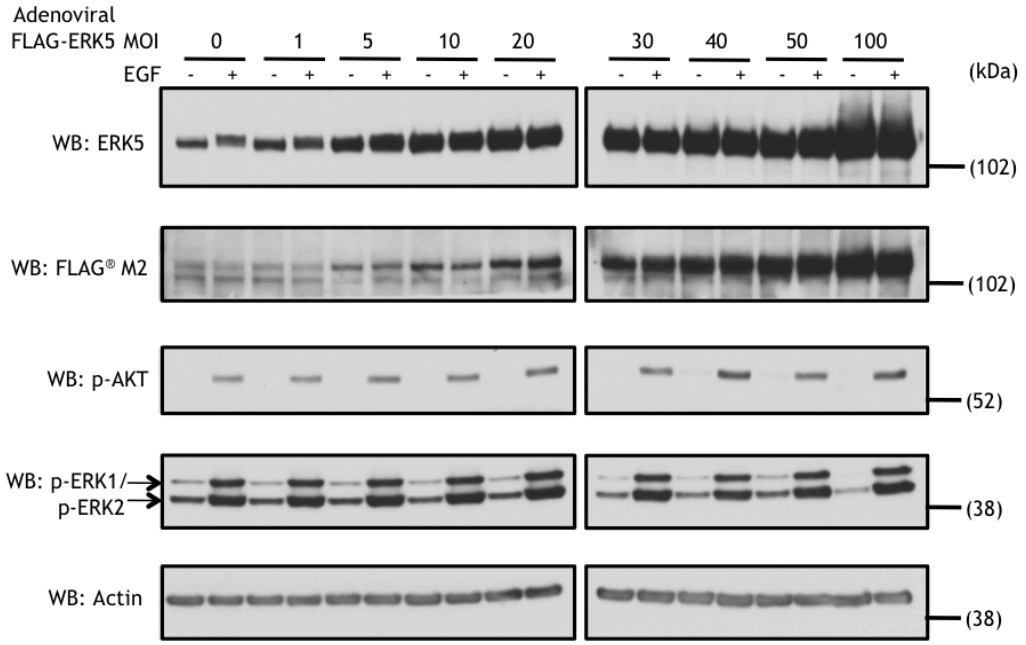

Figure 5.4 Adenoviral MOI response of adenoviral FLAG-ERK5 in HeLa.
HeLa were plated on 12-well plates for 24 h. Cells were either left untransduced, or transduced with adenoviral FLAG-ERK5 with a range of MOI: 1, 5, 10, 20, 30, 40, 50 or 100 for 30 h, prior to overnight serum starvation. Cells were then stimulated with EGF (50 ng/mL) for 10 min and lysed. Protein lysates were separated on 4-12% NuPAGE® gels and incubated with antibodies against ERK5, FLAG® M2, p-AKT, pERK1/2 and Actin. This result is representative of two individual experiments.

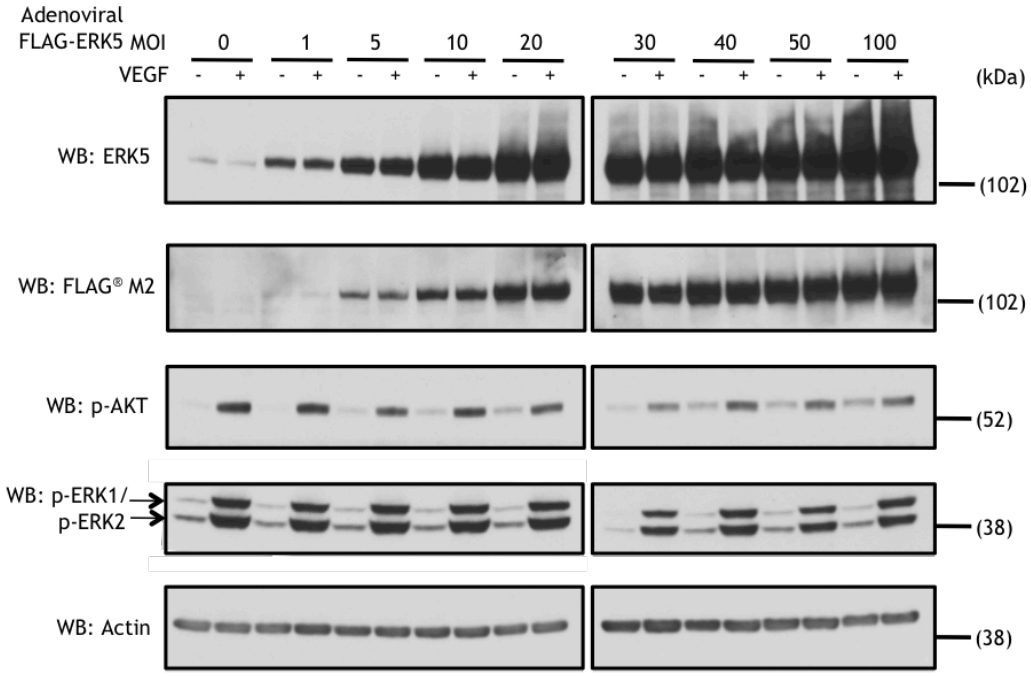

Figure 5.5 Adenoviral MOI response of adenoviral FLAG-ERK5 in HDMEC.
HDMEC were plated on 12-well plates for 24 h. Cells were either left untransduced, or transduced with adenoviral FLAG-ERK5 with a range of MOI: 1, 5, 10, 20, 30, 40, 50 or 100 for 30 h, prior to overnight serum starvation. Cells were then stimulated with VEGF (50 ng/mL) for 10 min and lysed. Protein lysates were separated on 4-12% NuPAGE® gels and incubated with antibodies against ERK5, FLAG® M2, p-AKT, pERK1/2 and Actin. This result is representative of two individual experiments.

From these adenoviral MOI response experiments, it was important to ascertain a MOI that would enable sufficient ERK5 overexpression, without inducing artefacts, or affecting other parallel signalling pathways such as ERK1/2; thus a MOI of 20 was utilised for subsequent IP experiments.

HeLa and HDMEC transduced with adenoviral FLAG-ERK5 and stimulated with EGF or VEGF (50 ng/mL) for 10 min or 30 min were precipitated with an anti-FLAG® M2 antibody covalently coupled to agarose beads (A2220) (Figure 5.6).

Western blotting with an antibody against AKT revealed that this protein was co-precipitated along with FLAG-tagged ERK5 in HDMEC but not in HeLa cells. AKT appeared to co-precipitate with ERK5 in the unstimulated condition, however the amount increased upon stimulation with VEGF for 10 min and 30 min (Figure 5.6). These results support the subcellular fractionation data from the previous chapter whereby an increase in ERK5 at the membrane after VEGF stimulation, resulted in increased levels of AKT (Figure 4.5).

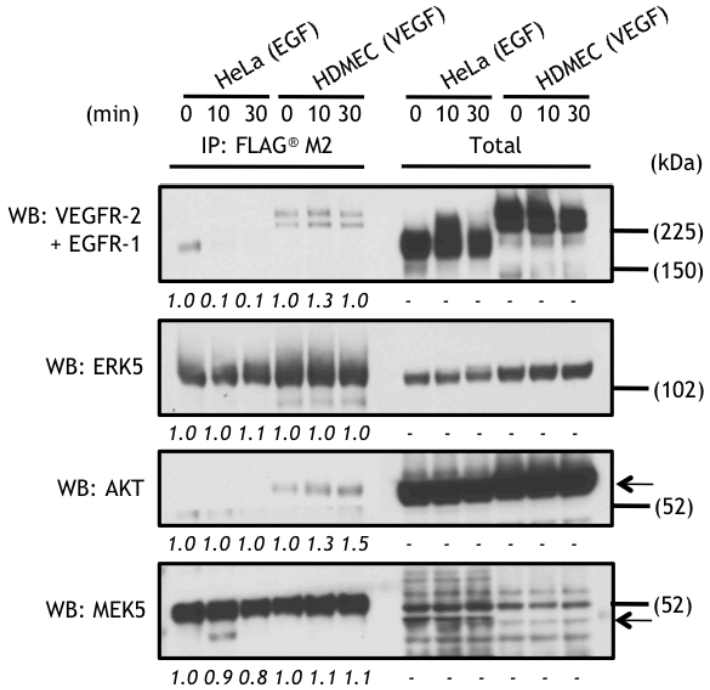

Figure 5.6 Immunoprecipitation of overexpressed ERK5 in HeLa and HDMEC.
HeLa and HDMEC were seeded on 10 cm dishes for 24 h, prior to 48 h incubation with adenoviral FLAG-ERK5 MOI 20. Cells were then serum starved overnight, then stimulated with EGF or VEGF (50 ng/mL) for 10 or 30 min, followed by sucrose lysis. Lysates were immunoprecipitated (IP) overnight, at 4°C with an anti-FLAG® M2 antibody covalently coupled to agarose beads (A2220). The beads were then spun down and washed, prior to the addition of 1 volume of LDS and boiling at 90°C. Samples were separated on 4-12% NuPAGE® gels and membranes were incubated with antibodies against VEGFR-2+EGFR-1, ERK5, AKT and MEK5 for Western blotting (WB). Arrows indicate the protein band of interest amongst other non-specific bands. This result is representative of two individual experiments.

A rather interesting discovery during this IP experiment was the co-immunoprecipitation of the relevant RTKS. In HeLa cells, EGFR-1 appeared to co-precipitate with ERK5 in the unstimulated condition, whereas in HDMEC, VEGFR-2 co-precipitated with ERK5 in all conditions, with a noticeable increase at 10 min following VEGF stimulation (Figure 5.6).

The reciprocal IP using an antibody against AKT for precipitation was conducted in order to validate the co-precipitation of AKT with ERK5 (Figure 5.7). Although the heavy IgG-γ chains yet again masked the 50 kDa region, Western blotting against ERK5 demonstrated that HeLa cells did not reveal an ERK5-AKT interaction, whereas once more ERK5 co-precipitated with AKT in HDMEC (Figure 5.7). It was observed that in the two VEGF-stimulated conditions, the levels of ERK5 was more than that of the unstimulated condition, with the 30 min stimulation revealing the greatest amount of ERK5 (Figure 5.7).

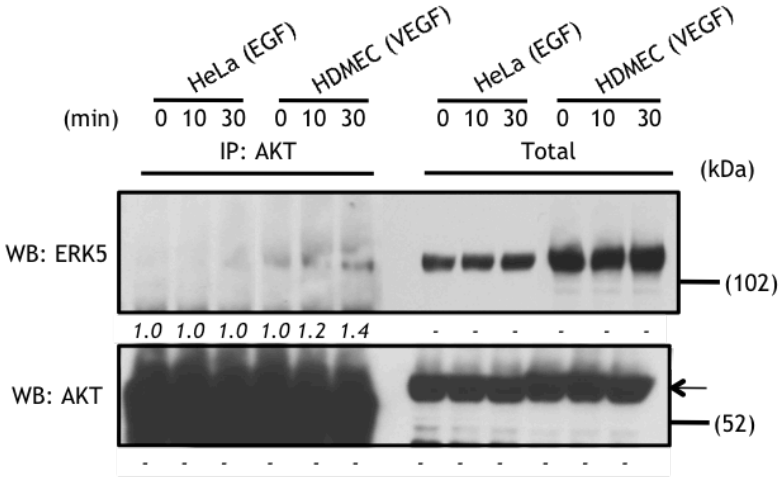

Figure 5.7 Immunoprecipitation of AKT in HeLa and HDMEC overexpressing ERK5.
HeLa and HDMEC were seeded on 10 cm dishes for 24 h, prior to 48 h incubation with adenoviral FLAG-ERK5 MOI 20. Cells were then serum starved overnight, then stimulated with EGF or VEGF (50 ng/mL) for 10 or 30 min, followed by sucrose lysis. Lysates were immunoprecipitated (IP) overnight, at 4°C with an antibody against AKT that had been previously bound to Protein G Plus agarose beads. The beads were then spun down and washed, prior to the addition of 1 volume of LDS and boiling at 90°C. Samples were separated on 4-12% NuPAGE® gels and membranes were incubated with antibodies against VEGFR-2+EGFR, ERK5, AKT and MEK5 for Western blotting (WB). Arrows indicate the protein band of interest amongst other non-specific bands. This result is representative of one experiment.

5.4 Discovery proteomics

In an attempt to further substantiate the novel finding that ERK5 and AKT may interact with one another in HDMEC, this protein-protein interaction was examined with the use of mass spectrometry (LC-MS/MS). HDMEC were transduced with adenoviral FLAG-ERK5 for 30 h in order to induce ERK5 overexpression. Three conditions of HDMEC were investigated: 1.

Untransduced, basal control, 2. Transduced, basal control and 3. Transduced, 30 min VEGF-stimulated condition. HDMEC samples prepared for analysis by mass spectrometry, were initially immunoprecipitated with an antibody against FLAG® M2 and evaluated using SDS-PAGE and Western blotting (Figure 5.8), as well as with silver staining (Figure 5.9).

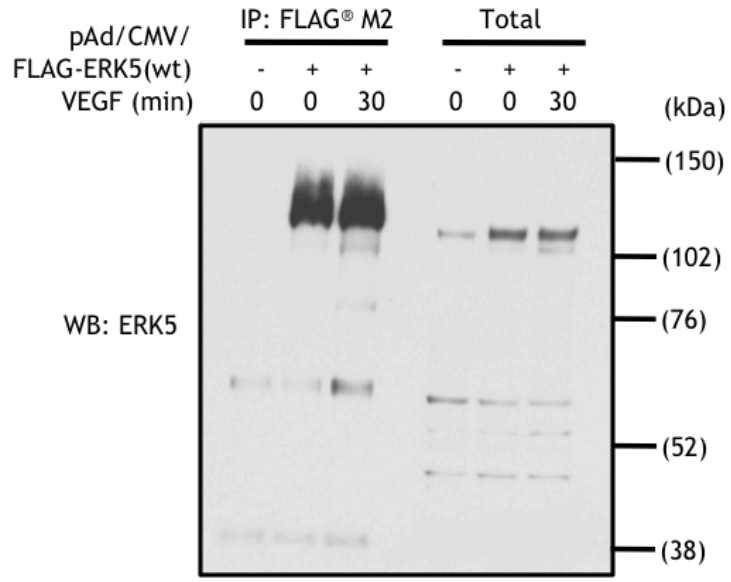

Figure 5.8 Western blot of samples to be run on LC-MS/MS.
HDMEC were seeded on multiple 10 cm dishes for 24 h, prior to 30 h incubation with adenoviral FLAG-ERK5 MOI 20. Cells were then serum starved overnight, then stimulated with VEGF (50 ng/mL) for 30 min, followed by sucrose lysis. Lysates were immunoprecipitated (IP) overnight, at 4°C C with an agarose conjugated antibody against FLAG® tag. The beads were then spun down and washed, prior to the removal of a fraction of bead lysates, addition of 1 volume of LDS and boiling at 90°C. Protein samples were separated on 4-12% NuPAGE® gels and membranes were incubated with antibodies against ERK5 for Western blotting (WB). This result is representative of three individual experiments.

It was evident that in both the Western blot (Figure 5.8) and silver stain (Figure 5.9), proteins in addition to ERK5 were detected in these samples and consequently sent to Professor Rob Beynon (Proteomics Group, Institute of Integrative Biology, University of Liverpool, Crown Street, Liverpool L69 7ZB) for proteomic analysis.

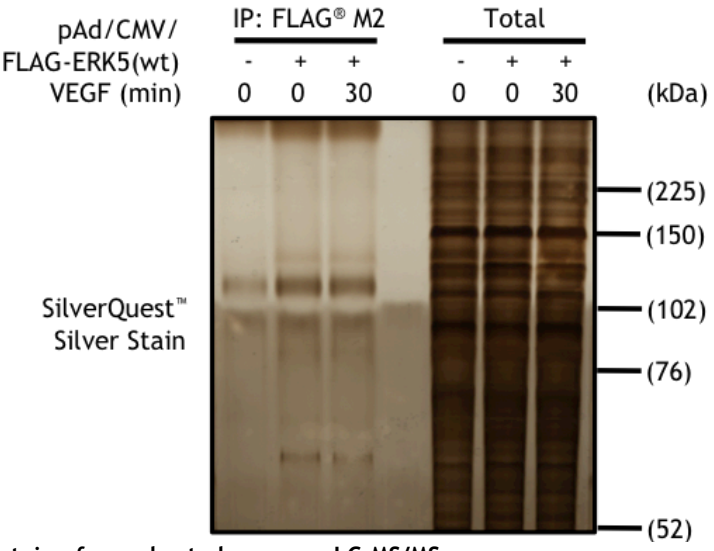

Figure 5.9 Silver stain of samples to be run on LC-MS/MS.
Protein samples used in Figure 5.8 were separated on 4-12% NuPAGE® gels prior to membrane fixation, sensitisation and development, as per the SilverQuest™ Silver Staining kit (Life Technologies™) protocol.

The results obtained from the three separate runs were consolidated. Proteins present in the untransduced basal condition were subtracted from each transduced condition, after which only proteins present in two out of the three independent runs were retained (Figure 5.10). The remaining proteins were further whittled down according to the number of unique peptides, with a cut-off point of 2 unique peptides (Figure 5.10). The protein hits for each experimental condition, after applying the aforementioned restrictions are summarised in Table 5.1, Table 5.2 and Table 5.3, with the comprehensive tables available to view in Appendix V.

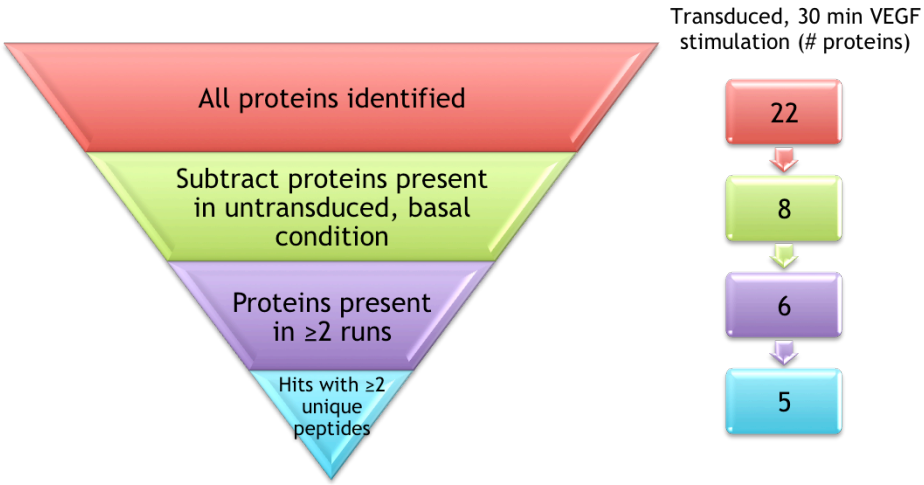

Figure 5.10 Flowchart of resultant proteins from proteomic analysis for the transduced, 30 min VEGF-stimulated condition.
Proteins initially detected in the transduced, 30 min VEGF-stimulated condition, were subjected to subtraction of proteins present in the untranduced, basal condition, then restricted to those only present in two of the three independent runs conducted, followed by elimination of proteins with <2 unique peptides.

It was evident that of the remaining candidate proteins detected in the transduced 30 min VEGF-stimulated condition, ERK5 (termed MAPK7 in the proteomic readout) was noticeably present with an average of 10 unique peptides across the three runs (Table 5.3). The use of STRING 9.1 (http://string-db.org), a network analysis program, enabled the creation of Figure 5.11 providing known and predicted protein-protein interactions for the resultant candidate proteins.

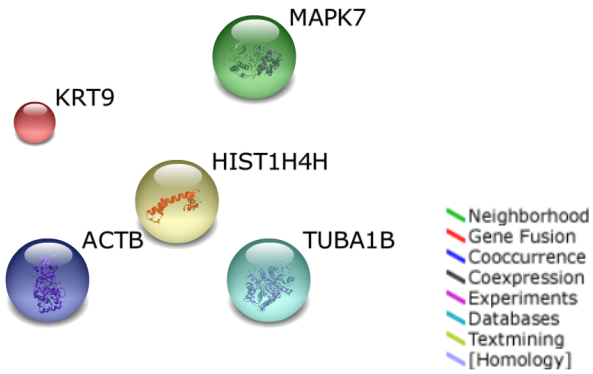

Figure 5.11 Original STRING network analysis.
Resultant candidate proteins in the transduced, 30 min VEGF-stimulated condition were interpreted by STRING 9.1 to produce a visual network analysis. Key: KRT9 (Keratin), ACTB (Actin), HIST1H4H (Histone), TUBA1B (Tubulin), MAPK7 (Mitogen-activated protein kinase 7; ERK5).

Table 5.1 Readout of proteins discovered in the untransduced, basal condition after LC-MS/MS
Peptides: total number of peptides identified as belonging to each protein; # Unique Peptides: number of peptides identified with high confidence for each protein

		Run 1		Run 2		Run 3			
Accession	Description	# Unique Peptides	# Peptides	# Unique Peptides	# Peptides	# Unique Peptides	# Peptides	Average Unique	Average peptides
O14744	Protein arginine N-methyltransferase 5 OS=Homo sapiens GN=PRMT5 PE=1 SV=4 - [ANM5_HUMAN]	2	7	2	8	2	9	2	8
O60814	Histone H2B type 1-K OS=Homo sapiens GN=HIST1H2BK PE=1 SV=3 - [H2B1K_HUMAN]	1	2	1	1	N/A	N/A	1	2
P01616	Ig kappa chain V-II region MIL OS=Homo sapiens PE=1 SV=1 - [KV203_HUMAN]	1	1	1	1	1	1	1	1
P01859	Ig gamma-2 chain C region OS=Homo sapiens GN=IGHG2 PE=1 SV=2 - [IGHG2_HUMAN]	1	1	1	1	N/A	N/A	1	1
P02768	Serum albumin OS=Homo sapiens GN=ALB PE=1 SV=2 - [ALBU_HUMAN]	2	6	N/A	N/A	3	5	3	6
P04264	Keratin, type II cytoskeletal 1 OS=Homo sapiens GN=KRT1 PE=1 SV=6 - [K2C1_HUMAN]	2	6	13	17	2	5	6	9
P13645	Keratin, type I cytoskeletal 10 OS=Homo sapiens GN=KRT10 PE=1 SV=6 - [K1C10_HUMAN]	1	4	6	14	N/A	N/A	4	9
P19474	E3 ubiquitin-protein ligase TRIM21 OS=Homo sapiens GN=TRIM21 PE=1 SV=1 - [RO52_HUMAN]	N/A	N/A	1	1	1	1	1	1
P35908	Keratin, type II cytoskeletal 2 epidermal OS=Homo sapiens GN=KRT2 PE=1 SV=2 - [K22E_HUMAN]	N/A	N/A	3	9	1	3	2	6
P52732	Kinesin-like protein KIF11 OS=Homo sapiens GN=KIF11 PE=1 SV=2 - [KIF11_HUMAN]	N/A	N/A	1	2	1	12	1	7
P62805	Histone H4 OS=Homo sapiens GN=HIST1H4A PE=1 SV=2 - [H4_HUMAN]	N/A	N/A	1	3	1	3	1	3
Q92851	Caspase-10 OS=Homo sapiens GN=CASP10 PE=1 SV=3 - [CASPA_HUMAN]	N/A	N/A	1	1	1	1	1	1
Q9BQA1	Methylosome protein 50 OS=Homo sapiens GN=WDR77 PE=1 SV=1 - [MEP50_HUMAN]	1	2	1	3	2	4	1	3
Q9BQE3	Tubulin alpha-1C chain OS=Homo sapiens GN=TUBA1C PE=1 SV=1 - [TBA1C_HUMAN]	1	5	N/A	N/A	3	4	2	5

Table 5.2 Readout of proteins discovered in the transduced, basal condition after LC-MS/MS
Peptides: total number of peptides identified as belonging to each protein; # Unique Peptides: number of peptides identified with high confidence for each protein

		Run 1		Run 2		Run 3			
Accession	Description	# Unique Peptides	# Peptides	# Unique Peptides	# Peptides	# Unique Peptides	# Peptides	Average Unique	Average peptides
P07437	Tubulin beta chain OS=Homo sapiens GN=TUBB PE=1 SV=2 - [TBB5_HUMAN]	N/A	N/A	3	4	2	7	3	6
P60709	Actin, cytoplasmic 1 OS=Homo sapiens GN=ACTB PE=1 SV=1 - [ACTB_HUMAN]	N/A	N/A	1	6	1	8	1	7
P68363	Tubulin alpha-1B chain OS=Homo sapiens GN=TUBA1B PE=1 SV=1 - [TBA1B_HUMAN]	N/A	N/A	4	6	5	6	5	6
Q13164	Mitogen-activated protein kinase 7 OS=Homo sapiens GN=MAPK7 PE=1 SV=2 - [MK07_HUMAN]	2	14	12	21	12	26	9	20

Table 5.3 Readout of proteins discovered in the transduced, 30 min VEGF stimulated condition after LC-MS/MS
Peptides: total number of peptides identified as belonging to each protein; # Unique Peptides: number of peptides identified with high confidence for each protein

		Run 1		Run 2		Run 3			
Accession	Description	# Unique Peptides	# Peptides	# Unique Peptides	# Peptides	# Unique Peptides	# Peptides	Average Unique	Average peptides
P35527	Keratin, type I cytoskeletal 9 OS=Homo sapiens GN=KRT9 PE=1 SV=3 - [K1C9_HUMAN]	1	4	3	6	N/A	N/A	2	5
P60709	Actin, cytoplasmic 1 OS=Homo sapiens GN=ACTB PE=1 SV=1 - [ACTB_HUMAN]	2	5	1	6	1	6	1	6
P62805	Histone H4 OS=Homo sapiens GN=HIST1H4A PE=1 SV=2 - [H4_HUMAN]	1	2	1	2	1	3	1	2
P68363	Tubulin alpha-1B chain OS=Homo sapiens GN=TUBA1B PE=1 SV=1 - [TBA1B_HUMAN]	5	5	2	5	5	6	4	5
Q13164	Mitogen-activated protein kinase 7 OS=Homo sapiens GN=MAPK7 PE=1 SV=2 - [MK07_HUMAN]	9	22	9	26	11	25	10	24

ERK5 was present in the original network analysis, however there were no immediate protein-protein interactions (either known or predicted) with any of the other candidate proteins. Thus, an expanded network was created to include 10 additional predicted partners (Figure 5.12).

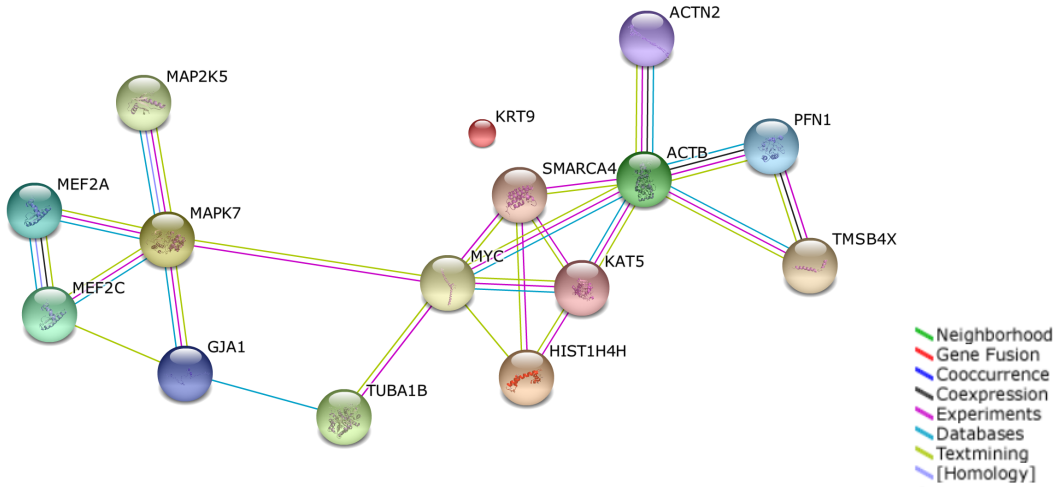

Figure 5.12 Expanded STRING network analysis.
STRING 9.1 included an additional 10 protein partners into the original network analysis to produce an expanded network. Key: KRT9 (Keratin), HIST1H4H (Histone), MAPK7 (ERK5), TUBA1B (Tubulin), ACTB (Actin), MEF2C (Myocyte enhancer factor 2C), MEF2A (Myocyte enhancer factor 2A), PFN1 (Profilin 1), GJA1 (Gap junction protein, alpha 1), ACTN2 (Actinin, alpha 2), KAT5 (Lysine acetyltransferase 5), SMARCA4 (SWI/SNF related, matrix associated, actin dependent regulator of chromatin, subfamily a, member 4), TMSB4X (Thymosin beta 4, X-linked), MYC (v-myc myelocytomatosis viral oncogene homolog), MAP2K5 (Mitogen-activated protein kinase kinase 5; MEK5).

The expanded network analysis provided a new and rather interesting association between ERK5 and tubulin alpha-1B chain, via gap junction alpha-1 protein (GJA1). Thus, the inclusion of GJA1 as an intermediary junction increases the scope of additional proteins acting as interacting partners of ERK5.

5.5 Discussion

Early data from this chapter (Figure 5.6 and Figure 5.7) provides additional evidence to support the intriguing association between ERK5 and AKT in HDMEC, initially uncovered in Chapter 3. This chapter utilised an adenovirus generated to encode for FLAG-ERK5, which could then be added to HDMEC and HeLa cells to transduce an overexpression of ERK5. As previously mentioned, primary human cells are particularly difficult to transfect with high

efficiency. The use of a current, commercially available transfection reagent is only able to achieve <2% transfection efficiency in HUVECs, thus adenovirus-mediated gene delivery was preferred.

Immunoprecipitation experiments revealed the presence of AKT upon ERK5 overexpression and precipitation in HDMEC (Figure 5.6). Additionally, a greater amount of AKT appeared to co-precipitate at the 30 min stimulation time point rather than the 10 min time point. The subsequent experiment conducting a reciprocal IP (IP: AKT and WB: ERK5), further confirmed that ERK5 could also be detected as co-precipitating with AKT in HDMEC, and once again a larger amount was observed at the 30 min time point (Figure 5.7). There appeared to be no association evident between ERK5 and AKT in HeLa (Figure 5.6 and Figure 5.7) potentially suggesting a differential role for VEGF- and EGF- stimulation of ERK5 and AKT activity. Few studies have investigated the role of VEGF-mediated ERK5 phosphorylation in regulating AKT activity, however the study from which this project has progressed, initially highlighted the requirement for ERK5 in VEGF-stimulated AKT phosphorylation in HDMEC (Roberts *et al.*, 2010). Instead, data from this project suggest a possible co-localisation (Figure 4.5) and interaction between ERK5 and AKT in HDMEC (Figure 5.6 and Figure 5.7).

Subsequently, mass spectrometry was utilised in conjunction with ERK5 overexpression, in an attempt to further confirm AKT as a potential binding partner of activated ERK5 in HDMEC (Table 5.3). The results obtained from the proteomic analysis however, did not identify AKT in the immunoprecipitated proteins, which may have been due to the binding of ERK5 and AKT being transient. Thus, in an attempt to ascertain this potential transient interaction between ERK5 and AKT, additional proteomic experiments would require the inclusion of extra VEGF-stimulated time points such as 1, 5, 10 and 20 mins.

However, with the ERK5-AKT interaction evident during Western blotting (Figure 5.8), it may suggest that it is instead necessary to optimise the sample conditions for mass spectrometry, especially considering the somewhat disconcerting lack of known binding partners such as MEK5, which would be expected to be identified by mass spectrometry following ERK5 immunoprecipitation. It is apparent that the conditions were correct for the mass spectrometry process, as our bait protein, ERK5, was present in the proteomic readout. Nevertheless, these conditions may not have been appropriate for the interacting complex itself. The samples were frozen at -80°C after preparation, however they were only processed 6 weeks later, enabling the potential occurrence of protein degradation. This remains a possibility as the average number of ERK5 peptides discovered was only 24, a relatively low quantity considering the protein appeared to be adequately overexpressed

as detected by Western blotting and silver staining (Figure 5.8 and Figure 5.9). Thus, bearing in mind that AKT itself was not overexpressed, the endogenous number of peptides may have been degraded to levels undetectable by the mass spectrometry instrument. Consequently, the overexpression of both ERK5 and AKT with two different epitope tags, may be required to ascertain the nature of the interaction either as direct binding of the two proteins, or their existence as a complex.

The network analysis program STRING 9.1 was used to process candidate proteins originally discovered during mass spectrometry. This analysis schematic displayed ERK5 and tubulin alpha-1B chain present, yet with no direct association with one another, or any of the other resultant proteins (Figure 5.11). However, by including additional interacting partners into the network, these two proteins were connected via the intermediary protein, gap junction alpha-1 protein (GJA1).

GJA1, also known as Connexin43 or Cx43, is a membrane-spanning protein that is able to form channels between adjacent cells, thereby bridging the gap and enabling intercellular exchange of information. Initial studies involving ERK5 and Cx43, reported the phosphorylation of Cx43 on Ser^{255} by ERK5 both *in vitro* and *in vivo* in EGF-stimulated HEK293 cells (Cameron *et al.*, 2003), however in 2006 Park and colleagues demonstrated a "mode-1" interaction of 14-3-3 θ with phospho-Ser^{373} of Cx43 (Park *et al.*, 2006). Previous evidence has shown AKT to often mediate 14-3-3 interactions by phosphorylating target proteins (Kovacina *et al.*, 2003), thus Park et al., were subsequently able to demonstrate Cx43 as being a substrate for AKT in EGF-stimulated Rat-1 fibroblasts (Park *et al.*, 2007).

In the context of these previous studies, data from this project may provide an additional aspect whereby VEGF-stimulated ERK5 initially presents in the cytoplasm followed by an interaction with, and consequent phosphorylation of, Cx43 at the plasma membrane. Cx43 in turn may complex with AKT either directly as a substrate, or indirectly via 14-3-3. It is important to note that although data from this project did not demonstrate a direct ERK5-AKT interaction, the possibility of these two proteins interacting in this manner must not be neglected. In view of the possible connection of Cx43 occurring between ERK5 and AKT, it may be that the presence of the transmembranous protein, Cx43, has obscured the proteomic result. The hydrophobic domains of the membrane protein would not have solubilised appropriately in the sucrose lysis buffer, resulting in its precipitation prior to being processed by mass spectrometry. Therefore, it would be necessary to optimise the conditions to include membrane proteins, such as the addition of a mass spectrometry-compatible detergent.

Chapter Six
General Discussion

6.1 The role and regulation of ERK5 in endothelial cells

The ubiquitously expressed ERK5 protein plays different, yet specific roles in various cell types (Sohn *et al.*, 2002; Hayashi *et al.*, 2004; Wang and Tournier, 2006; Spiering *et al.*, 2009) and in addition to regulating normal cellular processes such as proliferation, differentiation and survival (Kato *et al.*, 1998; Dinev *et al.*, 2001; Wang and Tournier, 2006), ERK5 has been implicated in the progression of pathologies such as cancer and ischaemia (Takeishi *et al.*, 1999; Montero *et al.*, 2009).

Global gene ablation techniques highlighted the critical role of ERK5 in normal vascular development (Hayashi and Lee, 2004), with the initial defect discovered to occur within the endothelium (Hayashi *et al.*, 2004). Since these findings however, only a handful of studies have characterised the activation of ERK5 within endothelial cells (Abe *et al.*, 1996; Yan *et al.*, 1999; Roberts *et al.*, 2010), yet numerous studies focussed on EGF-stimulated ERK5 activation in the context of tumour cell proliferation and intracellular localisation, thus leading to the development of small-molecule inhibitors (Kato *et al.*, 1998; Kamakura *et al.*, 1999; Hayashi *et al.*, 2001; Raviv *et al.*, 2004; Kondoh *et al.*, 2006; Tatake *et al.*, 2008; Yang *et al.*, 2010a).

This thesis has addressed key differences in ERK5 activation by different growth factors in both endothelial and HeLa cells, and as a consequence several novel discoveries have been revealed, which are discussed forthwith.

6.1.1 VEGF appears unique in its ability to stimulate ERK5 phosphorylation in HDMECs

The characterisation of ERK5 activation in HDMEC was initially investigated with the use of various growth factors, however it was VEGF that appeared to be unique in its ability to stimulate ERK5 phosphorylation in this cell type. Interestingly, VEGF was also able to induce phosphorylation of AKT (Figure 3.6) and with the use of the MEK5 inhibitor BIX 02189 (Figure 4.8), it was later discovered that ERK5 might play a role in the regulation of AKT activity. The association between AKT and ERK5 became more evident as subcellular protein fractionation experiments revealed a cytoplasmic/plasma membranous intracellular localisation of the two proteins (Figure 4.5), which was further supported by immunofluorescence experiments showing co-localisation of p-AKT and ERK5 in the cytoplasm and at the cell periphery (Figure 4.6).

It is important to note however, that the activation of both ERK5 and AKT in HDMEC are not events that are mutually inclusive of one another; stimulation with HGF acting through the c-Met receptor, demonstrates AKT activation in the absence of ERK5 phosphorylation (Figure 3.6). Instead, it appears that VEGF-mediated ERK5 activation requires the phosphorylation of PLCγ, as data utilising MAE cells stably expressing the Flk-1 $Y^{1173}F$ mutant receptor highlighted the significant decrease in ERK5 activation upon loss of PLCγ phosphorylation (Figure 3.8).

PLCγ phosphorylation hydrolyses IP_3 from PIP_2, which in turn mediates intracellular levels Ca^{2+} and DAG, a PKC activator; thus, it is possible that ERK5 activity maybe regulated by PKC. Numerous studies have implicated various PKC isoforms in the regulation of ERK5 activity (Diaz-Meco and Moscat, 2001; Li *et al.*, 2005; Zhao *et al.*, 2010), however others have shown that ERK5 activation does not occur via PKC (Abe *et al.*, 1996; Kato *et al.*, 1998; Yan *et al.*, 1999), thereby suggesting cell dependency with regards to activation of this pathway. VEGF-mediated proliferation in HDMEC has been shown to act through a PLCγ>PKC pathway, consequently activating ERK1/2 (Xia *et al.*, 1996; Wellner *et al.*, 1999; Takahashi *et al.*, 2001); the observed decrease in ERK1/2 activation in the MAE cells stably expressing Flk-1 $Y^{1173}F$ reflects this (Figure 3.8), however the presence of some residual ERK1/2 phosphorylation suggests the possibility of an alternative pathway feeding into its activation. Ras hyperactivation has been shown to induce a pro-angiogenic phenotype (Meadows *et al.*, 2004; Bajaj *et al.*, 2010), therefore it may be that an unidentified adaptor molecule directly couples VEGFR-2 to the GrbB2-Sos-Ras pathway thereby activating ERK1/2.

6.1.2 VEGF and EGF induce differential phosphorylation of ERK5 and intracellular localisation

Thus far, the majority of studies have adhered to the initial characterisation of ERK5 activation whereby the Thr^{218}/Tyr^{220} residues in the kinase domain are dual-phosphorylated, followed by the autophosphorylation of numerous C-terminal tail residues (Mody *et al.*, 2003). In light of the fact that reliable reagents for the detection of ERK5 activation are lacking, in particular a consistent phospho-ERK5 (Thr^{218}/Tyr^{220}) antibody for Western blotting and immunofluorescence, progress in the field has been limited to detecting ERK5 activation through electrophoretic mobility bandshift on conventional SDS-PAGE. This however presented a significant issue, as ERK5 activation in HDMEC could not be detected by mobility bandshift (Figure 3.1*b*). This project was able to overcome this hurdle with the use of the novel Phos-tag™ reagent in SDS-PAGE, and as a consequence this study revealed a novel difference in the phosphorylation events of ERK5 in VEGF-stimulated HDMEC and EGF-stimulated HeLa.

The activation of ERK5 resembles that of JNK, whereby phosphorylation by its upstream MAPKK preferentially phosphorylates the threonine residue of the T-X-Y motif (Lawler *et al.*, 1998; Mody *et al.*, 2003), in contrast to p38 MAPK and ERK1/2, which are preferentially phosphorylated on the tyrosine residue of the T-X-Y motif (Haystead *et al.*, 1992; Fleming *et al.*, 2000). However, unlike JNK, p38 MAPK and ERK1/2, in addition to dual-phosphorylation of the Thr/Tyr residues of the T-X-Y motif, ERK5 is able to undergo autophosphorylation of multiple residues of its C-terminal tail (Mody *et al.*, 2003; Buschbeck and Ullrich, 2005; Morimoto *et al.*, 2007).

This project discovered that in line with current literature regarding ERK5 activation, EGF-stimulated HeLa cells undergo phosphorylation of the Thr^{218}/Tyr^{220} residues in the activation loop of the kinase domain, but also at additional residues, such as Thr^{732}, thought to be in the C-terminal tail. This resulted in a mobility bandshift with conventional SDS-PAGE (Figure 3.1*a*) and a dual bandshift with Phos-tag™ SDS-PAGE (p-ERK5 and hyper p-ERK5) (Figure 3.5). It was subsequently ascertained that the p-ERK5 band corresponded to phosphorylation of Thr^{218}/Tyr^{220} (Figure 4.1*a*), and that the hyper p-ERK5 band comprised of phosphorylation of these same two residues as well as additional C-terminal residues (Figure 4.1*b*).

VEGF-stimulation of HDMEC did not induce an ERK5 mobility bandshift using conventional SDS-PAGE (Figure 3.1*b*, however a single bandshift was detected with Phos-tag™ SDS-PAGE (Figure 3.6), which was subsequently shown to correspond to phosphorylation of Thr^{218}/Tyr^{220} (Figure 4.1*a*). These data suggest that VEGF was only able to induce dual-

phosphorylation of the kinase domain residues (p-ERK5) with no apparent phosphorylation of C-terminal residues (Figure 4.1*b*). Taken together, these data infer that kinase activity and phosphorylation of C-terminal residues are not necessarily mutually inclusive events.

Furthermore, this result along with dose-response data of the ERK5 inhibitor XMD8-92 on HeLa, proposed the possibility that an alternative pathway may feed in the phosphorylation of C-terminal residues upon EGF stimulation (Figure 3.13). If ERK5 alone was responsible for autophosphorylation of its C-terminal residues, the hyper p-ERK5 band should not be evident upon XMD8-92 inhibition, however the observed partial reduction in intensity of this hyper p-ERK5 band suggests that both ERK5-dependent and –independent pathways contribute towards the phosphorylation of the C-terminal tail (Figure 3.13). The novel discovery that XMD8-92 inhibits C-terminal autophosphorylation, but not ERK5-independent C-terminal phosphorylation, would not have been detected on conventional SDS-PAGE; inhibition with XMD8-92 resulted in a loss of mobility bandshift, indicating conventional SDS-PAGE is unable to fully discriminate between the ERK5-dependent and –independent phosphorylation events.

This project utilised siRNA against signalling proteins, known to be differentially activated by VEGFR-2 and EGFR-1, to reveal the possible involvement of HRAS in EGF-mediated C-terminal phosphorylation of ERK5 (Figure 4.2*b*). Recent studies have linked phosphorylation of the C-terminal residues of ERK5 to a MEK5-independent pathway during mitosis via CDK activity (Diaz-Rodriguez and Pandiella, 2010; Inesta-Vaquera *et al.*, 2010). Focussing on Thr^{732}, as this residue was investigated in this project, it is unlikely that RAS activates CDK-1 and as a consequence phosphorylates Thr^{732}, as numerous studies have highlighted the ability of RAS to induce cell cycle arrest in primary mammalian cells (Land *et al.*, 1983; Hirakawa and Ruley, 1988; Daar *et al.*, 1991). More recently, albeit in a different system of *Xenopus* egg extracts, RAS has been shown to suppress CDK-1 (Huang *et al.*, 2013).

Utilising the kinase-specific phosphorylation profiling tool NetPhosK 1.0 (CBS, 2014) revealed p38 MAPK, CDK5 and GSK3 as possible kinases that may phosphorylate this specific residue. These kinases are predicted with a low confidence (0.51-0.58) and in conjunction with the knowledge that this profiling tool does not cover an exhaustive list of kinases, further delineation of the potential pathways feeding into C-terminal phosphorylation would be necessary. p38 MAPK activity has previously been implicated in increased vascular permeability and shear stress-induced angiogenesis upon VEGF stimulation of VEGFR-2 in endothelial cells (Issbrucker *et al.*, 2003; Gee *et al.*, 2010), thus

any potential involvement of this pathway in ERK5 phosphorylation would prove an interesting future avenue.

The ERK5 signalling pathway is one that is associated with cancers of the breast and prostate, and additionally, tumours presenting with a strong nuclear localisation of ERK5 often result in poor disease prognosis (Esparís-Ogando *et al.*, 2002; Mehta *et al.*, 2003; McCracken *et al.*, 2008; Montero *et al.*, 2009). This project revealed that the nuclear localisation of ERK5 required phosphorylation of its numerous C-terminal residues, in addition to its Thr^{218}/Tyr^{220} residues (Figure 4.3). Consequently, VEGF-mediated dual-phosphorylation of ERK5 did not undergo translocation to the nucleus, but instead appeared to localise in the cytoplasm and at the plasma membrane (Figure 4.4 and Figure 4.5).

6.1.3 VEGF-mediated ERK5 activation regulates AKT phosphorylation in HDMECs

The discovery that VEGF-stimulated ERK5 activity was required in mediating AKT activity in HDMEC (Roberts *et al.*, 2010), as well as the implication of ERK5 in growth factor-mediated activation of AKT in other cell types (Lennartsson *et al.*, 2010; Razumovskaya *et al.*, 2011), led to the investigation of AKT activity with respect to ERK5 phosphorylation in this project.

Experiments utilising the specific MEK5 inhibitor (BIX 02189) revealed a novel discovery in that VEGF-mediated AKT activity was dependent upon MEK5 kinase activity (Figure 4.8). The previous finding that the ERK5 kinase inhibitor (XMD8-92) blocked phosphorylation of ERK5-dependent C-terminal residues, but not that of Thr^{218}/Tyr^{220} (Figure 3.12 and Figure 3.13), supported the data highlighting the inability of XMD8-92 to affect VEGF-stimulated AKT activation; phosphorylation of Thr^{218}/Tyr^{220} alone was sufficient in regulating VEGF-mediated AKT activity (Figure 4.8).

It was evident that the role ERK5 played in regulating the phosphorylation of AKT was specific to VEGF-stimulated HDMEC; inhibiting EGF-mediated ERK5 phosphorylation in HeLa with the use of BIX 02189 and XMD8-92 did not appear to affect AKT activity (Figure 4.9). This significant discovery provides a rationale behind the lack of vascular toxicity seen with XMD8-92 on the human tumour xenograft study in mice (Yang *et al.*, 2010a); VEGF-stimulated ERK5 regulation of AKT activity remains unaffected by XMD8-92, whereas BIX 02189 could potentially induce vascular toxicity due to blocking VEGF-mediated AKT activity and consequently endothelial cell survival. It remains to be determined what the

extent of *in vivo* toxicity is with BIX 02189 as to date, no animal studies have utilised this, or any other MEK5 inhibitor.

AKT appeared to have a similar intracellular localisation to that of ERK5, i.e. a cytoplasmic/plasma membranous localisation (Figure 4.5 and Figure 4.6) in HDMEC, with no apparent co-localisation between the two proteins in HeLa (Figure 4.7). Thus it was proposed that a potential interaction between ERK5 and AKT might exist in HDMEC. It is important to note however, that the antibody used in this study to detect the presence of AKT, recognised all three isoforms of AKT, i.e. AKT1, AKT2 and AKT3, therefore elucidation of which isoform interacts with ERK5 remains to be determined.

6.1.4 VEGFR-2, ERK5 and AKT co-immunoprecipitate in HDMECs

Immunoprecipitation experiments provided evidence to support the hypothesis that ERK5 and AKT might interact with one another; HDMEC transduced with adenoviral FLAG-ERK5, revealed a co-immunoprecipitation of AKT along with FLAG-ERK5 upon VEGF stimulation (Figure 5.6) as well as the reciprocal result of FLAG-ERK5 co-precipitating with AKT (Figure 5.7). As previously mentioned, the lack of association between ERK5 and AKT in HeLa was once again observed during both these immunoprecipitation experiments (Figure 5.6 and Figure 5.7), thus providing further evidence to suggest a differential role for EGF-mediated ERK5 phosphorylation in this cell type.

A considerably interesting finding was the co-precipitation of the relevant receptors in each cell type with FLAG-ERK5 (Figure 5.6*)*. Unstimulated HeLa demonstrated co-precipitation of EGFR-1 with ERK5, whereas all conditions of HDMEC resulted in VEGFR-2 co-precipitating with ERK5, with an evident increase at 10 min post-VEGF stimulation (Figure 5.6). These data, along with previous intracellular localisation results (Figure 4.4 and Figure 4.5 suggest that VEGF may induce ERK5 activation via VEGFR-2 internalisation, thereby enabling it to complex with, and consequently activate, ERK5. Findings from co-stimulation experiments that utilised MAE cells stably expressing the Flk-1 receptor, revealed the hyper p-ERK5 generated by EGF stimulation alone decreased upon co-stimulation with VEGF (Figure 3.9). This provides additional evidence that VEGFR-2 and EGFR-1 may be able to activate different intracellular pools of ERK5, possibly due to VEGFR-2 sequestering ERK5 in an intracellular localisation that precludes it from being further phosphorylated by EGFR-1.

VEGFR-2 internalisation is similar to that of EGFR-1 in that it undergoes clathrin-dependent endocytosis upon binding to VEGF-A (Lampugnani *et al.*, 2006), however the

ability of VEGFR-2 to signal in cooperation with the non-catalytic co-receptor NRP-1, lends itself to a difference in internalisation compared to EGFR-1 (Horowitz and Seerappu, 2012). Consequently, this difference in internalisation may enable VEGFR-2, ERK5 and AKT to exist in a complex, possibly linked via the membrane-spanning protein Cx43, at a region between the plasma membrane and cytoplasm.

Cx43 has previously been shown to be phosphorylated on Ser^{255} by ERK5, but not ERK1/2, both *in vitro* and *in vivo* in EGF-stimulated HEK293 cells (Cameron *et al.*, 2003). Furthermore, with the observation of a "mode-1" interaction of 14-3-3 θ with phospho-Ser^{373} of Cx43 (Park *et al.*, 2006), and evidence showing AKT as a mediator of 14-3-3 interactions by phosphorylation of target proteins (Kovacina *et al.*, 2003), Cx43 has since been shown to be a substrate for AKT (Park *et al.*, 2007). Thus VEGF-stimulated ERK5 activity may phosphorylate and interact with Cx43 at the plasma membrane, which in turn may complex with AKT either directly as a substrate, or indirectly via 14-3-3. If this is the case, endothelial cell apoptosis in *Erk5* knockout mice reported to be due to a lack of MEF2C phosphorylation by ERK5 (Hayashi *et al.*, 2004), may in fact be due to a decrease in AKT activity.

Interestingly, $Akt1^{-/-}$ mice show increased neonatal mortality (Chen *et al.*, 2001b; Cho *et al.*, 2001) due to defects in placental function such as fewer blood vessels and scarce vascular branching (Yang *et al.*, 2003b). These phenotypes have been observed *in vitro* as a decrease in tubular morphogenesis and cellular survival in HDMEC, upon ERK5 knockdown with siRNA (Roberts *et al.*, 2010). Furthermore, the study from which this project has progressed showed that PI3K inhibition affected VEGF-mediated AKT phosphorylation but not ERK5 phosphorylation, suggesting that PI3K may lie downstream of, or parallel to, the ERK5 pathway in HDMEC (Roberts *et al.*, 2010). The role of EGF-mediated AKT activity in HeLa cells remains to be elucidated; a previous study has implicated EGFR in playing an important role in mediating oxidative stress-induced AKT activation (Wang *et al.*, 2000).

Figure 6.1 and Figure 6.2 demonstrates the proposed mechanisms though which ERK5 is differentially phosphorylated upon EGF or VEGF stimulation in HeLa or HDMEC.

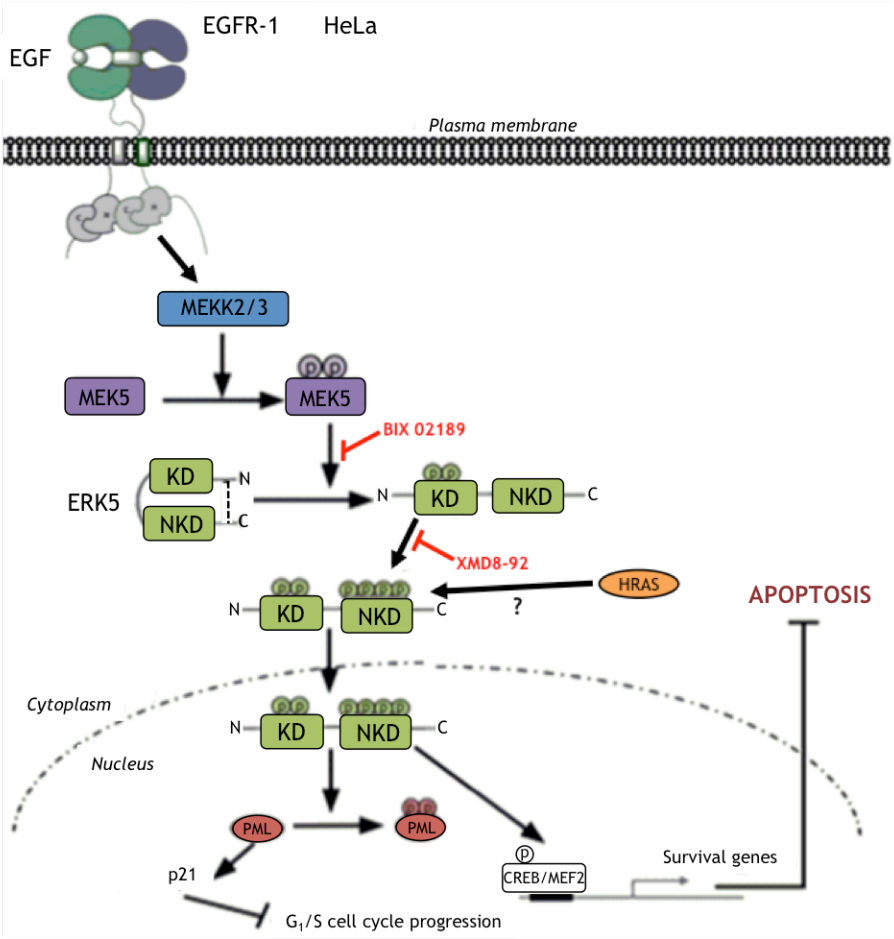

Figure 6.1 EGF-mediated ERK5 activity in HeLa.
EGF stimulation of HeLa results in phosphorylation of Thr^{218}/Tyr^{220} in the kinase domain by MEK5. Inhibition of this phosphorylation can occur using the MEK5-selective inhibitor, BIX 02189. Phosphorylation of C-terminal residues of ERK5 may occur by ERK5-dependent and -independent pathways. The ERK5-selective inhibitor, XMD8-92 is able to inhibit autophosphorylation of ERK5 C-terminal residues. ERK5-independent phosphorylation of C-terminal residues is thought to occur via EGF-mediated HRAS activation. Phosphorylation of C-terminal residues enables nuclear shuttling of ERK5 wherein phosphorylation of promyelocytic leukemia protein (PML) occurs in the PML-nuclear body (PML-NB). Phosphorylated PML is unable to upregulated p21, which is required for G_1/S cell cycle progression. Additionally, nuclear ERK5 is able to phosphorylate transcription factors such as CREB and MEF2, leading to a survival response.

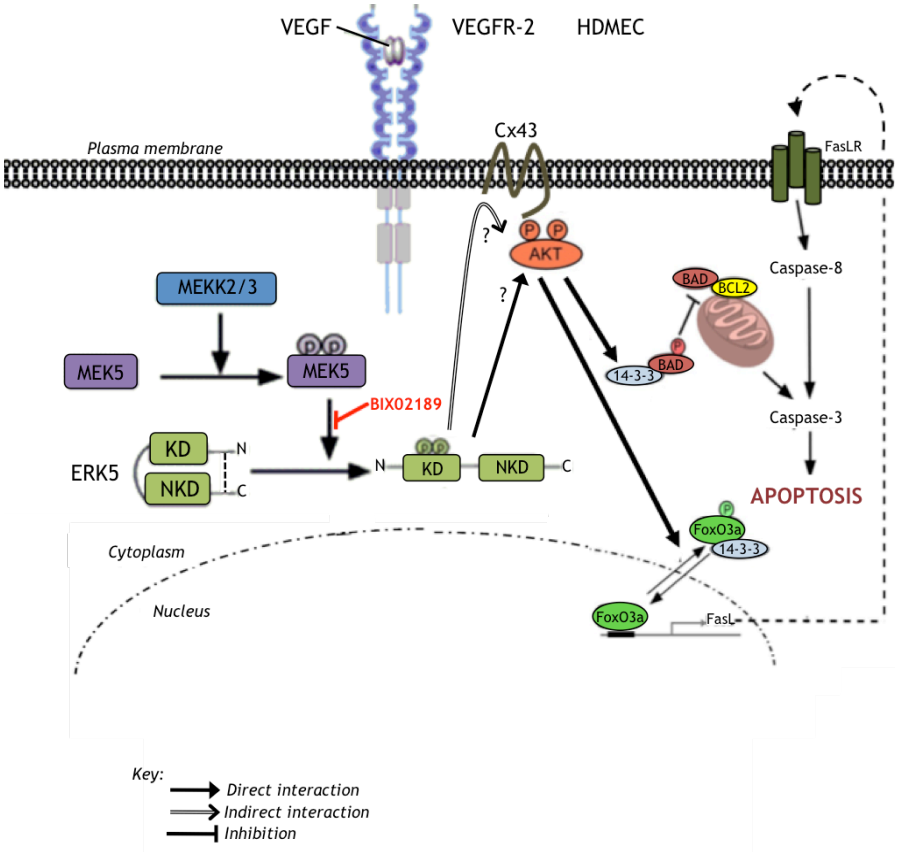

Figure 6.2 VEGF-mediated ERK5 activity in HDMEC.
VEGF stimulation of HDMEC results in phosphorylation of Thr^{218}/Tyr^{220} in the kinase domain by MEK5. BIX 02189 is able to inhibit this phosphorylation. VEGF is unable to induce C-terminal phosphorylation of ERK5. Instead, ERK5 phosphorylated at Thr^{218}/Tyr^{220}, is thought to complex with VEGFR-2 and MEK5 at the plasma membrane whereby it is able to complex with, and mediate AKT activation, possibly via Cx43, or via an unknown direct mechanism. Phosphorylated AKT is consequently able to phosphorylate BAD, sequestering it to the 14-3-3 protein, inhibiting its interaction with BCL2 and its translocation to the mitochondria. FoxO3a phosphorylation by AKT is also sequestered by the 14-3-3 protein in the cytoplasm, thereby preventing it from upregulating the Fas ligand (FasL), which subsequently results in an apoptotic feedback loop and FasL-mediated caspase activation.

6.2 Future perspectives

This novel discovery that ERK5 is differentially phosphorylated by EGF and VEGF, which in turn leads to a divergence in downstream activation, provides key insight into the diverse functional role of ERK5 in various cell types upon growth factor simulation.

The observation that C-terminal phosphorylation was required for the nuclear translocation of ERK5, could be further investigated regarding ERK5-dependent and ERK5-independent phosphorylation of these C-terminal residues. Future studies should aim to observe the effect of reduced C-terminal phosphorylation on nuclear translocation; HeLa cells treated with XMD8-92 would inhibit ERK5-dependent C-terminal phosphorylation and intracellular localisation could then be observed using immunofluorescent staining. Furthermore, aberrations in the transcriptional activity of ERK5 as a result of decreased C-terminal phosphorylation would be revealed by investigating levels of transcription factors such as CREB and MEF2, c-Myc and Sap1a with qRT-PCR.

Thus far, studies have not observed the activation of RAS isoforms in response to VEGF stimulation in HDMEC; a future line of investigation would require a VEGF-activated RAS assay to determine potential RAS isoforms activated in HDMEC. Further to this, with the knowledge that HRAS plays a potential role in EGF-stimulated C-terminal phosphorylation, it may then be possible to utilise a dominant-active (G12V) RAS in VEGF-stimulated HDMEC to force phosphorylation of certain C-terminal residues. Immunofluorescent staining could be utilised in order to detect whether this results in a change in the intracellular localisation of VEGF-stimulated ERK5. Consequently, it would be necessary to determine any changes in downstream signalling, i.e. from VEGF-induced, ERK5-mediated AKT activity to EGF-stimulated, ERK5-mediated cell proliferation.

As previously mentioned, VEGFR-2 is able to signal in cooperation with the co-receptor NRP-1. It may be that dimerisation of these two receptors and their subsequent internalisation may play a role in activating a different intracellular pool of ERK5 compared to that of EGFR-1. To determine whether or not this may be the case, the use of VEGF-A_{121} an isoform that does not bind NRP-1, would provide further insight into the potential role NRP-1 plays in the activation of ERK5. Prior to this however, it would be necessary to assess the ability and extent of ERK5 phosphorylation in response to VEGF-A_{121} stimulation.

The interesting discovery that ERK5 may exist within a complex with VEGFR-2 and AKT near the plasma membrane would require much further exploration; time and funding

constraints limited further investigation in this project. As mentioned in Chapter 5, a more detailed proteomic study with additional VEGF-stimulated time-points, such as 1, 5, 10 and 20 min would benefit the proteomic analysis in order to ascertain the potential transiency of the interaction between ERK5 and AKT. Additionally, in view of the relatively low quantity of the bait protein (FLAG-ERK5) after transduced overexpression, it would be necessary to ensure that proteomic samples are processed immediately, to prevent protein degradation upon freezing. Furthermore, with the possibility that the transmembrane protein Cx43, may be an intermediary molecule in the ERK5-AKT complex, optimisation of the proteomic lysis buffer would be required to take account of the insoluble, hydrophobic domains of the membrane protein.

Finally, phospho-proteomics would potentially be the major line of future investigation, whereby point mutations of ERK5 could be overexpressed in both VEGF-stimulated HDMEC and EGF-stimulated HeLa. An adenoviral FLAG-ERK5(AEF) mutant, in which Thr^{218}/Tyr^{220} are mutated to Ala^{218}/Phe^{220} respectively, and a constitutively-active HA_3-MEK5(D), in which Ser^{311}/Thr^{315} are mutated to Asp^{311}/Asp^{315}, were generated during this project, however time constraints prevented their use in proteomic experiments. The use of the adenoviral HA_3-MEK5(D) in conjunction with adenoviral FLAG-ERK5(wt), would enable their overexpression, but also the constitutive phosphorylation of the Thr^{218}/Tyr^{220} residues. This would overcome the transient nature of phosphorylated events, thereby facilitating detection of ERK5-interacting proteins. Phospho-proteomic profiling would reveal the specific residues phosphorylated following VEGF and EGF stimulation. Furthermore, point mutations of C-terminal phosphorylation residues in EGF-stimulated HeLa cells would facilitate identification of the precise kinase implicated in phosphorylating the ERK5-independent C-terminal residues.

This thesis has revealed a hitherto unknown difference in ERK5 phosphorylation and consequently its intracellular localisation in endothelial cells. These findings taken together with the discovery of novel interacting partners of ERK5, has brought to light several new interesting avenues for future investigation. One in particular involves the novel finding that C-terminal residues of ERK5 may be phosphorylated by ERK5-dependent and –independent pathways. The selective ERK5 inhibitor XMD8-92, although able to prevent autophosphorylation of C-terminal residues of ERK5, cannot inhibit other potential kinases from phosphorylating alternative C-terminal residues. Thus, in order to prevent ERK5-independent pathways from offering a compensatory mechanism for C-terminal phosphorylation in the presence of promising drugs such as XMD8-92, it is essential that these kinases are identified; hence, the critical component of pathological ERK5 activation can be targeted, without affecting its physiological role.

References

abcam®. (2014). "http://www.abcam.com/index.html?pageconfig=resource&rid=11379." Retrieved 11th November 2014.

Abe, J., Kusuhara, M., Ulevitch, R. J., Berk, B. C. and Lee, J. D. (1996). Big mitogen-activated protein kinase 1 (BMK1) is a redox-sensitive kinase. *J Biol Chem,* **271**(28): 16586-16590.

Abe, J., Takahashi, M., Ishida, M., Lee, J. D. and Berk, B. C. (1997). c-Src Is Required for Oxidative Stress-mediated Activation of Big Mitogen-activated Protein Kinase 1 (BMK1). *J Biol Chem,* **272**: 20389-20394.

Aird, W. C. (2007). Phenotypic heterogeneity of the endothlium: I. Structure, function and mechanisms. *Circulation research,* **100**: 158-173.

Aird, W. C. (2012). Endothelial cell heterogeneity. *Cold Spring Harb Perspect Med,* **2**: a006429.

Akaike, M., Che, W., Marmarosh, N. L., Ohta, S., Osawa, M., Ding, B., Berk, B. C., Yan, C. and Abe, J. (2004). The hinge-helix 1 region of peroxisome proliferator-activated receptor gamma1 (PPARgamma1) mediates interaction with extracellular signal-regulated kinase 5 and PPARgamma1 transcriptional activation: involvement in flow-induced PPARgamma activation in endothelial cells. *Mol Cell Biol,* **24**(19): 8691-8704.

Alessi, D. R., Andjelkovic, M., Caudwell, B., Cron, P., Morrice, N., Cohen, P. and Hemmings, B. A. (1996). Mechanism of activation of protein kinase B by insulin and IGF-1. *Embo J,* **15**: 6541-6551.

Alessi, D. R., James, S. R., Downes, C. P., Holmes, A. B., Gaffney, P. R., Reese, C. B. and Cohen, P. (1997). Characterization of a 3-phosphoinositide-dependent protein kinase which phosphorylates and activates protein kinase B alpha. *Curr Biol,* **7**: 261-269.

Altomare, D. A., You, H., Xiao, G. H., Ramos-Nino, M. E., Skele, K. L., De Rienzo, A., Jhanwar, S. C., Mossman, B. T., Kane, A. B. and Testa, J. R. (2005). Human and mouse mesotheliomas exhibit elevated AKT/PKB activity, which can be targeted pharmacologically to inhibit tumor cell growth. *Oncogene,* **24**: 6080-6089.

Anderson, K. E., Coadwell, J., Stephens, L. R. and Hawkins, P. T. (1998). Translocation of PDK-1 to the plasma membrane is important in allowing PDK-1 to activated protein kinase B. *Curr Biol,* **8**: 684-691.

Anton, M., Wolf, A., Mykhaylyk, O., Koch, C., Gansbacher, B. and Plank, C. (2012). Optimizing adenoviral transduction of endothelial cells under flow conditions. *Pharm Res,* **29**: 1219-1231.

Bajaj, A., Zheng, Q., Adam, A., Vincent, P. and Pumiglia, K. (2010). Activation of endothelial Ras signaling bypasses senescence and causes abnormal vascular morphogenesis. *Cancer Res,* **70**: 3803-3812.

Barros, J. C. and Marshall, C. J. (2005). Activation of either ERK1/2 or ERK5 MAP kinase pathways can lead to disruption of the actin cytoskeleton. *J Cell Sci,* **118**: 1663-1671.

Batzer, A. G., Rotin, D., Urena, J. M., Skolnik, E. Y. and Schlessinger, J. (1994). Hierarchy of binding sites for Grb2 and Shc on the epidermal growth factor receptor. *Mol Cell Biol,* **14**: 5192-5201.

Benjamin, L. E., Hemo, I. and Keshet, E. (1998). A plasticity window for blood vessel remodelling is defined by pericyte coverage of the preformed endothelial network and is regulated by PDGF-B and VEGF. *Development,* **125**: 1591-1598.

Bera, A., Das, F., Ghosh-Choudhry, N., Li, X., Pal, S., Gorin, Y., Kasinath, B. S., Abboud, H. E. and Ghosh Choudhury, G. (2014). A positive feedback loop involving Erk5 and Akt turns on mesangial cell proliferation in response to PDGF. *Am J Physiol Cell Physiol,* **306**: C1089-C1100.

Bergelson, J. M., cunningham, J. A., Droguett, G., Kurt-Jones, E. A., Krithivas, A., Hong, J. S., Horwitz, M. S., Crowell, R. L. and Finberg, R. W. (1997). Isolation of a common receptor for Coxsackie B viruses and Adenoviruses 2 and 5. *Science,* **275**: 1320-1323.

Bergers, G. and Hanahan, D. (2008). Modes of resistance to anti-angiogenic therapy. *Nat Rev Cancer,* **8**: 592-603.

Bergers, G. and Song, S. (2005). The role of pericytes in blood-vessel formation and maintenance. *Neuro Oncol,* **7**: 452-464.

Berkers, J. A., van Bergen en Henegouwen, P. M. and Boonstra, J. (1991). Three classes of epidermal growth factor receptors on HeLa cells. *J Biol Chem,* **266**: 922-927.

Bernstein, E., Caudy, A. A., Hammond, S. M. and Hannon, G. J. (2001). Role for a bidentate ribonuclease in the initiation step of RNA interference. *Nature,* **409**: 363-366.

Berse, B., Brown, L. F., Van De Water, L., Dvorak, H. F. and Senger, D. R. (1992). Vascular permeability factor (vascular endothelial growth factor) gene is expressed differentially in normal tissues, macrophages, and tumors. *Mol Biol Cell,* **3**: 211-220.

Bi, W., Drake, C. J. and Schwarz, J. J. (1999). The transcription factor MEF2C-null mouse exhibits complex vascular malformations and reduced cardiac expression of angiopoietin 1 and VEGF. *Dev Biol,* **211**: 255-267.

Blanes, M. G., Oubaha, M., Rautureau, Y. and Gratton, J. P. (2007). Phosphorylation of tyrosine 801 of vascular endothelial growth factor receptor-2 is necessary for Akt-dependent endothelial nitric-oxide synthase activation and nitric oxide release from endothelial cells. *J Biol Chem,* **282**: 10660-10669.

Blank, J. L., Gerwins, P., Elliott, E. M., Sather, S. and Johnson, G. L. (1996). Molecular cloning of mitogen-activated protein/ERK kinase kinases (MEKK) 2 and 3. Regulation of sequential phosphorylation pathways involving mitogen-activated protein kinase and c-Jun kinase. *J Biol Chem,* **271**(10): 5361-5368.

Boon, R. A. and Horrevoets, A. J. (2009). Key transcriptional regulators of the vasoprotective effects of shear stress. *Hamostaseologie,* **29**: 39-43.

Boulton, T. G., Nye, S. H., Robbins, D. J., Ip, N. Y., Radziejewska, E., Morgenbesser, S. D., DePinho, R. A., Panayotatos, N., Cobb, M. H. and Yancopoulos, G. D. (1991). ERKs: a family of protein-serine/threonine kinases that are activated and tyrosine phosphorylated in response to insulin and NGF. *Cell,* **65**(4): 663-675.

Brauckmann, S. and Gilbert, S. F. (2004). Gastrulation: From Cells to Embryo, Cold Spring Harbor Laboratory Press.

Brunet, A., Bonni, A., Zigmond, M. J., Lin, M. Z., Juo, P., Hu, L. S., Anderson, M. J., Arden, K. C., Blenis, J. and Greenberg, M. E. (1999). Akt promotes cell survival by phosphorylating and inhibiting a Forkhead transcription factor. *Cell,* **96**: 857-868.

Buschbeck, M. and Ullrich, A. (2005). The unique C-terminal tail of the mitogen-activated protein kinase ERK5 regulates its activation and nuclear shuttling. *J Biol Chem,* **280**(4): 2659-2667.

Cameron, S. J., Malik, S., Akaike, M., Lerner-Marmarosh, N., Yan, C., Lee, J. D., Abe, J. and Yang, J. (2003). Regulation of epidermal growth factor-induced connexin 43 gap junction communication by big mitogen-activated protein kinase 1/ERK5 but not ERK1/2 kinase activation. *J Biol Chem,* **278**: 18682-18688.

Cantley, L. C. (2002). The phosphoinositide 3-kinase pathway. *Science,* **296**: 1655-1657.

Cardone, M. H., Roy, N., Stennicke, H. R., Salvesen, G. S., Franke, T. F., Stanbridge, E., Frisch, S. and Reed, J. C. (1998). Regulation of cell death protease caspase-9 by phosphorylation. *Science,* **282**: 1318-1321.

Carmeliet, P. (2000). Mechanisms of angiogenesis and arteriogenesis. *Nat Med,* **6**: 389-395.

Carmeliet, P. (2005). Angiogenesis in life, disease and medicine. *Nature,* **438**: 932-936.

Carmeliet, P., Ferreira, V., Breier, G., Pollefeyt, S., Kieckens, L., Gertsenstein, M., Fahrig, M., Vandenhoeck, A., Harpal, K., Eberhardt, C., Declercq, C., Pawling, J., Moons, L., Collen, D., Risau, W. and Nagy, A. (1996). Abnormal blood vessel development and lethality in embryos lacking a single VEGF allele. *Nature,* **380**: 435-439.

Carmeliet, P. and Jain, R. K. (2000). Angiogenesis in cancer and other diseases. *Nature,* **407**: 249-257.

Caron, C., Spring, K., Laramée, M., Chabot, C., Cloutier, M., Gu, H. and Royal, I. (2009). Non-redundant roles of the Gab1 and Gab2 scaffolding adapters in VEGF-mediated

signalling, migration, and survival of endothelial cells. *Cellular signalling,* **21**: 943-953.

Carter, E. J., Cosgrove, R. A., Gonzalez, I., Eisemann, J. H., Lovett, F. A., Cobb, L. J. and Pell, J. M. (2009). MEK5 and ERK5 are mediators of the pro-myogenic actions of IGF-2. *J Cell Sci,* **122**: 3104-3112.

Carvajal-Vergara, X., Tabera, S., Montero, J. C., Esparis-Ogando, A., Lopez-Perez, R., Mateo, G., Gutierrez, N., Parmo-Cabanas, M., Teixido, J., San Miguel, J. F. and Pandiella, A. (2005). Multifunctional role of Erk5 in multiple myeloma. *Blood,* **105**(11): 4492-4499.

Cavanaugh, J. E., Ham, J., Hetman, M., Poser, S., Yan, C. and Xia, Z. (2001). Differential regulation of mitogen-activated protein kinases ERK1/2 and ERK5 by neurotrophins, neuronal activity, and cAMP in neurons. *J Neurosci,* **21**(2): 434-443.

CBS. (2014). "http://www.cbs.dtu.dk/services/NetPhosK/." Retrieved 22nd October 2014.

Chang, L. and Karin, M. (2001). Mammalian MAP kinase signalling cascades. *Nature,* **410**(6824): 37-40.

Chao, T. H., Hayashi, M., Tapping, R. I., Kato, Y. and Lee, J. D. (1999). MEKK3 directly regulates MEK5 activity as part of the big mitogen-activated protein kinase 1 (BMK1) signaling pathway. *J Biol Chem,* **274**(51): 36035-36038.

Chen, J.-H., Wang, X.-C., Kan, M. and Sato, J. D. (2001a). Effect of FGF-1 and FGF-2 on VEGF binding to human umbilical vein endothelial cells. *Cell Biol Int,* **25**: 257-260.

Chen, W. S., Xu, P.-Z., Gottlob, K., Chen, M.-L., Sokol, K., Shiyanova, T., Roninson, I., Weng, W., Suzuki, R., Tobe, K., Kadowaki, T. and Hay, N. (2001b). Growth retardation and increased apoptosis in mice with homozygous disruption of the akt1 gene. *Genes Dev,* **15**: 2203-2208.

Cho, H., Thorvaldsen, J. L., Chu, Q., Feng, F. and Birnbaum, M. J. (2001). Akt1/PKBalpha is required for normal growth but dispensible for maintenance of glucose homeostasis in mice. *J Biol Chem,* **276**: 38349-38352.

Christoffersson, G., Zang, G., Zhuang, Z. W., Vågesjö, E., Simons, M., Phillipson, M. and Welsh, M. (2012). Vascular adaptation to a dysfunctional endothelium as a consequence of Shb deficiency. *Angiogenesis,* **15**: 469-480.

Ciardiello, F., McGeady, M. L., Kim, N., Basolo, F., Hynes, N., Langton, B. C., Yokozaki, H., Saeki, T., Elliott, J. W., Masui, H. and al., e. (1990). Transforming growth factor-alpha expression is enhanced in human mammary epithelial cells transformed by an activated c-Ha-ras protooncogene but not by the c-neu protooncogene, and overexpression of the transforming growth factor-alpha complementary DNA leads to transformation. *Cell Growth Diff,* **1**: 407-420.

Clark, P. R., Jensen, T. J., Kluger, M. S., Morelock, M., Hanidu, A., Qi, Z., Tatake, R. J. and Pober, J. S. (2011). MEK5 is activated by shear stress, activates ERK5 and induces KLF4 to modulate TNF responses in human dermal microvascular endothelial cells. *Microcirculation,* **18**: 102-117.

Coffer, P. J., Jin, J. and Woodgett, J. R. (1998). Protein kinase B (c-Akt): a multifunctional mediator of phosphatidylinositol 3-kinase activation. *The Biochemical journal,* **335**: 1-13.

Cohen, S. and Carpenter, G. (1975). Human epidermal growth factor: isolation and chemical and biological properties. *Proc Natl Acad Sci U S A,* **72**: 1317-1321.

Cohen, S. and Elliot, G. A. (1963). The stimulation of epidermal keratinization by a protein isolated from the submaxillary gland of the mouse. *J Invest Dermatol,* **40**: 1-5.

Cohen, S. and Levi-Montalcini, R. (1957). Purification and properties of a nerve growth-promoting factor isolated from mouse sarcoma 180. *Cancer Res,* **17**: 15-20.

Conway, E. M. and Carmeliet, P. (2004). The diversity of endothelial cells: a challenge for therapeutic angiogenesis. *J Clin Invest,* **84**: 1470-1478.

Coultas, L., Chawengsaksophak, K. and Rossant, J. (2005). Endothelial cells and VEGF in vascular development. *Nature,* **438**: 937-945.

Cude, K., Wang, Y., Choi, H. J., Hsuan, S. L., Zhang, H., Wang, C. Y. and Xia, Z. (2007). Regulation of the G2-M cell cycle progression by the ERK5-NFkappaB signaling pathway. *The Journal of cell biology,* **177**(2): 253-264.

Cunningham, S. A., Arrate, M. P., Brock, T. A. and Waxham, M. N. (1997). Interactions of FLT-1 and KDR with phospholipase C gamma: identification of the phosphotyrosine binding sites. *Biochem Biophys Res Commun,* **240**: 635-639.

Daar, I., Nebreda, A. R., Yew, N., Sass, P., Paules, R., Santos, E., Wigler, M. and Vande Woude, G. F. (1991). The ras oncoprotein and M-phase activity. *Science,* **253**: 74-76.

Dance, M., Montagner, A., Yart, A., Masri, B., Audigier, Y., Perret, B., Salles, J. P. and Raynal, P. (2006). The adaptor protein Gab1 couples the stimulation of vascular endothelial growth factor receptor-2 to the activation of phophoinositide 3-kinase. *J Biol Chem,* **281**: 23285-23295.

Datta, S. R., Dudek, H., Tao, X., Masters, S., Fu, H., Gotoh, Y. and Greenberg, M. E. (1997). Akt phosphorylation of BAD couples survival signals to the cell-intrinsic death machinery. *Cell,* **91**: 231-241.

Dawson, J. P., Berger, M. B., Lin, C. C., Schlessinger, J., Lemmon, M. A. and Ferguson, K. M. (2005). Epidermal growth factor receptor dimerization and activation require ligand-induced conformational changes in the dimer interface. *Mol Cell Biol,* **25**: 7734-7742.

De Bock, K., Cauwenberghs, S. and Carmeliet, P. (2011). Vessel abnormalization: another hallmark of cancer? Molecular mechanisms and therapeutic implications. *Curr Opin Genet Dev,* **21**: 73-79.

Dekker, R. J., van Soest, S., Fontijn, R. D., Salamanca, S., de Groot, P. G., VanBavel, E., Pannekoek, H. and Horrevoets, A. J. (2002). Prolonged fluid shear stress induces a distinct set of endothelial cell genes, most specifically lung Krüppel-like factor (KLF2). *Blood,* **100**: 1689-1698.

Deng, X., Yang, Q., Kwiatkowski, N., Sim, T., McDermott, U., Settleman, J. E., Lee, J. D. and Gray, N. S. (2011). Discovery of a benzo[e]pyrimido-[5,4-b][1,4]diazepin-6(11H)-one as a potent and selective inhibitor of big MAP kinase 1. *ACS Med Chem Lett,* **2**: 195-200.

Dhillon, A. S., Hagan, S., Rath, O. and Kolch, W. (2007). MAP kinase signalling pathways in cancer. *Oncogene,* **26**: 3279-3290.

Di Marco, E., Pierce, J. H., Fleming, T. P., Kraus, M. H., Molloy, C. J., Aaronson, S. A. and Di Fiore, P. P. (1989). Autocrine interaction between TGF alpha and the EGF-receptor: quantitative requirements for induction of the malignant phenotype. *Oncogene,* **4**: 831-838.

Diaz-Meco, M. T. and Moscat, J. (2001). MEK5, a new target of the atypical protein kinase C isoforms in mitogenic signaling. *Mol Cell Biol,* **21**: 1218-1227.

Diaz-Rodriguez, E. and Pandiella, A. (2010). Multisite phosphorylation of Erk5 in mitosis. *J Cell Sci,* **123**: 3146-3156.

Dickinson, R. J. and Keyse, S. M. (2006). Diverse physiological functions for dual-specificity MAP kinase phosphatases. *J Cell Sci,* **119**(Pt 22): 4607-4615.

Dietz, M. S., HaBe, D., Ferraris, D. M., Gohler, A., Niemann, H. H. and Heilemann, M. (2013). Single-molecule photobleaching reveals increased MET receptor dimerization upon ligand binding in intact cells. *BMC Biophysics,* **6**(6): http://www.biomedcentral.com/2046-1682/2046/2046.

Dinev, D., Jordan, B. W., Neufeld, B., Lee, J. D., Lindemann, D., Rapp, U. R. and Ludwig, S. (2001). Extracellular signal regulated kinase 5 (ERK5) is required for the differentiation of muscle cells. *EMBO Rep,* **2**: 829-834.

Doanes, A. M., Hegland, D. D., Sethi, R., Kovesdi, I., Bruder, J. T. and Finkel, T. (1999). VEGF stimulates MAPK through a pathway that is unique for receptor tyrosine kinases. *Biochem Biophys Res Commun,* **255**: 545-548.

Domingues, I., Rino, J., Demmers, J. A. A., de Lanerolle, P. and Santos, S. C. (2011). VEGFR2 translocates to the nucleus to regulate its own transcription. *PLoS ONE,* **6**: e25668.

Dong, L. Q. and Liu, F. (2005). PDK2: the missing piece in the receptor tyrosine kinase signaling pathway puzzle. *Am J Physiol Endocrinol Metab,* **289**: E187-196.

Dor, Y., Porat, R. and Keshet, E. (2001). Vascular endothelial growth factor and vascular adjustments to perturbations in oxygen homeostasis. *Am J Physiol Cell Physiol,* **280**: C1367-1374.

Duff, J. L., Monia, B. P. and Berk, B. C. (1995). Mitogen-activated Protein (MAP) Kinase Is Regulated by the MAP Kinase Phosphatase (MKP-1) in Vascular Smooth Muscle Cells. *J Biol Chem,* **270**: 7161-7166.

Dumont, D. J., Jussila, L., Taipale, J., Lymboussaki, A., Mustonen, T., Pajusola, K., Breitman, M. L. and Alitalo, K. (1998). Cardiovascular failure in mouse embryos deficient in VEGFR receptor-3. *Science,* **282**: 946-949.

Ebner, R. and Derynck, R. (1991). Epidermal growth factor and transforming growth factor-alpha: differential intracellular routing and processing of ligand-receptor complexes. *Cell Regul,* **2**: 599-612.

EducationalForum. (2014). "Caring for diabetes: http://www.caringfordiabetes.com/impdemo/hyper_artilce.html." Retrieved 10th November 2014.

Eikesdal, H. P. and Kalluri, R. (2009). Drug resistance associated with antiangiogenesis therapy. *Semin Cancer Biol,* **19**: 310-317.

English, J. M., Pearson, G., Baer, R. and Cobb, M. H. (1998). Identification of substrates and regulators of the mitogen-activated protein kinase ERK5 using chimeric protein kinases. *J Biol Chem,* **273**(7): 3854-3860.

Escudier, B., Eisen, T., Stadler, W. M., Szczylik, C., Oudard, S., Siebels, M., Negrier, S., Chevreau, C., Solska, E., Desai, A. A., Rolland, F., Demkow, T., Hutson, T. E., Gore, M., S., F., Schwartz, B., Shan, M., Simantov, R. and Bukowski, R. M. (2007a). Sorafenib in advanced clear-cell renal-cell carcinoma. *N Engl J Med,* **356**: 125-134.

Escudier, B., Pluzanska, A., Koralewski, P., Ravaud, A., Bracarda, S., Szczylik, C., Chevreau, C., Filipek, M., Melichar, B., Bajetta, E., Gorbunova, V., Bay, J. O., Bodrogi, I., Jagiello-Gruszfeld, A. and Moore, N. (2007b). Bevacizumab plus interferon alfa-2a for treatment of metastatic renal cell carcinoma: a randomised, double-blind phase III trial. *Lancet,* **370**: 2103-2111.

Esparís-Ogando, A., Díaz-Rodríguez, E., Montero, J. C., Yuste, L., Crespo, P. and Pandiella, A. (2002). Erk5 participates in neuregulin signal transduction and is constitutively active in breast cancer cells overexpressing ErbB2. *Mol Cell Biol,* **22**: 270-285.

Fantin, A., Vieira, J. M., Gestri, G., Denti, L., Schwarz, Q., Prykhozhij, S., Peri, F., Wilson, S. W. and Ruhrberg, C. (2010). Tissue macrophages act as cellular chaperones for vascular anastomosis downstream of VEGF-mediated endothelial tip cell induction. *Blood,* **116**: 829-840.

Favier, B., Alam, A., Barron, P., Bonnin, J., Laboudie, P., Fons, P., Mandron, M., Herault, J. P., Neufeld, G., Savi, P., Herbert, J. M. and Bono, F. (2006). Neuropilin-2

interacts with VEGFR-2 and VEGFR-3 and promotes human endothelial cell survival and migration. *Blood,* **108**: 1243-1250.

Fenn, J. B., Mann, M., Meng, c. K., Wong, S. F. and Whitehouse, C. M. (1989). Electrospray ionization for mass spectrometry of large biomolecules. *Science,* **246**: 64-71.

Ferguson, K. M., Berger, M. B., Mendrola, J. M., Cho, H. S., Leahy, D. J. and Lemmon, M. A. (2003). EGF activates its receptor by removing interactions that autoinhibit ectodomain dimerization. *Mol Cell,* **11**: 507-517.

Ferrara, N. (2004). Vascular endothelial growth factor: basic science and clinical progress. *Endocr Rev,* **25**: 581-611.

Ferrara, N. (2009). Vascular endothelial growth factor. *Arterioscler Thromb Vasc Biol,* **29**: 789-791.

Ferrara, N., Carver-Moore, K., Chen, H., Dowd, M., Lu, L., O'Shea, K. S., Powell-Braxton, L., Hillan, K. J. and Moore, M. W. (1996). Heterozygous embryonic lethality induced by targeted inactivation of the VEGF gene. *Nature,* **380**: 439-442.

Ferrara, N. and Davis-Smyth, T. (1997). The biology of vascular endothelial growth factor. *Endocr Rev,* **18**: 4-25.

Finegan, K. G., Wang, X., Lee, E. J., Robinson, A. C. and Tournier, C. (2009). Regulation of neuronal survival by the extracellular signal-regulated protein kinase 5. *Cell death and differentiation,* **16**(5): 674-683.

Fleming, Y., Armstrong, C. G., Morrice, N., Paterson, A., Goedert, M. and Cohen, P. (2000). Synergistic activation of stress-activated protein kinase 1/c-Jun N-terminal kinase (SAPK1/JNK) isoforms by mitogen-activated protein kinase kinase 4 (MKK4) and MKK7. *The Biochemical journal,* **352**: 145-154.

Folkman, J. (1971). Tumor angiogenesis: therapeutic implications. *N Engl J Med,* **285**: 1182-1186.

Folkman, J. (1990). What is the evidence that tumors are angiogenesis dependent? *J Natl Cancer Inst,* **82**: 4-6.

Folkman, J. (1995). Angiogenesis in cancer, vascular, rheumatoid and other disease. *Nat Med,* **1**: 27-31.

Folkman, J. and Shing, Y. (1992). Angiogenesis. *J Biol Chem,* **267**: 10931-10934.

Fong, G. H., Rossant, J., Gertsenstein, M. and Breitman, M. L. (1995). Role of the Flt-1 receptor tyrosine kinase in regulating the assembly of vascular endothelium. *Nature,* **376**: 66-70.

Fong, G. H., Zhang, L., Bryce, D. M. and Peng, J. (1999). Increased hemangioblast commitment, not vascular disorganization, is the primary defect in flt-1 knock-out mice. *Development,* **126**: 3015-3025.

Franovic, A., Gunaratnam, L., Smith, K., Robert, I., Patten, D. and Lee, S. C. (2007). Translational up-regulation of the EGFR by tumor hypoxia provides a nonmutational explanation for its overexpression in human cancer. *Proc Natl Acad Sci U S A,* **104**: 13092-13097.

Fuh, G., Li, B., Crowley, C., Cunningham, B. and Wells, J. A. (1998). Requirements for binding and signaling of the kinase domain receptor for vascular endothelial growth factor. *J Biol Chem,* **273**: 11197-11204.

Funa, N. S., Kriz, V., Zang, G., Calounova, G., Åkerblomg, B., Mares, J., Larsson, E., Sun, Y., Betsholtz, C. and Welsh, M. (2009). Dysfunctional microvasculature as a consequnce of Shb gene inactivation causes impaired tumor growth. *Cancer Res,* **69**: 2141-2148.

Gallagher, P. J. and van der Wal, A. C. (2006). Blood vessels. Philadelphia, Lippincott, Williams and Wilkins.

Garlanda, C. and Dejana, E. (1997). Heterogeneity of endothelial cells: specific markers. *Arterioscler Thromb Vasc Biol,* **17**: 1193-1202.

Garrington, T. P., Ishizuka, T., Papst, P. J., Chayama, K., Webb, S., Yujiri, T., Sun, W., Sather, S., Russell, D. M., Gibson, S. B., Keller, G., Gelfand, E. W. and Johnson, G. L. (2000). MEKK2 gene disruption causes loss of cytokine production in response to IgE and c-Kit ligand stimulation of ES cell-derived mast cells. *Embo J,* **19**: 5387-5395.

Gee, E., Milkiewicz, M. and Haas, T. L. (2010). p38 MAPK is activated by vascular endothelial growth factor receptor 2 and is essential for shear stress-induced angiogenesis. *Journal of cellular physiology,* **222**: 120-126.

Gerber, H.-P., Hillan, K. J., Ryan, A. M., Kowalski, J., Keller, G. A., Rangell, L., Wright, B. D., Radtke, F., Aguet, M. and Ferrara, N. (1999). VEGF is required for growth and survival in neonatal mice. *Development,* **126**: 1149-1159.

Gerber, H.-P., McMurtrey, A., Kowalski, J., Yan, M., Keyt, B. A., Dixit, V. and Ferrara, N. (1998). Vascular Endothelial Growth Factor Regulates Endothelial Cell Survival through the Phosphatidylinositol 3'-Kinase/Akt Signal Transduction Pathway. *J Biol Chem,* **273**: 30336-30343.

Gerhardt, H. and Betsholtz, C. (2003). Endothelial-pericyte interactions in angiogenesis. *Cell Tissue Res,* **314**: 15-23.

Girard, J. P. and Springer, t. A. (1995). High endothelial venules (HEVs): specialized endothelium for lymphocyte migration. *Immunol Today,* **16**: 449-457.

Gregory, H. (1975). Isolation and structure of urogastrone and its relationship to epidermal growth factor. *Nature,* **257**: 325-327.

Groothuis, P. G., Nap, A. W., Winterhager, E. and Grummer, R. (2005). Vascular development in endometriosis. *Angiogenesis,* **8**: 147-156.

Gu, C., Rodriguez, E. R., Reimert, D. V., Shu, T., Fritsch, B., Richards, L. J., Kolodkin, A. L. and Ginty, D. D. (2003). Neuropilin-1 conveys semaphorin and VEGF signaling during neural and cardiovascular development. *Developmental cell,* **5**: 45-57.

Guo, D., Jia, Q., Song, H.-Y., Warren, R. S. and Donner, D. B. (1995). Vascular Endothelial Cell Growth Factor Promotes Tyrosine Phosphorylation of Mediators of Signal Transduction That Contain SH2 Domains. *J Biol Chem,* **270**: 6729-6733.

Guo, Z., Clydesdale, G., Cheng, J., Kim, K., Gan, L., McConkey, D. J., Ullrich, S. E., Zhuang, Y. and Su, B. (2002). Disruption of Mekk2 in mice reveals an unexpected role for MEKK2 in modulating T-cell receptor signal transduction. *Mol Cell Biol,* **22**: 5761-5768.

Gygi, S. P., Rist, B., Gerber, S. A., Turecek, F., Gelb, M. H. and Aebersold, R. (1999). Quantitative analysis of complex protein mixtures using isotope-coded affinity tags. *Nat Biotechnol,* **17**: 994-999.

Haar, J. L. and Ackerman, G. A. (1971). A phase and electron microscopic study of vasculogenesis and erythropoiesis in the yolk sac of the mouse. *Anat Rec,* **170**: 199-224.

Haeussler, D. J., Pimentel, D. R., Hou, X., Burgoyne, J. R., Cohen, R. A. and Bachschmid, M. M. (2013). Endomembrane H-Ras controls vascular endothelial growth factor-induced nitric-oxide synthase-mediated endothelial cell migration. *J Biol Chem,* **288**: 15380-15389.

Hallberg, B., Rayter, S. I. and Downward, J. (1994). Interaction of Ras and Raf in intact mammalian cells upon extracellular stimulation. *J Biol Chem,* **269**: 3913-3916.

Hammond, S. M., Bernstein, E., Beach, D. and Hannon, G. J. (2000). An RNA-directed nuclease mediates post-transcriptional gene silencing in Drosophila cells. *Nature,* **404**: 293-296.

Han, J., Jiang, Y., Li, Z., Kravchenko, V. V. and Ulevitch, R. J. (1997). Activation of the transcription factor MEF2C by the MAP kinase p38 in inflammation. *Nature,* **386**(6622): 296-299.

Hanahan, D. and Folkman, J. (1996). Patterns and emerging mechanisms of the angiogenic switch during tumorigenesis. *Cell,* **86**: 353-364.

Hanahan, D. and Weinberg, R. A. (2011). Hallmarks of cancer: the next generation. *Cell,* **144**: 646-674.

Harper, S. J. and Bates, D. O. (2008). VEGF-A splicing: The key to anti-angiogenic therapeutics? *Nat Rev Cancer,* **8**: 880-887.

Harris, R. C., Chung, E. and Coffey, R. J. (2003). EGF receptor ligands. *Experimental cell research,* **284**: 2-13.

Hashimoto, A., Kurosaki, M., Gotoh, N., Shibuya, M. and Kurosaki, T. (1999). Shc regulates epidermal growth factor-induced activation of the JNK signaling pathway. *J Biol Chem,* **274**: 20139-20143.

Hashizume, H., Baluk, P., Morikawa, S., McLean, J. W., Thurston, G., Roberge, S., Jain, R. K. and McDonald, D. M. (2000). Openings between defective endothelial cells explain tumor vessel leakiness. *Am J Pathol,* **156**: 1363-1380.

Hayashi, M., Fearns, C., Eliceiri, B., Yang, Y. and Lee, J. D. (2005). Big mitogen-activated protein kinase 1/Extracellular signal-regulated kinase 5 signaling pathway is essential for tumor-associated angiogenesis. *Cancer Res,* **65**: 7699-7706.

Hayashi, M., Kim, S. W., Imanaka-Yoshida, K., Yoshida, T., Abel, E. D., Eliceiri, B., Yang, Y., Ulevitch, R. J. and Lee, J. D. (2004). Targeted deletion of BMK1/ERK5 in adult mice perturbs vascular integrity and leads to endothelial failure. *J Clin Invest,* **113**(8): 1138-1148.

Hayashi, M. and Lee, J. D. (2004). Role of the BMK1/ERK5 signaling pathway: lessons from knockout mice. *J Mol Med (Berl),* **82**(12): 800-808.

Hayashi, M., Tapping, R. I., Chao, T. H., Lo, J. F., King, C. C., Yang, Y. and Lee, J. D. (2001). BMK1 mediates growth factor-induced cell proliferation through direct cellular activation of serum and glucocorticoid-inducible kinase. *J Biol Chem,* **276**(12): 8631-8634.

Hayes, D. F. (2011). Bevacizumab treatment for solid tumors: boon or bust? *JAMA,* **305**: 506-508.

Haystead, T. A., Dent, P., Wu, J., Haystead, C. and Sturgill, T. W. (1992). Ordered phosphorylation of p42mapk by MAP kinase kinase. *FEBS Lett,* **305**: 17-22.

Heinke, J., Patterson, C. and Moser, M. (2012). Life is a pattern: vascular assembly within the embryo. *Front Biosci,* **E4**: 2269-2288.

Hellström, M., Gerhardt, H., Kalén, M., Li, X., Eriksson, U., Wolburg, H. and Betsholtz, C. (2001). Lack of pericytes leads to endothelial hyperplasia and abnormal vascular morphogenesis. *The Journal of cell biology,* **153**: 543-554.

Henry, T. D., Annex, B. H., McKendall, G. R., Azrin, M. A., Lopez, J. J., Giordano, F. J., Shah, P. K., Willerson, J. T., Benza, R. L., Berman, D. S., Gibson, C. M., Bajamonde, A., Rundle, A. C., Fine, J. and McCluskey, E. R. (2003). The VIVA trial: Vascular endothelial growth factor in Ischemia for Vascular Angiogenesis. *Circulation,* **107**: 1359-1365.

Hewett, P. W. (2009). Vascular endothelial cells from human micro- and macrovessels: isolation, characterisation and culture. *Methods Mol Biol,* **467**: 95-111.

Higashiyama, S., Lau, K. E., Besner, G. A., Abraham, J. and Klagsbrun, M. (1992). Structure of heparin-binding EGF-like growth factor. Multiple forms, primary structure, and glycosylation of the mature protein. *J Biol Chem,* **267**: 6205-6212.

Hirakawa, T. and Ruley, H. E. (1988). Rescue of cells from ras oncogene-induced growth arrest by a second, complementing, oncogene. *Proc Natl Acad Sci U S A,* **85**: 19-23.

Hiratsuka, S., Minowa, O., Kuno, J., Noda, T. and Shibuya, M. (1998). Flt-1 lacking the tyrosine kinase domain is sufficient for normal development and angiogenesis in mice. *Proc Natl Acad Sci U S A,* **95**: 9349-9354.

Hiratsuka, S., Nakao, K., Nakamura, K., Katsuki, M., Maru, Y. and Shibuya, M. (2005). Membrane fixation of vascular endothelial growth factor receptor 1 ligand-binding domain is important for vasculogenesis and angiogenesis in mice. *Mol Cell Biol,* **25**: 346-354.

Holgado-Madruga, M., Emlet, D. R., Moscatello, D. K., Godwin, A. K. and Wong, A. J. (1996). A Grb2-associated docking protein in EGF- and insulin-receptor signalling. *Nature,* **379**: 560-564.

Holmes, K., Chapman, E., See, V. and Cross, M. J. (2010). VEGF stimulates RCAN1.4 expression in endothelial cells via a pathway requiring Ca2+/Calcineurin and Protein Kinase C-d. *PLoS ONE,* **5**: e11435.

Holmes, K., Roberts, O. L., Thomas, A. M. and Cross, M. J. (2007). Vascular endothelial growth factor receptor-2: Structure, function, intracellular signalling and therapeutic inhibition. *Cellular signalling,* **19**: 2003-2012.

Holmgren, L., O'Reilly, M. S. and Folkman, J. (1995). Dormancy of micrometastases: balanced proliferation and apoptosis in the presence of angiogenesis suppression. *Nat Med,* **1**: 149-153.

Holmqvist, K., Cross, M. J., Rolny, C., Hagerkvist, R., Rahimi, N., Matsumoto, T., Claesson-Welsh, L. and Welsh, M. (2004). The adaptor protein Shb binds to tyrosine 1175 in vascular endothelial growth factor (VEGF) receptor-2 and regulates VEGF-dependent cellular migration. *J Biol Chem,* **279**: 22267-22275.

Horowitz, A. and Seerappu, H. R. (2012). Regulation of VEGF signaling by membrane traffic. *Cellular signalling,* **24**: 1810-1820.

Houck, K. A., Ferrara, N., Winer, J., Cachianes, G., Li, B. and Leung, D. W. (1991). The vascular endothelial growth factor family - identification of a fourth molecular species and characterization of alternative splicing of RNA. *Mol Endocrinol,* **5**: 1806-1814.

Huang, J. and Manning, B. D. (2009). A complex interplay between Akt, TSC2, and the two mTOR complexes. *Biochem Soc Trans,* **37**: 217-222.

Huang, T.-L., Pian, J. P. and Pan, B.-T. (2013). Oncogenic Ras suprresses Cdk1 in a complex manner during the incubation of activated Xenopus egg extracts. *Arch Biochem Biophys,* **532**: 10.1016/j.abb.2013.1001.1006.

Hurwitz, H., Fehrenbacher, L., Novotny, W., Cartwright, T., Hainsworth, J., Heim, W., Berlin, J., Baron, A., Griffing, S., Holmgren, E., Ferrara, N., Fyfe, G., Rogers, B., Ross, R. and Kabbinavar, F. (2004). Bevacizumab plus irinotecan, fluorouracil, and leucovorin for metastatic colorectal cancer. *N Engl J Med,* **350**: 2335-2342.

Imoukhuede, P. I. and Popel, A. S. (2011). Quantification and cell-to-cell variation of vascular endothelial growth factor receptors. *Experimental cell research,* **317**: 955-965.

Inai, T., Mancuso, M., Hashizume, H., Baffert, F., Haskell, A., Baluk, P., Hu-Lowe, D. D., Shalinsky, D. R., Thurston, G., Yancopoulos, G. D. and McDonald, D. M. (2004). Inhibition of vascular endothelial growth factor (VEGF) signaling in cancer causes loss of endothelial fenestrations, regression of tumor vessels, and appearance of basement membrane ghosts. *Am J Pathol,* **165**: 35-52.

Inesta-Vaquera, F. A., Campbell, D. G., Tournier, C., Gomez, N., Lizcano, J. M. and Cuenda, A. (2010). Alternative ERK5 regulation by phosphorylation during the cell cycle. *Cellular signalling,* **22**(12): 1829-1837.

Issbrucker, K., Marti, H. H., Hippenstiel, S., Springmann, G., Voswinckel, R., Gaumann, A., Breier, G., Drexler, H. C. A., Suttorp, N. and Clauss, M. (2003). p38 MAP kinase - a molecular switch between VEGF-induced angiogenesis and vascular hyperpermeability. *Faseb J,* **17**: 262-264.

Jacinto, E., Facchinetti, V., Liu, D., Soto, N., Wei, S., Jung, S. Y., Huang, Q., Qin, J. and Su, B. (2006). SIN1/MIP1 maintains rictor-mTOR complex integrity and regulates Akt phosphorylation and substrate specificity. *Cell,* **127**: 125-137.

Jackson, C. J. and Nguyen, M. (1997). Human microvascular endothelial cells differ from macrovascular endothelial cells in their expression of matrix metalloproteinases. *Int J Biochem Cell Biol,* **29**: 1167-1177.

Jain, R. K. (2003). Molecular regulation of vessel maturation. *Nat Med,* **9**: 685-693.

Jain, R. K. (2005). Normalization of tumor vasculature: an emerging concept in antiangiogenic therapy. *Science,* **307**: 58-62.

Ji, Q. S., Winnier, G. E., Niswender, K. D., Horstman, D., Wisdom, R., Magnuson, M. A. and Carpenter, G. (1997). Essential role of the tyrosine kinase substrate phospholipase C-gamma1 in mammalian growth and development. *Proc Natl Acad Sci U S A,* **94**: 2999-3003.

Jingjing, L., Xue, Y., Agarwal, N. and Roque, R. S. (1999). Human Muller cells express VEGF183, a novel spliced variant of vascular endothelial growth factor. *Invest Opthalmol Vis Sci,* **40**: 752-759.

Johnson, G. L. and Vaillancourt, R. R. (1994). Sequential protein kinase reactions controlling cell growth and differentiation. *Curr Opin Cell Biol,* **6**: 230-238.

Kamakura, S., Moriguchi, T. and Nishida, E. (1999). Activation of the protein kinase ERK5/BMK1 by receptor tyrosine kinases. Identification and characterization of a signaling pathway to the nucleus. *J Biol Chem,* **274**(37): 26563-26571.

Kappas, N. C., Zeng, G., Chappell, J. C., Kearney, J. B., Hazarika, S., Kallianos, K. G., Patterson, C., Annex, B. H. and Bautch, V. L. (2008). The VEGF receptor Flt-1 spatially modulates Flk-1 signaling and blood vessel branching. *The Journal of cell biology,* **181**: 847-858.

Karas, M. and Hillenkamp, F. (1988). Laser desorption ionization of proteins with molecular masses exceeding 10,000 daltons. *Anal Chem,* **60**: 2299-2301.

Karkkainen, M. J., Haiko, P., Sainio, K., Partanen, J., Taipale, J., Petrova, T. V., Jeltsch, M., Jackson, D. G., Talikka, M., Rauvala, H., Betsholtz, C. and Alitalo, K. (2004). Vascular endothelial growth factor C is required for sprouting of the first lymphatic vessels from embryonic veins. *Nat Immunol,* **5**: 74-80.

Karkkainen, M. J., Makinen, T. and Alitalo, K. (2002). Lymphatic endothelium: a new frontier of metastasis research. *Nat Cell Biol,* **4**: E2-E5.

Kasler, H. G., Victoria, J., Duramad, O. and Winoto, A. (2000). ERK5 is a novel type of mitogen-activated protein kinase containing a transcriptional activation domain. *Mol Cell Biol,* **20**(22): 8382-8389.

Kato, Y., Kravchenko, V. V., Tapping, R. I., Han, J., Ulevitch, R. J. and Lee, J. D. (1997). BMK1/ERK5 regulates serum-induced early gene expression through transcription factor MEF2C. *Embo J,* **16**(23): 7054-7066.

Kato, Y., Tapping, R. I., Huang, S., Watson, M. H., Ulevitch, R. J. and Lee, J. D. (1998). Bmk1/Erk5 is required for cell proliferation induced by epidermal growth factor. *Nature,* **395**(6703): 713-716.

Kato, Y., Zhao, M., Morikawa, A., Sugiyama, T., Chakravortty, D., Koide, N., Yoshida, T., Tapping, R. I., Yang, Y., Yokochi, T. and Lee, J. D. (2000). Big mitogen-activated kinase regulates multiple members of the MEF2 protein family. *J Biol Chem,* **275**(24): 18534-18540.

Kawasaki, T., Kitsukawa, T., Bekku, Y., Matsuda, Y., Sanbo, M., Yagi, T. and Fujisawa, H. (1999). A requirement for neuropilin-1 in embryonic vessel formation. *Development,* **126**: 4895-4902.

Kazerounian, S., Yee, K. O. and Lawler, J. (2008). Thrombospondins in cancer. *Cellular and molecular life sciences : CMLS,* **65**: 700-712.

Kendall, R. L. and Thomas, K. A. (1993). Inhibition of vascular endothelial cell growth factor activity by an endogenously encoded soluble recepotr. *Proc Natl Acad Sci U S A,* **90**: 10705-10709.

Kerbel, R. S. (2006). Antiangiogenic therapy: a universal chemosensitization strategy for cancer? *Science,* **312**: 1171-1175.

Kesavan, K., Lobel-Rice, K., Sun, W., Lapadat, R., Webb, S., Johnson, G. L. and Garrington, T. P. (2004). MEKK2 regulates the coordinate activation of ERK5 and JNK in response to FGF-2 in fibroblasts. *Journal of cellular physiology,* **199**(1): 140-148.

Kim, M., Kim, S., Lim, J. H., Lee, C. M., Choi, H. C. and Woo, C. H. (2012). Laminar flow activation of ERK5 in vascular endothelium leads to atheroprotective effect via NF-E2-related factor2 (Nrf2) activation. *J Biol Chem,* **287**: 40722-40731.

Kimura, T. E., Jin, J., Zi, M., Prehar, S., Liu, W., Oceandy, D., Abe, J., Neyses, L., Weston, A. H., Cartwright, E. J. and Wang, X. (2010). Targeted deletion of the extracellular signal-regulated protein kinase 5 attenuates hypertrophic response and promotes pressure overload-induced apoptosis in the heart. *Circulation research,* **106**(5): 961-970.

Kinoshita, E., Kinoshita-Kikuta, E., Takiyama, K. and Koike, T. (2006). Phosphate-binding tag, a new tool to visualize phosphorylated proteins. *Mol Cell Proteomics,* **5**: 749-757.

Kitamoto, Y., Tokunaga, H. and Tomita, K. (1997). Vascular endothelial growth factor is an essential molecule for mouse kidney development: glomerulogenesis and nephrogenesis. *J Clin Invest,* **99**: 2351-2357.

Klagsbrun, M. and Moses, M. A. (1999). Molecular angiogenesis. *Chem Blol,* **6**: R217-224.

Koch, S. and Claesson-Welsh, L. (2012). Signal transduction by vascular endothelial growth factor receptors. *Cold Spring Harb Perspect Med,* **2**: a006502.

Kondoh, K., Terasawa, K., Morimoto, H. and Nishida, E. (2006). Regulation of nuclear translocation of extracellular signal-regulated kinase 5 by active nuclear import and export mechanisms. *Mol Cell Biol,* **26**(5): 1679-1690.

Kovacina, K. S., Park, G. Y., Bae, S. S., Guzzetta, A. W., Schaefer, E., Birnbaum, M. J. and Roth, R. A. (2003). Identification of a proline-rich AKT substrate as a 14-3-3 binding partner. *J Biol Chem,* **278**: 10189-10194.

Ku, D. D., Zaleski, J. K., Liu, S. and Brock, T. A. (1993). Vascular endothelial gorwht factor induces EDRF-dependent relaxation in coronary arteries. *Am J Physiol,* **265**: H586-592.

Kumanogoh, A. and Kikutani, H. (2013). Immunological functions of the neuropilins and plexins as receptors for semaphorins. *Nature Reviews Immunology,* **13**: 802-814.

Kumar, S., West, D. C. and Ager, A. (1987). Heterogeneity in endothelial cells from large vessels and microvessels. *Differentiation,* **36**: 57-70.

Lafleur, M. A., Handsley, M. M. and Edwards, D. R. (2003). Metalloproteinases and their inhibitors in angiogenesis. *Expert Rev Mol Med,* **5**: 1-39.

Lamalice, L., Houle, F. and Huot, J. (2006). Phosphorylation of Tyr1214 within VEGFR-2 triggers the recruitment of Nck and activation of Fyn leading to SAPK2/p38 activation and endothelial cell migration in response to VEGF.

Lamark, T., Perander, M., Outzen, H., Kristiansen, K., Overvatn, A., Michaelsen, E., Bjorkoy, G. and Johansen, T. (2003). Interaction codes within the family of mammalian Phox and Bem1p domain-containing proteins. *J Biol Chem,* **278**(36): 34568-34581.

Lampugnani, M. G., Orsenigo, F., Gagliani, M. C., Tacchetti, C. and Dejana, E. (2006). Vascular endothelial cadherin controls VEGFR-2 internalization and signaling from intracellular compartments. *The Journal of cell biology,* **174**: 593-604.

Land, H., Parada, L. F. and Weinberg, R. A. (1983). Tumorigenic conversion of primary embryo fibroblasts require at least two cooperating oncogenes. *Nature,* **304**: 596-602.

Langlois, W. J., Sasaoka, T., Saltiel, A. R. and Olefsky, J. M. (1995). Negative feedback regulation and desensitization of insulin- and epidermal growth factor-stimulated p21ras activation. *J Biol Chem,* **270**: 25320-25323.

Lawler, S., Fleming, Y., Goedert, M. and Cohen, P. (1998). Synergistic activation of SAPK1/JNK1 by two MAP kinase kinases in vitro. *Curr Blol,* **8**: 1387-1390.

Lawlor, M. A. and Alessi, D. R. (2001). PKB/Akt: a key mediator of cell proliferation, survival and insulin responses? *J Cell Sci,* **114**: 2903-2910.

Lawson, N. D., Mugford, J. W., Diamond, B. A. and Weinstein, B. M. (2003). Phospholipase C gamma-1 is required downstream of vascular endothelial growth factor during arterial development. *Genes Dev,* **17**: 1346-1351.

Le, N. T., Heo, K. S., Takei, Y., Lee, H., Woo, C. H., Chang, E., McClain, C., Hurley, C., Wang, X., Li, F., Xu, H., Morrell, C., Sullivan, M. A., Cohen, M. S., Serafimova, I. M., Taunton, J., Fujiwara, K. and Abe, J. (2013). A crucial role for p90RSK-mediated reduction of ERK5 transcriptional activity in endothelial dysfunction and atherosclerosis. *Circulation,* **127**: 486-499.

Lee, J. D., Ulevitch, R. J. and Han, J. (1995). Primary structure of BMK1: a new mammalian map kinase. *Biochem Biophys Res Commun,* **213**(2): 715-724.

Lemmon, M. A. and Schlessinger, J. (2010). Cell signaling by receptor tyrosine kinases. *Cell,* **141**: 1117-1134.

Lennartsson, J., Burovic, F., Witek, B., Jurek, A. and Heldin, C. H. (2010). Erk 5 is necessary for sustained PDGF-induced Akt phosphorylation and inhibition of apoptosis. *Cellular signalling,* **22**: 955-960.

Levi-Montalcini, R. and Hamburger, V. (1951). Selective growth stimulating effects of mouse sarcoma on the sensory and sympathetic nervous system of the chick embryos. *J Exp Zool,* **116**: 321-362.

Lewis, T. S., Shapiro, P. S. and Ahn, N. G. (1998). Signal transduction through MAP kinase cascades. *Advances in cancer research,* **74**: 49-139.

Li, G., Lucas, J. J. and Gelfand, E. W. (2005). Protein kinase C alpha, betaI, and betaII isozymes regulate cytokine production in mast cells through MEKK2/ERK5-dependent and -independent pathways. *Cell Immunol,* **238**: 10-18.

Li, J., Zhang, Y. P. and Kirsner, R. S. (2003). Angiogeneis in wound repair: angiogenic growth factors and the extracellular matrix. *Microsc Res Tech,* **2003**: 107-114.

Li, L., Tatake, R. J., Natarajan, K., Taba, Y., Garin, G., Tai, C., Leung, E., Surapisitchat, J., Yoshiziumi, M., Yan, C., Abe, J. and Berk, B. C. (2008). Fluid shear stress inhibits TNF-mediated JNK activation via MEK5-BMK1 in endothelial cells. *Biochem Biophys Res Commun,* **370**: 159-163.

Li, T., Pan, Y.-W., Wang, W., Abel, G., Zou, J., Xu, L., Storm, D. R. and Xia, Z. (2013). Targeted deletion of the ERK5 MAP kinase impairs neuronal differentiation, migration, and survival during adult neurogenesis in the olfactory bulb. *PLoS ONE,* **8**: e61948.

Liao, H. J., Kume, T., McKay, C., Xu, M. J., Ihle, J. N. and Carpenter, G. (2002). Absence of erythrogenesis and vasculogenesis in Plcg1-deficient mice. *J Biol Chem,* **277**: 9335-9341.

LifeTechnologies™. (2014). "http://tools.lifetechnologies.com/Content/SFS/ProductNotes/F_Lipofectamineht tp://www.lifetechnologies.com/order/catalog/product/11668027." Retrieved 9th November 2014.

Lin, Q., Lu, J., Yanagisawa, H., Webb, R., Lyons, G. E., Richardson, J. A. and Olson, E. N. (1998). Requirement of the MADS-box transcription factor MEF2C for vascular development. *Development,* **125**: 4565-4574.

Lin, Q., Schwarz, J., Bucana, C. and Olson, E. N. (1997). Control of mouse cardiac morphogenesis and myogenesis by transcription factor MEF2C. *Science,* **276**: 1404-1407.

Llovet, J. M., Ricci, S., Mazzaferro, V., Hilgard, P., Gane, E., Blanc, J. F., de Oliveira, A. C., Santoro, A., Raoul, J. L., Forner, A., Schwartz, M., Porta, C., Zeuzum, S., Bolondi, L., Greten, T. F., Galle, P. R., Seitz, J. F., Borbath, I., Haussinger, D., Giannaris, T., Shan, M., Moscovici, M., Voliotis, D. and Bruix, J. (2008). Sorafenib in advanced hepatocellular carcinoma. *N Engl J Med,* **359**: 378-390.

Lochhead, P. A., Gilley, R. and Cook, S. J. (2012). ERK5 and its role in tumour development. *Biochem Soc Trans,* **40**: 251-256.

Lohela, M., Bry, M., Tammela, T. and Alitalo, K. (2009). VEGFs and receptors involved in angiogenesis versus lymphangiogenesis. *Curr Opin Cell Biol,* **21**: 154-164.

Lonza. (2014). "http://www.lonza.com/products-services/bio-research/transfection/nucleofector-technology.aspx." Retrieved 11th November 2014.

Lowenstein, E. J., Daly, R. J., Batzer, A. G., Li, W., Margolis, B., Lammers, A., Ullrich, A., Skolnik, E. Y., Bar-Sagi, D. and Schlessinger, J. (1992). The SH2 and SH3 domain-containing protein GRB2 links receptor tyrosine kinases to ras signaling. *Cell,* **70**: 431-442.

Lyttle, D. J., Fraser, K. M., Fleming, S. B., Mercer, A. A. and Robinson, A. J. (1994). Homologs of vascular endothelial growth factor are encoded by the poxvirus orf virus. *J Virol,* **68**: 84-92.

Mancuso, M., Davis, R., Norberg, S. M., O'Brien, S., Sennino, B., Nakahara, T., Yao, V. J., Inai, T., Brooks, P., Freimark, B., Shalinsky, D. R., Hu-Lowe, D. D. and McDonald, D. M. (2006). Rapid vascular regrowth in tumors after reversal of VEGF inhibition. *J Clin Invest,* **116**: 2610-2621.

Massague, J. (1990). Transforming growth factors-α. *J Biol Chem,* **265**: 21393-21396.

Matsumoto, T., Bohman, S., Dixellus, J., Berge, T., Dimberg, A., Magnusson, P., Wang, L., Wikner, C., Qi, J. H., Wernstedt, C., Wu, J., Bruheim, S., Mugishima, H., Mukhopadhyay, D., Spurkland, A. and Claesson-Welsh, L. (2005). VEGF receptor-2 Y951 signaling and a role for the adaptor molecule TSAd in tumor angiogenesis. *Embo J,* **24**: 2342-2353.

Mattoon, D. R., Lamothe, B., Lax, I. and Schlessinger, J. (2004). The docking protein Gab1 is the primary mediator of EGF-stimulated activation of the PI-3K/Akt cell survival pathway. *BMC Biology,* **2**(24).

McCracken, S. R., Ramsay, A., Heer, R., Mathers, M. E., Jenkins, B. L., Edwards, J., Robson, C. N., Marquez, R., Cohen, P. and Leung, H. Y. (2008). Aberrant expression of extracellular signal-regulated kinase 5 in human prostate cancer. *Oncogene,* **27**: 2978-2988.

McGeachie, J. (2014). "Vascular system: http://www.lab.anhb.uwa.edu.au/mb140/corepages/vascular/vascular.htm." Retrieved 10th November 2014.

Meadows, K. N., Bryant, P. and Pumiglia, K. (2001). Vascular endothelial growth factor induction of the angiogenic phenotype requires Ras activation. *J Biol Chem,* **276**: 49289-49298.

Meadows, K. N., Bryant, P., Vincent, P. A. and Pumiglia, K. M. (2004). Activated Ras induces a proangiogenic phenotype in primary endothelial cells. *Oncogene,* **23**: 192-200.

Mehta, P. B., Jenkins, B. I., McCarthy, L., Thilak, L., Robson, C. N., Neal, D. E. and Leung, H. Y. (2003). MEK5 overexpression is associated with metastatic prostate cancer, and stimulates proliferation, MMP-9 expression and invasion. *Oncogene,* **22**: 1381-1389.

Miquerol, L., Langille, B. L. and Nagy, A. (2000). Embryonic development is disrupted by modest increases in vascular endothelial growth factor gene expression. *Development,* **127**(18): 3941-3946.

Miyasaka, M. and Tanaka, T. (2004). Lymphocyte trafficking across high endothelial venules: dogmas and enigmas. *Nat Rev Immunol,* **4**: 360-370.

Mody, N., Campbell, D. G., Morrice, N., Peggie, M. and Cohen, P. (2003). An analysis of the phosphorylation and activation of extracellular-signal-regulated protein kinase 5 (ERK5) by mitogen-activated protein kinase kinase 5 (MKK5) in vitro. *The Biochemical journal,* **372**(Pt 2): 567-575.

Mohammadi, M., Honegger, A. M., Rotin, D., Fischer, R., Bellot, F., Li, W., Dionne, C. A., Jaye, M., Rubinstein, M. and Schlessinger, J. (1991). A tyrosine-phosphorylated carboxy-terminal peptide of the fibroblast growth factor receptor (Flg) is a binding site for the SH2 domain of phospholipase C-gamma 1. *Mol Cell Biol,* **11**: 5068-5078.

Montero, J. C., Ocaña, A., Abad, M., Ortiz-Ruiz, M. J., Pandiella, A. and Esparís-Ogando, A. (2009). Expression of Erk5 in early stage breast cancer and association with disease free survival identifies this kinase as a potential therapeutic target. *PLoS ONE,* **4**: e5565.

Morikawa, S., Baluk, P., Kaidoh, T., Haskell, A., Jain, R. K. and McDonald, D. M. (2002). Abnormalities in pericytes on blood vessels and endothelial sprouts in tumors. *Am J Pathol,* **160**: 985-1000.

Morimoto, H., Kondoh, K., Nishimoto, S., Terasawa, K. and Nishida, E. (2007). Activation of a C-terminal transcriptional activation domain of ERK5 by autophosphorylation. *J Biol Chem,* **282**(49): 35449-35456.

Morrison, D. K. and Davis, R. J. (2003). Regulation of MAP kinase signaling modules by scaffold proteins in mammals. *Annual review of cell and developmental biology,* **19**: 91-118.

Motzer, R. J., Hutson, T. E., Tomczak, P., Michaelson, M. D., Bukowski, R. M., Rixe, O., Oudard, S., Negrier, S., Szczylik, C., Kim, S. T., Chen, I., Bycott, P. W., Baum, C. M. and Figlin, R. A. (2007). Sunitinib versus interferon alfa in metastatic renal-cell carcinoma. *N Engl J Med,* **356**(115-124).

Muller, Y. A., Li, B., Christinger, H. W., Wells, J. A., Cunningham, B. C. and de Vos, A. M. (1997). Vascular endothelial growth factor: crystal structure and functional

mapping of the kinase domain receptor binding site. *Proc Natl Acad Sci U S A,* **94**: 7192-7197.

Mulloy, R., Salinas, S., Philips, A. and Hipskind, R. A. (2003). Activation of cyclin D1 expression by the ERK5 cascade. *Oncogene,* **22**(35): 5387-5398.

Muthukkaruppan, V. R., Kubai, L. and Auerbach, R. (1982). Tumor-induced neovascularization in the mouse eye. *J Natl Cancer Inst,* **69**: 699-708.

Nakagami, H., Morishita, R., Yamamoto, K., Taniyama, Y., Aoki, M., Matsumoto, K., Nakamura, T., Kaneda, Y., Horiuchi, M. and Ogihara, T. (2001). Mitogenic and antiapoptotic action of hepatocyte growth factor through ERK, STAT3 and Akt in endothelial cells. *Hypertension,* **37**(581-586).

Nakamura, K. and Johnson, G. L. (2003). PB1 domains of MEKK2 and MEKK3 interact with the MEK5 PB1 domain for activation of the ERK5 pathway. *J Biol Chem,* **278**(39): 36989-36992.

Nakamura, K., Uhlik, M. T., Johnson, N. L., Hahn, K. M. and Johnson, G. L. (2006). PB1 domain-dependent signaling complex is required for extracellular signal-regulated kinase 5 activation. *Mol Cell Biol,* **26**: 2065-2079.

NCBI. (2014). "http://www.ncbi.nlm.nih.gov/gene/5598 MAPK7 mitogen-activated protein kinase 7 [Homo sapiens (human)] - Gene ID: 5598." Retrieved 15th June 2014.

NEB®. (2013). "https://www.neb.com/products/m2558-transpass-huvec-transfection-reagent." Retrieved 9th November 2014.

Neufeld, G., Cohen, T., Shraga, N., Lange, T., Kessler, O. and Herzog, Y. (2002). The neuropilins: multifunctional semaphorin and VEGF receptors that modulate axon guidance and angiogenesis. *Trends Cardiovasc Med,* **12**: 13-19.

Nishibe, S., Wahl, M. I., Hernández-Sotomayor, S. M., Tonks, N. K., Rhee, S. G. and Carpenter, G. (1990). Increase of the catalytic activity of phospholipase C-gamma 1 by tyrosine phosphorylation. *Science,* **250**: 1253-1256.

Nishida, E. and Gotoh, Y. (1993). The MAP kinase cascade is essential for diverse signal transduction pathways. *Trends Biochem Sci,* **18**(4): 128-131.

Nishida, N., Yano, H., Nishida, T., Kamura, T. and Kojiro, M. (2006). Angiogenesis in Cancer. *Vasc Health Risk Manag,* **2**: 213-219.

Nithianandarajah-Jones, G. N., Wilm, B., Goldring, C. E. P., Muller, J. and Cross, M. J. (2012). ERK5: Structure, regulation and function. *Cellular signalling,* **24**: 2187-2196.

Normanno, N., Bianco, C., De Luca, A., Maiello, M. R. and Salomon, D. S. (2003). Target-based agents against ErbB receptors and their ligands: a novel approach to cancer treatment. *Endocr Relat Cancer,* **10**: 1-21.

Normanno, N., Bianco, C., De Luca, A. and Salomon, D. S. (2001). The role of EGF-related peptides in tumor growth. *Front Biosci,* **6**: d685-d707.

Normanno, N., De Luca, A., Bianco, C., Strizzi, L., Mancino, M., Maiello, M. R., Carotenuto, A., De Feo, G., Caponigro, F. and Salomon, D. S. (2006). Epidermal growth factor receptor (EGFR) signaling in cancer. *Gene,* **366**: 2-16.

Obara, Y., Yamauchi, A., Takehara, S., Nemoto, W., Takahashi, M., Stork, P. J. and Nakahata, N. (2009). ERK5 activity is required for nerve growth factor-induced neurite outgrowth and stabilization of tyrosine hydroxylase in PC12 cells. *J Biol Chem,* **284**: 23564-23573.

Ohnesorge, N., Viemann, D., Schmidt, N., Czymai, T., Spiering, D., Schmolke, M., Ludwig, S., Roth, J., Goebeler, M. and Schmidt, M. (2010). Erk5 activation elicits a vasoprotective endothelial phenotype via induction of Kruppel-like factor 4 (KLF4). *J Biol Chem,* **285**: 26199-26210.

Okano, Y., Mizuno, K., Osada, S., Nakamura, T. and Nozawa, Y. (1993). Tyrosine phosphorylation of phospholipase C gamma in c-met/HGF receptor-stimulated hepatocytes: comparison with HepG2 hepatocarcinoma cells. *Biochem Biophys Res Commun,* **190**: 842-848.

Olson, E. N. (2004). Undermining the endothelium by ablation of MAPK-MEF2 signaling. *J Clin Invest,* **113**: 1110-1112.

Olsson, A. K., Dimberg, A., Kreuger, L. and Claesson-Welsh, L. (2006). VEGF receptor signalling - in control of vascular function. *Nat Rev Mol Cell Biol,* **7**: 359-371.

Omerovic, J., Clague, M. J. and Prior, I. A. (2010). Phosphatome profiling reveals PTPN2, PTPRJ and PTEN as potent negative regulators of PKB/Akt activation in Ras-mutated cancer cells. *The Biochemical journal,* **426**: 65-72.

Omerovic, J., Hammond, D. E., Clague, M. J. and Prior, I. A. (2008). Ras isoform abundance and signalling in human cancer cell lines. *Oncogene,* **27**: 2754-2762.

Ong, S. E., Blagoev, B., Kratchmarova, I., Kristensen, D. B., Steen, H., Pandey, A. and Mann, M. (2002). Stable isotope labeling by amino acids in cell culture, SILAC, as a simple and accurate approach to expression proteomics. *Mol Cell Proteomics,* **1**: 376-386.

Ornatsky, O. I., Cox, D. M., Tangirala, P., Andreucci, J. J., Quinn, Z. A., Wrana, J. L., Prywes, R., Yu, Y. T. and McDermott, J. C. (1999). Post-translational control of the MEF2A transcriptional regulatory protein. *Nucleic Acids Res,* **27**(13): 2646-2654.

Pankov, R., Cukierman, E., Clark, K., Matsumoto, K., Hahn, C., Poulin, B. and Yamada, K. M. (2003). Specific beta1 integrin site selectively regulates Akt/protein kinase B signaling via local activation of protein phosphatase 2A. *J Biol Chem,* **278**: 18671-18681.

Park, D. J., Freitas, T. A., Wallick, C. J., Guyette, C. V. and Warn-Cramer, B. J. (2006). Molecular dyamics and in vitro analysis of Connexin43: a new 14-3-3 mode-1 interacting protein. *Protein Sci,* **15**: 2344-2355.

Park, D. J., Wallick, C. J., Martyn, K. D., Lau, A. F., Jin, C. and Warn-Cramer, B. J. (2007). Akt phosphorylates Connexin43 on Ser373, a "mode-1" binding site for 14-3-3. *Cell Commun Adhes,* **14**: 211-226.

Park, J. E., Keller, G. A. and Ferrara, N. (1993). Vascular endothelial growth factor (VEGF) isoforms - differential deposition into the subepithelial extracellular matrix and bioactivity of extracellular matrix-bound VEGF. *Mol Biol Cell,* **4**: 1317-1326.

Parker, M. W., Xu, P., Li, X. and Vander Kooi, C. W. (2012). Structural basis for selective vascular endothelial growth factor-A (VEGF-A) binding to neuropilin-1. *J Biol Chem,* **287**(14): 11082-11089.

Parmar, K. M., Larman, H. B., Dai, G., Zhang, Y., Wang, E. T., Moorthy, S. N., Kratz, J. R., Lin, Z., Jain, M. K., Gimbrone Jr, M. A. and Garcia-Cardena, G. (2006). Integration of flow-dependent endothelial phenotypes by Kruppel-like factor 2. *J Clin Invest,* **116**: 49-58.

Pearson, J. D. (2000). Normal endothelial cell function. *Lupus,* **9**: 183-188.

Pi, X., Garin, G., Xie, L., Zheng, Q., Wei, H., Abe, J., Yan, C. and Berk, B. C. (2005). BMK1/ERK5 is a novel regulator of angiogenesis by destabilizing hypoxia inducible factor 1alpha. *Circulation research,* **96**(11): 1145-1151.

Plate, K. H., Breier, G., Millauer, B., Ullrich, A. and Risau, W. (1993). Up-regulation of vascular endothelial growth factor and its cognate receptors in a rat glioma model of tumor angiogenesis. *Cancer Res,* **53**: 5822-5827.

Plotnikov, A., Zehorai, E., Procaccia, S. and Seger, R. (2011). The MAPK cascades: Signaling components, nuclear roles and mechanisms of nuclear translocation. *Biochim Biophys Acta,* **1813**: 1619-1633.

Poltorak, Z., Cohen, T., Sivan, R., Kandelis, Y., Spira, G., Vlodavsky, I., Keshet, E. and Neufeld, G. (1997). VEGF145: a secreted VEGF form that binds to extracellular matrix. *J Biol Chem,* **72**: 7151-7158.

Pötgens, A. J. G., Lubsen, N. H., van Altena, M. C., Vermeulen, R., Bakker, A., Schoenmakers, J. G. G., Ruiter, D. J. and de Waal, R. M. W. (1994). Covalent dimerization of vascular permeability factor/vascular endothelial growth factor is essential for its biological activity. *J Biol Chem,* **269**: 32879-32885.

Prior, I., Lewis, P. D. and Mattos, C. (2012). A comprehensive survey of Ras mutations in cancer. *Cancer Research,* **72**: 2457-2467.

Qi, M. and Elion, E. A. (2005). MAP kinase pathways. *J Cell Sci,* **118**(Pt 16): 3569-3572.

Raman, M., Chen, W. and Cobb, M. H. (2007). Differential regulation and properties of MAPKs. *Oncogene,* **26**(22): 3100-3112.

Ramos-Nino, M. E., Blumen, S. R., Sabo-Attwood, T., Pass, H., Carbone, M., Testa, J. R., Altomare, D. A. and Mossman, B. T. (2008). HGF mediates cell proliferation of human mesothelioma cells through a PI3K/MEK5/Fra-1 pathway. *American Journal of Respiratory Cell and Molecular Biology,* **38**: 209-217.

Ramsay, A. K., McCracken, S. R., Soofi, M., Fleming, J., Yu, A. X., Ahmad, I., Morland, R., Machesky, L., Nixon, C., Edwards, D. R., Nuttall, R. K., Seywright, M., Marquez, R., Keller, E. and Leung, H. Y. (2011). ERK5 signalling in prostate cancer promotes an invasive phenotype. *Br J Cancer,* **104**: 664-672.

Randi, A. M., Sperone, A., Dryden, N. H. and Birdsey, G. M. (2009). Regulation of angiogenesis by ETS transcription factors. *Biochem Soc Trans,* **37**: 1248-1253.

Raviv, Z., Kalie, E. and Seger, R. (2004). MEK5 and ERK5 are localized in the nuclei of resting as well as stimulated cells, while MEKK2 translocates from the cytosol to the nucleus upon stimulation. *J Cell Sci,* **117**(Pt 9): 1773-1784.

Razmara, M., Eger, G., Rorsman, C., Heldin, C. H. and Lennartsson, J. (2012). MKP3 negatively modulates PDGF-induced Akt and Erk5 phosphorylation as well as chemotaxis. *Cellular signalling,* **24**: 635-640.

Razumovskaya, E., Sun, J. and Rönnstrand, L. (2011). Inhibition of MEK5 by BIX02188 induces apoptosis in cells expressing the oncogenic mutant FLT3-ITD. *Biochem Biophys Res Commun,* **412**: 307-312.

Regan, C. P., Li, W., Boucher, D. M., Spatz, S., Su, M. S. and Kuida, K. (2002). Erk5 null mice display multiple extraembryonic vascular and embryonic cardiovascular defects. *Proc Natl Acad Sci U S A,* **99**(14): 9248-9253.

Rini, B. I., Escudier, B., Tomczak, P., Kaprin, A., Szczylik, C., Hutson, T. E., Michaelson, M. D., Gorbunova, V., Gore, M. E., Rusakov, I. G., Negrier, S., Ou, Y. C., Castellano, D., Lim, H. Y., Uemura, H., Tarazi, J., Cella, D., Chen, C., Rosbrook, B., Kim, S. and Motzer, R. J. (2011). Comparative effectiveness of axitinib versus sorafenib in advanced renal cell carcinoma (AXIS): a randomised phase 3 trial. *Lancet,* **378**: 1931-1939.

Rini, B. I., Halabi, S., Rosenberg, J. E., Stadler, W. M., Vaena, D. A., Archer, L., Atkins, J. N., Picus, J., Czaykowski, P., Dutcher, J. and Small, E. J. (2010). Phase III trial of bevacizumab plus interferon alfa versus interferon alfa monotherapy in patients with metastatic renal cell carcinoma: final results of CALGB 90206. *J Clin Oncol,* **28**: 2137-2143.

Risau, W. (1997). Mechanisms of angiogenesis. *Nature,* **386**: 671-674.

Risau, W. and Flamme, I. (1995). Vasculogenesis. *Annual review of cell and developmental biology,* **11**: 73-91.

Roberts, D. M., Kearney, J. B., Johnson, J. H., Rosenberg, M. P., Kumar, R. and Bautch, V. L. (2004). The vascular endothelial growth factor (VEGF) receptor Flt-1 (VEGFR-1) modulates Flk-1 (VEGFR-2) signaling during blood vessel formation. *Am J Pathol,* **164**: 1531-1535.

Roberts, O. L., Holmes, K., Muller, J., Cross, D. A. and Cross, M. J. (2009). ERK5 and the regulation of endothelial cell function. *Biochem Soc Trans,* **37**(Pt 6): 1254-1259.

Roberts, O. L., Holmes, K., Muller, J., Cross, D. A. and Cross, M. J. (2010). ERK5 is required for VEGF-mediated survival and tubular morphogenesis of primary human microvascular endothelial cells. *J Cell Sci,* **123**: 3189-3200.

Robinson, M. J. and Cobb, M. H. (1997). Mitogen-activated protein kinase pathways. *Curr Opin Cell Biol,* **9**(2): 180-186.

Rosenthal, A., Lindquist, P. B., Bringman, T. S., Goeddel, D. V. and Derynck, R. (1986). Expression in rat fibroblasts of a human transforming growth factor-alpha cDNA results in transformation. *Cell,* **46**: 301-309.

Ross, P. L., Huang, Y. N., Marchese, J. N., Williamson, B., Parker, K., Hattan, S., Khainovski, N., Pillai, S., Dey, S., Daniels, S., Purkayastha, S., Juhasz, P., Martin, S., Bartlet-Jones, M., He, F., Jacobson, A. and Pappin, D. J. (2004). Multiplexed protein quantitation in Saccharomyces cerevisiae using amine-reactive isobaric tagging reagents. *Mol Cell Proteomics,* **3**: 1154-1169.

Rossant, J. and Howard, L. (2002). Signaling pathways in vascular development. *Annual review of cell and developmental biology,* **18**: 541-573.

Ruch, C., Skiniotis, G., Steinmetz, M. O., Walz, T. and Ballmer-Hofer, K. (2007). Structure of a VEGF-VEGF receptor complex determined by electon microscopy. *Nat Struct Mol Biol,* **14**: 249-250.

Russell, W. C. (2000). Update on Adenovirus and its Vectors. *J Gen Virol,* **81**: 2573-2604.

Sakaguchi, K., Okabayashi, Y., Kido, Y., Kimura, S., Matsumura, Y., Inushima, K. and Kasuga, M. (1998). Shc phosphotyrosine-binding domain dominantly interacts with epidermal growth factor receptors and mediates Ras activation in intact cells. *Mol Endocrinol,* **12**: 536-543.

Sakurai, Y., Ohgimoto, K., Kataoka, Y., Yoshida, N. and Shibuya, M. (2005). Essential role of Flk-1 (VEGF receptor 2) tyrosine residue 1173 in vasculogenesis in mice. *Proc Natl Acad Sci U S A,* **102**: 1076-1081.

Salmena, L., Carracedo, A. and Pandolfi, P. P. (2008). Tenets of PTEN tumor suppression. *Cell,* **133**(403-414).

Salomon, D. S., Brandt, R., Ciardiello, F. and Normanno, N. (1995). Epidermal growth factor-related peptides and their receptors in human malignancies. *Crit Rev Oncol Hematol,* **19**: 183-232.

Santos, S. C., Miguel, C., Domingues, I., Calado, A., Zhu, Z., Wu, Y. and Dias, S. (2007). VEGF and VEGFR-2 (KDR) internalization is required for endothelial recovery during wound healing. *Experimental cell research,* **313**: 1561-1574.

Sarbassov, D. D., Ali, S. M., Sengupta, S., Sheen, J. H., Hsu, P. P., Bagley, A. F., Markhard, A. L. and Sabatini, D. M. (2006). Prolonged rapamycin treatment inhibits mTORC2 assembly and Akt/PKB. *Mol Cell,* **22**: 159-168.

Sarbassov, D. D., Guertin, D. A., Ali, S. M. and Sabatini, D. M. (2005). Phosphorylation and regulation of Akt/PKB by the rictor-mTOR complex. *Science,* **307**: 1098-1101.

Sasaoka, T., Langlois, W. J., Leitner, J. W., Draznin, B. and Olefsky, J. M. (1994). The signaling pathway coupling epidermal growth factor receptors to activation of p21ras. *J Biol Chem,* **269**: 32621-32625.

Sawhney, R. S., Liu, W. and Brattain, M. G. (2009). A novel role of ERK5 in integrin-mediated cell adhesion and motility in cancer cells via Fak signaling. *Journal of cellular physiology,* **219**(1): 152-161.

Schmidt, A., Kellermann, J. and Lottspeich, F. (2005). A novel strategy for quantitative proteomics using isotop-coded protein labels. *Proteomics,* **5**: 4-15.

Schramp, M., Ying, O., Kim, T. Y. and Martin, G. S. (2008). ERK5 promotes Src-induced podosome formation by limiting Rho activation. *The Journal of cell biology,* **181**: 1195-1210.

Schreiber, A. B., Winkler, M. E. and Derynck, R. (1986). Transforming Growth Factor-alpha: A More Potent Angiogenic Mediator Than Epidermal Growth Factor. Science. **232:** 1250-1253.

Seaman, S., Stevens, J., Yang, M. Y., Logsdon, D., Graff-Cherry, C. and St Croix, B. (2007). Genes that distinguish physiological and pathological angiogenesis. *Cancer Cell,* **11**: 539-554.

Semenza, G. L. (2007). Hypoxia-inducible factor 1 (HIF-1) pathway. *Sci STKE,* **2007**: cm8.

SenBanerjee, S., Lin, Z., Atkins, G. B., Greif, D. M., Rao, R. M., Kumar, A., Feinberg, M. W., Chen, Z., Simon, D. I., Luscinskas, F. W., Michel, T. M., Gimbrone Jr, M. A., Garcia-Cardena, G. and Jain, M. K. (2004). KLF2 Is a novel transcriptional regulator of endothelial proinflammatory activation. *J Exp Med,* **199**: 1305-1315.

Senger, D. R., Galli, S. J., Dvorak, A. M., Perruzzi, C. A., Harvey, V. S. and Dvorak, H. F. (1983). Tumor cells secrete a vascular permeability factor that promotes accumulation of ascites fluid. *Science,* **219**: 983-985.

Shalaby, F., Rossant, J., Yamaguchi, T. P., Gertsenstein, M., Wu, X. F., Breitman, M. L. and Schuh, A. C. (1995). Failure of blood-island formation and vasculaogenesis in Flk-1 deficient mice. *Nature,* **376**: 62-66.

Shankar, V., Ciardiello, F., Kim, N., Derynck, R., Liscia, D. S., Merlo, G., Langton, B. C., Sheer, D., Callahan, R., Bassin, R. H. and et al. (1989). Transformation of an established mouse mammary epithelial cell line following transfection with a human transforming growth factor alpha cDNA. *Mol Carcinog,* **2**: 1-11.

Sharma, G. and Goalstone, M. L. (2005). Dominant negative FTase (DNFTα) inhibits ERK5, MEF2C and CREB activation in adipogenesis. *Mol Cell Endocrinol,* **245**: 93-104.

Sharp, P. A. (2001). RNA interference--2001. *Genes Dev,* **15**: 485-490.

Shibuya, M., Yamaguchi, S., Yamane, A., Ikeda, T., Tojo, A., Matsushime, H. and Sato, M. (1990). Nucleotide sequence and expression of a novel human receptor-type tyrosine kinase gene (flt) closely related to the fms family. *Oncogene,* **5**: 519-524.

Shinkai, A., Ito, M., Anazawa, H., Yamaguchi, S., Shitara, K. and Shibuya, M. (1998). Mapping of the sites involved in ligand association and dissociation at the extracellular domain of the kinase insert domain-containing receptor for vascular endothelial growth factor. *J Biol Chem,* **273**: 31283-31288.

Shoyab, M., McDonald, V. L., Bradley, J. G. and Todaro, G. J. (1988). Amphiregulin: a bifunctional growth-modulating glycoprotein produced by the phorbol 12-myristate 13-acetate-treated human breast adenocarcinoma cell line MCF-7. *Proc Natl Acad Sci U S A,* **85**: 6528-6532.

Shu, X., Wu, W., Mosteller, R. D. and Broek, D. (2002). Sphingosine kinase mediates vascular endothelial growth factor-induced activation of ras and mitogen-activated protein kinases. *Mol Cell Biol,* **22**: 7758-7768.

Shweiki, D., Itin, A., Soffer, D. and Keshet, E. (1992). Vascular endothelial growth factor induced by hypoxia may mediate hypoxia-initiated angiogenesis. *Nature,* **359**: 843-845.

Slater, S. C., Ramnath, R. D., Uttridge, K., Saleem, M. A., Cahill, P. A., Mathieson, P. W., Welsh, G. I. and Satchell, S. C. (2012). Chronic exposure to laminar shear stress induces Kruppel-like factor 2 in glomerular endothelial cells and modulates interactions with co-cultured podocytes. *Int J Biochem Cell Biol,* **44**: 1482-1490.

Sohn, S. J., Sarvis, B. K., Cado, D. and Winoto, A. (2002). ERK5 MAPK regulates embryonic angiogenesis and acts as a hypoxia-sensitive repressor of vascular endothelial growth factor expression. *J Biol Chem,* **277**(45): 43344-43351.

Soker, S., Miao, H. Q., Nomi, M., Takashima, S. and Klagsbrun, M. (2002). VEGF165 mediates formation of complexes containing VEGFR-2 and neuropilin-1 that enhance VEGF165-receptor binding. *2002,* **J Cell Biochem**(85).

Soker, S., Takashima, S., Miao, H. Q., Neufeld, G. and Klagsbrun, M. (1998). Neuropilin-1 is expressed by endothelial and tumour cells as an isoform-specific receptor for vascular endothelial growth factor. *Cell,* **92**(735-745).

Soltau, J. and Drevs, J. (2009). Mode of action and clinical impact of VEGF signaling inhibitors. *Expert Rev Anticancer Ther,* **9**: 649-662.

Sonpavde, G. and Hutson, T. E. (2007). Pazopanib: a novel multitargeted tyrosine kinase inhibitor. *Curr Oncol Rep,* **9**: 115-119.

Spiering, D., Schmolke, M., Ohnesorge, N., Schmidt, M., Goebeler, M., Wegener, J., Wixler, V. and Ludwig, S. (2009). MEK5/ERK5 signaling modulates endothelial cell migration and focal contact turnover. *J Biol Chem,* **284**: 24972-24980.

Srivastava, D. and Olson, E. N. (2000). A genetic blueprint for cardiac development. *Nature,* **407**: 221-226.

Starkey, R. H., Cohen, S. and Orth, D. N. (1975). Epidermal growth factor: identification of a new hormone in human urine. *Science,* **189**: 800-802.

Stavri, G. T., Zachary, I. C., Baskerville, P. A., Martin, J. F. and Erusalimsky, J. D. (1995). Basic fibroblast growth factor upregulates the expression of vascular endothelial growth factor in vascular smooth muscle cells. Synergistic interaction with hypoxia. *Circulation,* **92**: 11-14.

Sternberg, C. N., Davis, I. D., Mardiak, J., Szczylik, C., Lee, E., Wagstaff, J., Barrios, C. H., Salman, P., Gladkov, O. A., Kavina, A., Zarbá, J. J., Chen, M., McCann, L., Pandite, L., Roychowdhury, D. F. and Hawkins, R. E. (2010). Pazopanib in locally advanced or metastatic renal cell carcinoma: results of a randomized phase III trial. *J Clin Oncol,* **28**: 1061-1068.

Stokoe, D., Stephens, L. R., Copeland, T., Gaffney, P. R., Reese, C. B., Painter, G. F., Holmes, A. B., McCormick, F. and Hawkins, P. T. (1997). Dual role of phosphatidylinositol-3,4,5-trisphosphate in the activation of protein kinase B. *Science,* **277**: 567-570.

Stover, D. R., Becker, M., Liebetanz, J. and Lydon, N. B. (1995). Src phosphorylation of the epidermal growth factor receptor at novel sites mediates receptor interaction with Src and P85 alpha. *J Biol Chem,* **270**: 15591-15597.

Strachan, L., Murison, J. G., Prestidge, R. L., Sleeman, M. A., Watson, J. D. and Kumble, K. D. (2001). Cloning and biological activity of epigen, a novel member of the epidermal growth factor superfamily. *J Biol Chem,* **276**: 18265-18271.

Sun, W., Kesavan, K., Schaefer, B. C., Garrington, T. P., Ware, M., Johnson, N. L., Gelfand, E. W. and Johnson, G. L. (2001). MEKK2 associates with the adapter protein Lad/RIBP and regulates the MEK5-BMK1/ERK5 pathway. *J Biol Chem,* **276**(7): 5093-5100.

Sun, W., Wei, X., Kesavan, K., Garrington, T. P., Fan, R., Mei, J., Anderson, S. M., Gelfand, E. W. and Johnson, G. L. (2003). MEK kinase 2 and the adaptor protein Lad regulate extracellular signal-regulated kinase 5 activation by epidermal growth factor via Src. *Mol Cell Biol,* **23**(7): 2298-2308.

Suzuki, A., Hamada, K., Sasaki, T., Mak, T. W. and Nakano, T. (2007). Role of PTEN/PI3K pathway in endothelial cells. *Biochem Soc Trans,* **35**: 172-176.

Takahashi, H., Ueno, H. and Shibuya, M. (1999). VEGF activates protein kinase C-dependent, but Ras-independent Raf-MEK-MAP kinase pathway for DNA synthesis in primary endothelial cells. *Oncogene,* **18**: 2221-2230.

Takahashi, T. and Shibuya, M. (1997). The 230 kDa mature form of KDR/Flk-1 (VEGF receptor-2) activates the PLC-gamma pathway and partially induces mitotic signals in NIH3T3 fibroblasts. *Oncogene,* **14**: 2079-2089.

Takahashi, T., Yamaguchi, S., Chida, K. and Shibuya, M. (2001). A single autophosphorylation site on KDR/Flk-1 is essential for VEGF-A-dependent activation of PLC-gamma and DNA synthesis in vascular endothelial cells. *Embo J,* **20**: 2768-2778.

Takeishi, Y., Abe, J., Lee, J. D., Kawakatsu, H., Walsh, R. A. and Berk, B. C. (1999). Differential regulation of p90 ribosomal S6 kinase and big mitogen-activated protein kinase 1 by ischemia/reperfusion and oxidative stress in perfused guinea pig hearts. *Circulation research,* **85**(12): 1164-1172.

Tam, J. P., Marquardt, H., Rosberger, D. F., Wong, T. W. and Todaro, G. J. (1984). Synthesis of biologically active rat transforming growth factor I. *Nature,* **309**: 376-378.

Tan, W. H., Popel, A. S. and Mac Gabhann, F. (2013). Computational model of Gab1/2-dependent VEGFR2 pathway to Akt activation. *PLoS ONE,* **8**: e67438.

Tanoue, T. and Nishida, E. (2002). Docking interactions in the mitogen-activated protein kinase cascades. *Pharmacology & therapeutics,* **93**(2-3): 193-202.

Tanoue, T. and Nishida, E. (2003). Molecular recognitions in the MAP kinase cascades. *Cellular signalling,* **15**(5): 455-462.

Tatake, R. J., O'Neill, M. M., Kennedy, C. A., Wayne, A. L., Jakes, S., Wu, D., Kugler Jr, S. Z., Kashem, M. A., Kaplita, P. and Snow, R. J. (2008). Identification of pharmacological inhibitors of the MEK5/ERK5 pathway. *Biochem Biophys Res Commun,* **377**: 120-125.

Terasawa, K., Okazaki, K. and Nishida, E. (2003). Regulation of c-Fos and Fra-1 by the MEK5-ERK5 pathway. *Genes to cells : devoted to molecular & cellular mechanisms,* **8**(3): 263-273.

Terman, B. I., Carrion, M. E., Kovacs, E., Rasmussen, B. A., Eddy, R. L. and Shows, T. B. (1991). Identification of a new endothelial cell growth factor receptor tyrosine kinase. *Oncogene,* **6**: 1677-1683.

Tischer, E., Mitchell, R., Hartman, T., Silva, M., Gospodarowicz, D., Fiddes, J. C. and Abraham, J. A. (1991). The human gene for vascular endothelial growth factor.

Multiple protein forms are encoded through alternative exon splicing. *J Biol Chem,* **266**: 11947-11954.

Toyoda, H., Komurasaki, T., Uchida, D., Takayama, Y., Isobe, T., Okuyama, T. and Hanada, K. (1995). Epiregulin. A novel epidermal growth factor with mitogenic activity for rat primary hepatocytes. *J Biol Chem,* **270**: 7495-7500.

Traub, O. and Berk, B. C. (1998). Laminar shear stress: mechanisms by which endothelial cells transduce an atheroprotective force. *Arterioscler Thromb Vasc Biol,* **18**: 677-685.

Ushio-Fukai, M. and Nakamura, Y. (2008). Reactive oxygen species and angiogenesis: NADPH oxidase as target for cancer therapy. *Cancer Lett,* **266**: 37-52.

Vailhe, B., Vittet, D. and Feige, J.-J. (2001). In vitro models of vasculogenesis and angiogenesis. *Lab Invest,* **81**: 439-452.

van Belle, E., Witzenbichler, B., Chen, D., Silver, M., Chang, L., Schwall, R. and Isner, J. M. (1998). Potentiated angiogeneic effect of scatter factor/hepatocyte growth factor via induction of vascular endothelial growth factor. *Circulation,* **97**: 381-390.

van Drogen, F. and Peter, M. (2002). MAP kinase cascades: scaffolding signal specificity. *Curr Biol,* **12**(2): R53-55.

van Hinsbergh, V. W. M., Engelse, M. A. and Quax, P. H. (2006). Pericellular proteases in angiogenesis and vasculogenesis. *Arterioscler Thromb Vasc Biol,* **26**(716-728).

Wang, X., McCullough, K. D., Franke, T. F. and Holbrook, N. J. (2000). Epidermal growth factor receptor-dependent Akt activation by oxidative stress enhances cell survival. *J Biol Chem,* **275**: 14626-14631.

Wang, X., Merritt, A. J., Seyfried, J., Guo, C., Papadakis, E. S., Finegan, K. G., Kayahara, M., Dixon, J., Boot-Handford, R. P., Cartwright, E. J., Mayer, U. and Tournier, C. (2005). Targeted deletion of Mek5 causes early embryonic death and defects in the extracellular signal-regulated kinase 5/myocyte enhancer factor 2 cell survival pathway. *Mol Cell Biol,* **25**(1): 336-345.

Wang, X. and Tournier, C. (2006). Regulation of cellular functions by the ERK5 signalling pathway. *Cellular signalling,* **18**(6): 753-760.

Warner, A. J., Lopez-Dee, J., Knight, E. L., Feramisco, J. R. and Prigent, S. A. (2000). The Shc-related adaptor protein, Sck, forms a complex with the vascular-endothelial-growth-factor receptor KDR in transfected cells. *Biochemical Journal,* **347**: 501-509.

Watanabe, S., Lazar, E. and Sporn, M. B. (1987). Transformation of normal rat kidney (NRK) cells by an infectious retrovirus carrying a synthetic rat type alpha transforming growth factor gene. *Proc Natl Acad Sci U S A,* **84**: 1258-1262.

Watson, F. L., Heerssen, H. M., Bhattacharyya, A., Klesse, L., Lin, M. Z. and Segal, R. A. (2001). Neurotrophins use the Erk5 pathway to mediate a retrograde survival response. *Nature neuroscience,* **4**(10): 981-988.

Weis, S. M. and Cheresh, D. A. (2011). Tumor angiogenesis: molecular pathways and therapeutic targets. *Nat Med,* **17**: 1359-1370.

Wellner, M., Maasch, C., Kupprion, C., Lindschau, C., Luft, F. C. and Haller, H. (1999). The proliferative effect of vascular endothelial growth factor requires protein kinase C-alpha and protein kinase C-zeta. *Arterioscler Thromb Vasc Biol,* **19**: 178-185.

Whitaker, G. B., Limberg, B. J. and Rosenbaum, J. S. (2001). Vascular endothelial growth factor receptor-2 and neuropilin-1 form a receptor complex that is responsible for the differential signaling potency of VEGF(165) and VEGF(121). *J Biol Chem,* **276**: 25520-25531.

Whitmarsh, A. J. and Davis, R. J. (1998). Structural organization of MAP-kinase signaling modules by scaffold proteins in yeast and mammals. *Trends Biochem Sci,* **23**(12): 481-485.

Widmann, C., Gibson, S., Jarpe, M. B. and Johnson, G. L. (1999). Mitogen-activated protein kinase: conservation of a three-kinase module from yeast to human. *Physiol Rev,* **79**(1): 143-180.

Wilhelm, S. M., Adnane, L., Newell, P., Villanueva, A., Llovet, J. M. and Lynch, M. (2008). Preclinical overview of sorafenib, a multikinase inhibitor that target both Raf and VEGF and PDGF receptor tyrosine kinase signaling. *Mol Cancer Ther,* **7**: 3129-3140.

Woo, C. H., Shishido, T., McClain, C., Lim, J. H., Li, J. D., Yang, J., Yan, C. and Abe, J. (2008). Extracellular signal-regulated kinase 5 SUMOylation antagonizes shear stress-induced antiinflammatory response and endothelial nitric oxide synthase expression in endothelial cells. *Circulation research,* **102**(5): 538-545.

Wu, L. W., Mayo, L. D., Dunbar, J. D., Kessler, K. M., Baerwald, M. R., Jaffe, E. A., Wang, D., Warren, R. S. and Donner, D. B. (2000a). Utilization of distinct signaling pathways by receptors for vascular endothelial cell growth factor and other mitogens in the induction of endothelial cell proliferation. *J Biol Chem,* **275**: 5096-5103.

Wu, L. W., Mayo, L. D., Dunbar, J. D., Kessler, K. M., Ozes, O. N., Warren, R. S. and Donner, D. B. (2000b). VRAP is an adaptor protein that binds KDR, a receptor for vascular endothelial cell growth factor. *J Biol Chem,* **275**: 6059-6062.

Xia, P., Aiello, L. P., Ishii, H., Jiang, Z. Y., Park, D. J., Robinson, G. S., Takagi, H., Newsome, W. P., Jirousek, M. R. and King, G. L. (1996). Characterization of vascular endothelial growth factor's effect on the activation of protein kinase C, its isoforms, and endothelial cell growth. *J Clin Invest,* **98**: 2018-2026.

Xin, X., Yang, S. H., Ingle, G., Ziot, C., Rangell, L., Kowalski, J., Schwall, R., Ferrara, N. and Gerritsen, M. E. (2001). Hepatocyte growth factor enhances vascular

endothelial growth factor-induced angiogenesis in vitro and in vivo. *Am J Pathol,* **158**: 1111-1120.

Yamazaki, Y., Takani, K., Atoda, H. and Morita, T. (2003). Snake venom vascular endothelial growth factors (VEGFs) exhibit potent activity through their specific recognition of KDR (VEGF receptor 2). *J Biol Chem,* **278**: 51985-51988.

Yan, C., Luo, H., Lee, J. D., Abe, J. and Berk, B. C. (2001). Molecular cloning of mouse ERK5/BMK1 splice variants and characterization of ERK5 functional domains. *J Biol Chem,* **276**(14): 10870-10878.

Yan, C., Takahashi, M., Okuda, M., Lee, J. D. and Berk, B. C. (1999). Fluid shear stress stimulates big mitogen-activated protein kinase 1 (BMK1) activity in endothelial cells. Dependence on tyrosine kinases and intracellular calcium. *J Biol Chem,* **274**(1): 143-150.

Yan, L., Carr, J., Ashby, P. R., Murry-Tait, V., Thompson, C. and Arthur, J. S. (2003). Knockout of ERK5 causes multiple defects in placental and embryonic development. *BMC developmental biology,* **3**: 11.

Yang, C. C., Ornatsky, O. I., McDermott, J. C., Cruz, T. F. and Prody, C. A. (1998). Interaction of myocyte enhancer factor 2 (MEF2) with a mitogen-activated protein kinase, ERK5/BMK1. *Nucleic Acids Res,* **26**(20): 4771-4777.

Yang, J., Boerm, M., McCarty, M., Bucana, C., Fidler, I. J., Zhuang, Y. and Su, B. (2000). Mekk3 is essential for early embryonic cardiovascular development. *Nature genetics,* **24**(3): 309-313.

Yang, Q., Deng, X., Lu, B., Cameron, M., Fearns, C., Patricelli, M. P., Yates III, J. R., Gray, N. S. and Lee, J. D. (2010a). Pharmacological inhibition of BMK1 suppresses tumor growth through PML. *Cancer Cell,* **18**: 258-267.

Yang, Q. and Lee, J. D. (2011). Targeting the BMK1 MAP Kinase pathway in cancer therapy. *Clin Cancer Res,* **17**: 3527-3532.

Yang, S. H., Sharrocks, A. D. and Whitmarsh, A. J. (2003a). Transcriptional regulation by the MAP kinase signaling cascades. *Gene,* **320**: 3-21.

Yang, Y., Xie, P., Opatowsky, Y. and Schlessinger, J. (2010b). Direct contacts between extracellular membrane-proximal domains are required for VEGF receptor activation and cell signaling. *Proc Natl Acad Sci U S A,* **107**: 1906-1911.

Yang, Z.-Z., Tschopp, O., Hemmings-Mieszczak, M., Feng, J., Brodbeck, D., Perentes, E. and Hemmings, B. A. (2003b). Protein kinase Ba/Akt1 regulates placental development and fetal growth. *J Biol Chem,* **278**: 32124-32131.

Yarden, Y. and Sliwkowski, M. X. (2001). Untangling the ErbB signalling network. *Nat Rev Mol Cell Biol,* **2**: 127-137.

Yoon, S. and Seger, R. (2006). The extracellular signal-regulated kinase: multiple substrates regulate diverse cellular functions. *Growth Factors,* **24**(1): 21-44.

Yuan, L., Moyon, D., Pardanaud, L., Breant, C., Karkkainen, M. J., Alitalo, K. and Eichmann, A. (2002). Abnormal lymphatic vessel development in neuropilin-2 mutant mice. *Development,* **129**: 4797-4806.

Zachary, I. (2003). VEGF signalling: integration and multi-tasking in endothelial cell biology. *Biochem Soc Trans,* **31**: 1171-1177.

Zang, G., Christoffersson, G., Tian, G., Harun-Or-Rashid, M., Vågesjö, E., Phillipson, M., Barg, S., Tengholm, A. and Welsh, M. (2013). Aberrant association between vascular endothelial growth factor receptor-2 and VE-cadherin in response to vascular endothelial growth factor-a in Shb-deficient lung endothelial cells. *Cellular signalling,* **25**: 85-92.

Zhang, H., Kolb, F. A., Brondani, V., Billy, E. and Filipowicz, W. (2002). Human Dicer preferentially cleaves dsRNAs at their termini without a requirement for ATP. *Embo J,* **21**: 5875-5885.

Zhang, X., Gureasko, J., Shen, K., Cole, P. A. and Kuriyan, J. (2006). An allosteric mechanism for activation of the kinase domain of epidermal growth factor receptor. *Cell,* **125**: 1137-1149.

Zhang, Y. and Dong, C. (2007). Regulatory mechanisms of mitogen-activated kinase signaling. *Cellular and molecular life sciences : CMLS,* **64**(21): 2771-2789.

Zhao, Z., Wang, W., Geng, J., Wang, L., Su, G., Zhang, Y., Ge, Z. and Kang, W. (2010). Protein kinase C epsilon-dependent extracellular signal-regulated kinase 5 phosphorylation and nuclear translocation involved in cardiomyocyte hypertrophy with angiotensin II stimulation. *J Cell Biochem,* **109**: 653-662.

Zhou, G., Bao, Z. Q. and Dixon, J. E. (1995). Components of a new human protein kinase signal transduction pathway. *J Biol Chem,* **270**(21): 12665-12669.

Appendices

Appendix I – Complete adenoviral FLAG-ERK5 sequence

Final viral titer: 7.72 x 10^9 ifu/mL

Black: pAd/CMV/V5 DEST

Pink: pENTR1a region transferred following recombination

Blue: FLAG tag (Start codon in **BOLD**)

Green: ERK5 sequence (T^{218}/Y^{220} in **BOLD**)

Red: Stop codon in **BOLD**

CATCATCAATAATATACCTTATTTTGGATTGAAGCCAATATGATAATGAGGGGGTGGAGTTTGTGAC
GTGGCGCGGGGCGTGGGAACGGGGCGGGTGACGTAGTAGTGTGGCGGAAGTGTGATGTTGCAAG
TGTGGCGGAACACATGTAAGCGACGGATGTGGCAAAAGTGACGTTTTTGGTGTGCGCCGGTGTACA
CAGGAAGTGACAATTTTCGCGCGGTTTTAGGCGGATGTTGTAGTAAATTTGGGCGTAACCGAGTAA
GATTTGGCCATTTTCGCGGGAAAACTGAATAAGAGGAAGTGAAATCTGAATAATTTTGTGTTACTCA
TAGCGCGTAATATTTGTCTAGGGCCGCGGGGACTTTGACCGTTTACGTGGAGACTCGCCCAGGTGT
TTTTCTCAGGTGTTTTCCGCGTTCCGGGTCAAAGTTGGCGTTTTATTATTATAGTCAGTCGAAGCTT
GGATCCGGTACCTCTAGAATTCTCGAGCGGCCGCTAGCGACATCGGATCTCCCGATCCCCTATGGTC
GACTCTCAGTACAATCTGCTCTGATGCCGCATAGTTAAGCCAGTATCTGCTCCCTGCTTGTGTGTTG
GAGGTCGCTGAGTAGTGCGCGAGCAAAATTTAAGCTACAACAAGGCAAGGCTTGACCGACAATTGC
ATGAAGAATCTGCTTAGGGTTAGGCGTTTTGCGCTGCTTCGCGATGTACGGGCCAGATATACGCGT
TGACATTGATTATTGACTAGTTATTAATAGTAATCAATTACGGGGTCATTAGTTCATAGCCCATATAT
GGAGTTCCGCGTTACATAACTTACGGTAAATGGCCCGCCTGGCTGACCGCCCAACGACCCCCGCCCA
TTGACGTCAATAATGACGTATGTTCCCATAGTAACGCCAATAGGGACTTTCCATTGACGTCAATGGG
TGGACTATTTACGGTAAACTGCCCACTTGGCAGTACATCAAGTGTATCATATGCCAAGTACGCCCCC
TATTGACGTCAATGACGGTAAATGGCCCGCCTGGCATTATGCCCAGTACATGACCTTATGGGACTTT
CCTACTTGGCAGTACATCTACGTATTAGTCATCGCTATTACCATGGTGATGCGGTTTTGGCAGTACA
TCAATGGGCGTGGATAGCGGTTTGACTCACGGGGATTTCCAAGTCTCCACCCCATTGACGTCAATG
GGAGTTTGTTTTGGCACCAAAATCAACGGGACTTTCCAAAATGTCGTAACAACTCCGCCCCATTGAC
GCAAATGGGCGGTAGGCGTGTACGGTGGGAGGTCTATATAAGCAGAGCTCTCTGGCTAACTAGAGA
ACCCACTGCTTACTGGCTTATCGAAATTAATACGACTCACTATAGGGAGACCCAAGCTGGCTAGTTA
AGCTATCAACAAGTTTTGTACAAAAAAGCAGGCTTTTCGAG**ATG**GACTACAAGGACGACGATGACAA
GGCCGAGCCTCTGAAGGAGGAAGACGGCGAGGACGGCTCTGCGGAGCCCCCCGGGCCCGTGAAGG
CCGAACCCGCCCACACCGCTGCCTCTGTAGCGGCCAAGAACCTGGCCCTGCTTAAAGCCCGCTCCTT
CGATGTGACCTTTGACGTGGGCGACGAGTACGAGATCATCGAGACCATAGGCAACGGGGCCTATGG
AGTGGTGTCCTCCGCCCGCCGCCGCCTCACCGGCCAGCAGGTGGCCATCAAGAAGATCCCTAATGC
TTTCGATGTGGTGACCAATGCCAAGCGGACCCTCAGGGAGCTGAAGATCCTCAAGCACTTTAAACAC
GACAACATCATCGCCATCAAGGACATCCTGAGGCCCACCGTGCCCTATGGCGAATTCAAATCTGTCT
ACGTGGTCCTGGACCTGATGGAAAGCGACCTGCACCAGATCATCCACTCCTCACAGCCCCTCACACT

GGAACACGTGCGCTACTTCCTGTACCAACTGCTGCGGGGCCTGAAGTACATGCACTCGGCTCAGGT
CATCCACCGTGACCTGAAGCCCTCCAACCTATTGGTGAATGAGAACTGTGAGCTCAAGATTGGTGAC
TTTGGTATGGCTCGTGGCCTGTGCACCTCGCCCGCTGAACATCAGTACTTCATG**ACT**GAG**TAT**GTG
GCCACGCGCTGGTACCGTGCGCCCGAGCTCATGCTCTCTTTGCATGAGTATACACAGGCTATTGACC
TCTGGTCTGTGGGCTGCATCTTTGGTGAGATGCTGGCCCGGCGCCAGCTCTTCCCAGGCAAAAACT
ATGTACACCAGCTACAGCTCATCATGATGGTGCTGGGTACCCCATCACCAGCCGTGATTCAGGCTGT
GGGGGCTGAGAGGGTGCGGGCCTATATCCAGAGCTTGCCACCACGCCAGCCTGTGCCCTGGGAGA
CAGTGTACCCAGGTGCCGACCGCCAGGCCCTATCACTGCTGGGTCGCATGCTGCGTTTTGAGCCCA
GCGCTCGCATCTCAGCAGCTGCTGCCCTTCGCCACCCTTTCCTGGCCAAGTACCATGATCCTGATGA
TGAGCCTGACTGTGCCCCGCCCTTTGACTTTGCCTTTGACCGCGAAGCCCTCACTCGGGAGCGCATT
AAGGAGGCCATTGTGGCTGAAATTGAGGACTTCCATGCAAGGCGTGAGGGCATCCGCCAACAGATC
CGCTTCCAGCCTTCTCTACAGCCTGTGGCTAGTGAGCCTGGCTGTCCAGATGTTGAAATGCCCAGTC
CCTGGGCTCCCAGTGGGGACTGTGCCATGGAGTCTCCACCACCAGCCCCGCCACCATGCCCCGGCC
CTGCACCTGACACCATTGATCTGACCCTGCAGCCACCTCCACCAGTCAGTGAGCCTGCCCCACCAAA
GAAAGATGGTGCCATCTCAGACAATACTAAGGCTGCCCTTAAAGCTGCCCTGCTCAAGTCTTTGAGG
AGCCGGCTCAGAGATGGCCCCAGCGCACCCCTGGAGGCTCCTGAGCCTCGGAAGCCGGTGACAGCC
CAGGAGCGCCAGCGGGAGCGGGAGGAGAAGCGGCGGAGGCGGCAAGAACGAGCCAAGGAGCGGG
AGAAACGGCGGCAGGAGCGGGAGCGAAAGGAACGGGGGGCTGGGGCCTCTGGGGGCCCCTCCACT
GACCCCTTGGCTGGACTAGTGCTCAGTGACAATGACAGAAGCCTGTTGGAACGCTGGACTCGAATG
GCCCGGCCCGCAGCCCCAGCCCTCACCTCTGTGCCGGCCCCTGCCCCAGCGCCAACGCCAACCCCAA
CCCCAGTCCAACCTACCAGTCCTCCTCCTGGCCCTGTAGCCCAGCCCACTGGCCCGCAACCACAATC
TGCGGGCTCTACCTCTGGCCCTGTACCCCAGCCTGCCTGCCCACCCCCTGGCCCTGCACCCCACCCC
ACTGGCCCTCCTGGGCCCATCCCTGTCCCCGCGCCACCCCAGATTGCCACCTCCACCAGCCTCCTGG
CTGCCCAGTCACTTGTGCCACCCCCTGGGCTGCCTGGCTCCAGCACCCCAGGAGTTTTGCCTTACTT
CCCACCTGGCCTGCCGCCCCCAGACGCCGGGGGAGCCCCTCAGTCTTCCATGTCAGAGTCACCTGA
TGTCAACCTTGTGACCCAGCAGCTATCTAAGTCACAGGTGGAGGACCCCCTGCCCCCTGTGTTCTCA
GGCACACCAAAGGGCAGTGGGGCTGGCTACGGTGTTGGCTTTGACCTGGAGGAATTCTTAAACCAG
TCTTTCGACATGGGCGTGGCTGATGGGCCACAGGATGGCCAGGCAGATTCAGCCTCTCTCTCAGCC
TCCCTGCTTGCTGACTGGCTCGAAGGCCATGGCATGAACCCTGCCGATATTGAGTCCCTGCAGCGT
GAGATCCAGATGGACTCCCCAATGCTGCTGGCTGACCTGCCTGACCTCCAGGACCCC**TGA**ATCTAGA
CCCAGCTTTCTTGTACAAAGTGGTTGATCTAGAGGGCCCGCGGTTCGAAGGTAAGCCTATCCCTAAC
CCTCTCCTCGGTCTCGATTCTACGCGTACCGGTTAGTAATGAGTTTAAACGGGGGAGGCTAACTGAA
ACACGGAAGGAGACAATACCGGAAGGAACCCGCGCTATGACGGCAATAAAAAGACAGAATAAAACGC
ACGGGTGTTGGGTCGTTTGTTCATAAACGCGGGGTTCGGTCCCAGGGCTGGCACTCTGTCGATACC
CCACCGAGACCCCATTGGGGCCAATACGCCCGCGTTTCTTCCTTTTCCCCACCCCACCCCCCAAGTT
CGGGTGAAGGCCCAGGGCTCGCAGCCAACGTCGGGGCGGCAGGCCCTGCCATAGCAGATCCGATT
CGACAGATCACTGAAATGTGTGGGCGTGGCTTAAGGGTGGGAAAGAATATATAAGGTGGGGGTCTT
ATGTAGTTTTGTATCTGTTTTGCAGCAGCCGCCGCCGCCATGAGCACCAACTCGTTTGATGGAAGCA

TTGTGAGCTCATATTTGACAACGCGCATGCCCCCATGGGCCGGGGTGCGTCAGAATGTGATGGGCT
CCAGCATTGATGGTCGCCCCGTCCTGCCCGCAAACTCTACTACCTTGACCTACGAGACCGTGTCTGG
AACGCCGTTGGAGACTGCAGCCTCCGCCGCCGCTTCAGCCGCTGCAGCCACCGCCCGCGGGATTGT
GACTGACTTTGCTTTCCTGAGCCCGCTTGCAAGCAGTGCAGCTTCCCGTTCATCCGCCCGCGATGAC
AAGTTGACGGCTCTTTTGGCACAATTGGATTCTTTGACCCGGGAACTTAATGTCGTTTCTCAGCAGC
TGTTGGATCTGCGCCAGCAGGTTTCTGCCCTGAAGGCTTCCTCCCCTCCCAATGCGGTTTAAAACAT
AAATAAAAAACCAGACTCTGTTTGGATTTGGATCAAGCAAGTGTCTTGCTGTCTTTATTTAGGGGTT
TTGCGCGCGCGGTAGGCCCGGGACCAGCGGTCTCGGTCGTTGAGGGTCCTGTGTATTTTTTCCAGG
ACGTGGTAAAGGTGACTCTGGATGTTCAGATACATGGGCATAAGCCCGTCTCTGGGGTGGAGGTAG
CACCACTGCAGAGCTTCATGCTGCGGGGTGGTGTTGTAGATGATCCAGTCGTAGCAGGAGCGCTGG
GCGTGGTGCCTAAAAATGTCTTTCAGTAGCAAGCTGATTGCCAGGGGCAGGCCCTTGGTGTAAGTG
TTTACAAAGCGGTTAAGCTGGGATGGGTGCATACGTGGGGATATGAGATGCATCTTGGACTGTATT
TTTAGGTTGGCTATGTTCCCAGCCATATCCCTCCGGGGATTCATGTTGTGCAGAACCACCAGCACAG
TGTATCCGGTGCACTTGGGAAATTTGTCATGTAGCTTAGAAGGAAATGCGTGGAAGAACTTGGAGA
CGCCCTTGTGACCTCCAAGATTTTCCATGCATTCGTCCATAATGATGGCAATGGGCCCACGGGCGGC
GGCCTGGGCGAAGATATTTCTGGGATCACTAACGTCATAGTTGTGTTCCAGGATGAGATCGTCATA
GGCCATTTTTACAAAGCGCGGGCGGAGGGTGCCAGACTGCGGTATAATGGTTCCATCCGGCCCAGG
GGCGTAGTTACCCTCACAGATTTGCATTTCCCACGCTTTGAGTTCAGATGGGGGGATCATGTCTACC
TGCGGGGCGATGAAGAAAACGGTTTCCGGGGTAGGGGAGATCAGCTGGGAAGAAAGCAGGTTCCT
GAGCAGCTGCGACTTACCGCAGCCGGTGGGCCCGTAAATCACACCTATTACCGGGTGCAACTGGTA
GTTAAGAGAGCTGCAGCTGCCGTCATCCCTGAGCAGGGGGGCCACTTCGTTAAGCATGTCCCTGAC
TCGCATGTTTTCCCTGACCAAATCCGCCAGAAGGCGCTCGCCGCCCAGCGATAGCAGTTCTTGCAAG
GAAGCAAAGTTTTTCAACGGTTTGAGACCGTCCGCCGTAGGCATGCTTTTGAGCGTTTGACCAAGCA
GTTCCAGGCGGTCCCACAGCTCGGTCACCTGCTCTACGGCATCTCGATCCAGCATATCTCCTCGTTT
CGCGGGTTGGGGCGGCTTTCGCTGTACGGCAGTAGTCGGTGCTCGTCCAGACGGGCCAGGGTCAT
GTCTTTCCACGGGCGCAGGGTCCTCGTCAGCGTAGTCTGGGTCACGGTGAAGGGGTGCGCTCCGG
GCTGCGCGCTGGCCAGGGTGCGCTTGAGGCTGGTCCTGCTGGTGCTGAAGCGCTGCCGGTCTTCG
CCCTGCGCGTCGGCCAGGTAGCATTTGACCATGGTGTCATAGTCCAGCCCCTCCGCGGCGTGGCCC
TTGGCGCGCAGCTTGCCCTTGGAGGAGGCGCCGCACGAGGGGCAGTGCAGACTTTTGAGGGCGTA
GAGCTTGGGCGCGAGAAATACCGATTCCGGGGAGTAGGCATCCGCGCCGCAGGCCCCGCAGACGG
TCTCGCATTCCACGAGCCAGGTGAGCTCTGGCCGTTCGGGGTCAAAAACCAGGTTTCCCCCATGCTT
TTTGATGCGTTTCTTACCTCTGGTTTCCATGAGCCGGTGTCCACGCTCGGTGACGAAAAGGCTGTCC
GTGTCCCCGTATACAGACTTGAGAGGCCTGTCCTCGAGCGGTGTTCCGCGGTCCTCCTCGTATAGA
AACTCGGACCACTCTGAGACAAAGGCTCGCGTCCAGGCCAGCACGAAGGAGGCTAAGTGGGAGGG
GTAGCGGTCGTTGTCCACTAGGGGGTCCACTCGCTCCAGGGTGTGAAGACACATGTCGCCCTCTTC
GGCATCAAGGAAGGTGATTGGTTTGTAGGTGTAGGCCACGTGACCGGGTGTTCCTGAAGGGGGGC
TATAAAAGGGGGTGGGGGCGCGTTCGTCCTCACTCTCTTCCGCATCGCTGTCTGCGAGGGCCAGCT
GTTGGGGTGAGTACTCCCTCTGAAAAGCGGGCATGACTTCTGCGCTAAGATTGTCAGTTTCCAAAAA

CGAGGAGGATTTGATATTCACCTGGCCCGCGGTGATGCCTTTGAGGGTGGCCGCATCCATCTGGTC
AGAAAAGACAATCTTTTTGTTGTCAAGCTTGGTGGCAAACGACCCGTAGAGGGCGTTGGACAGCAA
CTTGGCGATGGAGCGCAGGGTTTGGTTTTTGTCGCGATCGGCGCGCTCCTTGGCCGCGATGTTTAG
CTGCACGTATTCGCGCGCAACGCACCGCCATTCGGGAAAGACGGTGGTGCGCTCGTCGGGCACCAG
GTGCACGCGCCAACCGCGGTTGTGCAGGGTGACAAGGTCAACGCTGGTGGCTACCTCTCCGCGTAG
GCGCTCGTTGGTCCAGCAGAGGCGGCCGCCCTTGCGCGAGCAGAATGGCGGTAGGGGGTCTAGCT
GCGTCTCGTCCGGGGGGTCTGCGTCCACGGTAAAGACCCCGGGCAGCAGGCGCGCGTCGAAGTAG
TCTATCTTGCATCCTTGCAAGTCTAGCGCCTGCTGCCATGCGCGGGCGGCAAGCGCGCGCTCGTAT
GGGTTGAGTGGGGGACCCCATGGCATGGGGTGGGTGAGCGCGGAGGCGTACATGCCGCAAATGTC
GTAAACGTAGAGGGGCTCTCTGAGTATTCCAAGATATGTAGGGTAGCATCTTCCACCGCGGATGCT
GGCGCGCACGTAATCGTATAGTTCGTGCGAGGGAGCGAGGAGGTCGGGACCGAGGTTGCTACGGG
CGGGCTGCTCTGCTCGGAAGACTATCTGCCTGAAGATGGCATGTGAGTTGGATGATATGGTTGGAC
GCTGGAAGACGTTGAAGCTGGCGTCTGTGAGACCTACCGCGTCACGCACGAAGGAGGCGTAGGAG
TCGCGCAGCTTGTTGACCAGCTCGGCGGTGACCTGCACGTCTAGGGCGCAGTAGTCCAGGGTTTCC
TTGATGATGTCATACTTATCCTGTCCCTTTTTTTTCCACAGCTCGCGGTTGAGGACAAACTCTTCGC
GGTCTTTCCAGTACTCTTGGATCGGAAACCCGTCGGCCTCCGAACGGTAAGAGCCTAGCATGTAGA
ACTGGTTGACGGCCTGGTAGGCGCAGCATCCCTTTTCTACGGGTAGCGCGTATGCCTGCGCGGCCT
TCCGGAGCGAGGTGTGGGTGAGCGCAAAGGTGTCCCTGACCATGACTTTGAGGTACTGGTATTTGA
AGTCAGTGTCGTCGCATCCGCCCTGCTCCCAGAGCAAAAAGTCCGTGCGCTTTTTGGAACGCGGAT
TTGGCAGGGCGAAGGTGACATCGTTGAAGAGTATCTTTCCCGCGCGAGGCATAAAGTTGCGTGTGA
TGCGGAAGGGTCCCGGCACCTCGGAACGGTTGTTAATTACCTGGGCGGCGAGCACGATCTCGTCAA
AGCCGTTGATGTTGTGGCCCACAATGTAAAGTTCCAAGAAGCGCGGGATGCCCTTGATGGAAGGCA
ATTTTTTAAGTTCCTCGTAGGTGAGCTCTTCAGGGGAGCTGAGCCCGTGCTCTGAAAGGGCCCAGT
CTGCAAGATGAGGGTTGGAAGCGACGAATGAGCTCCACAGGTCACGGGCCATTAGCATTTGCAGGT
GGTCGCGAAAGGTCCTAAACTGGCGACCTATGGCCATTTTTTCTGGGGTGATGCAGTAGAAGGTAA
GCGGGTCTTGTTCCCAGCGGTCCCATCCAAGGTTCGCGGCTAGGTCTCGCGCGGCAGTCACTAGAG
GCTCATCTCCGCCGAACTTCATGACCAGCATGAAGGGCACGAGCTGCTTCCCAAAGGCCCCCATCCA
AGTATAGGTCTCTACATCGTAGGTGACAAAGAGACGCTCGGTGCGAGGATGCGAGCCGATCGGGAA
GAACTGGATCTCCCGCCACCAATTGGAGGAGTGGCTATTGATGTGGTGAAAGTAGAAGTCCCTGCG
ACGGGCCGAACACTCGTGCTGGCTTTTGTAAAAACGTGCGCAGTACTGGCAGCGGTGCACGGGCTG
TACATCCTGCACGAGGTTGACCTGACGACCGCGCACAAGGAAGCAGAGTGGGAATTTGAGCCCCTC
GCCTGGCGGGTTTGGCTGGTGGTCTTCTACTTCGGCTGCTTGTCCTTGACCGTCTGGCTGCTCGAG
GGGAGTTACGGTGGATCGGACCACCACGCCGCGCGAGCCCAAAGTCCAGATGTCCGCGCGCGGCG
GTCGGAGCTTGATGACAACATCGCGCAGATGGGAGCTGTCCATGGTCTGGAGCTCCCGCGGCGTCA
GGTCAGGCGGGAGCTCCTGCAGGTTTACCTCGCATAGACGGGTCAGGGCGCGGGCTAGATCCAGG
TGATACCTAATTTCCAGGGGCTGGTTGGTGGCGGCGTCGATGGCTTGCAAGAGGCCGCATCCCCGC
GGCGCGACTACGGTACCGCGCGGCGGGCGGTGGGCCGCGGGGGTGTCCTTGGATGATGCATCTAA
AAGCGGTGACGCGGGCGAGCCCCCGGAGGTAGGGGGGGCTCCGGACCCGCCGGGAGAGGGGGCA

GGGGCACGTCGGCGCCGCGCGCGGGCAGGAGCTGGTGCTGCGCGCGTAGGTTGCTGGCGAACGC
GACGACGCGGCGGTTGATCTCCTGAATCTGGCGCCTCTGCGTGAAGACGACGGGCCCGGTGAGCTT
GAGCCTGAAAGAGAGTTCGACAGAATCAATTTCGGTGTCGTTGACGGCGGCCTGGCGCAAAATCTC
CTGCACGTCTCCTGAGTTGTCTTGATAGGCGATCTCGGCCATGAACTGCTCGATCTCTTCCTCCTGG
AGATCTCCGCGTCCGGCTCGCTCCACGGTGGCGGCGAGGTCGTTGGAAATGCGGGCCATGAGCTG
CGAGAAGGCGTTGAGGCCTCCCTCGTTCCAGACGCGGCTGTAGACCACGCCCCCTTCGGCATCGCG
GGCGCGCATGACCACCTGCGCGAGATTGAGCTCCACGTGCCGGGCGAAGACGGCGTAGTTTCGCA
GGCGCTGAAAGAGGTAGTTGAGGGTGGTGGCGGTGTGTTCTGCCACGAAGAAGTACATAACCCAGC
GTCGCAACGTGGATTCGTTGATATCCCCCAAGGCCTCAAGGCGCTCCATGGCCTCGTAGAAGTCCAC
GGCGAAGTTGAAAAACTGGGAGTTGCGCGCCGACACGGTTAACTCCTCCTCCAGAAGACGGATGAG
CTCGGCGACAGTGTCGCGCACCTCGCGCTCAAAGGCTACAGGGGCCTCTTCTTCTTCTTCAATCTCC
TCTTCCATAAGGGCCTCCCCTTCTTCTTCTTCTGGCGGCGGTGGGGGAGGGGGGACACGGCGGCG
ACGACGGCGCACCGGGAGGCGGTCGACAAAGCGCTCGATCATCTCCCCGCGGCGACGGCGCATGG
TCTCGGTGACGGCGCGGCCGTTCTCGCGGGGGCGCAGTTGGAAGACGCCGCCCGTCATGTCCCGG
TTATGGGTTGGCGGGGGGCTGCCATGCGGCAGGGATACGGCGCTAACGATGCATCTCAACAATTGT
TGTGTAGGTACTCCGCCGCCGAGGGACCTGAGCGAGTCCGCATCGACCGGATCGGAAAACCTCTCG
AGAAAGGCGTCTAACCAGTCACAGTCGCAAGGTAGGCTGAGCACCGTGGCGGGCGGCAGCGGGCG
GCGGTCGGGGTTGTTTCTGGCGGAGGTGCTGCTGATGATGTAATTAAAGTAGGCGGTCTTGAGAC
GGCGGATGGTCGACAGAAGCACCATGTCCTTGGGTCCGGCCTGCTGAATGCGCAGGCGGTCGGCC
ATGCCCCAGGCTTCGTTTTGACATCGGCGCAGGTCTTTGTAGTAGTCTTGCATGAGCCTTTCTACCG
GCACTTCTTCTTCTCCTTCCTCTTGTCCTGCATCTCTTGCATCTATCGCTGCGGCGGCGGCGGAGTT
TGGCCGTAGGTGGCGCCCTCTTCCTCCCATGCGTGTGACCCCGAAGCCCCTCATCGGCTGAAGCAG
GGCTAGGTCGGCGACAACGCGCTCGGCTAATATGGCCTGCTGCACCTGCGTGAGGGTAGACTGGAA
GTCATCCATGTCCACAAAGCGGTGGTATGCGCCCGTGTTGATGGTGTAAGTGCAGTTGGCCATAAC
GGACCAGTTAACGGTCTGGTGACCCGGCTGCGAGAGCTCGGTGTACCTGAGACGCGAGTAAGCCCT
CGAGTCAAATACGTAGTCGTTGCAAGTCCGCACCAGGTACTGGTATCCCACCAAAAAGTGCGGCGG
CGGCTGGCGGTAGAGGGGCCAGCGTAGGGTGGCCGGGGCTCCGGGGGCGAGATCTTCCAACATAA
GGCGATGATATCCGTAGATGTACCTGGACATCCAGGTGATGCCGGCGGCGGTGGTGGAGGCGCGC
GGAAAGTCGCGGACGCGGTTCCAGATGTTGCGCAGCGGCAAAAAGTGCTCCATGGTCGGGACGCTC
TGGCCGGTCAGGCGCGCGCAATCGTTGACGCTCTAGACCGTGCAAAAGGAGAGCCTGTAAGCGGGC
ACTCTTCCGTGGTCTGGTGGATAAATTCGCAAGGGTATCATGGCGGACGACCGGGGTTCGAGCCCC
GTATCCGGCCGTCCGCCGTGATCCATGCGGTTACCGCCCGCGTGTCGAACCCAGGTGTGCGACGTC
AGACAACGGGGGAGTGCTCCTTTTGGCTTCCTTCCAGGCGCGGCGGCTGCTGCGCTAGCTTTTTTG
GCCACTGGCCGCGCGCAGCGTAAGCGGTTAGGCTGGAAAGCGAAAGCATTAAGTGGCTCGCTCCCT
GTAGCCGGAGGGTTATTTTCCAAGGGTTGAGTCGCGGGACCCCCGGTTCGAGTCTCGGACCGGCC
GGACTGCGGCGAACGGGGGTTTGCCTCCCCGTCATGCAAGACCCCGCTTGCAAATTCCTCCGGAAA
CAGGGACGAGCCCCTTTTTTGCTTTTCCCAGATGCATCCGGTGCTGCGGCAGATGCGCCCCCCTCCT
CAGCAGCGGCAAGAGCAAGAGCAGCGGCAGACATGCAGGGCACCCTCCCCTCCTCCTACCGCGTCA

GGAGGGGCGACATCCGCGGTTGACGCGGCAGCAGATGGTGATTACGAACCCCCGCGGCGCCGGGC
CCGGCACTACCTGGACTTGGAGGAGGGCGAGGGCCTGGCGCGGCTAGGAGCGCCCTCTCCTGAGC
GGTACCCAAGGGTGCAGCTGAAGCGTGATACGCGTGAGGCGTACGTGCCGCGGCAGAACCTGTTTC
GCGACCGCGAGGGAGAGGAGCCCGAGGAGATGCGGGATCGAAAGTTCCACGCAGGGCGCGAGCTG
CGGCATGGCCTGAATCGCGAGCGGTTGCTGCGCGAGGAGGACTTTGAGCCCGACGCGCGAACCGG
GATTAGTCCCGCGCGCGCACACGTGGCGGCCGCCGACCTGGTAACCGCATACGAGCAGACGGTGAA
CCAGGAGATTAACTTTCAAAAAAGCTTTAACAACCACGTGCGTACGCTTGTGGCGCGCGAGGAGGT
GGCTATAGGACTGATGCATCTGTGGGACTTTGTAAGCGCGCTGGAGCAAAACCCAAATAGCAAGCC
GCTCATGGCGCAGCTGTTCCTTATAGTGCAGCACAGCAGGGACAACGAGGCATTCAGGGATGCGCT
GCTAAACATAGTAGAGCCCGAGGGCCGCTGGCTGCTCGATTTGATAAACATCCTGCAGAGCATAGT
GGTGCAGGAGCGCAGCTTGAGCCTGGCTGACAAGGTGGCCGCCATCAACTATTCCATGCTTAGCCT
GGGCAAGTTTTACGCCCGCAAGATATACCATACCCCTTACGTTCCCATAGACAAGGAGGTAAAGATC
GAGGGGTTCTACATGCGCATGGCGCTGAAGGTGCTTACCTTGAGCGACGACCTGGGCGTTTATCGC
AACGAGCGCATCCACAAGGCCGTGAGCGTGAGCCGGCGGCGCGAGCTCAGCGACCGCGAGCTGAT
GCACAGCCTGCAAAGGGCCCTGGCTGGCACGGGCAGCGGCGATAGAGAGGCCGAGTCCTACTTTG
ACGCGGGCGCTGACCTGCGCTGGGCCCCAAGCCGACGCGCCCTGGAGGCAGCTGGGGCCGGACCT
GGGCTGGCGGTGGCACCCGCGCGCGCTGGCAACGTCGGCGGCGTGGAGGAATATGACGAGGACGA
TGAGTACGAGCCAGAGGACGGCGAGTACTAAGCGGTGATGTTTCTGATCAGATGATGCAAGACGCA
ACGGACCCGGCGGTGCGGGCGGCGCTGCAGAGCCAGCCGTCCGGCCTTAACTCCACGGACGACTG
GCGCCAGGTCATGGACCGCATCATGTCGCTGACTGCGCGCAATCCTGACGCGTTCCGGCAGCAGCC
GCAGGCCAACCGGCTCTCCGCAATTCTGGAAGCGGTGGTCCCGGCGCGCGCAAACCCCACGCACGA
GAAGGTGCTGGCGATCGTAAACGCGCTGGCCGAAAACAGGGCCATCCGGCCCGACGAGGCCGGCC
TGGTCTACGACGCGCTGCTTCAGCGCGTGGCTCGTTACAACAGCGGCAACGTGCAGACCAACCTGG
ACCGGCTGGTGGGGGATGTGCGCGAGGCCGTGGCGCAGCGTGAGCGCGCGCAGCAGCAGGGCAA
CCTGGGCTCCATGGTTGCACTAAACGCCTTCCTGAGTACACAGCCCGCCAACGTGCCGCGGGGACA
GGAGGACTACACCAACTTTGTGAGCGCACTGCGGCTAATGGTGACTGAGACACCGCAAAGTGAGGT
GTACCAGTCTGGGCCAGACTATTTTTTCCAGACCAGTAGACAAGGCCTGCAGACCGTAAACCTGAGC
CAGGCTTTCAAAAACTTGCAGGGGCTGTGGGGGGTGCGGGCTCCCACAGGCGACCGCGCGACCGT
GTCTAGCTTGCTGACGCCCAACTCGCGCCTGTTGCTGCTGCTAATAGCGCCCTTCACGGACAGTGG
CAGCGTGTCCCGGGACACATACCTAGGTCACTTGCTGACACTGTACCGCGAGGCCATAGGTCAGGC
GCATGTGGACGAGCATACTTTCCAGGAGATTACAAGTGTCAGCCGCGCGCTGGGGCAGGAGGACAC
GGGCAGCCTGGAGGCAACCCTAAACTACCTGCTGACCAACCGGCGGCAGAAGATCCCCTCGTTGCA
CAGTTTAAACAGCGAGGAGGAGCGCATTTTGCGCTACGTGCAGCAGAGCGTGAGCCTTAACCTGAT
GCGCGACGGGGTAACGCCCAGCGTGGCGCTGGACATGACCGCGCGCGCAACATGGAACCGGGCATGT
ATGCCTCAAACCGGCCGTTTATCAACCGCCTAATGGACTACTTGCATCGCGCGGCCGCCGTGAACCC
CGAGTATTTCACCAATGCCATCTTGAACCCGCACTGGCTACCGCCCCCTGGTTTCTACACCGGGGGA
TTCGAGGTGCCCGAGGGTAACGATGGATTCCTCTGGGACGACATAGACGACAGCGTGTTTTCCCCG
CAACCGCAGACCCTGCTAGAGTTGCAACAGCGCGAGCAGGCAGAGGCGGCGCTGCGAAAGGAAAGC

TTCCGCAGGCCAAGCAGCTTGTCCGATCTAGGCGCTGCGGCCCCGCGGTCAGATGCTAGTAGCCCA
TTTCCAAGCTTGATAGGGTCTCTTACCAGCACTCGCACCACCCGCCCGCGCCTGCTGGGCGAGGAG
GAGTACCTAAACAACTCGCTGCTGCAGCCGCAGCGCGAAAAAAACCTGCCTCCGGCATTTCCCAACA
ACGGGATAGAGAGCCTAGTGGACAAGATGAGTAGATGGAAGACGTACGCGCAGGAGCACAGGGAC
GTGCCAGGCCCGCGCCCGCCCACCCGTCGTCAAAGGCACGACCGTCAGCGGGGTCTGGTGTGGGA
GGACGATGACTCGGCAGACGACAGCAGCGTCCTGGATTTGGGAGGGAGTGGCAACCCGTTTGCGC
ACCTTCGCCCCAGGCTGGGGAGAATGTTTTAAAAAAAAAAAAGCATGATGCAAAATAAAAAACTCAC
CAAGGCCATGGCACCGAGCGTTGGTTTTCTTGTATTCCCCTTAGTATGCGGCGCGCGGCGATGTAT
GAGGAAGGTCCTCCTCCCTCCTACGAGAGTGTGGTGAGCGCGGCGCCAGTGGCGGCGGCGCTGGG
TTCTCCCTTCGATGCTCCCCTGGACCCGCCGTTTGTGCCTCCGCGGTACCTGCGGCCTACCGGGGG
GAGAAACAGCATCCGTTACTCTGAGTTGGCACCCCTATTCGACACCACCCGTGTGTACCTGGTGGAC
AACAAGTCAACGGATGTGGCATCCCTGAACTACCAGAACGACCACAGCAACTTTCTGACCACGGTCA
TTCAAAACAATGACTACAGCCCGGGGGAGGCAAGCACACAGACCATCAATCTTGACGACCGGTCGCA
CTGGGGCGGCGACCTGAAAACCATCCTGCATACCAACATGCCAAATGTGAACGAGTTCATGTTTACC
AATAAGTTTAAGGCGCGGGTGATGGTGTCGCGCTTGCCTACTAAGGACAATCAGGTGGAGCTGAAA
TACGAGTGGGTGGAGTTCACGCTGCCCGAGGGCAACTACTCCGAGACCATGACCATAGACCTTATG
AACAACGCGATCGTGGAGCACTACTTGAAAGTGGGCAGACAGAACGGGGTTCTGGAAAGCGACATC
GGGGTAAAGTTTGACACCCGCAACTTCAGACTGGGGTTTGACCCCGTCACTGGTCTTGTCATGCCT
GGGGTATATACAAACGAAGCCTTCCATCCAGACATCATTTTGCTGCCAGGATGCGGGGTGGACTTCA
CCCACAGCCGCCTGAGCAACTTGTTGGGCATCCGCAAGCGGCAACCCTTCCAGGAGGGCTTTAGGA
TCACCTACGATGATCTGGAGGGTGGTAACATTCCCGCACTGTTGGATGTGGACGCCTACCAGGCGA
GCTTGAAAGATGACACCGAACAGGGCGGGGGTGGCGCAGGCGGCAGCAACAGCAGTGGCAGCGGC
GCGGAAGAGAACTCCAACGCGGCAGCCGCGGCAATGCAGCCGGTGGAGGACATGAACGATCATGCC
ATTCGCGGCGACACCTTTGCCACACGGGCTGAGGAGAAGCGCGCTGAGGCCGAAGCAGCGGCCGA
AGCTGCCGCCCCCGCTGCGCAACCCGAGGTCGAGAAGCCTCAGAAGAAACCGGTGATCAAACCCCT
GACAGAGGACAGCAAGAAACGCAGTTACAACCTAATAAGCAATGACAGCACCTTCACCCAGTACCGC
AGCTGGTACCTTGCATACAACTACGGCGACCCTCAGACCGGAATCCGCTCATGGACCCTGCTTTGCA
CTCCTGACGTAACCTGCGGCTCGGAGCAGGTCTACTGGTCGTTGCCAGACATGATGCAAGACCCCG
TGACCTTCCGCTCCACGCGCCAGATCAGCAACTTTCCGGTGGTGGGCGCCGAGCTGTTGCCCGTGC
ACTCCAAGAGCTTCTACAACGACCAGGCCGTCTACTCCCAACTCATCCGCCAGTTTACCTCTCTGACC
CACGTGTTCAATCGCTTTCCCGAGAACCAGATTTTGGCGCGCCCGCCAGCCCCCACCATCACCACCG
TCAGTGAAAACGTTCCTGCTCTCACAGATCACGGGACGCTACCGCTGCGCAACAGCATCGGAGGAG
TCCAGCGAGTGACCATTACTGACGCCAGACGCCGCACCTGCCCCTACGTTTACAAGGCCCTGGGCAT
AGTCTCGCCGCGCGTCCTATCGAGCCGCACTTTTTGAGCAAGCATGTCCATCCTTATATCGCCCAGC
AATAACACAGGCTGGGGCCTGCGCTTCCCAAGCAAGATGTTTGGCGGGGCCAAGAAGCGCTCCGAC
CAACACCCAGTGCGCGTGCGCGGGCACTACCGCGCGCCCTGGGGCGCGCACAAACGCGGCCGCACT
GGGCGCACCACCGTCGATGACGCCATCGACGCGGTGGTGGAGGAGGCGCGCAACTACACGCCCAC
GCCGCCACCAGTGTCCACAGTGGACGCGGCCATTCAGACCGTGGTGCGCGGAGCCCGGCGCTATGC

TAAAATGAAGAGACGGCGGAGGCGCGTAGCACGTCGCCACCGCCGCCGACCCGGCACTGCCGCCCA
ACGCGCGGCGGCGGCCCTGCTTAACCGCGCACGTCGCACCGGCCGACGGGCGGCCATGCGGGCCG
CTCGAAGGCTGGCCGCGGGTATTGTCACTGTGCCCCCCAGGTCCAGGCGACGAGCGGCCGCCGCA
GCAGCCGCGGCCATTAGTGCTATGACTCAGGGTCGCAGGGGCAACGTGTATTGGGTGCGCGACTC
GGTTAGCGGCCTGCGCGTGCCCGTGCGCACCCGCCCCCCGCGCAACTAGATTGCAAGAAAAAACTA
CTTAGACTCGTACTGTTGTATGTATCCAGCGGCGGCGGCGCGCAACGAAGCTATGTCCAAGCGCAA
AATCAAAGAAGAGATGCTCCAGGTCATCGCGCCGGAGATCTATGGCCCCCCGAAGAAGGAAGAGCA
GGATTACAAGCCCCGAAAGCTAAAGCGGGTCAAAAAGAAAAAGAAAGATGATGATGATGAACTTGAC
GACGAGGTGGAACTGCTGCACGCTACCGCGCCCAGGCGACGGGTACAGTGGAAAGGTCGACGCGT
AAAACGTGTTTTGCGACCCGGCACCACCGTAGTCTTTACGCCCGGTGAGCGCTCCACCCGCACCTAC
AAGCGCGTGTATGATGAGGTGTACGGCGACGAGGACCTGCTTGAGCAGGCCAACGAGCGCCTCGG
GGAGTTTGCCTACGGAAAGCGGCATAAGGACATGCTGGCGTTGCCGCTGGACGAGGGCAACCCAAC
ACCTAGCCTAAAGCCCGTAACACTGCAGCAGGTGCTGCCCGCGCTTGCACCGTCCGAAGAAAAGCG
CGGCCTAAAGCGCGAGTCTGGTGACTTGGCACCCACCGTGCAGCTGATGGTACCCAAGCGCCAGCG
ACTGGAAGATGTCTTGGAAAAAATGACCGTGGAACCTGGGCTGGAGCCCGAGGTCCGCGTGCGGCC
AATCAAGCAGGTGGCGCCGGGACTGGGCGTGCAGACCGTGGACGTTCAGATACCCACTACCAGTAG
CACCAGTATTGCCACCGCCACAGAGGGCATGGAGACACAAACGTCCCCGGTTGCCTCAGCGGTGGC
GGATGCCGCGGTGCAGGCGGTCGCTGCGGCCGCGTCCAAGACCTCTACGGAGGTGCAAACGGACC
CGTGGATGTTTCGCGTTTCAGCCCCCCGGCGCCCGCGCGGTTCGAGGAAGTACGGCGCCGCCAGC
GCGCTACTGCCCGAATATGCCCTACATCCTTCCATTGCGCCTACCCCCGGCTATCGTGGCTACACCT
ACCGCCCCAGAAGACGAGCAACTACCCGACGCCGAACCACCACTGGAACCCGCCGCCGCCGTCGCC
GTCGCCAGCCCGTGCTGGCCCCGATTTCCGTGCGCAGGGTGGCTCGCGAAGGAGGCAGGACCCTG
GTGCTGCCAACAGCGCGCTACCACCCCAGCATCGTTTAAAAGCCGGTCTTTGTGGTTCTTGCAGATA
TGGCCCTCACCTGCCGCCTCCGTTTCCCGGTGCCGGGATTCCGAGGAAGAATGCACCGTAGGAGGG
GCATGGCCGGCCACGGCCTGACGGGCGGCATGCGTCGTGCGCACCACCGGCGGCGGCGCGCGTCG
CACCGTCGCATGCGCGGCGGTATCCTGCCCCTCCTTATTCCACTGATCGCCGCGGCGATTGGCGCC
GTGCCCGGAATTGCATCCGTGGCCTTGCAGGCGCAGAGACACTGATTAAAAACAAGTTGCATGTGG
AAAAATCAAAATAAAAAGTCTGGACTCTCACGCTCGCTTGGTCCTGTAACTATTTTGTAGAATGGAA
GACATCAACTTTGCGTCTCTGGCCCCGCGACACGGCTCGCGCCCGTTCATGGGAAACTGGCAAGAT
ATCGGCACCAGCAATATGAGCGGTGGCGCCTTCAGCTGGGGCTCGCTGTGGAGCGGCATTAAAAAT
TTCGGTTCCACCGTTAAGAACTATGGCAGCAAGGCCTGGAACAGCAGCACAGGCCAGATGCTGAGG
GATAAGTTGAAAGAGCAAAATTTCCAACAAAAGGTGGTAGATGGCCTGGCCTCTGGCATTAGCGGG
GTGGTGGACCTGGCCAACCAGGCAGTGCAAAATAAGATTAACAGTAAGCTTGATCCCCGCCCTCCCG
TAGAGGAGCCTCCACCGGCCGTGGAGACAGTGTCTCCAGAGGGGCGTGGCGAAAAGCGTCCGCGC
CCCGACAGGGAAGAAACTCTGGTGACGCAAATAGACGAGCCTCCCTCGTACGAGGAGGCACTAAAG
CAAGGCCTGCCCACCACCCGTCCCATCGCGCCCATGGCTACCGGAGTGCTGGGCCAGCACACACCC
GTAACGCTGGACCTGCCTCCCCCCGCCGACACCCAGCAGAAACCTGTGCTGCCAGGCCCGACCGCC
GTTGTTGTAACCCGTCCTAGCCGCGCGTCCCTGCGCCGCGCCGCCAGCGGTCCGCGATCGTTGCGG

CCCGTAGCCAGTGGCAACTGGCAAAGCACACTGAACAGCATCGTGGGTCTGGGGGTGCAATCCCTG
AAGCGCCGACGATGCTTCTGAATAGCTAACGTGTCGTATGTGTGTCATGTATGCGTCCATGTCGCC
GCCAGAGGAGCTGCTGAGCCGCCGCGCGCCCGCTTTCCAAGATGGCTACCCCTTCGATGATGCCGC
AGTGGTCTTACATGCACATCTCGGGCCAGGACGCCTCGGAGTACCTGAGCCCCGGGCTGGTGCAGT
TTGCCCGCGCCACCGAGACGTACTTCAGCCTGAATAACAAGTTTAGAAACCCCACGGTGGCGCCTAC
GCACGACGTGACCACAGACCGGTCCCAGCGTTTGACGCTGCGGTTCATCCCTGTGGACCGTGAGGA
TACTGCGTACTCGTACAAGGCGCGGTTCACCCTAGCTGTGGGTGATAACCGTGTGCTGGACATGGC
TTCCACGTACTTTGACATCCGCGGCGTGCTGGACAGGGGCCCTACTTTTAAGCCCTACTCTGGCACT
GCCTACAACGCCCTGGCTCCCAAGGGTGCCCCAAATCCTTGCGAATGGGATGAAGCTGCTACTGCTC
TTGAAATAAACCTAGAAGAAGAGGACGATGACAACGAAGACGAAGTAGACGAGCAAGCTGAGCAGC
AAAAAACTCACGTATTTGGGCAGGCGCCTTATTCTGGTATAAATATTACAAAGGAGGGTATTCAAAT
AGGTGTCGAAGGTCAAACACCTAAATATGCCGATAAAACATTTCAACCTGAACCTCAAATAGGAGAA
TCTCAGTGGTACGAAACTGAAATTAATCATGCAGCTGGGAGAGTCCTTAAAAAGACTACCCCAATGA
AACCATGTTACGGTTCATATGCAAAACCCACAAATGAAAATGGAGGGCAAGGCATTCTTGTAAAGCA
ACAAAATGGAAAGCTAGAAAGTCAAGTGGAAATGCAATTTTTCTCAACTACTGAGGCGACCGCAGGC
AATGGTGATAACTTGACTCCTAAAGTGGTATTGTACAGTGAAGATGTAGATATAGAAACCCCAGACA
CTCATATTTCTTACATGCCCACTATTAAGGAAGGTAACTCACGAGAACTAATGGGCCAACAATCTATG
CCCAACAGGCCTAATTACATTGCTTTTAGGGACAATTTTATTGGTCTAATGTATTACAACAGCACGG
GTAATATGGGTGTTCTGGCGGGCCAAGCATCGCAGTTGAATGCTGTTGTAGATTTGCAAGACAGAA
ACACAGAGCTTTCATACCAGCTTTTGCTTGATTCCATTGGTGATAGAACCAGGTACTTTTCTATGTG
GAATCAGGCTGTTGACAGCTATGATCCAGATGTTAGAATTATTGAAAATCATGGAACTGAAGATGAA
CTTCCAAATTACTGCTTTCCACTGGGAGGTGTGATTAATACAGAGACTCTTACCAAGGTAAAACCTA
AAACAGGTCAGGAAAATGGATGGGAAAAAGATGCTACAGAATTTTCAGATAAAAATGAAATAAGAGT
TGGAAATAATTTTGCCATGGAAATCAATCTAAATGCCAACCTGTGGAGAAATTTCCTGTACTCCAACA
TAGCGCTGTATTTGCCCGACAAGCTAAAGTACAGTCCTTCCAACGTAAAAATTTCTGATAACCCAAAC
ACCTACGACTACATGAACAAGCGAGTGGTGGCTCCCGGGTTAGTGGACTGCTACATTAACCTTGGA
GCACGCTGGTCCCTTGACTATATGGACAACGTCAACCCATTTAACCACCACCGCAATGCTGGCCTGC
GCTACCGCTCAATGTTGCTGGGCAATGGTCGCTATGTGCCCTTCCACATCCAGGTGCCTCAGAAGTT
CTTTGCCATTAAAAACCTCCTTCTCCTGCCGGGCTCATACACCTACGAGTGGAACTTCAGGAAGGAT
GTTAACATGGTTCTGCAGAGCTCCCTAGGAAATGACCTAAGGGTTGACGGAGCCAGCATTAAGTTT
GATAGCATTTGCCTTTACGCCACCTTCTTCCCCATGGCCCACAACACCGCCTCCACGCTTGAGGCCA
TGCTTAGAAACGACACCAACGACCAGTCCTTTAACGACTATCTCTCCGCCGCCAACATGCTCTACCCT
ATACCCGCCAACGCTACCAACGTGCCCATATCCATCCCCTCCCGCAACTGGGCGGCTTTCCGCGGCT
GGGCCTTCACGCGCCTTAAGACTAAGGAAACCCCATCACTGGGCTCGGGCTACGACCCTTATTACAC
CTACTCTGGCTCTATACCCTACCTAGATGGAACCTTTTACCTCAACCACACCTTTAAGAAGGTGGCCA
TTACCTTTGACTCTTCTGTCAGCTGGCCTGGCAATGACCGCCTGCTTACCCCCAACGAGTTTGAAAT
TAAGCGCTCAGTTGACGGGGAGGGTTACAACGTTGCCCAGTGTAACATGACCAAAGACTGGTTCCT
GGTACAAATGCTAGCTAACTACAACATTGGCTACCAGGGCTTCTATATCCCAGAGAGCTACAAGGAC

CGCATGTACTCCTTCTTTAGAAACTTCCAGCCCATGAGCCGTCAGGTGGTGGATGATACTAAATACA
AGGACTACCAACAGGTGGGCATCCTACACCAACACAACAACTCTGGATTTGTTGGCTACCTTGCCCC
CACCATGCGCGAAGGACAGGCCTACCCTGCTAACTTCCCCTATCCGCTTATAGGCAAGACCGCAGTT
GACAGCATTACCCAGAAAAAGTTTCTTTGCGATCGCACCCTTTGGCGCATCCCATTCTCCAGTAACTT
TATGTCCATGGGCGCACTCACAGACCTGGGCCAAAACCTTCTCTACGCCAACTCCGCCCACGCGCTA
GACATGACTTTTGAGGTGGATCCCATGGACGAGCCCACCCTTCTTTATGTTTTGTTTGAAGTCTTTG
ACGTGGTCCGTGTGCACCGGCCGCACCGCGGCGTCATCGAAACCGTGTACCTGCGCACGCCCTTCT
CGGCCGGCAACGCCACAACATAAAGAAGCAAGCAACATCAACAACAGCTGCCGCCATGGGCTCCAGT
GAGCAGGAACTGAAAGCCATTGTCAAAGATCTTGGTTGTGGGCCATATTTTTTGGGCACCTATGACA
AGCGCTTTCCAGGCTTTGTTTCTCCACACAAGCTCGCCTGCGCCATAGTCAATACGGCCGGTCGCGA
GACTGGGGGCGTACACTGGATGGCCTTTGCCTGGAACCCGCACTCAAAAACATGCTACCTCTTTGA
GCCCTTTGGCTTTTCTGACCAGCGACTCAAGCAGGTTTACCAGTTTGAGTACGAGTCACTCCTGCGC
CGTAGCGCCATTGCTTCTTCCCCCGACCGCTGTATAACGCTGGAAAAGTCCACCCAAAGCGTACAGG
GGCCCAACTCGGCCGCCTGTGGACTATTCTGCTGCATGTTTCTCCACGCCTTTGCCAACTGGCCCCA
AACTCCCATGGATCACAACCCCACCATGAACCTTATTACCGGGGTACCCAACTCCATGCTCAACAGTC
CCCAGGTACAGCCCACCCTGCGTCGCAACCAGGAACAGCTCTACAGCTTCCTGGAGCGCCACTCGCC
CTACTTCCGCAGCCACAGTGCGCAGATTAGGAGCGCCACTTCTTTTTGTCACTTGAAAAACATGTAA
AAATAATGTACTAGAGACACTTTCAATAAAGGCAAATGCTTTTATTTGTACACTCTCGGGTGATTATT
TACCCCCACCCTTGCCGTCTGCGCCGTTTAAAAATCAAAGGGGTTCTGCCGCGCATCGCTATGCGCC
ACTGGCAGGGACACGTTGCGATACTGGTGTTTAGTGCTCCACTTAAACTCAGGCACAACCATCCGCG
GCAGCTCGGTGAAGTTTTCACTCCACAGGCTGCGCACCATCACCAACGCGTTTAGCAGGTCGGGCG
CCGATATCTTGAAGTCGCAGTTGGGGCCTCCGCCCTGCGCGCGCGAGTTGCGATACACAGGGTTGC
AGCACTGGAACACTATCAGCGCCGGGTGGTGCACGCTGGCCAGCACGCTCTTGTCGGAGATCAGAT
CCGCGTCCAGGTCCTCCGCGTTGCTCAGGGCGAACGGAGTCAACTTTGGTAGCTGCCTTCCCAAAA
AGGGCGCGTGCCCAGGCTTTGAGTTGCACTCGCACCGTAGTGGCATCAAAAGGTGACCGTGCCCGG
TCTGGGCGTTAGGATACAGCGCCTGCATAAAAGCCTTGATCTGCTTAAAAGCCACCTGAGCCTTTGC
GCCTTCAGAGAAGAACATGCCGCAAGACTTGCCGGAAAACTGATTGGCCGGACAGGCCGCGTCGTG
CACGCAGCACCTTGCGTCGGTGTTGGAGATCTGCACCACATTTCGGCCCCACCGGTTCTTCACGATC
TTGGCCTTGCTAGACTGCTCCTTCAGCGCGCGCTGCCCGTTTTCGCTCGTCACATCCATTTCAATCA
CGTGCTCCTTATTTATCATAATGCTTCCGTGTAGACACTTAAGCTCGCCTTCGATCTCAGCGCAGCG
GTGCAGCCACAACGCGCAGCCCGTGGGCTCGTGATGCTTGTAGGTCACCTCTGCAAACGACTGCAG
GTACGCCTGCAGGAATCGCCCCATCATCGTCACAAAGGTCTTGTTGCTGGTGAAGGTCAGCTGCAA
CCCGCGGTGCTCCTCGTTCAGCCAGGTCTTGCATACGGCCGCCAGAGCTTCCACTTGGTCAGGCAG
TAGTTTGAAGTTCGCCTTTAGATCGTTATCCACGTGGTACTTGTCCATCAGCGCGCGCGCAGCCTCC
ATGCCCTTCTCCCACGCAGACACGATCGGCACACTCAGCGGGTTCATCACCGTAATTTCACTTTCCG
CTTCGCTGGGCTCTTCCTCTTCCTCTTGCGTCCGCATACCACGCGCCACTGGGTCGTCTTCATTCAG
CCGCCGCACTGTGCGCTTACCTCCTTTGCCATGCTTGATTAGCACCGGTGGGTTGCTGAAACCCACC
ATTTGTAGCGCCACATCTTCTCTTTCTTCCTCGCTGTCCACGATTACCTCTGGTGATGGCGGGCGCT

CGGGCTTGGGAGAAGGGCGCTTCTTTTTCTTCTTGGGCGCAATGGCCAAATCCGCCGCCGAGGTCG
ATGGCCGCGGGCTGGGTGTGCGCGGCACCAGCGCGTCTTGTGATGAGTCTTCCTCGTCCTCGGACT
CGATACGCCGCCTCATCCGCTTTTTTGGGGGCGCCCGGGGAGGCGGCGGCGACGGGGACGGGGAC
GACACGTCCTCCATGGTTGGGGGACGTCGCGCCGCACCGCGTCCGCGCTCGGGGGTGGTTTCGCG
CTGCTCCTCTTCCCGACTGGCCATTTCCTTCTCCTATAGGCAGAAAAAGATCATGGAGTCAGTCGAG
AAGAAGGACAGCCTAACCGCCCCCTCTGAGTTCGCCACCACCGCCTCCACCGATGCCGCCAACGCGC
CTACCACCTTCCCCGTCGAGGCACCCCCGCTTGAGGAGGAGGAAGTGATTATCGAGCAGGACCCAG
GTTTTGTAAGCGAAGACGACGAGGACCGCTCAGTACCAACAGAGGATAAAAAGCAAGACCAGGACA
ACGCAGAGGCAAACGAGGAACAAGTCGGGCGGGGGGACGAAAGGCATGGCGACTACCTAGATGTG
GGAGACGACGTGCTGTTGAAGCATCTGCAGCGCCAGTGCGCCATTATCTGCGACGCGTTGCAAGAG
CGCAGCGATGTGCCCCTCGCCATAGCGGATGTCAGCCTTGCCTACGAACGCCACCTATTCTCACCGC
GCGTACCCCCCAAACGCCAAGAAAACGGCACATGCGAGCCCAACCCGCGCCTCAACTTCTACCCCGT
ATTTGCCGTGCCAGAGGTGCTTGCCACCTATCACATCTTTTTCCAAAACTGCAAGATACCCCTATCCT
GCCGTGCCAACCGCAGCCGAGCGGACAAGCAGCTGGCCTTGCGGCAGGGCGCTGTCATACCTGATA
TCGCCTCGCTCAACGAAGTGCCAAAAATCTTTGAGGGTCTTGGACGCGACGAGAAGCGCGCGGCAA
ACGCTCTGCAACAGGAAAACAGCGAAAATGAAAGTCACTCTGGAGTGTTGGTGGAACTCGAGGGTG
ACAACGCGCGCCTAGCCGTACTAAAACGCAGCATCGAGGTCACCCACTTTGCCTACCCGGCACTTAA
CCTACCCCCCAAGGTCATGAGCACAGTCATGAGTGAGCTGATCGTGCGCCGTGCGCAGCCCCTGGA
GAGGGATGCAAATTTGCAAGAACAAACAGAGGAGGGCCTACCCGCAGTTGGCGACGAGCAGCTAGC
GCGCTGGCTTCAAACGCGCGAGCCTGCCGACTTGGAGGAGCGACGCAAACTAATGATGGCCGCAGT
GCTCGTTACCGTGGAGCTTGAGTGCATGCAGCGGTTCTTTGCTGACCCGGAGATGCAGCGCAAGCT
AGAGGAAACATTGCACTACACCTTTCGACAGGGCTACGTACGCCAGGCCTGCAAGATCTCCAACGTG
GAGCTCTGCAACCTGGTCTCCTACCTTGGAATTTTGCACGAAAACCGCCTTGGGCAAAACGTGCTTC
ATTCCACGCTCAAGGGCGAGGCGCGCCGCGACTACGTCCGCGACTGCGTTTACTTATTTCTATGCTA
CACCTGGCAGACGGCCATGGGCGTTTGGCAGCAGTGCTTGGAGGAGTGCAACCTCAAGGAGCTGCA
GAAACTGCTAAAGCAAAACTTGAAGGACCTATGGACGGCCTTCAACGAGCGCTCCGTGGCCGCGCA
CCTGGCGGACATCATTTTCCCCGAACGCCTGCTTAAAACCCTGCAACAGGGTCTGCCAGACTTCACC
AGTCAAAGCATGTTGCAGAACTTTAGGAACTTTATCCTAGAGCGCTCAGGAATCTTGCCCGCCACCT
GCTGTGCACTTCCTAGCGACTTTGTGCCCATTAAGTACCGCGAATGCCCTCCGCCGCTTTGGGGCCA
CTGCTACCTTCTGCAGCTAGCCAACTACCTTGCCTACCACTCTGACATAATGGAAGACGTGAGCGGT
GACGGTCTACTGGAGTGTCACTGTCGCTGCAACCTATGCACCCCGCACCGCTCCCTGGTTTGCAATT
CGCAGCTGCTTAACGAAAGTCAAATTATCGGTACCTTTGAGCTGCAGGGTCCCTCGCCTGACGAAAA
GTCCGCGGCTCCGGGGTTGAAACTCACTCCGGGGCTGTGGACGTCGGCTTACCTTCGCAAATTTGT
ACCTGAGGACTACCACGCCCACGAGATTAGGTTCTACGAAGACCAATCCCGCCCGCCAAATGCGGAG
CTTACCGCCTGCGTCATTACCCAGGGCCACATTCTTGGCCAATTGCAAGCCATCAACAAAGCCCGCC
AAGAGTTTCTGCTACGAAAGGGACGGGGGGTTTACTTGGACCCCCAGTCCGGCGAGGAGCTCAACC
CAATCCCCCCGCCGCCGCAGCCCTATCAGCAGCAGCCGCGGGCCCTTGCTTCCCAGGATGGCACCC
AAAAAGAAGCTGCAGCTGCCGCCGCCACCCACGGACGAGGAGGAATACTGGGACAGTCAGGCAGAG

GAGGTTTTGGACGAGGAGGAGGAGGACATGATGGAAGACTGGGAGAGCCTAGACGAGGAAGCTTC
CGAGGTCGAAGAGGTGTCAGACGAAACACCGTCACCCTCGGTCGCATTCCCCTCGCCGGCGCCCCA
GAAATCGGCAACCGGTTCCAGCATGGCTACAACCTCCGCTCCTCAGGCGCCGCCGGCACTGCCCGT
TCGCCGACCCAACCGTAGATGGGACACCACTGGAACCAGGGCCGGTAAGTCCAAGCAGCCGCCGCC
GTTAGCCCAAGAGCAACAACAGCGCCAAGGCTACCGCTCATGGCGCGGGCACAAGAACGCCATAGT
TGCTTGCTTGCAAGACTGTGGGGGCAACATCTCCTTCGCCCGCCGCTTTCTTCTCTACCATCACGGC
GTGGCCTTCCCCCGTAACATCCTGCATTACTACCGTCATCTCTACAGCCCATACTGCACCGGCGGCA
GCGGCAGCGGCAGCAACAGCAGCGGCCACACAGAAGCAAAGGCGACCGGATAGCAAGACTCTGACA
AAGCCCAAGAAATCCACAGCGGCGGCAGCAGCAGGAGGAGGAGCGCTGCGTCTGGCGCCCAACGAA
CCCGTATCGACCCGCGAGCTTAGAAACAGGATTTTTCCCACTCTGTATGCTATATTTCAACAGAGCA
GGGGCCAAGAACAAGAGCTGAAAATAAAAAACAGGTCTCTGCGATCCCTCACCCGCAGCTGCCTGTA
TCACAAAAGCGAAGATCAGCTTCGGCGCACGCTGGAAGACGCGGAGGCTCTCTTCAGTAAATACTG
CGCGCTGACTCTTAAGGACTAGTTTCGCGCCCTTTCTCAAATTTAAGCGCGAAAACTACGTCATCTC
CAGCGGCCACACCCGGCGCCAGCACCTGTCGTCAGCGCCATTATGAGCAAGGAAATTCCCACGCCCT
ACATGTGGAGTTACCAGCCACAAATGGGACTTGCGGCTGGAGCTGCCCAAGACTACTCAACCCGAAT
AAACTACATGAGCGCGGGACCCCACATGATATCCCGGGTCAACGGAATCCGCGCCCACCGAAACCGA
ATTCTCTTGGAACAGGCGGCTATTACCACCACACCTCGTAATAACCTTAATCCCCGTAGTTGGCCCG
CTGCCCTGGTGTACCAGGAAAGTCCCGCTCCCACCACTGTGGTACTTCCCAGAGACGCCCAGGCCG
AAGTTCAGATGACTAACTCAGGGGCGCAGCTTGCGGGCGGCTTTCGTCACAGGGTGCGGTCGCCCG
GGCAGGGTATAACTCACCTGACAATCAGAGGGCGAGGTATTCAGCTCAACGACGAGTCGGTGAGCT
CCTCGCTTGGTCTCCGTCCGGACGGGACATTTCAGATCGGCGGCGCCGGCCGTCCTTCATTCACGC
CTCGTCAGGCAATCCTAACTCTGCAGACCTCGTCCTCTGAGCCGCGCTCTGGAGGCATTGGAACTCT
GCAATTTATTGAGGAGTTTGTGCCATCGGTCTACTTTAACCCCTTCTCGGGACCTCCCGGCCACTAT
CCGGATCAATTTATTCCTAACTTTGACGCGGTAAAGGACTCGGCGGACGGCTACGACTGAATGTTAA
GTGGAGAGGCAGAGCAACTGCGCCTGAAACACCTGGTCCACTGTCGCCGCCACAAGTGCTTTGCCC
GCGACTCCGGTGAGTTTTGCTACTTTGAATTGCCCGAGGATCATATCGAGGGCCCGGCGCACGGCG
TCCGGCTTACCGCCCAGGGAGAGCTTGCCCGTAGCCTGATTCGGGAGTTTACCCAGCGCCCCCTGC
TAGTTGAGCGGGACAGGGGACCCTGTGTTCTCACTGTGATTTGCAACTGTCCTAACCTTGGATTACA
TCAAGATCTTTGTTGCCATCTCTGTGCTGAGTATAATAAATACAGAAATTAAAATATACTGGGGCTCC
TATCGCCATCCTGTAAACGCCACCGTCTTCACCCGCCCAAGCAAACCAAGGCGAACCTTACCTGGTA
CTTTTAACATCTCTCCCTCTGTGATTTACAACAGTTTCAACCCAGACGGAGTGAGTCTACGAGAGAA
CCTCTCCGAGCTCAGCTACTCCATCAGAAAAAACACCACCCTCCTTACCTGCCGGGAACGTACGAGT
GCGTCACCGGCCGCTGCACCACACCTACCGCCTGACCGTAAACCAGACTTTTTCCGGACAGACCTCA
ATAACTCTGTTTACCAGAACAGGAGGTGAGCTTAGAAAACCCTTAGGGTATTAGGCCAAAGGCGCAG
CTACTGTGGGGTTTATGAACAATTCAAGCAACTCTACGGGCTATTCTAATTCAGGTTTCTCTAGAAA
TGGACGGAATTATTACAGAGCAGCGCCTGCTAGAAAGACGCAGGGCAGCGGCCGAGCAACAGCGCA
TGAATCAAGAGCTCCAAGACATGGTTAACTTGCACCAGTGCAAAAGGGGTATCTTTTGTCTGGTAAA
GCAGGCCAAAGTCACCTACGACAGTAATACCACCGGACACCGCCTTAGCTACAAGTTGCCAACCAAG

CGTCAGAAATTGGTGGTCATGGTGGGAGAAAAGCCCATTACCATAACTCAGCACTCGGTAGAAACC
GAAGGCTGCATTCACTCACCTTGTCAAGGACCTGAGGATCTCTGCACCCTTATTAAGACCCTGTGCG
GTCTCAAAGATCTTATTCCCTTTAACTAATAAAAAAAAATAATAAAGCATCACTTACTTAAAATCAGTT
AGCAAATTTCTGTCCAGTTTATTCAGCAGCACCTCCTTGCCCTCCTCCCAGCTCTGGTATTGCAGCTT
CCTCCTGGCTGCAAACTTTCTCCACAATCTAAATGGAATGTCAGTTTCCTCCTGTTCCTGTCCATCCG
CACCCACTATCTTCATGTTGTTGCAGATGAAGCGCGCAAGACCGTCTGAAGATACCTTCAACCCCGT
GTATCCATATGACACGGAAACCGGTCCTCCAACTGTGCCTTTTCTTACTCCTCCCTTTGTATCCCCCA
ATGGGTTTCAAGAGAGTCCCCCTGGGGTACTCTCTTTGCGCCTATCCGAACCTCTAGTTACCTCCAA
TGGCATGCTTGCGCTCAAAATGGGCAACGGCCTCTCTCTGGACGAGGCCGGCAACCTTACCTCCCAA
AATGTAACCACTGTGAGCCCACCTCTCAAAAAAACCAAGTCAAACATAAACCTGGAAATATCTGCACC
CCTCACAGTTACCTCAGAAGCCCTAACTGTGGCTGCCGCCGCACCTCTAATGGTCGCGGGCAACACA
CTCACCATGCAATCACAGGCCCCGCTAACCGTGCACGACTCCAAACTTAGCATTGCCACCCAAGGAC
CCCTCACAGTGTCAGAAGGAAAGCTAGCCCTGCAAACATCAGGCCCCCTCACCACCACCGATAGCAG
TACCCTTACTATCACTGCCTCACCCCCTCTAACTACTGCCACTGGTAGCTTGGGCATTGACTTGAAA
GAGCCCATTTATACACAAAATGGAAAACTAGGACTAAAGTACGGGGCTCCTTTGCATGTAACAGACG
ACCTAAACACTTTGACCGTAGCAACTGGTCCAGGTGTGACTATTAATAATACTTCCTTGCAAACTAAA
GTTACTGGAGCCTTGGGTTTTGATTCACAAGGCAATATGCAACTTAATGTAGCAGGAGGACTAAGG
ATTGATTCTCAAAACAGACGCCTTATACTTGATGTTAGTTATCCGTTTGATGCTCAAAACCAACTAAA
TCTAAGACTAGGACAGGGCCCTCTTTTTATAAACTCAGCCCACAACTTGGATATTAACTACAACAAAG
GCCTTTACTTGTTTACAGCTTCAAACAATTCCAAAAAGCTTGAGGTTAACCTAAGCACTGCCAAGGG
GTTGATGTTTGACGCTACAGCCATAGCCATTAATGCAGGAGATGGGCTTGAATTTGGTTCACCTAAT
GCACCAAACACAAATCCCCTCAAAACAAAAATTGGCCATGGCCTAGAATTTGATTCAAACAAGGCTAT
GGTTCCTAAACTAGGAACTGGCCTTAGTTTTGACAGCACAGGTGCCATTACAGTAGGAAACAAAAAT
AATGATAAGCTAACTTTGTGGACCACACCAGCTCCATCTCCTAACTGTAGACTAAATGCAGAGAAAG
ATGCTAAACTCACTTTGGTCTTAACAAAATGTGGCAGTCAAATACTTGCTACAGTTTCAGTTTTGGCT
GTTAAAGGCAGTTTGGCTCCAATATCTGGAACAGTTCAAAGTGCTCATCTTATTATAAGATTTGACG
AAAATGGAGTGCTACTAAACAATTCCTTCCTGGACCCAGAATATTGGAACTTTAGAAATGGAGATCT
TACTGAAGGCACAGCCTATACAAACGCTGTTGGATTTATGCCTAACCTATCAGCTTATCCAAAATCTC
ACGGTAAAACTGCCAAAAGTAACATTGTCAGTCAAGTTTACTTAAACGGAGACAAAACTAAACCTGTA
ACACTAACCATTACACTAAACGGTACACAGGAAACAGGAGACACAACTCCAAGTGCATACTCTATGTC
ATTTTCATGGGACTGGTCTGGCCACAACTACATTAATGAAATATTTGCCACATCCTCTTACACTTTTT
CATACATTGCCCAAGAATAAAGAATCGTTTGTGTTATGTTTCAACGTGTTTATTTTTCAATTGCAGAA
AATTTCGAATCATTTTTCATTCAGTAGTATAGCCCCACCACCACATAGCTTATACAGATCACCGTACC
TTAATCAAACTCACAGAACCCTAGTATTCAACCTGCCACCTCCCTCCCAACACACAGAGTACACAGTC
CTTTCTCCCCGGCTGGCCTTAAAAAGCATCATATCATGGGTAACAGACATATTCTTAGGTGTTATATT
CCACACGGTTTCCTGTCGAGCCAAACGCTCATCAGTGATATTAATAAACTCCCCGGGCAGCTCACTT
AAGTTCATGTCGCTGTCCAGCTGCTGAGCCACAGGCTGCTGTCCAACTTGCGGTTGCTTAACGGGC
GGCGAAGGAGAAGTCCACGCCTACATGGGGGTAGAGTCATAATCGTGCATCAGGATAGGGCGGTG

GTGCTGCAGCAGCGCGCGAATAAACTGCTGCCGCCGCCGCTCCGTCCTGCAGGAATACAACATGGC
AGTGGTCTCCTCAGCGATGATTCGCACCGCCCGCAGCATAAGGCGCCTTGTCCTCCGGGCACAGCA
GCGCACCCTGATCTCACTTAAATCAGCACAGTAACTGCAGCACAGCACCACAATATTGTTCAAAATCC
CACAGTGCAAGGCGCTGTATCCAAAGCTCATGGCGGGGACCACAGAACCCACGTGGCCATCATACC
ACAAGCGCAGGTAGATTAAGTGGCGACCCCTCATAAACACGCTGGACATAAACATTACCTCTTTTGG
CATGTTGTAATTCACCACCTCCCGGTACCATATAAACCTCTGATTAAACATGGCGCCATCCACCACCA
TCCTAAACCAGCTGGCCAAAACCTGCCCGCCGGCTATACACTGCAGGGAACCGGGACTGGAACAAT
GACAGTGGAGAGCCCAGGACTCGTAACCATGGATCATCATGCTCGTCATGATATCAATGTTGGCACA
ACACAGGCACACGTGCATACACTTCCTCAGGATTACAAGCTCCTCCCGCGTTAGAACCATATCCCAG
GGAACAACCCATTCCTGAATCAGCGTAAATCCCACACTGCAGGGAAGACCTCGCACGTAACTCACGT
TGTGCATTGTCAAAGTGTTACATTCGGGCAGCAGCGGATGATCCTCCAGTATGGTAGCGCGGGTTT
CTGTCTCAAAAGGAGGTAGACGATCCCTACTGTACGGAGTGCGCCGAGACAACCGAGATCGTGTTG
GTCGTAGTGTCATGCCAAATGGAACGCCGGACGTAGTCATATTTCCTGAAGCAAAACCAGGTGCGG
GCGTGACAAACAGATCTGCGTCTCCGGTCTCGCCGCTTAGATCGCTCTGTGTAGTAGTTGTAGTATA
TCCACTCTCTCAAAGCATCCAGGCGCCCCCTGGCTTCGGGTTCTATGTAAACTCCTTCATGCGCCGC
TGCCCTGATAACATCCACCACCGCAGAATAAGCCACACCCAGCCAACCTACACATTCGTTCTGCGAG
TCACACACGGGAGGAGCGGGAAGAGCTGGAAGAACCATGTTTTTTTTTTTATTCCAAAAGATTATCC
AAAACCTCAAAATGAAGATCTATTAAGTGAACGCGCTCCCCTCCGGTGGCGTGGTCAAACTCTACAG
CCAAAGAACAGATAATGGCATTTGTAAGATGTTGCACAATGGCTTCCAAAAGGCAAACGGCCCTCAC
GTCCAAGTGGACGTAAAGGCTAAACCCTTCAGGGTGAATCTCCTCTATAAACATTCCAGCACCTTCA
ACCATGCCCAAATAATTCTCATCTCGCCACCTTCTCAATATATCTCTAAGCAAATCCCGAATATTAAG
TCCGGCCATTGTAAAAATCTGCTCCAGAGCGCCCTCCACCTTCAGCCTCAAGCAGCGAATCATGATT
GCAAAAATTCAGGTTCCTCACAGACCTGTATAAGATTCAAAAGCGGAACATTAACAAAAATACCGCGA
TCCCGTAGGTCCCTTCGCAGGGCCAGCTGAACATAATCGTGCAGGTCTGCACGGACCAGCGCGGCC
ACTTCCCCGCCAGGAACCTTGACAAAAGAACCCACACTGATTATGACACGCATACTCGGAGCTATGC
TAACCAGCGTAGCCCCGATGTAAGCTTTGTTGCATGGGCGGCGATATAAAATGCAAGGTGCTGCTC
AAAAAATCAGGCAAAGCCTCGCGCAAAAAAGAAAGCACATCGTAGTCATGCTCATGCAGATAAAGGC
AGGTAAGCTCCGGAACCACCACAGAAAAAGACACCATTTTTCTCTCAAACATGTCTGCGGGTTTCTG
CATAAACACAAAATAAAATAACAAAAAAACATTTAAACATTAGAAGCCTGTCTTACAACAGGAAAAAC
AACCCTTATAAGCATAAGACGGACTACGGCCATGCCGGCGTGACCGTAAAAAAACTGGTCACCGTGA
TTAAAAAGCACCACCGACAGCTCCTCGGTCATGTCCGGAGTCATAATGTAAGACTCGGTAAACACAT
CAGGTTGATTCACATCGGTCAGTGCTAAAAAGCGACCGAAATAGCCCGGGGGAATACATACCCGCA
GGCGTAGAGACAACATTACAGCCCCCATAGGAGGTATAACAAAATTAATAGGAGAGAAAAACACATA
AACACCTGAAAAACCCTCCTGCCTAGGCAAAATAGCACCCTCCCGCTCCAGAACAACATACAGCGCTT
CCACAGCGGCAGCCATAACAGTCAGCCTTACCAGTAAAAAAGAAAACCTATTAAAAAAACACCACTCG
ACACGGCACCAGCTCAATCAGTCACAGTGTAAAAAAGGGCCAAGTGCAGAGCGAGTATATATAGGAC
TAAAAAATGACGTAACGGTTAAAGTCCACAAAAAACACCCAGAAAACCGCACGCGAACCTACGCCCA
GAAACGAAAGCCAAAAAACCCACAACTTCCTCAAATCGTCACTTCCGTTTTCCCACGTTACGTCACTT

CCCATTTTAAGAAAACTACAATTCCCAACACATACAAGTTACTCCGCCCTAAAACCTACGTCACCCGC
CCCGTTCCCACGCCCCGCGCCACGTCACAAACTCCACCCCCTCATTATCATATTGGCTTCAATCCAAA
ATAAGGTATATTATTGATGATGTTAATTAATTTAAATCCGCATGCGATATCGAGCTCTCCCGGGAAT
TCGGATCTGCGACGCGAGGCTGGATGGCCTTCCCCATTATGATTCTTCTCGCTTCCGGCGGCATCG
GGATGCCCGCGTTGCAGGCCATGCTGTCCAGGCAGGTAGATGACGACCATCAGGGACAGCTTCACG
GCCAGCAAAAGGCCAGGAACCGTAAAAAGGCCGCGTTGCTGGCGTTTTTCCATAGGCTCCGCCCCC
CTGACGAGCATCACAAAAATCGACGCTCAAGTCAGAGGTGGCGAAACCCGACAGGACTATAAAGATA
CCAGGCGTTTCCCCCTGGAAGCTCCCTCGTGCGCTCTCCTGTTCCGACCCTGCCGCTTACCGGATAC
CTGTCCGCCTTTCTCCCTTCGGGAAGCGTGGCGCTTTCTCAATGCTCACGCTGTAGGTATCTCAGTT
CGGTGTAGGTCGTTCGCTCCAAGCTGGGCTGTGTGCACGAACCCCCCGTTCAGCCCGACCGCTGCG
CCTTATCCGGTAACTATCGTCTTGAGTCCAACCCGGTAAGACACGACTTATCGCCACTGGCAGCAGC
CACTGGTAACAGGATTAGCAGAGCGAGGTATGTAGGCGGTGCTACAGAGTTCTTGAAGTGGTGGCC
TAACTACGGCTACACTAGAAGGACAGTATTTGGTATCTGCGCTCTGCTGAAGCCAGTTACCTTCGGA
AAAAGAGTTGGTAGCTCTTGATCCGGCAAACAAACCACCGCTGGTAGCGGTGGTTTTTTTGTTTGCA
AGCAGCAGATTACGCGCAGAAAAAAAGGATCTCAAGAAGATCCTTTGATCTTTTCTACGGGGTCTGA
CGCTCAGTGGAACGAAAACTCACGTTAAGGGATTTTGGTCATGAGATTATCAAAAAGGATCTTCACC
TAGATCCTTTTAAATCAATCTAAAGTATATATGAGTAAACTTGGTCTGACAGTTACCAATGCTTAATC
AGTGAGGCACCTATCTCAGCGATCTGTCTATTTCGTTCATCCATAGTTGCCTGACTCCCCGTCGTGT
AGATAACTACGATACGGGAGGGCTTACCATCTGGCCCCAGTGCTGCAATGATACCGCGAGACCCAC
GCTCACCGGCTCCAGATTTATCAGCAATAAACCAGCCAGCCGGAAGGGCCGAGCGCAGAAGTGGTC
CTGCAACTTTATCCGCCTCCATCCAGTCTATTAATTGTTGCCGGGAAGCTAGAGTAAGTAGTTCGCC
AGTTAATAGTTTGCGCAACGTTGTTGCCATTGNTGCAGGCATCGTGGTGTCACGCTCGTCGTTTGG
TATGGCTTCATTCAGCTCCGGTTCCCAACGATCAAGGCGAGTTACATGATCCCCCATGTTGTGCAAA
AAAGCGGTTAGCTCCTTCGGTCCTCCGATCGTTGTCAGAAGTAAGTTGGCCGCAGTGTTATCACTCA
TGGTTATGGCAGCACTGCATAATTCTCTTACTGTCATGCCATCCGTAAGATGCTTTTCTGTGACTGG
TGAGTACTCAACCAAGTCATTCTGAGAATAGTGTATGCGGCGACCGAGTTGCTCTTGCCCGGCGTCA
ACACGGGATAATACCGCGCCACATAGCAGAACTTTAAAAGTGCTCATCATTGGAAAACGTTCTTCGG
GGCGAAAACTCTCAAGGATCTTACCGCTGTTGAGATCCAGTTCGATGTAACCCACTCGTGCACCCAA
CTGATCTTCAGCATCTTTTACTTTCACCAGCGTTTCTGGGTGAGCAAAAACAGGAAGGCAAAATGCC
GCAAAAAAGGGAATAAGGGCGACACGGAAATGTTGAATACTCATACTCTTCCTTTTTCAATATTATT
GAAGCATTTATCAGGGTTATTGTCTCATGAGCGGATACATATTTGAATGTATTTAGAAAAATAAACA
AATAGGGGTTCCGCGCACATTTCCCCGAAAAGTGCCACCTGACGTCTAAGAAACCATTATTATCATG
ACATTAACCTATAAAAATAGGCGTATCACGAGGCCCTTTCGTCTTCAAGGATCCGAATTCCCGGGAG
AGCTCGATATCGCATGCGGATTTAAATTAATTAA

Appendix II – siRNA duplexes

Protein	Dharmacon product	Catalogue Number	Target (NCBI accession)
Non-targeting control	siGENOME Non-Targeting siRNA #3	D-001210-03	N/A
ERK5	ON-TARGETplus MAPK7 siRNA	J-003513-07 J-003513-08 J-003513-09 J-003513-10	NM_002749, NM_139033, NM_139034, NM_139032 (ORF)
RAF1	ON-TARGETplus RAF1 siRNA	J-003601-13 J-003601-14 J-003601-15 J-003601-16	NM_002880 (ORF)
HRAS	ON-TARGETplus HRAS siRNA	J-004142-07 J-004142-10	NM_001130442, NM_005343 (ORF), NM_176795 (3'UTR)
KRAS	ON-TARGETplus KRAS siRNA	J-005069-08 J-005069-10	NM_004985, NM_033360 (ORF)
		J-005069-09	NM_004985 (ORF), NM_033360 (3'UTR)
		J-005069-11	NM_004985, NM_033360 (3'UTR)
NRAS	ON-TARGETplus NRAS siRNA	J-003919-05 J-003919-06 J-003919-07	NM_002524 (ORF)

Appendix III – ERK5 mRNA sequence data

ERK5 mRNA sequence data for HeLa and HDMEC, compared against ERK5 NCBI reference sequence: NM_139033.2. Highlighted codons represent start (green) and stop codon (red).

```
ERK5  AGCGTGGCCTTGGGAGGCGGGGCGGAGGGGGACGGACAGGGCAGCTCAAGACGCTGAGGT
HeLa  ------------------------------------------------------------
HDMEC ------------------------------------------------------------


ERK5  GGTGGCTGCGGCCTTTGAACAAGTAAGTGAGCCACCCTCGGAGACCCCCGCGCTGGGGAC
HeLa  ------------------------------------------------------------
HDMEC ----------------------------------------------------TGGGGAC


ERK5  GGGAGGCCGGCGAGCCTCGGGACCTCTGAAAGCCTTGAGGAGGCGCGGGGACACCATGGC
HeLa  ---------------CTCGGGACCTCTGAAAGCCTTGAGGAGGCGCGGGGACACCATGGC
HDMEC GGGAGGCCGGCGAGCCTCGGGACCTCTGAAAGCCTTGAGGAGGCGCGGGGACACCATGGC
                         ****************************************

ERK5  CGAGCCTCTGAAGGAGGAAGACGGCGAGGACGGCTCTGCGGAGCCCCCCGGGCCCGTGAA
HeLa  CGAGCCTCTGAAGGAGGAAGACGGCGAGGACGGCTCTGCGGAGCCCCCCGGGCCCGTGAA
HDMEC CGAGCCTCTGAAGGAGGAAGACGGCGAGGACGGCTCTGCGGAGCCCCCCGGGCCCGTGAA
      ************************************************************

ERK5  GGCCGAACCCGCCCACACCGCTGCCTCTGTAGCGGCCAAGAACCTGGCCCTGCTTAAAGC
HeLa  GGCCGAACCCGCCCACACCGCTGCCTCTGTAGCGGCCAAGAACCTGGCCCTGCTTAAAGC
HDMEC GGCCGAACCCGCCCACACCGCTGCCTCTGTAGCGGCCAAGAACCTGGCCCTGCTTAAAGC
      ************************************************************

ERK5  CCGCTCCTTCGATGTGACCTTTGACGTGGGCGACGAGTACGAGATCATCGAGACCATAGG
HeLa  CCGCTCCTTCGATGTGACCTTTGACGTGGGCGACGAGTACGAGATCATCGAGACCATAGG
HDMEC CCGCTCCTTCGATGTGACCTTTGACGTGGGCGACGAGTACGAGATCATCGAGACCATAGG
      ************************************************************

ERK5  CAACGGGGCCTATGGAGTGGTGTCCTCCGCCCGCCGCCGCCTCACCGGCCAGCAGGTGGC
HeLa  CAACGGGGCCTATGGAGTGGTGTCCTCCGCCCGCCGCCGCCTCACCGGCCAGCAGGTGGC
HDMEC CAACGGGGCCTATGGAGTGGTGTCCTCCGCCCGCCGCCGCCTCACCGGCCAGCAGGTGGC
      ************************************************************

ERK5  CATCAAGAAGATCCCTAATGCTTTCGATGTGGTGACCAATGCCAAGCGGACCCTCAGGGA
HeLa  CATCAAGAAGATCCCTAATGCTTTCGATGTGGTGACCAATGCCAAGCGGACCCTCAGGGA
HDMEC CATCAAGAAGATCCCTAATGCTTTCGATGTGGTGACCAATGCCAAGCGGACCCTCAGGGA
      ************************************************************

ERK5  GCTGAAGATCCTCAAGCACTTTAAACACGACAACATCATCGCCATCAAGGACATCCTGAG
HeLa  GCTGAAGATCCTCAAGCACTTTAAACACGACAACATCATCGCCATCAAGGACATCCTGAG
HDMEC GCTGAAGATCCTCAAGCACTTTAAACACGACAACATCATCGCCATCAAGGACATCCTGAG
      ************************************************************

ERK5  GCCCACCGTGCCCTATGGCGAATTCAAATCTGTCTACGTGGTCCTGGACCTGATGGAAAG
HeLa  GCCCACCGTGCCCTATGGCGAATTCAAATCTGTCTACGTGGTCCTGGACCTGATGGAAAG
HDMEC GCCCACCGTGCCCTATGGCGAATTCAAATCTGTCTACGTGGTCCTGGACCTGATGGAAAG
      ************************************************************
```

```
ERK5  CGACCTGCACCAGATCATCCACTCCTCACAGCCCCTCACACTGGAACACGTGCGCTACTT
HeLa  CGACCTGCACCAGATCATCCACTCCTCACAGCCCCTCACACTGGAACACGTGCGCTACTT
HDMEC CGACCTGCACCAGATCATCCACTCCTCACAGCCCCTCACACTGGAACACGTGCGCTACTT
      ************************************************************

ERK5  CCTGTACCAACTGCTGCGGGGCCTGAAGTACATGCACTCGGCTCAGGTCATCCACCGTGA
HeLa  CCTGTACCAACTGCTGCGGGGCCTGAAGTACATGCACTCGGCTCAGGTCATCCACCGTGA
HDMEC CCTGTACCAACTGCTGCGGGGCCTGAAGTACATGCACTCGGCTCAGGTCATCCACCGTGA
      ************************************************************

ERK5  CCTGAAGCCCTCCAACCTATTGGTGAATGAGAACTGTGAGCTCAAGATTGGTGACTTTGG
HeLa  CCTGAAGCCCTCCAACCTATTGGTGAATGAGAACTGTGAGCTCAAGATTGGTGACTTTGG
HDMEC CCTGAAGCCCTCCAACCTATTGGTGAATGAGAACTGTGAGCTCAAGATTGGTGACTTTGG
      ************************************************************

ERK5  TATGGCTCGTGGCCTGTGCACCTCGCCCGCTGAACATCAGTACTTCATGACTGAGTATGT
HeLa  TATGGCTCGTGGCCTGTGCACCTCGCCCGCTGAACATCAGTACTTCATGACTGAGTATGT
HDMEC TATGGCTCGTGGCCTGTGCACCTCGCCCGCTGAACATCAGTACTTCATGACTGAGTATGT
      ************************************************************

ERK5  GGCCACGCGCTGGTACCGTGCGCCCGAGCTCATGCTCTCTTTGCATGAGTATACACAGGC
HeLa  GGCCACGCGCTGGTACCGTGCGCCCGAGCTCATGCTCTCTTTGCATGAGTATACACAGGC
HDMEC GGCCACGCGCTGGTACCGTGCGCCCGAGCTCATGCTCTCTTTGCATGAGTATACACAGGC
      ************************************************************

ERK5  TATTGACCTCTGGTCTGTGGGCTGCATCTTTGGTGAGATGCTGGCCCGGCGCCAGCTCTT
HeLa  TATTGACCTCTGGTCTGTGGGCTGCATCTTTGGTGAGATGCTGGCCCGGCGCCAGCTCTT
HDMEC TATTGACCTCTGGTCTGTGGGCTGCATCTTTGGTGAGATGCTGGCCCGGCGCCAGCTCTT
      ************************************************************

ERK5  CCCAGGCAAAAACTATGTACACCAGCTACAGCTCATCATGATGGTGCTGGGTACCCCATC
HeLa  CCCAGGCAAAAACTATGTACACCAGCTACAGCTCATCATGATGGTGCTGGGTACCCCATC
HDMEC CCCAGGCAAAAACTATGTACACCAGCTACAGCTCATCATGATGGTGCTGGGTACCCCATC
      ************************************************************

ERK5  ACCAGCCGTGATTCAGGCTGTGGGGGCTGAGAGGGTGCGGGCCTATATCCAGAGCTTGCC
HeLa  ACCAGCCGTGATTCAGGCTGTGGGGGCTGAGAGGGTGCGGGCCTATATCCAGAGCTTGCC
HDMEC ACCAGCCGTGATTCAGGCTGTGGGGGCTGAGAGGGTGCGGGCCTATATCCAGAGCTTGCC
      ************************************************************

ERK5  ACCACGCCAGCCTGTGCCCTGGGAGACAGTGTACCCAGGTGCCGACCGCCAGGCCCTATC
HeLa  ACCACGCCAGCCTGTGCCCTGGGAGACAGTGTACCCAGGTGCCGACCGCCAGGCCCTATC
HDMEC ACCACGCCAGCCTGTGCCCTGGGAGACAGTGTACCCAGGTGCCGACCGCCAGGCCCTATC
      ************************************************************

ERK5  ACTGCTGGGTCGCATGCTGCGTTTTGAGCCCAGCGCTCGCATCTCAGCAGCTGCTGCCCT
HeLa  ACTGCTGGGTCGCATGCTGCGTTTTGAGCCCAGCGCTCGCATCTCAGCAGCTGCTGCCCT
HDMEC ACTGCTGGGTCGCATGCTGCGTTTTGAGCCCAGCGCTCGCATCTCAGCAGCTGCTGCCCT
      ************************************************************

ERK5  TCGCCACCCTTTCCTGGCCAAGTACCATGATCCTGATGATGAGCCTGACTGTGCCCCGCC
HeLa  TCGCCACCCTTTCCTGGCCAAGTACCATGATCCTGATGATGAGCCTGACTGTGCCCCGCC
HDMEC TCGCCACCCTTTCCTGGCCAAGTACCATGATCCTGATGATGAGCCTGACTGTGCCCCGCC
      ************************************************************

ERK5  CTTTGACTTTGCCTTTGACCGCGAAGCCCTCACTCGGGAGCGCATTAAGGAGGCCATTGT
HeLa  CTTTGACTTTGCCTTTGACCGCGAAGCCCTCACTCGGGAGCGCATTAAGGAGGCCATTGT
HDMEC CTTTGACTTTGCCTTTGACCGCGAAGCCCTCACTCGGGAGCGCATTAAGGAGGCCATTGT
      ************************************************************
```

```
ERK5  GGCTGAAATTGAGGACTTCCATGCAAGGCGTGAGGGCATCCGCCAACAGATCCGCTTCCA
HeLa  GGCTGAAATTGAGGACTTCCATGCAAGGCGTGAGGGCATCCGCCAACAGATCCGCTTCCA
HDMEC GGCTGAAATTGAGGACTTCCATGCAAGGCGTGAGGGCATCCGCCAACAGATCCGCTTCCA
      ************************************************************
ERK5  GCCTTCTCTACAGCCTGTGGCTAGTGAGCCTGGCTGTCCAGATGTTGAAATGCCCAGTCC
HeLa  GCCTTCTCTACAGCCTGTGGCTAGTGAGCCTGGCTGTCCAGATGTTGAAATGCCCAGTCC
HDMEC GCCTTCTCTACAGCCTGTGGCTAGTGAGCCTGGCTGTCCAGATGTTGAAATGCCCAGTCC
      ************************************************************

ERK5  CTGGGCTCCCAGTGGGGACTGTGCCATGGAGTCTCCACCACCAGCCCCGCCACCATGCCC
HeLa  CTGGGCTCCCAGTGGGGACTGTGCCATGGAGTCTCCACCACCAGCCCCGCCACCATGCCC
HDMEC CTGGGCTCCCAGTGGGGACTGTGCCATGGAGTCTCCACCACCAGCCCCGCCACCATGCCC
      ************************************************************

ERK5  CGGCCCTGCACCTGACACCATTGATCTGACCCTGCAGCCACCTCCACCAGTCAGTGAGCC
HeLa  CGGCCCTGCACCTGACACCATTGATCTGACCCTGCAGCCACCTCCACCAGTCAGTGAGCC
HDMEC CGGCCCTGCACCTGACACCATTGATCTGACCCTGCAGCCACCTCCACCAGTCAGTGAGCC
      ************************************************************

ERK5  TGCCCCACCAAAGAAAGATGGTGCCATCTCAGACAATACTAAGGCTGCCCTTAAAGCTGC
HeLa  TGCCCCACCAAAGAAAGATGGTGCCATCTCAGACAATACTAAGGCTGCCCTTAAAGCTGC
HDMEC TGCCCCACCAAAGAAAGATGGTGCCATCTCAGACAATACTAAGGCTGCCCTTAAAGCTGC
      ************************************************************

ERK5  CCTGCTCAAGTCTTTGAGGAGCCGGCTCAGAGATGGCCCCAGCGCACCCCTGGAGGCTCC
HeLa  CCTGCTCAAGTCTTTGAGGAGCCGGCTCAGAGATGGCCCCAGCGCACCCCTGGAGGCTCC
HDMEC CCTGCTCAAGTCTTTGAGGAGCCGGCTCAGAGATGGCCCCAGCGCACCCCTGGAGGCTCC
      ************************************************************

ERK5  TGAGCCTCGGAAGCCGGTGACAGCCCAGGAGCGCCAGCGGGAGCGGGAGGAGAAGCGGCG
HeLa  TGAGCCTCGGAAGCCGGTGACAGCCCAGGAGCGCCAGCGGGAGCGGGAGGAGAAGCGGCG
HDMEC TGAGCCTCGGAAGCCGGTGACAGCCCAGGAGCGCCAGCGGGAGCGGGAGGAGAAGCGGCG
      ************************************************************

ERK5  GAGGCGGCAAGAACGAGCCAAGGAGCGGGAGAAACGGCGGCAGGAGCGGGAGCGAAAGGA
HeLa  GAGGCGGCAAGAACGAGCCAAGGAGCGGGAGAAACGGCGGCAGGAGCGGGAGCGAAAGGA
HDMEC GAGGCGGCAAGAACGAGCCAAGGAGCGGGAGAAACGGCGGCAGGAGCGGGAGCGAAAGGA
      ************************************************************

ERK5  ACGGGGGGCTGGGGCCTCTGGGGGCCCCTCCACTGACCCCTTGGCTGGACTAGTGCTCAG
HeLa  ACGGGGGGCTGGGGCCTCTGGGGGCCCCTCCACTGACCCCTTGGCTGGACTAGTGCTCAG
HDMEC ACGGGGGGCTGGGGCCTCTGGGGGCCCCTCCACTGACCCCTTGGCTGGACTAGTGCTCAG
      ************************************************************

ERK5  TGACAATGACAGAAGCCTGTTGGAACGCTGGACTCGAATGGCCCGGCCCGCAGCCCCAGC
HeLa  TGACAATGACAGAAGCCTGTTGGAACGCTGGACTCGAATGGCCCGGCCCGCAGCCCCAGC
HDMEC TGACAATGACAGAAGCCTGTTGGAACGCTGGACTCGAATGGCCCGGCCCGCAGCCCCAGC
      ************************************************************

ERK5  CCTCACCTCTGTGCCGGCCCCTGCCCCAGCGCCAACGCCAACCCCAACCCCAGTCCAACC
HeLa  CCTCACCTCTGTGCCGGCCCCTGCCCCAGCGCCAACGCCAACCCCAACCCCAGTCCAACC
HDMEC CCTCACCTCTGTGCCGGCCCCTGCCCCAGCGCCAACGCCAACCCCAACCCCAGTCCAACC
      ************************************************************

ERK5  TACCAGTCCTCCTCCTGGCCCTGTAGCCCAGCCCACTGGCCCGCAACCACAATCTGCGGG
HeLa  TACCAGTCCTCCTCCTGGCCCTGTAGCCCAGCCCACTGGCCCGCAACCACAATCTGCGGG
HDMEC TACCAGTCCTCCTCCTGGCCCTGTAGCCCAGCCCACTGGCCCGCAACCACAATCTGCGGG
      ************************************************************
```

```
ERK5   CTCTACCTCTGGCCCTGTACCCCAGCCTGCCTGCCCACCCCCTGGCCCTGCACCCCACCC
HeLa   CTCTACCTCTGGCCCTGTACCCCAGCCTGCCTGCCCACCCCCTGGCCCTGCACCCCACCC
HDMEC  CTCTACCTCTGGCCCTGTACCCCAGCCTGCCTGCCCACCCCCTGGCCCTGCACCCCACCC
       ************************************************************

ERK5   CACTGGCCCTCCTGGGCCCATCCCTGTCCCCGCGCCACCCCAGATTGCCACCTCCACCAG
HeLa   CACTGGCCCTCCTGGGCCCATCCCTGTCCCCGCGCCACCCCAGATTGCCACCTCCACCAG
HDMEC  CACTGGCCCTCCTGGGCCCATCCCTGTCCCCGCGCCACCCCAGATTGCCACCTCCACCAG
       ************************************************************

ERK5   CCTCCTGGCTGCCCAGTCACTTGTGCCACCCCCTGGGCTGCCTGGCTCCAGCACCCCAGG
HeLa   CCTCCTGGCTGCCCAGTCACTTGTGCCACCCCCTGGGCTGCCTGGCTCCAGCACCCCAGG
HDMEC  CCTCCTGGCTGCCCAGTCACTTGTGCCACCCCCTGGGCTGCCTGGCTCCAGCACCCCAGG
       ************************************************************

ERK5   AGTTTTGCCTTACTTCCCACCTGGCCTGCCGCCCCCAGACGCCGGGGGAGCCCCTCAGTC
HeLa   AGTTTTGCCTTACTTCCCACCTGGCCTGCCGCCCCCAGACGCCGGGGGAGCCCCTCAGTC
HDMEC  AGTTTTGCCTTACTTCCCACCTGGCCTGCCGCCCCCAGACGCCGGGGGAGCCCCTCAGTC
       ************************************************************

ERK5   TTCCATGTCAGAGTCACCTGATGTCAACCTTGTGACCCAGCAGCTATCTAAGTCACAGGT
HeLa   TTCCATGTCAGAGTCACCTGATGTCAACCTTGTGACCCAGCAGCTATCTAAGTCACAGGT
HDMEC  TTCCATGTCAGAGTCACCTGATGTCAACCTTGTGACCCAGCAGCTATCTAAGTCACAGGT
       ************************************************************

ERK5   GGAGGACCCCCTGCCCCCTGTGTTCTCAGGCACACCAAAGGGCAGTGGGGCTGGCTACGG
HeLa   GGAGGACCCCCTGCCCCCTGTGTTCTCAGGCACACCAAAGGGCAGTGGGGCTGGCTACGG
HDMEC  GGAGGACCCCCTGCCCCCTGTGTTCTCAGGCACACCAAAGGGCAGTGGGGCTGGCTACGG
       ************************************************************

ERK5   TGTTGGCTTTGACCTGGAGGAATTCTTAAACCAGTCTTTCGACATGGGCGTGGCTGATGG
HeLa   TGTTGGCTTTGACCTGGAGGAATTCTTAAACCAGTCTTTCGACATGGGCGTGGCTGATGG
HDMEC  TGTTGGCTTTGACCTGGAGGAATTCTTAAACCAGTCTTTCGACATGGGCGTGGCTGATGG
       ************************************************************

ERK5   GCCACAGGATGGCCAGGCAGATTCAGCCTCTCTCTCAGCCTCCCTGCTTGCTGACTGGCT
HeLa   GCCACAGGATGGCCAGGCAGATTCAGCCTCTCTCTCAGCCTCCCTGCTTGCTGACTGGCT
HDMEC  GCCACAGGATGGCCAGGCAGATTCAGCCTCTCTCTCAGCCTCCCTGCTTGCTGACTGGCT
       ************************************************************

ERK5   CGAAGGCCATGGCATGAACCCTGCCGATATTGAGTCCCTGCAGCGTGAGATCCAGATGGA
HeLa   CGAAGGCCATGGCATGAACCCTGCCGATATTGAGTCCCTGCAGCGTGAGATCCAGATGGA
HDMEC  CGAAGGCCATGGCATGAACCCTGCCGATATTGAGTCCCTGCAGCGTGAGATCCAGATGGA
       ************************************************************

ERK5   CTCCCCAATGCTGCTGGCTGACCTGCCTGACCTCCAGGACCCCTGAGGCCCCCAGCCTGT
HeLa   CTCCCCAATGCTGCTGGCTGACCTGCCTGACCTCCAGGACCCCTGAGGCCCCCAGCCTGT
HDMEC  CTCCCCAATGCTGCTGGCTGACCTGCCTGACCTCCAGGACCCCTGAGGCCCCCAGCCTGT
       ************************************************************

ERK5   GCCTTGCTGCCACAGTAGACCTAGTTCCAGGATCCATGGGAGCATTCTCAAAGGCTTTAG
HeLa   GCCTTGCTGC----------------------------------------------------
HDMEC  GCCTTGCTGCCACAGTAGACCTAGTTCCAGGATCCATGGGAGCATTCTCAAAGGCTTTAG
       **********

ERK5   CCCTGGACCCAGCAGGTGAGGCTCGGCTTGGATTATTCTGCAGGTTCATCTCAGACCCAC
HeLa   ------------------------------------------------------------
HDMEC  CCCTGGACCCAGCAGGTGAGGCTCGGCTTGGATTATTCTGCAGGTTCATCTCAGACCCAC
```

```
ERK5  CTTTCAGCCTTAAGCAGCCACCTGAGCCACCACCGAGCCATGGCAGGATCGGGAGACCCC
HeLa  ------------------------------------------------------------
HDMEC CTTTCAGCCTTAAGCAGCCACCTGAGCCAC------------------------------

ERK5  AACTCCCCCTGAACAATCCTTTTCAGTATTATATTTTTATTATTATTATGTTATTATTAC
HeLa  ------------------------------------------------------------
HDMEC ------------------------------------------------------------


ERK5  ACTGTCTTTTTGCCATCAAAATGAGGCCTGTGAAATACAAGGTTCCCTTCTGCACCTGAA
HeLa  ------------------------------------------------------------
HDMEC ------------------------------------------------------------


ERK5            AAAAAAAAAAAAAAAAAAAAAAAAAAAAAA
HeLa            --------------------------------
HDMEC           --------------------------------
```

Appendix IV - Subcellular protein fractionation controls

HDMEC were seeded on 10 cm plates for 24 h prior to overnight serum starvation and stimulation with 50 ng/mL VEGF for 10, 30 and 60 min. Cells were then lysed with the appropriate buffers from the Thermo Fischer Subcellular Fractionation Kit. Lysates were separated on a 4-12% NuPAGE gel as well as a 7% (w/v) acrylamide, 70 μM Phos-tag™ gel, followed by Western blotting (WB) with antibodies against CD31 (membrane control), Lamin (nuclear control) and GAPDH (cytoplasm control). *Densitometric analysis of protein expression relative to the whole cell lysate of each subcellular region, is displayed beneath each blot to highlight protein enrichment. The whole cell lysate was set arbitrarily as 1.0 for each protein. This result is representative of two independent experiments.*

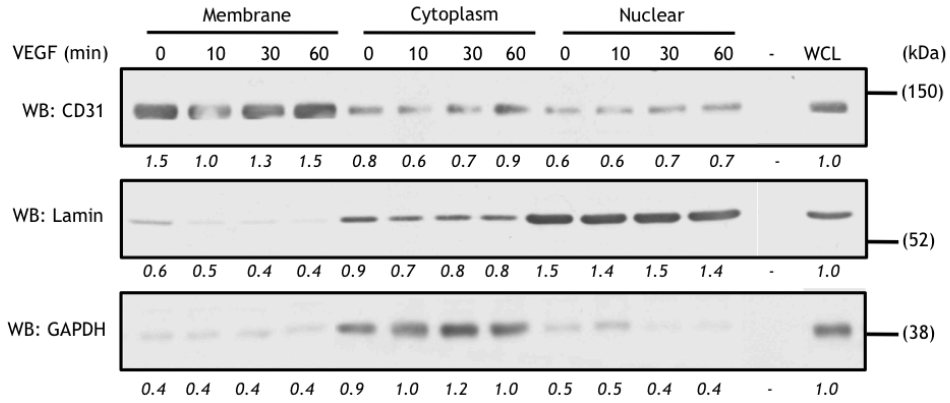

Appendix V – Readout of ERK5-interacting proteins in HDMEC discovered by LC-MS/MS

Proteins discovered in the untransduced, basal condition after LC-MS/MS, in Run 1 (blue), Run 2 (green) and Run 3 (pink)

Accession	Description	Score	Coverage	# Proteins	# Unique Peptides	# Peptides	# PSMs	# AAs	MW [kDa]	calc. pI
P01616	Ig kappa chain V-II region MIL OS=Homo sapiens PE=1 SV=1 - [KV203_HUMAN]	208.47	11.61	5	1	1	5	112	12.0	9.29
O14744	Protein arginine N-methyltransferase 5 OS=Homo sapiens GN=PRMT5 PE=1 SV=4 - [ANM5_HUMAN]	48.24	10.52	1	2	7	7	637	72.6	6.29
O14744	Protein arginine N-methyltransferase 5 OS=Homo sapiens GN=PRMT5 PE=1 SV=4 - [ANM5_HUMAN]	65.66	10.52	1	2	8	8	637	72.6	6.29
O14744	Protein arginine N-methyltransferase 5 OS=Homo sapiens GN=PRMT5 PE=1 SV=4 - [ANM5_HUMAN]	61.81	13.50	1	2	9	9	637	72.6	6.29
O60814	Histone H2B type 1-K OS=Homo sapiens GN=HIST1H2BK PE=1 SV=3 - [H2B1K_HUMAN]	56.54	19.05	14	1	2	2	126	13.9	10.32
O60814	Histone H2B type 1-K OS=Homo sapiens GN=HIST1H2BK PE=1 SV=3 - [H2B1K_HUMAN]	70.59	11.90	14	1	1	1	126	13.9	10.32
P01616	Ig kappa chain V-II region MIL OS=Homo sapiens PE=1 SV=1 - [KV203_HUMAN]	195.39	11.61	5	1	1	5	112	12.0	9.29
P01616	Ig kappa chain V-II region MIL OS=Homo sapiens PE=1 SV=1 - [KV203_HUMAN]	181.96	11.61	5	1	1	5	112	12.0	9.29
P01859	Ig gamma-2 chain C region OS=Homo sapiens GN=IGHG2 PE=1 SV=2 - [IGHG2_HUMAN]	38.74	2.76	1	1	1	1	326	35.9	7.59
P01859	Ig gamma-2 chain C region OS=Homo sapiens GN=IGHG2 PE=1 SV=2 - [IGHG2_HUMAN]	39.79	2.76	1	1	1	1	326	35.9	7.59
P02768	Serum albumin OS=Homo sapiens GN=ALB PE=1 SV=2 - [ALBU_HUMAN]	80.28	8.21	1	2	6	9	609	69.3	6.28
P02768	Serum albumin OS=Homo sapiens GN=ALB PE=1 SV=2 - [ALBU_HUMAN]	66.39	8.21	1	3	5	5	609	69.3	6.28
P04264	Keratin, type II cytoskeletal 1 OS=Homo sapiens GN=KRT1 PE=1 SV=6 - [K2C1_HUMAN]	62.83	9.47	6	2	6	6	644	66.0	8.12
P04264	Keratin, type II cytoskeletal 1 OS=Homo sapiens GN=KRT1 PE=1 SV=6 - [K2C1_HUMAN]	344.82	27.64	6	13	17	17	644	66.0	8.12
P04264	Keratin, type II cytoskeletal 1 OS=Homo sapiens GN=KRT1 PE=1 SV=6 - [K2C1_HUMAN]	53.03	7.92	2	2	5	5	644	66.0	8.12

P07437	Tubulin beta chain OS=Homo sapiens GN=TUBB PE=1 SV=2 - [TBB5_HUMAN]	71.09	9.68	11	2	4	4	444	49.6	4.89
P13645	Keratin, type I cytoskeletal 10 OS=Homo sapiens GN=KRT10 PE=1 SV=6 - [K1C10_HUMAN]	41.16	6.34	17	1	4	4	584	58.8	5.21
P13645	Keratin, type I cytoskeletal 10 OS=Homo sapiens GN=KRT10 PE=1 SV=6 - [K1C10_HUMAN]	156.28	24.32	10	6	14	14	584	58.8	5.21
P19474	E3 ubiquitin-protein ligase TRIM21 OS=Homo sapiens GN=TRIM21 PE=1 SV=1 - [RO52_HUMAN]	42.08	1.89	1	1	1	1	475	54.1	6.38
P19474	E3 ubiquitin-protein ligase TRIM21 OS=Homo sapiens GN=TRIM21 PE=1 SV=1 - [RO52_HUMAN]	45.39	1.89	1	1	1	1	475	54.1	6.38
P35527	Keratin, type I cytoskeletal 9 OS=Homo sapiens GN=KRT9 PE=1 SV=3 - [K1C9_HUMAN]	161.52	27.61	7	7	14	15	623	62.0	5.24
P35908	Keratin, type II cytoskeletal 2 epidermal OS=Homo sapiens GN=KRT2 PE=1 SV=2 - [K22E_HUMAN]	92.24	15.18	12	3	9	9	639	65.4	8.00
P35908	Keratin, type II cytoskeletal 2 epidermal OS=Homo sapiens GN=KRT2 PE=1 SV=2 - [K22E_HUMAN]	53.75	5.32	1	1	3	3	639	65.4	8.00
P52732	Kinesin-like protein KIF11 OS=Homo sapiens GN=KIF11 PE=1 SV=2 - [KIF11_HUMAN]	41.48	2.08	1	1	2	2	1056	119.1	5.64
P52732	Kinesin-like protein KIF11 OS=Homo sapiens GN=KIF11 PE=1 SV=2 - [KIF11_HUMAN]	35.87	10.70	1	1	12	12	1056	119.1	5.64
P53999	Activated RNA polymerase II transcriptional coactivator p15 OS=Homo sapiens GN=SUB1 PE=1 SV=3 - [TCP4_HUMAN]	59.85	8.66	1	1	1	1	127	14.4	9.60
P60709	Actin, cytoplasmic 1 OS=Homo sapiens GN=ACTB PE=1 SV=1 - [ACTB_HUMAN]	0.00	13.87	14	1	5	5	375	41.7	5.48
P62805	Histone H4 OS=Homo sapiens GN=HIST1H4A PE=1 SV=2 - [H4_HUMAN]	42.26	29.13	1	1	3	3	103	11.4	11.36
P62805	Histone H4 OS=Homo sapiens GN=HIST1H4A PE=1 SV=2 - [H4_HUMAN]	44.41	29.13	1	1	3	3	103	11.4	11.36
P68363	Tubulin alpha-1B chain OS=Homo sapiens GN=TUBA1B PE=1 SV=1 - [TBA1B_HUMAN]	114.63	22.17	8	5	7	8	451	50.1	5.06
P68371	Tubulin beta-4B chain OS=Homo sapiens GN=TUBB4B PE=1 SV=1 - [TBB4B_HUMAN]	68.61	14.83	11	1	6	6	445	49.8	4.89
Q92851	Caspase-10 OS=Homo sapiens GN=CASP10 PE=1 SV=3 - [CASPA_HUMAN]	36.56	0.96	2	1	1	1	521	58.9	7.33
Q92851	Caspase-10 OS=Homo sapiens GN=CASP10 PE=1 SV=3 - [CASPA_HUMAN]	36.61	0.96	2	1	1	1	521	58.9	7.33
Q9BQA1	Methylosome protein 50 OS=Homo sapiens GN=WDR77 PE=1 SV=1 - [MEP50_HUMAN]	58.94	5.56	1	1	2	2	342	36.7	5.17

Q9BQA1	Methylosome protein 50 OS=Homo sapiens GN=WDR77 PE=1 SV=1 - [MEP50_HUMAN]	47.34	12.57	1	1	3	3	342	36.7	5.17
Q9BQA1	Methylosome protein 50 OS=Homo sapiens GN=WDR77 PE=1 SV=1 - [MEP50_HUMAN]	57.60	16.96	1	2	4	4	342	36.7	5.17
Q9BQE3	Tubulin alpha-1C chain OS=Homo sapiens GN=TUBA1C PE=1 SV=1 - [TBA1C_HUMAN]	43.07	17.37	5	1	5	5	449	49.9	5.10
Q9BQE3	Tubulin alpha-1C chain OS=Homo sapiens GN=TUBA1C PE=1 SV=1 - [TBA1C_HUMAN]	92.55	12.69	8	3	4	4	449	49.9	5.10

Proteins discovered in the transduced, basal condition after LC-MS/MS, in Run 1 (blue), Run 2 (green) and Run 3 (pink)

Accession	Description	Score	Coverage	# Proteins	# Unique Peptides	# Peptides	# PSMs	# AAs	MW [kDa]	calc. pI
P01616	Ig kappa chain V-II region MIL OS=Homo sapiens PE=1 SV=1 - [KV203_HUMAN]	244.54	11.61	5	1	1	6	112	12.0	9.29
O14744	Protein arginine N-methyltransferase 5 OS=Homo sapiens GN=PRMT5 PE=1 SV=4 - [ANM5_HUMAN]	81.94	14.60	1	3	10	10	637	72.6	6.29
O14744	Protein arginine N-methyltransferase 5 OS=Homo sapiens GN=PRMT5 PE=1 SV=4 - [ANM5_HUMAN]	83.57	20.72	1	4	13	13	637	72.6	6.29
O60814	Histone H2B type 1-K OS=Homo sapiens GN=HIST1H2BK PE=1 SV=3 - [H2B1K_HUMAN]	36.69	19.05	14	1	2	2	126	13.9	10.32
P01616	Ig kappa chain V-II region MIL OS=Homo sapiens PE=1 SV=1 - [KV203_HUMAN]	198.69	11.61	5	1	1	5	112	12.0	9.29
P01616	Ig kappa chain V-II region MIL OS=Homo sapiens PE=1 SV=1 - [KV203_HUMAN]	246.65	11.61	5	1	1	9	112	12.0	9.29
P01700	Ig lambda chain V-I region HA OS=Homo sapiens PE=1 SV=1 - [LV102_HUMAN]	34.08	4.46	8	1	1	1	112	11.9	8.91
P01859	Ig gamma-2 chain C region OS=Homo sapiens GN=IGHG2 PE=1 SV=2 - [IGHG2_HUMAN]	36.59	2.76	1	1	1	1	326	35.9	7.59
P02768	Serum albumin OS=Homo sapiens GN=ALB PE=1 SV=2 - [ALBU_HUMAN]	145.41	8.21	1	2	6	17	609	69.3	6.28
P02768	Serum albumin OS=Homo sapiens GN=ALB PE=1 SV=2 - [ALBU_HUMAN]	51.02	3.61	1	1	2	2	609	69.3	6.28

P02768	Serum albumin OS=Homo sapiens GN=ALB PE=1 SV=2 - [ALBU_HUMAN]	50.79	3.61	1	1	2	2	609	69.3	6.28
P04264	Keratin, type II cytoskeletal 1 OS=Homo sapiens GN=KRT1 PE=1 SV=6 - [K2C1_HUMAN]	301.08	26.86	5	14	16	16	644	66.0	8.12
P04264	Keratin, type II cytoskeletal 1 OS=Homo sapiens GN=KRT1 PE=1 SV=6 - [K2C1_HUMAN]	70.76	8.39	2	3	6	6	644	66.0	8.12
P07437	Tubulin beta chain OS=Homo sapiens GN=TUBB PE=1 SV=2 - [TBB5_HUMAN]	69.44	10.36	11	3	4	4	444	49.6	4.89
P07437	Tubulin beta chain OS=Homo sapiens GN=TUBB PE=1 SV=2 - [TBB5_HUMAN]	61.90	17.57	11	2	7	7	444	49.6	4.89
P08238	Heat shock protein HSP 90-beta OS=Homo sapiens GN=HSP90AB1 PE=1 SV=4 - [HS90B_HUMAN]	46.19	2.21	4	1	2	2	724	83.2	5.03
P13645	Keratin, type I cytoskeletal 10 OS=Homo sapiens GN=KRT10 PE=1 SV=6 - [K1C10_HUMAN]	220.72	22.60	21	8	13	13	584	58.8	5.21
P19474	E3 ubiquitin-protein ligase TRIM21 OS=Homo sapiens GN=TRIM21 PE=1 SV=1 - [RO52_HUMAN]	43.49	1.89	1	1	1	1	475	54.1	6.38
P35527	Keratin, type I cytoskeletal 9 OS=Homo sapiens GN=KRT9 PE=1 SV=3 - [K1C9_HUMAN]	123.58	18.78	2	5	8	9	623	62.0	5.24
P35908	Keratin, type II cytoskeletal 2 epidermal OS=Homo sapiens GN=KRT2 PE=1 SV=2 - [K22E_HUMAN]	106.25	16.28	10	5	10	10	639	65.4	8.00
P35908	Keratin, type II cytoskeletal 2 epidermal OS=Homo sapiens GN=KRT2 PE=1 SV=2 - [K22E_HUMAN]	40.11	3.44	1	1	2	2	639	65.4	8.00
P52732	Kinesin-like protein KIF11 OS=Homo sapiens GN=KIF11 PE=1 SV=2 - [KIF11_HUMAN]	37.07	7.95	1	1	9	9	1056	119.1	5.64
P53999	Activated RNA polymerase II transcriptional coactivator p15 OS=Homo sapiens GN=SUB1 PE=1 SV=3 - [TCP4_HUMAN]	63.64	8.66	1	1	1	1	127	14.4	9.60
P60709	Actin, cytoplasmic 1 OS=Homo sapiens GN=ACTB PE=1 SV=1 - [ACTB_HUMAN]	40.65	18.93	10	1	6	6	375	41.7	5.48
P60709	Actin, cytoplasmic 1 OS=Homo sapiens GN=ACTB PE=1 SV=1 - [ACTB_HUMAN]	43.22	21.87	10	1	8	8	375	41.7	5.48
P62805	Histone H4 OS=Homo sapiens GN=HIST1H4A PE=1 SV=2 - [H4_HUMAN]	44.71	29.13	1	1	3	3	103	11.4	11.36
P62805	Histone H4 OS=Homo sapiens GN=HIST1H4A PE=1 SV=2 - [H4_HUMAN]	50.58	29.13	1	1	3	3	103	11.4	11.36
P68363	Tubulin alpha-1B chain OS=Homo sapiens GN=TUBA1B PE=1 SV=1 - [TBA1B_HUMAN]	101.64	20.62	6	4	6	6	451	50.1	5.06
P68363	Tubulin alpha-1B chain OS=Homo sapiens GN=TUBA1B PE=1 SV=1 - [TBA1B_HUMAN]	148.18	18.63	8	5	6	7	451	50.1	5.06

Q13164	Mitogen-activated protein kinase 7 OS=Homo sapiens GN=MAPK7 PE=1 SV=2 - [MK07_HUMAN]	80.09	18.87	1	2	14	20	816	88.3	5.88
Q13164	Mitogen-activated protein kinase 7 OS=Homo sapiens GN=MAPK7 PE=1 SV=2 - [MK07_HUMAN]	264.73	28.43	3	12	21	26	816	88.3	5.88
Q13164	Mitogen-activated protein kinase 7 OS=Homo sapiens GN=MAPK7 PE=1 SV=2 - [MK07_HUMAN]	309.01	32.84	1	12	26	33	816	88.3	5.88
Q92851	Caspase-10 OS=Homo sapiens GN=CASP10 PE=1 SV=3 - [CASPA_HUMAN]	33.80	0.96	2	1	1	1	521	58.9	7.33
Q92851	Caspase-10 OS=Homo sapiens GN=CASP10 PE=1 SV=3 - [CASPA_HUMAN]	0.00	0.96	2	1	1	1	521	58.9	7.33
Q9BQA1	Methylosome protein 50 OS=Homo sapiens GN=WDR77 PE=1 SV=1 - [MEP50_HUMAN]	70.73	9.94	1	2	3	3	342	36.7	5.17
Q9BQA1	Methylosome protein 50 OS=Homo sapiens GN=WDR77 PE=1 SV=1 - [MEP50_HUMAN]	86.33	9.94	1	3	3	3	342	36.7	5.17
Q9BQE3	Tubulin alpha-1C chain OS=Homo sapiens GN=TUBA1C PE=1 SV=1 - [TBA1C_HUMAN]	55.09	7.57	5	1	3	3	449	49.9	5.10
Q9UHT4	Putative uncharacterized protein PRO1854 OS=Homo sapiens GN=PRO1854 PE=5 SV=1 - [YG001_HUMAN]	27.17	7.46	6	1	1	2	67	8.3	10.08

Proteins discovered in the transduced, 30 min VEGF stimulated condition after LC-MS/MS, in Run 1 (blue), Run 2 (green) and Run 3 (pink)

Accession	Description	Score	Coverage	# Proteins	# Unique Peptides	# Peptides	# PSMs	# AAs	MW [kDa]	calc. pI
O14744	Protein arginine N-methyltransferase 5 OS=Homo sapiens GN=PRMT5 PE=1 SV=4 - [ANM5_HUMAN]	87.37	19.31	1	4	13	13	637	72.6	6.29
O14744	Protein arginine N-methyltransferase 5 OS=Homo sapiens GN=PRMT5 PE=1 SV=4 - [ANM5_HUMAN]	71.42	18.68	1	3	13	13	637	72.6	6.29
O14744	Protein arginine N-methyltransferase 5 OS=Homo sapiens GN=PRMT5 PE=1 SV=4 - [ANM5_HUMAN]	68.57	15.86	1	3	11	11	637	72.6	6.29
O60814	Histone H2B type 1-K OS=Homo sapiens GN=HIST1H2BK PE=1 SV=3 - [H2B1K_HUMAN]	59.52	19.05	14	1	2	2	126	13.9	10.32
O60814	Histone H2B type 1-K OS=Homo sapiens GN=HIST1H2BK PE=1 SV=3 - [H2B1K_HUMAN]	61.77	19.05	14	1	2	2	126	13.9	10.32
P01616	Ig kappa chain V-II region MIL OS=Homo sapiens PE=1 SV=1 - [KV203_HUMAN]	234.26	11.61	5	1	1	6	112	12.0	9.29
P01616	Ig kappa chain V-II region MIL OS=Homo sapiens PE=1 SV=1 - [KV203_HUMAN]	200.82	11.61	5	1	1	5	112	12.0	9.29
P01616	Ig kappa chain V-II region MIL OS=Homo sapiens PE=1 SV=1 - [KV203_HUMAN]	249.65	11.61	5	1	1	7	112	12.0	9.29
P01859	Ig gamma-2 chain C region OS=Homo sapiens GN=IGHG2 PE=1 SV=2 - [IGHG2_HUMAN]	36.95	2.76	1	1	1	1	326	35.9	7.59
P02768	Serum albumin OS=Homo sapiens GN=ALB PE=1 SV=2 - [ALBU_HUMAN]	50.62	2.46	1	1	1	1	609	69.3	6.28
P02768	Serum albumin OS=Homo sapiens GN=ALB PE=1 SV=2 - [ALBU_HUMAN]	45.91	5.09	1	1	3	3	609	69.3	6.28
P04264	Keratin, type II cytoskeletal 1 OS=Homo sapiens GN=KRT1 PE=1 SV=6 - [K2C1_HUMAN]	116.09	11.96	2	4	8	8	644	66.0	8.12
P04264	Keratin, type II cytoskeletal 1 OS=Homo sapiens GN=KRT1 PE=1 SV=6 - [K2C1_HUMAN]	177.97	21.27	5	9	13	13	644	66.0	8.12
P04264	Keratin, type II cytoskeletal 1 OS=Homo sapiens GN=KRT1 PE=1 SV=6 - [K2C1_HUMAN]	81.82	11.80	2	4	8	8	644	66.0	8.12
P07437	Tubulin beta chain OS=Homo sapiens GN=TUBB PE=1 SV=2 - [TBB5_HUMAN]	61.09	13.06	11	2	5	5	444	49.6	4.89
P08670	Vimentin OS=Homo sapiens GN=VIM PE=1 SV=4 - [VIME_HUMAN]	37.12	4.51	1	1	2	2	466	53.6	5.12

P13645	Keratin, type I cytoskeletal 10 OS=Homo sapiens GN=KRT10 PE=1 SV=6 - [K1C10_HUMAN]	43.92	9.59	1	1	6	6	584	58.8	5.21
P13645	Keratin, type I cytoskeletal 10 OS=Homo sapiens GN=KRT10 PE=1 SV=6 - [K1C10_HUMAN]	137.35	16.61	17	5	10	10	584	58.8	5.21
P13645	Keratin, type I cytoskeletal 10 OS=Homo sapiens GN=KRT10 PE=1 SV=6 - [K1C10_HUMAN]	41.49	9.59	8	1	6	6	584	58.8	5.21
P19474	E3 ubiquitin-protein ligase TRIM21 OS=Homo sapiens GN=TRIM21 PE=1 SV=1 - [RO52_HUMAN]	43.25	1.89	1	1	1	1	475	54.1	6.38
P35527	Keratin, type I cytoskeletal 9 OS=Homo sapiens GN=KRT9 PE=1 SV=3 - [K1C9_HUMAN]	63.55	6.58	1	1	4	4	623	62.0	5.24
P35527	Keratin, type I cytoskeletal 9 OS=Homo sapiens GN=KRT9 PE=1 SV=3 - [K1C9_HUMAN]	88.04	11.40	1	3	6	6	623	62.0	5.24
P35908	Keratin, type II cytoskeletal 2 epidermal OS=Homo sapiens GN=KRT2 PE=1 SV=2 - [K22E_HUMAN]	87.65	8.14	4	3	5	5	639	65.4	8.00
P35908	Keratin, type II cytoskeletal 2 epidermal OS=Homo sapiens GN=KRT2 PE=1 SV=2 - [K22E_HUMAN]	52.16	5.32	1	1	3	3	639	65.4	8.00
P52732	Kinesin-like protein KIF11 OS=Homo sapiens GN=KIF11 PE=1 SV=2 - [KIF11_HUMAN]	55.70	2.46	1	1	3	3	1056	119.1	5.64
P53999	Activated RNA polymerase II transcriptional coactivator p15 OS=Homo sapiens GN=SUB1 PE=1 SV=3 - [TCP4_HUMAN]	66.77	8.66	1	1	1	1	127	14.4	9.60
P53999	Activated RNA polymerase II transcriptional coactivator p15 OS=Homo sapiens GN=SUB1 PE=1 SV=3 - [TCP4_HUMAN]	41.88	8.66	1	1	1	1	127	14.4	9.60
P53999	Activated RNA polymerase II transcriptional coactivator p15 OS=Homo sapiens GN=SUB1 PE=1 SV=3 - [TCP4_HUMAN]	53.42	8.66	1	1	1	1	127	14.4	9.60
P60709	Actin, cytoplasmic 1 OS=Homo sapiens GN=ACTB PE=1 SV=1 - [ACTB_HUMAN]	62.25	13.87	14	2	5	5	375	41.7	5.48
P60709	Actin, cytoplasmic 1 OS=Homo sapiens GN=ACTB PE=1 SV=1 - [ACTB_HUMAN]	56.30	16.00	10	1	6	6	375	41.7	5.48
P60709	Actin, cytoplasmic 1 OS=Homo sapiens GN=ACTB PE=1 SV=1 - [ACTB_HUMAN]	36.82	16.00	14	1	6	6	375	41.7	5.48
P62805	Histone H4 OS=Homo sapiens GN=HIST1H4A PE=1 SV=2 - [H4_HUMAN]	42.55	17.48	1	1	2	2	103	11.4	11.36
P62805	Histone H4 OS=Homo sapiens GN=HIST1H4A PE=1 SV=2 - [H4_HUMAN]	55.72	17.48	1	1	2	2	103	11.4	11.36
P62805	Histone H4 OS=Homo sapiens GN=HIST1H4A PE=1 SV=2 - [H4_HUMAN]	53.03	29.13	1	1	3	3	103	11.4	11.36

P68363	Tubulin alpha-1B chain OS=Homo sapiens GN=TUBA1B PE=1 SV=1 - [TBA1B_HUMAN]	114.98	14.86	8	5	5	5	451	50.1	5.06
P68363	Tubulin alpha-1B chain OS=Homo sapiens GN=TUBA1B PE=1 SV=1 - [TBA1B_HUMAN]	75.52	16.63	5	2	5	5	451	50.1	5.06
P68363	Tubulin alpha-1B chain OS=Homo sapiens GN=TUBA1B PE=1 SV=1 - [TBA1B_HUMAN]	123.83	18.63	8	5	6	6	451	50.1	5.06
P68371	Tubulin beta-4B chain OS=Homo sapiens GN=TUBB4B PE=1 SV=1 - [TBB4B_HUMAN]	59.41	15.73	11	2	6	6	445	49.8	4.89
Q13164	Mitogen-activated protein kinase 7 OS=Homo sapiens GN=MAPK7 PE=1 SV=2 - [MK07_HUMAN]	266.01	28.19	1	9	22	27	816	88.3	5.88
Q13164	Mitogen-activated protein kinase 7 OS=Homo sapiens GN=MAPK7 PE=1 SV=2 - [MK07_HUMAN]	223.86	34.68	1	9	26	30	816	88.3	5.88
Q13164	Mitogen-activated protein kinase 7 OS=Homo sapiens GN=MAPK7 PE=1 SV=2 - [MK07_HUMAN]	292.05	30.15	1	11	25	30	816	88.3	5.88
Q92851	Caspase-10 OS=Homo sapiens GN=CASP10 PE=1 SV=3 - [CASPA_HUMAN]	33.89	0.96	2	1	1	1	521	58.9	7.33
Q92851	Caspase-10 OS=Homo sapiens GN=CASP10 PE=1 SV=3 - [CASPA_HUMAN]	36.55	0.96	2	1	1	1	521	58.9	7.33
Q92851	Caspase-10 OS=Homo sapiens GN=CASP10 PE=1 SV=3 - [CASPA_HUMAN]	36.52	0.96	2	1	1	1	521	58.9	7.33
Q9BQA1	Methylosome protein 50 OS=Homo sapiens GN=WDR77 PE=1 SV=1 - [MEP50_HUMAN]	68.68	9.94	1	3	3	3	342	36.7	5.17
Q9BQA1	Methylosome protein 50 OS=Homo sapiens GN=WDR77 PE=1 SV=1 - [MEP50_HUMAN]	40.92	5.56	1	1	2	2	342	36.7	5.17
Q9BQA1	Methylosome protein 50 OS=Homo sapiens GN=WDR77 PE=1 SV=1 - [MEP50_HUMAN]	58.19	12.57	1	2	3	3	342	36.7	5.17
Q9UHT4	Putative uncharacterized protein PRO1854 OS=Homo sapiens GN=PRO1854 PE=5 SV=1 - [YG001_HUMAN]	36.63	7.46	6	1	1	2	67	8.3	10.08